Title
Robust Coordination and Control of Networked Systems with Intermittent Communication

Author
Phillips, Sean

Publication Date
2018

Peer reviewed|Thesis/dissertation

UNIVERSITY OF CALIFORNIA
SANTA CRUZ

ROBUST COORDINATION AND CONTROL OF NETWORKED SYSTEMS WITH INTERMITTENT COMMUNICATION

A dissertation submitted in partial satisfaction of the
requirements for the degree of

DOCTOR OF PHILOSOPHY

in

COMPUTER ENGINEERING
with an emphasis in ROBOTICS AND CONTROL

by

Sean A. Phillips

March 2018

The Dissertation of Sean A. Phillips
is approved:

Professor Ricardo G. Sanfelice, Chair

Professor Dejan Milutinovic

Professor Qi Gong

Dean Tyrus Miller
Vice Provost and Dean of Graduate Studies

Table of Contents

List of Figures **vi**

List of Tables **viii**

List of Symbols **ix**

Abstract **xii**

Dedication **xiv**

Acknowledgments **xv**

1 Introduction **1**
1.1 Motivation and Historical Relevance 1
1.2 Contributions 4
1.2.1 Consensus and Synchronization in Networked Systems with Intermittent Information 5
1.2.2 Desynchronization of Impulse-coupled oscillators 9
1.3 Organization 11

2 Preliminaries **16**
2.1 Hybrid Systems 16
2.1.1 Autonomous Hybrid Systems 16
2.1.2 Hybrid Systems with Inputs 21
2.2 Graph Theory 22

I Synchronization and Consensus in Networks with Intermittent Communication **25**

3 A Hybrid Consensus Protocol for Pointwise Exponential Stability **26**
3.1 Introduction 26
3.2 Consensus using Intermittent Information 27
3.3 Pointwise Asymptotic Stability through Synchronous Communication 30
3.3.1 Hybrid Modeling 30
3.3.2 Properties of maximal solutions 31
3.3.3 Coordinate change 33

3.3.4 Basic properties and equivalencies of $\mathcal{H}$ and $\widetilde{\mathcal{H}}$ . . . 34
3.3.5 Consensus Convergent Point . . . 40
3.3.6 Partial pointwise exponential stability for $\mathcal{H}$ . . . 42
3.3.7 Robustness to Perturbations on Communication Noise . . . 45
3.4 Numerical Examples . . . 49
3.5 Summary . . . 51

4 Decentralized Synchronization of Linear Time-invariant Systems 52
4.1 Introduction . . . 52
4.2 Robust Global Synchronization with Intermittent Information . . . 55
4.2.1 Hybrid Modeling . . . 55
4.2.2 Properties of Maximal Solutions to $\mathcal{H}$ . . . 58
4.2.3 Sufficient Conditions for Synchronization . . . 59
4.2.4 Time to Synchronize . . . 68
4.2.5 Robustness of Synchronization . . . 75
4.2.6 Robustness to Information Loss . . . 84
4.3 Numerical Examples . . . 86
4.3.1 Synchronization under Nominal Conditions . . . 86
4.3.2 Synchronization under Perturbations and Information Loss . . . 93
4.4 Summary . . . 94

5 On Synchronization in General Hybrid Systems 95
5.1 Introduction . . . 95
5.2 Interconnected Agents with Hybrid Dynamics . . . 96
5.2.1 Hybrid Modeling and General Properties . . . 96
5.2.2 Partial Synchronization Notions . . . 99
5.2.3 Results for Partial Synchronization . . . 101
5.3 Summary . . . 106

II Impulse-Coupled Oscillators 107

6 Desynchronization in Impulse-Coupled Oscillators 108
6.1 Introduction . . . 108
6.2 Hybrid System Model of Impulse-Coupled Oscillators . . . 111
6.2.1 Mathematical Model . . . 111
6.2.2 Basic Properties of $\mathcal{H}_N$ . . . 113
6.3 Dynamical Properties of $\mathcal{H}_N$ . . . 116
6.3.1 Construction of the set $\mathcal{A}$ for $\mathcal{H}_N$ . . . 116
6.3.2 Lyapunov Stability . . . 119
6.3.3 Characterization of Time of Convergence . . . 124
6.3.4 Robustness Analysis . . . 126
6.4 Numerical Analysis . . . 131
6.4.1 Nominal Case . . . 131
6.4.2 Perturbed Case . . . 134
6.5 Summary . . . 141

7 Synchronization and Desynchronization in Interconnected Neurons **142**
7.1 Introduction . . . 142
7.2 A Framework For Analysis for Spiking Neurons . . . 143
7.2.1 Introduction to Neuron Models . . . 143
7.2.2 Hybrid Modeling . . . 144
7.2.3 Basic Properties of $\mathcal{H}$ . . . 145
7.3 Stability Analysis of Synchronization and Desynchronization with Zero Inputs . . 146
7.3.1 Proposed Approach . . . 146
7.3.2 Simplified Hodgkin-Huxley (HH) Model ($n = 2$) . . . 147
7.3.3 Inhibited Simplified Hodgkin-Huxley (IHH) Model ($n = 2$) . . . 153
7.3.4 SNIPER (S) Model ($n = 2$) . . . 156
7.3.5 Hopf (H) Model ($n = 2$) . . . 162
7.4 Summary . . . 163

8 Frequency Hopping Rendezvous **165**
8.1 Introduction . . . 165
8.2 Modeling Impulsive Oscillators with Channel Dependency . . . 167
8.2.1 Hybrid Modeling . . . 168
8.2.2 Basic Properties of $\mathcal{H}_{2,2}$ . . . 172
8.3 Synchronization Properties of the Hybrid System Model for Two Impulsive Oscillators with Channel Dependency . . . 172
8.3.1 Asymptotic Stability Analysis of $\mathcal{H}_{2,2}$ . . . 173
8.4 Numerical Analysis . . . 197
8.4.1 Numerical Simulation of $\mathcal{H}_{2,2}$ . . . 197
8.4.2 Performance Analysis: Time to synchronize . . . 198
8.4.3 Robustness analysis to interference . . . 200
8.5 Experimental Results . . . 201
8.6 Summary . . . 204

III Final Remarks **205**

9 Conclusion and Future Directions **206**

Bibliography **209**

A List of Publications **219**

List of Publications **219**

List of Figures

3.1 (top) The x and τ components of a solution $\phi = (\phi_x, \phi_\eta, \phi_\tau)$ to $\mathcal{H}$ with $\mathcal{G}$ in (3.48) using Protocol 3.3.1 which satisfies Proposition 3.3.5. (bottom) Note that since $V_2(\chi)$ for $\widetilde{\mathcal{H}}$ deceases to zero with respect to flow time, it indicates that the solution reaches consensus. 50

4.1 Numerical solutions of 6 interconnected linear oscillators communicating over a ring graph. 87

4.2 A numerical solution of the first component of the state ϕ_{x_i} for each $i \in \{1, 2, 3\}$ where $\phi_{x_i} = (\phi_{x_{i1}}, \phi_{x_{i2}})$ and ϕ_τ for Example 4.3.2. (top and middle, respectively) The Lyapunov function V in (4.45) evaluated along the solution to $\mathcal{H}_\varepsilon$ decreases to zero, indicating that the solution synchronizes over hybrid time. (bottom) . . 89

4.3 (left) Randomly generated undirected small-world network containing 100 agents. (upper right) The first component of the states of each agent in the network. Note that over time all agents converge to synchrony. (bottom right) The norm of the relative error over ordinary time converges to zero. 92

4.4 When communication noise is present, solutions converge to a neighborhood about the synchronization set as indicated by the norm of the relative error converging to an average value of 0.1147. 92

4.5 The norm of the average relative error ε_i for 10 averaged trajectories for each dropout rate $d_r = \{0, 0.2, 0.4, 0.6, 0.8, 1\}$ 94

6.1 An example of two impulse-coupled oscillators reaching desynchronization (as Δt_i converges to a constant.) The internal resets (dark red circles) map the timers to zero. The external resets (light green circles) map the timers to a fraction $(1+\varepsilon)$ of their current value. 112

6.2 Time to converge (over $\bar{\tau} + 1$) as a function of $\varepsilon \in [-0.9, -0.1]$, with $c_2 = 0.99\bar{\tau}$ and $c_1 \in \{0.5\bar{\tau}, 0.3\bar{\tau}, 0.1\bar{\tau}, 0.05\bar{\tau}\}$ 125

6.3 Solutions to $\mathcal{H}_N$ with $N \in \{2, 3\}$ that are initially in the set $\mathcal{A}$. 131

6.4 Solutions to $\mathcal{H}_N$ that asymptotically converge to the desynchronization set $\mathcal{A}$ for $N \in \{2, 3, 7, 10\}$. 132

6.5 Solutions to $\mathcal{H}_N$ initialized in $\mathcal{X}_N$ is outside the basin of attraction $\mathcal{B}_\mathcal{A}$ and, therefore, never converge to the set $\mathcal{A}$ 133

6.6 Solutions to $\mathcal{H}_N$ for $N \in \{2, 3\}$ that initially evolve in $\mathcal{X}$ and eventually become desynchronized due to the set-valuedness of the jump map. 134

6.7 Solutions to the hybrid system with perturbed threshold, namely, with $D_\rho = \{\tau : \exists i \in \{1,2\}$ s.t. $\tau_i = \bar{\tau} + \rho_i\}$ for $\rho_1 = \rho_2 = 0.2$. 135
6.8 Numerical simulations of the perturbed version of $\mathcal{H}_2$ with jump set given by $D_\rho = \{\tau : \exists i \in \{1,2\}$ s.t. $\tau_i = \bar{\tau} + \rho_i\}$ for different values of ρ_i. 136
6.9 Solutions to the hybrid system $\mathcal{H}_2$ with the perturbed jump in (6.17) map with $\rho_1 = \rho_2 = 0.2$. 138
6.10 Solutions to the hybrid system $\mathcal{H}_2$ with the perturbed jump map with $\rho_1 \neq \rho_2$. . 138
6.11 Solutions to the hybrid system with perturbed "bump" on the jump map, with $\widetilde{\rho}_1 = \widetilde{\rho}_2 = 0.1$. 139
6.12 Numerical simulations of the perturbed version of $\mathcal{H}_2$ with the perturbed "bump" on the jump map with $\widetilde{\rho}_1 \neq \widetilde{\rho}_2$. 139
6.13 Solutions to the hybrid system $\mathcal{H}_2$ with perturbed flow map given by the cases covered in Section 6.4.2.2. Figures (a) and (b) show solutions given by the flow perturbation $\Delta\omega = [0.120, 0.134]^\top$ given in Section 6.4.2.2. Note that these figures have a dashed black line denoting the calculated distance from $\widetilde{\mathcal{A}}$ in (6.18). . . . 141

7.1 A solution θ to the simplified Hodgkin-Huxley hybrid system $\mathcal{H}_{HH}$ with $\theta(0,0) = [0, 3.1]^\top$. Note that solutions become synchronized ($\theta_1(t,j) = \theta_2(t,j)$) and $V(\theta(t,j)) = 0$ at $(t,j) = (7.5, 9)$. 150
7.2 A solution θ to the simplified Inverse Hodgkin-Huxley hybrid system $\mathcal{H}_{IHH}$ with $\theta(0,0) = [0, 0.1]^\top$. 153
7.3 A solution to $\mathcal{H}_S$ that never converges to $\mathcal{A}_S$ with $z(\theta) = 1 - \cos(\theta)$, $h = \pi/8$, and initial condition $\theta(0,0) = [0, 2\pi - \theta^*]^\top \in \mathcal{X}$. 157
7.4 The (θ_1, θ_2)-plane for the hybrid system $\mathcal{H}_S$ with $h = 2.67$. 158
7.5 Numerical solutions to $\mathcal{H}_H$ with initial conditions $\theta(0,0) \in [0, 2\pi]^2$. The red regions correspond to the points that converge to $\mathcal{A}_H$ (dashed cyan) while the blue region corresponds to the points that "get stuck" near $\mathcal{A}_H$ due to the offset θ_0. 164

8.1 (a) Trajectories (τ_1, q_1) of a single pulse-coupled oscillator over two channels. (b) Trajectories (τ_1, q_1) and (τ_2, q_2) of two pulse-coupled oscillators over two channels. 168
8.2 A plot of the Lyapunov function V in (8.6) for each x in $C \cup D$ 190
8.3 The flow set (red), the jump set (solid black), and basin of attraction with μ-level sets $L_V(\bar{\tau})$ (in blue) and $L_V(0)$ (in green) for each pair $(q_1.q_2)$ 196
8.4 Time to converge to $\mathcal{A}$, i.e., time to synchronize timers and channel selections, for $\varepsilon = 0.1, 0.2, 0.3, 0.4, 0.7, 1$ 199
8.5 Time to synchronize as a function of the timer advance constant, ε, with x(0,0) = [1.2,2,0,1] 200
8.6 Percentage of time on the same channel versus number of interfering packets. . . 201
8.7 Test bed for experimentation with pulse-coupled oscillators Explorer16 demo boards with ZeroG wireless modules (bottom), wireless routers (top). 201
8.8 Experimental data obtained with the test bed in Figure 8.7. 204

List of Tables

4.1 Comparison of convergence times for different gains K and E for the hybrid system $\mathcal{H}$ with asynchronous communication in Section 4.2.1. The ✓ indicates that the conditions are satisfied, and the $\times$ indicates that the conditions are not satisfied but solutions converge to the synchronization set. 88
4.2 Comparison of convergence times and results for different choices of gains K and E for the hybrid system $\mathcal{H}_\varepsilon$ with synchronous communication. The ✓ indicates that the conditions are satisfied, and the $\times$ indicates that the conditions are not satisfied but solutions converge to the synchronization set. 91

List of Symbols

$\mathbb{B}$	The closed unit ball, of appropriate dimension, in the Euclidean norm
$\mathbb{C}$	The set of all complex numbers
$\mathbb{N}$	The set of all positive integers including zero, i.e., $\{0, 1, 2, \dots\}$
$\mathbb{R}$	The set of all real numbers
$\mathbb{R}_{\geq 0}$	The set of all non-negative real numbers
$\mathbb{Z}_{\geq 1}$	The set of all positive integers, i.e., $\{1, 2, \dots\}$
$\overline{\mathrm{con}}(S)$	The convex hull of a set S
$\overline{S}$	The closure of a set $S \subset \mathbb{R}^n$ defined by the intersection of all closed sets containing S
(ν, w)	Given vectors $\nu \in \mathbb{R}^n$, $w \in \mathbb{R}^m$, $[\nu^\top \ w^\top]^\top$ is equivalent to (ν, w)
1_N	The vector of N ones
$\langle u, v \rangle$	The inner product of u and v, namely, $u^\intercal v$ for $u, v \in \mathbb{R}^n$
$\lvert\nu\rvert$	The Euclidean vector norm $\lvert\nu\rvert := \sqrt{\nu^\top \nu}$
$\{v_i\}_{i=1}^n$	An orthonormal basis for $\mathbb{R}^n$, each column vector v_i is a vector full of zeros with a 1 in the i-th entry
$x^\top$	The transpose of x
$\mathrm{dom}\, f$	The domain of a function $f : \mathbb{R}^m \to \mathbb{R}^n$ is defined as $\mathrm{dom}\, f := \{x \in \mathbb{R}^m : f(x) \text{ is defined}\}$

$\mathcal{K}$	A function $\alpha : \mathbb{R}_{\geq 0} \to \mathbb{R}_{\geq 0}$ is a class-$\mathcal{K}$ function, also written $\alpha \in \mathcal{K}$, if α is zero at zero, continuous, strictly increasing
$\lfloor x \rfloor$	Defines the largest integer that is less than or equal to $x \in \mathbb{R}$
gph$f$	The graph of a function $f : \mathbb{R}^m \to \mathbb{R}^n$ is defined as gph$f := \{(x, y) : x \in \mathbb{R}^m, y \in G(x)\}$
$\|m\|_\infty$	Given a function $m : \mathbb{R}_{\geq 0} \to \mathbb{R}^n$, $\|m\|_\infty := \sup_{t \geq 0} \|m(t)\|$ and $\|m\|_\delta := \sup_{t \in [0,\delta]} \|m(t)\|$
$\|y\|_{\mathcal{A}}$	$\|y\|_{\mathcal{A}} := \inf_{x \in \mathcal{A}} \|x - y\|$ for a given point $y \in \mathbb{R}^n$ and a closed set $\mathcal{A} \subset \mathbb{R}^n$
$L_V(\mu)$	The μ-sublevel set of V, i.e., $L_V(\mu) = \{x \in \operatorname{dom} V : V(x) \leq \mu\}$
$V^{-1}(\mu)$	The μ-level set of V, i.e., $V^{-1}(\mu) = \{x \in \operatorname{dom} V : V(x) = \mu\}$
diag(A, B)	A block diagonal matrix which has A and B on the diagonal and matrix full of zeros elsewhere
exp(At)	Given a scalar t, and matrix A, exp(At) is the matrix exponential of At
exp(x)	Given a scalar value x, exp(x) is the exponential to the power of x
$\lambda(A)$	The set containing all eigenvalues of the matrix A
$\mu(A)$	$\max\{Re(\lambda)/2 : \ \lambda \in \operatorname{eig}(A + A^\top)\}$ for a matrix A
$\overline{\lambda}(A)$	$\max\{Re(\lambda) : \ \lambda \in \operatorname{eig}(A)\}$ for a matrix A
$\underline{\lambda}(A)$	$\min\{Re(\lambda) : \ \lambda \in \operatorname{eig}(A)\}$ for a matrix A
$\|A\|$	$\max\{\|\lambda\|^{\frac{1}{2}} : \ \lambda \in \lambda(A^\top A)\}$
$A * B$	The Khatri-Rao product between two matrices A and B with proper dimensions. The Khatri-Rao product is defined as a block wise matrix Kronecker product, namely, $A * B = (A_{ij} \otimes B_{ij})_{ij}$

$A \otimes B$	The Kronecker product between two matrices A and B, namely, $$A \otimes B = \begin{bmatrix} a_{11}B & \dots a_{1n}B & \\ \vdots & \ddots & \vdots \\ a_{m1}B & \dots & a_{mn}B \end{bmatrix}$$
I_N	$I_N \in \mathbb{R}^{N \times N}$ defines the identity matrix given $N \in \mathbb{N}$
$Re(\lambda)$	The real component of the eigenvalue λ.
$\mathrm{He}(A, B)$	The operator $\mathrm{He}(A, B) := A^\top B + B^\top A$ for two matrices A, B with proper dimensions
$\mathcal{S}_\mathcal{H}$	The set of all maximal solutions to $\mathcal{H}$.
$\mathcal{S}_\mathcal{H}(\zeta)$	The set of all maximal solutions to $\mathcal{H}$ from ζ.
$\mathcal{K}_\infty$	An unbounded $\mathcal{K}$ function.
$\mathcal{KL}$	A function $\beta : \mathbb{R}_{\geq 0} \times \mathbb{R}_{\geq 0} \to \mathbb{R}_{\geq 0}$ is a class-$\mathcal{KL}$ function, also written $\beta \in \mathcal{KL}$, if it is nondecreasing in its first argument, nonincreasing in its second argument, $\lim_{r \to 0^+} \beta(r, s) = 0$ for each $s \in \mathbb{R}_{\geq 0}$, and $\lim_{s \to \infty} \beta(r, s) = 0$ for each $r \in \mathbb{R}_{\geq 0}$

Abstract

Robust Coordination and Control of Networked Systems with Intermittent Communication

by

Sean A. Phillips

Networked systems characterize many modern real-world interactions, ranging from the internet and social media networks, to communication networks and power distribution networks, to interconnected neuron and biological models. For such networks, agents in the network utilize information from its neighbors to achieve a common task, however, in practical applications the information available to each agent may not be continuously available. Moreover, such information may be subjected to environmental perturbations. Therefore, in this dissertation, robust coordination and control algorithms are studied for networked systems when the coupling between them are naturally intermittent. Namely, coordination in terms of synchronization and desynchronization for different interconnected networked systems are analyzed. The intermittency of the communication structure implies some impulsive instances in the dynamics, therefore, for each case, a hybrid systems approach is utilized to model and analyze the dynamics of such systems. Namely, results for set stability using Lyapunov stability and invariance principles are utilized to study the dynamical properties of the coordination algorithms. This dissertation is divided into two enveloping parts: 1) controller design for the synchronization of continuous-time agents where the information transmitted between the agents is intermittent; 2) a dynamical study of desynchronization in impulse-coupled oscillators with some resulting applications. More specifically, the first part considers a distributed controller design for the case when each agent has linear time-invariant continuous-time dynamics, however, the com-

munication triggering information transfer between agents occurs intermittently. For this case, the robust exponential stability of the set characterizing synchronization in continuous linear time-invariant systems when information from neighbors is received impulsively at isolated time instances. The second part considers the case of a network of impulse-coupled oscillators. Impulse coupled oscillators are systems which evolve continuously, until a threshold is reached, at which point, releases an impulse and affects neighboring agents. Due to the oscillatory nature of such systems, under certain parameters the times at which impulses occur separate in time, this action is referred to as desynchronization. The set of points describing desynchronization is characterized and recast as a set stabilization problem, it is shown that the desynchronization set is robustly asymptotically stable. Utilizing recent results for impulse coupled oscillators, applications to the study of dynamical behavior of spiking neurons and to frequency rendezvous for communication systems are given. Numerical examples illustrating the results are presented throughout.

Dedicated to my parents:

Lisa and Brian Gregg

and

Gordon Phillips.

Acknowledgments

Foremost, I would like to express my thanks to Dr. Ricardo Sanfelice, who has had endless patience with helping me advance towards the completion of this degree. Your guidance has been a valued asset from the time I began working with you all those years ago, through my masters program and into writing this dissertation. It is impossible to express how much you've taught me. I enjoyed the thought provoking conversations and rigor you instilled on me while discussing and producing new results, ideas and papers. I hope that we can continue working together as colleagues and friends.

Thank you to my other committee members, Dr. Qi Gong and Dr. Dejan Milutinovic. I thoroughly appreciate your encouraging words and guidance before and during my defense.

I'm thankful for my wonderful girlfriend, Savannah Rodgers, thank you for your unending love and support. Though my move to Santa Cruz has been a difficult road, I am ever grateful for having you in my life.

To all of the lab members at the University of Arizona and University of California, Santa Cruz: Thank you Jun Chai, Yuchun Li, Bharani Malladi, Nathalie Risso, Pedro Casau, Pablo Nanez and Hyejin Han. I will cherish our time together discussing the mundane to the involved. I'm looking forward to future collaborations and conversations with you all.

Thank you Jun for being there and adventuring with me in California. Thank you for catching me every time I fell.

Thank you to R. Scott Erwin for mentoring me and helping me navigate the transition into the real-world. I'm looking forward to working closely with you in the coming years.

Chapter 1

Introduction

1.1 Motivation and Historical Relevance

One of the first descriptions of automatically driven devices comes in Aristotle's *'Politics'*, wherein, he describes what household life could be like with autonomous processes, namely, as written on the cover page of [1]:

> *"... if every instrument could accomplish its own work, obeying or anticipating the will of others ... if the shuttle would weave and the pick touch the lyre with a hand to guide them, chief workmen would not need servants, nor masters slaves.*

However, there would not be any rigor in the development in a field called control theory until much later. The first such article which is frequently attributed to the creation of the field of control dates back to the late 19th century with J. C. Maxwell's famous paper titled "On governors" published in the Proceedings of the Royal Society in 1868, [2]. In this article, Maxwell discusses the design of *a governor* (such devices, were used to regulate velocity in steam engines) using a rigorous mathematical analysis.

The time between the industrial revolutions and World War I, control theory was given a written language, namely, the language of mathematical analyses. With the Wright

Brother's monumental flight in 1903 the world of control theory continued to progress and weave itself into a variety of applications. In the 1930's, the number of applications of automatic control increased into power distribution systems, stabilization of aircraft, telecommunication amplifiers, petroleum production, and much more. Modern control theory is now one of the most interdisciplinary areas of science, where engineering and mathematics are symbiotically driven. Such techniques are now found in every major industry, from space based applications, manufacturing automation, and even in mining and chemical processes.

From the inception of control theory, the control of a single (potentially large and complex) system has seen a majority of attention. Under these modeling structures, numerous methodologies were developed and applied to every aspect of modern life, such methods include, proportional-integral-derivative (PID) control, adaptive control, robust control, optimal control, model predictive control and hybrid control. Beginning in the 1970's, the study of interconnected networked systems has seen increased attention. Networked systems are typically considered as multiple smaller systems (also called subsystems) interconnected together into a larger system. The control of which has been separated into two distinct paradigms, a centralized approach and a decentralized approach. In the centralized approach, the actions of each system within the networked systems are governed via a monolithic centralized controller; however, this is becoming a less viable due to the expensive mainframe maintenance. Therefore, the necessity of a decentralized approach is needed.

Recently with the advent of inexpensive communication methods and the miniaturization of electronics, the control algorithms can be designed in a distributed way for each system in the network to accomplish a common task. Indeed, one motivation of coordination of networked distributed systems is to achieve the same performance that monolithic classical control structures (which instructs agents from a centralized controller) yields, but over a distributed network of agents. More specifically, instead of having a large centralized mainframe computer governing

the actions of each agent, the designer designs the controller to allow the agents themselves to govern their own actions. This distributed structure allows the designer to consider multiple small inexpensive computers to distribute the computational effort to achieve the agents' goals.

With the distribution of the control to the agents, an effort to coordinate their actions is now a current discussion. Coordination in multiagent and networked systems is a rather broad term which encompasses a variety of ideologies. However, it is generally defined as designing control algorithms for agents to utilize available assets and make decisions in a distributed fashion to complete a common task. As Boutilier discusses in [3], the solutions to such problems are typically approached from three different perspectives: communication based; convention based; and learning based. These three categories are explicitly defined as follows:

- **Communication based**: Agents communicate in order to determine task allocation. Such an algorithm requires a common language, at least, to coordinate their actions. Namely, the connected agents need to adhere to a structure of communication to articulate their actions. In large systems of connected agents, such as the cases considered in this work, there must be some form of communication in order to share information between agents in the network; it would be impossible otherwise to effectively coordinate their efforts.

- **Convention based**: Conventions are systems that are designed so that joint actions are assured. Typically, a convention is a commonly-known rule which agents follow to coordinate their actions. There are many real-world precedents for coordination by convention. For example, traffic control is a typical model for such algorithms wherein traffic flow is controlled via stop signals. An open-loop coordination design is another example of convention based coordination, for instance, each agent knows that it must do a pre-specified task; for instance, role-based structured control as implemented in many Robocup robotic

soccer teams [4].

- **Learning based**: A coordinated policy might be learned. It may combine both of the previous methods to achieve its task; namely, conventions may be learned through communications. There are many different ways of applying learning algorithms to coordination, from learning to choose to between optimal protocols, to leaning to use simple communication techniques. However, such algorithms are difficult to setup, implement and may have a high bandwidth consumption.

In this dissertation, two main enveloping topics are discussed. The first is a communication based approach to a consensus/synchronization of linear continuous-time equations where communication between the agents is not continuous. More specifically, the agents can only communicate at some unknown intermittent time instances. The second topic is on interconnected impulse-coupled oscillators which are networked systems with state variables that evolve continuously until a state dependent event triggers an instantaneous update of their state values. Specifically, the tendency for desynchronizing impulse-coupled oscillators separating their impulses to occur with equal spacing in time is studied, this configuration is also referred to as a splay-state configuration. Moreover, the communication structure of these impulse-coupled oscillators lends itself into numerous applications studied here: networks of interconnected spiking neurons and a frequency hopping rendezvous problem for cognitive radios. Insights into the aforementioned problems are given in the following section.

1.2 Contributions

The main topics covered in this work utilize communication over the network to coordinate their actions. The specific topics are introduced in the subsequent sections.

1.2.1 Consensus and Synchronization in Networked Systems with Intermittent Information

1.2.1.1 Motivation

The topics of consensus and synchronization in multiagent networked systems has gained massive traction in recent years due to the wide range of applications science and engineering. In general, consensus is defined on multiple agents connected together via a graph agree to a common value. Synchronization, however, is also an agreement of states where each agent has its own local dynamics. Consensus is seen in spiking neurons, formation control and flocking maneuvers [5, 6, 7, 8], distributed sensor networks [9, 10], satellite constellation formation [11], and in communication of computer network systems [12]. Synchronization is seen in spiking neurons [13, 14], formation control and flocking maneuvers [5, 7], distributed sensor networks [10], and satellite constellation formation [11], to name a few.

Some of the main challenges for designing protocols for consensus and synchronization problems are:

- *Impulsive communication events*: Continuous communication between agents may not occur continuously. Due to the computerized and digital controllers, the communication structures occur at impulsive events. Moreover, such communications between agents (especially, if the agents are dynamic) may not occur periodic (due to potential line of sight or range issues).

- *Asynchronous and heterogenous communication events at unknown times*: the time instances at which each agent receives information are not synchronized and do not necessarily occur periodically. Namely, each agent may receive information from its neighbors at different and unknown time instances. Furthermore, the amount of ordinary time elapsed

between consecutive communication events for each agent is not constant and not predefined beforehand; for example, one agent may receive information at a much faster "rate" than others.

- *Instability of nominal dynamics:* each of the systems may not be stable, potentially leading to unbounded trajectories in each system. In particular, the individual dynamics of the agents to be synchronized could be such that their origin is marginally stable or unstable, in which case the state trajectories of the agents need to converge to each other while potentially escaping to infinity.

- *Perturbations in the dynamics, parameters, and measurements:* unknown dynamics in the model makes it difficult to design an algorithm that guarantees exact synchronization. Synchronization algorithms that are not robust to perturbations on the transmitted information and on the times at which such information arrives could prevent the state trajectories of the agents to converge to nearby values.

1.2.1.2 Related Work

The wide applicability of consensus and synchronization in science and engineering has promoted a rich set of theoretical results for a variety of class of dynamical systems using a diverse set of tools. Consensus was initially proposed in [6] which proposed an algorithm that utilized the graphical properties of the network to ensure global convergence to an average value of the states initial conditions. The study of convergence and stability of synchronization come through the use of systems theory tools such as Lyapunov functions [15, 16], contraction theory [17], and incremental input-to-state stability [18, 19]. Results for asymptotic synchronization with continuous coupling between agents exist in both the continuous-time domain and the discrete-time domain; see, e.g., [20, 21, 22], where the latter is a detailed survey of coordina-

tion and consensus for first-order integrator dynamics, in continuous-time and discrete-time. In [20], both for continuous-time and discrete-time interconnected linear time-invariant systems a dynamic control law is shown to guarantee that the solution of each agent converge to that of an homogeneous system with the same dynamics. In [21], the author provides a brief survey on the convergence to synchronization through Lyapunov and set convexity analysis. As pointed out therein, a typical approach to guarantee that the interconnected agents converge to synchronization is to leverage the properties of the graph structure inherent in the connection of multiple agents. Namely, the approach is to use the properties of the graph Laplacian matrix to show that every agent converges to the synchronization manifold. Typically only convergence of the solutions to this manifold is discussed and stability is typically left out of the definitions of asymptotic synchronization; see, e.g., [15, 20, 22].

Synchronization in continuous-time systems where communication coupling occurs at discrete events is an emergent area of study. In [19], the authors study a case of synchronization where agents have nonlinear continuous-time dynamics with continuous coupling and impulsive perturbations. In [23], the authors use Lyapunov-like analysis to derive sufficient conditions for the synchronization of continuously coupled nonlinear systems with impulsive resets on the difference between neighboring agents. Similar to impulsive systems, synchronization in systems where feedback controllers are designed as state-triggered discrete events appeared [24, 25]. In [24], a distributed event-triggered control strategy was developed to drive the outputs of the agents in a network to synchronization. Through a Laplacian analysis on solutions of the closed-loop system, an observer-based event policy was developed in [25] for a network of linear time-invariant systems where communication is triggered when the distance between the local state and its estimate is large than a threshold. Using a sample-and-hold self-triggered controller policy, a practical synchronization result was established in [26] for the case of first-order integrator dynamics. To the best of our knowledge, methods for the design of algorithms

that guarantee synchronization of multi-agent systems with information arriving at impulsive, asynchronous time instances are not available.

1.2.1.3 Contributions

This part deals with the problem of consensus of first-order integrator systems communicating at stochastically determined time instances over a network and the case of synchronization when each agent is a higher dimensional linear time-invariant system. The problem considered here consists of designing a control structure that guarantees the state of each agent converges to a common value by only using intermittent information from their neighbors. To solve this problem, a hybrid state-feedback protocol is designed which undergoes an instantaneous change in its internal states when new information is available, and evolves continuously between such events. Due to the combination of continuous and impulsive dynamics, the hybrid systems framework developed in [27, 28] is capable of modeling such interconnected systems, the controller, and the network topologies as well as to design the protocols, for which, levy the graphical properties and nature of the update laws to apply Lyapunov theorems for asymptotic stability of sets for hybrid systems. Aside from asymptotic stability, when the communications graph is strongly connected and weight balanced, the point to which the consensus states converge to is determined. Through a Lyapunov based analysis, a diagonal-like set is shown to be partially pointwise globally exponentially stable with respect to the agent's states. Such a notion is stronger than the typical notions of asymptotic stability due to the additional requirement that each point in the set is Lyapunov stable; see e.g. [29] and [30] for similar non-partial state notions. Furthermore, when information is asynchronously received by each agent, under certain conditions, it is possible to guarantee that the consensus set is globally asymptotically stable using a invariance principle with a Lyapunov-like function. Similarly, when the agents have dynamics, synchronization is shown through recasting the problem as a set stability problem.

Then, sufficient conditions for exponential stability are given. Moreover, in-depth robustness analyses are presented, wherein several key robustness properties are established. In part, this is enabled by the proposed hybrid controller which is designed to satisfy certain regularity conditions that, under nominal conditions has uniform global asymptotic stability of the synchronization set, guarantees robustness to small enough perturbations. Numerous examples are presented to showcase the nominal and robustness results.

1.2.2 Desynchronization of Impulse-coupled oscillators

1.2.2.1 Motivation

Impulse-coupled oscillators are multi-agent systems with state variables consisting of timers that evolve continuously until a state-dependent event triggers an instantaneous update of their values. Networks of such oscillators have been employed to model the dynamics of a wide range of biological and engineering systems. In fact, impulse-coupled oscillators have been used to model groups of fireflies [31], spiking neurons [32, 33], muscle cells [34], wireless networks [35], and sensor networks [36]. With synchronization being a property of particular interest, such complex networks have been found to coordinate the values of their state variables by sharing information only at the times the events/impulses occur [31, 37].

The opposite of synchronization is *desynchronization*. In simple words, desynchronization in multi-agent systems is the notion that the agents' periodic actions are separated "as far apart" as possible in time. Desynchronization is similar to clustering or splay-state configurations, and is sometimes referred in the literature as inhibited behavior [38, 39]. For impulse-coupled oscillators, desynchronization is given as the behavior in which the separation between all of the timers impulses is equal [40]. This behavior has been found to be present in communication schemes in fish [41] and in networks of spiking neurons [42, 43]. Desynchro-

nization of oscillators has recently been shown to be of importance in the understanding of Parkinson's disease [44, 45], in the design of algorithms that limit the amount of overlapping data transfer and data loss in wireless digital networks [35], and in the design of round-robin scheduling schemes for sensor networks [36].

Motivated by the applications mentioned above and the lack of a full understanding of desynchronization in multi-agent systems, this chapter pertains to the study of the dynamical properties of desynchronization in a network of impulse-coupled oscillators with an all-to-all communication graph. The uniqueness of the approach emerges from the use of hybrid systems tools, which not only conveniently capture the continuous and impulsive behavior in the networks of interest, but also are suitable for analytical study of asymptotic stability and robustness to perturbations.

1.2.2.2 Contributions

The dynamics of the proposed hybrid system capture the (linear) continuous evolution of the states as well their impulsive/discontinuous behavior due to state triggered events. Analysis of the asymptotic behavior of the trajectories (or solutions) to these systems is performed using the framework of hybrid systems introduced in [28, 27]. To this end, the study of desynchronization is recast as a set stabilization problem. Unlike synchronization, for which the set of points to stabilize is obvious, the complexity of desynchronization requires first to determine such a collection of points, which is referred to as the *desynchronization set*. Then, an algorithm to compute such set of points in the desynchronization set is proposed. Using Lyapunov stability theory for hybrid systems, it is shown that the desynchronization set is asymptotically stable by defining a Lyapunov-like function as the distance between the state and (an inflated version of) the desynchronization set. In our context, asymptotic stability of the desynchronization set implies that the distance between the state and the desynchronization set converges to zero

as the amount of time and the number of jumps get large. Using the proposed Lyapunov-like function and invoking an invariance principle, the basin of attraction is characterized and shown to be the entire state space minus a set of measure zero, which turns out to actually be an exact estimate of the basin of attraction. Furthermore, also exploiting the availability of a Lyapunov-like function, the time for the solutions to reach a neighborhood of the desynchronization set is analytically characterized. In particular, this characterization provides key insight for the design of algorithms used in applications in which desynchronization is crucial, such as wireless digital networks and sensor networks.

The asymptotic stability property of the desynchronization configuration is shown to be robust to several types of perturbations. The perturbations studied here include a generic perturbation in the form of an inflation of the dynamics of the proposed hybrid system model of the network of interest and several kinds of perturbations on the timer rates. Using the tools presented in [28, 27], the effect of such perturbations on the already established asymptotic stability property of the desynchronization set are rigorously charactered. In particular, these perturbations capture situations where the agents in the network are heterogeneous due to having differing timer rates, threshold values, and update laws. Networks of impulse-coupled oscillators under several classes of perturbations are simulated to exemplify the results.

1.3 Organization

In light of the contributions listed above, this dissertation is divided into two parts. First, the main notions and modeling frameworks are introduced. Then, Part 1 includes the results on synchronization and consensus of multiagent systems where information is communicated intermittently over a graph. The second part of this dissertation presents the main results on impulse-couple oscillators. The specific chapters of this work is given below:

Chapter 2: Preliminaries

In this chapter, the hybrid systems framework, basic properties used throughout this dissertation and main results utilized are given. Moreover, in this chapter, a brief introduction into the graph theoretical notions are given.

Part I: Robust Decentralized Consensus and Synchronization through Networks with Intermittent Communication

Chapter 3: A Hybrid Consensus Protocol for Pointwise-Exponential Stability

In this chapter, the problem of achieving consensus of the states of multiagent systems is considered, where connected over a network in which communication events are triggered intermittently. The solution proposed consists of a protocol design that, using intermittent information obtained over the network, asymptotically drives the values of their states to agreement, with stability, globally and with robustness to perturbations. More precisely, the protocol jumps at the communication events and evolves continuously in-between such events. Then, by recasting the consensus problem as a set stabilization problem, Lyapunov stability tools for hybrid systems can be applied. Sufficient conditions for exponential stability of the consensus set are given. Furthermore, under additional network structure requirements, this set is also shown to be partially pointwise globally exponentially stable. Robustness of consensus to certain classes of perturbations is also established.

Chapter 4: Decentralized Synchronization of Linear Time-Invariant Systems

In this chapter, the problem of synchronization of multiple linear time-invariant systems connected over a network with both synchronous and asynchronous intermittently available communication events is studied. To solve this problem, similar to the consensus problem,

the controller utilizes information transmitted to it during discrete communication events and exhibits continuous dynamics between such events. Due to the additional continuous and discrete dynamics inherent to the interconnected networked systems and communication structure, the hybrid systems framework in [28] is utilized to model and analyze the closed-loop system. The problem of synchronization is then recast as a set stabilization problem and, by employing Lyapunov stability tools for hybrid systems, sufficient conditions for asymptotic stability of the synchronization set are provided. Furthermore, the stability property of synchronization is robust to perturbations. Numerical examples illustrating the main results are included.

Chapter 5: Synchronization of General Hybrid Systems

In this chapter, a brief discussion on the synchronization of the states of a multiagent networked system, each agent exhibits hybrid behavior. Namely, the state of each agent may evolve continuously according to a differential inclusion, and, at times, jump discretely according to a difference inclusion. A notion of asymptotic synchronization for a partition of the state of the system. The definition of asymptotic synchronization imposes both Lyapunov stability and attractivity on the difference between the agents' states. Synchronization recast as a set stability problem, for which tools for the study of asymptotic stability of sets for hybrid systems are suitable.

Part II: Networks of Impulse-coupled Oscillators

Chapter 6: Desynchronization in Impulse-coupled Oscillators

In this chapter, the property of desynchronization in a completely connected network of homogeneous impulse-coupled oscillators is studied. Each impulse-coupled oscillator is modeled as a hybrid system with a single time state that self-resets to zero when it reaches a threshold, at which event all other impulse-coupled oscillators adjust their timers following a common reset

law. In this setting, desynchronization is considered as each impulse-coupled oscillator's timer having equal separation between successive resets. For the considered model, desynchronization is shown to be an asymptotically stable property. For this purpose, desynchronization is recast as a set stabilization problem and employ Lyapunov stability tools for hybrid systems. Furthermore, several perturbation cases are considered showing that desynchronization is a robust property. Perturbations on both the continuous and discrete dynamics are considered.

Chapter 7: Synchronization and Desynchronization in Interconnected Spiking Neurons

Using the network of interconnected impulse-coupled oscillators in Chapter 6, a framework for analysis for a population of n interconnected neurons. Several well-known neuron models are studied with the framework, including both excitatory and inhibitory simplified Hodgkin-Huxley, Hopf, and SNIPER models. For each model, the sets that the solutions to each system converge to are characterized and, using Lyapunov stability tools for hybrid systems, stability properties for each case are established. Numerical simulation provide insight on the results and capabilities of the proposed framework.

Chapter 8: Frequency Hopping Rendezvous

An algorithm to find, link and synchronize the actions of cognitive radios is considered, known as frequency hopping rendezvous. The algorithm is modeled as an impulse-coupled oscillator, which updates its state when information arrives, however, if the agents are on different channels it is not possible to receive information. Under such a communication constraint, the impulse-coupled oscillators (almost globally) synchronize their channel selections. To establish this result, the interconnection of oscillators are modeled as a hybrid system and recent Lyapunov stability tools are applied to. Numerical simulation are included to illustrate the

results.

Chapter 9: Conclusion and Future Directions

A summary of the contributions and potential future directions are presented. A complete list of publications can be found in the authors CV attached in Appendix A.

Chapter 2

Preliminaries

2.1 Hybrid Systems

2.1.1 Autonomous Hybrid Systems

A hybrid system $\mathcal{H}$ has data (C, f, D, G) and is defined by

$$\begin{aligned} \dot{\xi} &= f(\xi) \qquad \xi \in C, \\ \xi^{+} &\in G(\xi) \qquad \xi \in D, \end{aligned} \tag{2.1}$$

where $\xi \in \mathbb{R}^n$ is the state, f defines the flow map capturing the continuous dynamics and C defines the flow set on which f is effective. The set-valued map G defines the jump map and models the discrete behavior, while D defines the jump set, which is the set of points from where jumps are allowed.

A solution to generic hybrid systems ϕ to $\mathcal{H}$ defined in (2.1) is parametrized by $(t, j) \in \mathbb{R}_{\geq 0} \times \mathbb{N}$, where t denotes ordinary time and j denotes jump time. More specifically, solutions are given by *hybrid arcs* on *hybrid time domains* defined below.

Definition 2.1.1 *(hybrid time domain) A subset $S \subset \mathbb{R}_{\geq 0} \times \mathbb{N}$ is a compact hybrid time domain*

if $S = \bigcup_{j=0}^{J-1} ([t_j, t_{j+1}], j)$ *for some finite sequence of times* $0 = t_0 \leq t_1 \leq t_2 \ldots \leq t_J$. *A subset* $S \subset \mathbb{R}_{\geq 0} \times \mathbb{N}$ *is a hybrid time domain if for all* $(T, J) \in S$, $S \cap ([0, T] \times \{0, 1, \ldots J\})$ *is a compact hybrid time domain.*

Definition 2.1.2 *(hybrid arc) A function* $x : \operatorname{dom} x \to \mathbb{R}^n$ *is a hybrid arc if* $\operatorname{dom} x$ *is a hybrid time domain and if for each* $j \in \mathbb{N}$, *the function* $t \mapsto x(t, j)$ *is locally absolutely continuous.*

Definition 2.1.3 *(solution) A hybrid arc* ϕ *is a* solution to the hybrid system $\mathcal{H}$ *if* $\phi(0, 0) \in C \cup D$ *and:*

(S1) For all $j \in \mathbb{N}$ *and almost all* t *such that* $(t, j) \in \operatorname{dom} \phi$, *the solution* $\phi(t, j) \in C, \quad \dot{\phi}(t, j) = f(\phi(t, j))$.

(S2) For all $(t, j) \in \operatorname{dom} \phi$ *such that* $(t, j + 1) \in \operatorname{dom} \phi$, $\phi(t, j) \in D, \quad \phi(t, j + 1) \in G(\phi(t, j))$.

A solution to $\mathcal{H}$ is called maximal if it cannot be extended, i.e., it is not a truncated version of another solution. It is called complete if its domain is unbounded. A solution is Zeno if it is complete and its domain is bounded in the t direction. A solution is precompact if it is complete and bounded.

Next, we define several notions of stability for a closed set $\mathcal{A} \subset \mathbb{R}^n$ for a hybrid system $\mathcal{H}$.

Definition 2.1.4 *(global exponential stability) Let a hybrid system* $\mathcal{H}$ *be defined on* $\mathbb{R}^n$. *Let* $\mathcal{A} \subset \mathbb{R}^n$ *be closed. The set* $\mathcal{A}$ *is said to be global exponential stability for* $\mathcal{H}$ *if there exist* $\kappa, \alpha > 0$ *such that every maximal solution* ϕ *to* $\mathcal{H}$ *is complete and satisfies*

$$|\phi(t, j)|_{\mathcal{A}} \leq \kappa e^{-\alpha(t+j)} |\phi(0, 0)|_{\mathcal{A}}$$

for each $(t, j) \in \operatorname{dom} \phi$

Definition 2.1.5 *(global asymptotic stability) Let $\mathcal{H}$ be a hybrid system in $\mathbb{R}^n$. A compact set is said to be*

- stable *for $\mathcal{H}$ if for every $\varepsilon > 0$ there exists $\delta > 0$ such that every solution ϕ to $\mathcal{H}$ $|\phi(0,0)|_{\mathcal{A}} \leq \delta$ satisfies $|\phi(t,j)|_{\mathcal{A}} \leq \varepsilon$ for all $(t,j) \in \operatorname{dom}\phi$;*

- locally attractive *for $\mathcal{H}$ if there exists $\mu > 0$ such that every solution ϕ to $\mathcal{H}$ with $|\phi(0,0)|_{\mathcal{A}} \leq \mu$ is bounded and, if ϕ is complete, then it also satisfies $\lim_{t+j\to\infty} |\phi(t,j)|_{\mathcal{A}} = 0$;*

- locally asymptotically stable *for $\mathcal{H}$ if it is both stable and locally attractive for $\mathcal{H}$.*

Note that attractivity can be considered to be *global* if local attractivity can be satisfied for every $\mu > 0$.

Definition 2.1.6 *(uniform global asymptotic stability) Let a hybrid system $\mathcal{H}$ be defined on $\mathbb{R}^n$. Let $\mathcal{A} \subset \mathbb{R}^n$ be closed. The set $\mathcal{A}$ is said to be*

- *uniformly globally stable (UGS) for $\mathcal{H}$ if there exists a class-$\mathcal{K}_\infty$ function α such that any solution ϕ to $\mathcal{H}$ satisfies $|\phi(t,j)|_{\mathcal{A}} \leq \alpha(|\phi(0,0)|_{\mathcal{A}})$ for all $(t,j) \in$ dom ϕ;*

- *uniformly globally attractive (UGA) for $\mathcal{H}$ if for each $\varepsilon > 0$ and $r > 0$ there exists $T > 0$ such that, every maximal solution ϕ to $\mathcal{H}$ is complete and if $|\phi(0,0)|_{\mathcal{A}} \leq r$, $(t,j) \in$ dom ϕ and $t + j \geq T$ then $|\phi(t,j)|_{\mathcal{A}} \leq \varepsilon$;*

- *uniformly globally asymptotically stable (UGAS) for $\mathcal{H}$ if it is both uniformly globally stable and uniformly globally attractive.* □

Definition 2.1.7 *(partial pointwise global exponential stability) Consider a hybrid system $\mathcal{H}$ with state $\xi = (p,q) \in \mathbb{R}^n$. The closed set $\mathcal{A} \subset \mathbb{R}^r \times \mathbb{R}^{n-r}$ where $r \in \mathbb{N}$ and $0 < r \leq n$ is* partially pointwise global exponentially stable *with respect to the state component p for $\mathcal{H}$ if*

1) every maximal solution ϕ to $\mathcal{H}$ is complete and has a limit belonging to $\mathcal{A}$;

2) $\mathcal{A}$ is globally exponentially stable for $\mathcal{H}$, namely, for each $\phi \in \mathcal{S}_{\mathcal{H}}$ there exist $\kappa, \alpha > 0$ such that $|\phi(t,j)|_{\mathcal{A}} \leq \kappa e^{-\alpha(t+j)} |\phi(0,0)|_{\mathcal{A}}$ for all $(t,j) \in \operatorname{dom} \phi$; and

3) for each $p^* \in \mathbb{R}^r$ such that there exists $q \in \mathbb{R}^{n-r}$ satisfying $(p^*, q) \in \mathcal{A}$, it follows that for each $\varepsilon > 0$ there exists $\delta > 0$ such that every solution $\phi = (\phi_p, \phi_q)$ to $\mathcal{H}$ with $\phi_p(0,0) \in p^* + \delta\mathbb{B}$ satisfies $|\phi_p(t,j) - p^*| \leq \varepsilon$ for all $(t,j) \in \operatorname{dom} \phi$. □

The asymptotic version of the notion in Definition 3.3.12 can be found in [46].

To apply some results for hybrid systems, the data (C, f, D, G) of the hybrid system may have to satisfy some mild regularity conditions known as the hybrid basic conditions.

Definition 2.1.8 (Hybrid Basic Conditions) *A hybrid system $\mathcal{H} = (C, f, D, G)$ is said to satisfy the hybrid basic conditions if*

(a) the sets C and D are closed;

(b) the function $f : \mathbb{R}^n \to \mathbb{R}^n$ is continuous;

(c) the set valued mapping $G : \mathbb{R}^n \rightrightarrows \mathbb{R}^n$ is outer semicontinuous and locally bounded relative to D, and $D \subset \operatorname{dom} G$.

A set-valued mapping $G : \mathbb{R}^n \rightrightarrows \mathbb{R}^n$ is *outer semicontinuous* if its graph $\{(x,y) : x \in \mathbb{R}^n, y \in G(x)\}$ is closed. In terms of set convergence, G is outer semicontinuous if and only if, for each $x \in \mathbb{R}^n$ and each sequence $x_i \to x$, the outer limit $\limsup_{i\to\infty} G(x_i)$ is contained in $G(x)$. The mapping G is *locally bounded* on a set D if, for each compact set $K \subset D$, $G(K)$ is bounded.

For the analysis of robustness to noise, an exogenous signal m defining measurement noise will play the role of an input u. A mapping m is admissible if $\operatorname{dom} m$ is a hybrid time domain and, for each $j \in \mathbb{N}$, the function $t \mapsto m(t,j)$ for all $t \in I_j$ is measurable.

Similar to continuous-time and discrete-time systems, a Lyapunov function candidate typically denoted by $V : \mathbb{R}^n \to \mathbb{R}_{\geq 0}$ may be found to ensure asymptotic stability of a set $\mathcal{A}$ for a hybrid system $\mathcal{H}$. We define a Lyapunov function candidate V as follows.

Definition 2.1.9 (Lyapunov function candidate) *Given the hybrid system $\mathcal{H}$ with data (C, f, D, G) and the compact set $\mathcal{A} \subset \mathbb{R}^n$, the function $V : \operatorname{dom} V \to \mathbb{R}$ is a* Lyapunov function candidate *for $(\mathcal{H}, \mathcal{A})$ if*

i) V is continuous and nonnegative on $(C \cup D) \setminus \mathcal{A} \subset \operatorname{dom} V$,

ii) V is continuously differentiable on an open set $\mathcal{O}$ satisfying $C \setminus \mathcal{A} \subset \mathcal{O} \subset \operatorname{dom} V$, and

iii) $\lim_{\{x \to \mathcal{A},\, x \in \operatorname{dom} V \cap (C \cup D)\}} V(x) = 0$.

Conditions i) and iii) hold when $\operatorname{dom} V$ contains $\mathcal{A} \cup C \cup D$, V is continuous and nonnegative on its domain, and $V(z) = 0$ for all $x \in \mathcal{A}$.

There exist numerous sufficient condition notions to guarantee UGAS of a closed set $\mathcal{A}$. Two such results utilized in this work are as follows.

Theorem 2.1.10 *[[27, Theorem 23]] Consider a hybrid system $\mathcal{H} = (C, f, D, G)$ satisfying the Basic Assumptions and a compact set $\mathcal{A} \subset \mathbb{R}^n$ satisfying $G(D \cap \mathcal{A}) \subset \mathcal{A}$. If there exists a Lyapunov function candidate V for $(\mathcal{H}, \mathcal{A})$ that is positive on $(C \cup D) \setminus \mathcal{A}$ and satisfies*

$$\langle \nabla V(x), f(x) \rangle \leq 0 \quad \textit{for all } x \in C \setminus \mathcal{A},$$

$$V(g) - V(x) \leq 0 \quad \textit{for all } x \in D \setminus \mathcal{A}, g \in G(x) \setminus \mathcal{A}$$

then the set $\mathcal{A}$ is stable. If, furthermore, there exists a compact neighborhood K of $\mathcal{A}$ such that, for each $\mu > 0$, no complete solution to $\mathcal{H}$ remains in $L_V(\mu) \cap K$, then the set $\mathcal{A}$ is asymptotically

stable. In this case, the basin of attraction contains every compact set contained in K that is forward invariant.

Theorem 2.1.11 *Consider a hybrid system $\mathcal{H}$ with state $\xi \in \mathbb{R}^n$ and let $\mathcal{A} \subset \mathbb{R}^n$ be closed. Suppose V is a Lyapunov function candidate for $\mathcal{H}$ and there exist $\alpha_1, \alpha_2 \in \mathcal{K}_\infty$, and a continuous $\rho \in \mathcal{PD}$ such that*

$$\alpha_1(|\xi|_\mathcal{A}) \leq V(x) \leq \alpha_2(|\xi|_\mathcal{A}) \qquad \forall \xi \in C \cup D \cup G(D) \tag{2.2}$$

$$\langle \nabla V(\xi), f(\xi) \rangle \leq -\rho(|\xi|_\mathcal{A}) \qquad \forall \xi \in C \tag{2.3}$$

$$V(g) - V(\xi) \leq 0 \qquad \forall \xi \in D, g \in G(x) \tag{2.4}$$

and every maximal solution to $\mathcal{H}$ is complete. If, for each $r > 0$, there exists $\gamma_r \in \mathcal{K}_\infty$, $N_r \geq 0$ such that for every solution ϕ to $\mathcal{H}$, $|\phi(0,0)|_\mathcal{A} \in (0,r], (,j) \in \operatorname{dom}\phi, t + j \geq T$ implies $t \geq \gamma_r(T) - N_r$, then $\mathcal{A}$ is uniformly globally asymptotically stable.

2.1.2 Hybrid Systems with Inputs

Building on the autonomous hybrid systems, such systems can also be defined with inputs, [47]. Namely, in compact form with state ξ and input u (or disturbance), a hybrid system $\mathcal{H}$ is given by

$$\begin{aligned} \dot{\xi} &= f(\xi, u) \qquad (\xi, u) \in C, \\ \xi^+ &\in G(\xi, u) \qquad (\xi, u) \in D. \end{aligned} \tag{2.5}$$

Similar to (2.5), a solution to (2.1) is given by a solution pair (ϕ, u) with $\operatorname{dom}\phi = \phi u (= \operatorname{dom}(\phi, u))$ that satisfies the dynamics therein with the property that, for each $j \in \mathbb{N}, t \mapsto \phi(t,j)$ is absolutely continuous and $t \mapsto u(t,j)$ is Lebesgue measureable and locally essentially bounded on $\{t : (t,j) \in \operatorname{dom}(\phi, u)\}$. We use the following input-to-state stability notion.

Definition 2.1.12 ([47, Definition 2.1]) *Given a compact set $\mathcal{A}$, the hybrid system with state z, and input u given by* (2.5) *is input-to-state stable (ISS) with respect to $\mathcal{A}$ if there exist $\beta \in \mathcal{KL}$ and $\gamma \in \mathcal{K}$ such that, for each $\phi(0,0) \in \mathbb{R}^n$, every solution pair (ϕ, u) satisfies*

$$|\phi(t,j)|_{\mathcal{A}} \leq \max\{\beta(|\phi(0,0)|_{\mathcal{A}}, t+j), \gamma(|u|_\infty)\} \tag{2.6}$$

for each $(t,j) \in \operatorname{dom}\phi$.

The $\mathcal{L}_\infty$ norm of $(t,j) \mapsto u(t,j)$ is given by

$$||u||_(t,j) := \max\left\{ \operatorname*{ess\,sup}_{(t',j')\in \operatorname{dom} u \setminus R(u), t'+j' \leq t+j} |u(t',j')|, \sup_{(t',j')\in R(u), t'+j' \leq t+j} \right\} \tag{2.7}$$

where R captures the jump points in the domain of the signal u, i.e., $R(u) = \{(t, j_\in \operatorname{dom} u : (t, j+1_\in \operatorname{dom} u\}$; see [47, Definition 2.1] for details.

We also consider perturbed hybrid systems and present results on the nominal robustness, we refer the reader to [28] for details on such systems.

2.2 Graph Theory

A directed graph (digraph) is defined as $\Gamma = (\mathcal{V}, \mathcal{E}, \mathcal{G})$. The set of nodes of the digraph are indexed by the elements of $\mathcal{V} = \{1, 2, \ldots, N\}$ and the edges are pairs in the set $\mathcal{E} \subset \mathcal{V} \times \mathcal{V}$. Each edge directly links two different nodes, i.e., an edge from i to k, denoted by (i,k), implies that agent i can send information to agent k. The adjacency matrix of the digraph Γ is denoted by $\mathcal{G} = (g_{ik}) \in \mathbb{R}^{N\times N}$, where $g_{ik} = 1$ if $(i,k) \in \mathcal{E}$, and $g_{ik} = 0$ otherwise. The in-degree and out-degree of agent i are defined by $d^{in}(i) = \sum_{k=1}^N g_{ki}$ and $d^{out}(i) = \sum_{k=1}^N g_{ik}$. The largest (smallest) in-degree in the digraph is given by $\overline{d} = \max_{i\in\mathcal{V}} d^{in}(i)$ ($\underline{d} = \min_{i\in\mathcal{V}} d^{in}(i)$). The in-degree matrix $\mathcal{D}$ is the diagonal matrix with entries $\mathcal{D}_{ii} = d^{in}(i)$ for all $i \in \mathcal{V}$. The Laplacian matrix of the digraph Γ, denoted by $\mathcal{L}$, is defined as $\mathcal{L} = \mathcal{D} - \mathcal{G}$. The Laplacian has the property

that $\mathcal{L}\mathbf{1}_N = 0$. The set of indices corresponding to the neighbors that can send information to the i-th agent is denoted by $\mathcal{N}(i) := \{k \in \mathcal{V} : (k, i) \in \mathcal{E}\}$.

In this article, we will make varying assumptions on the complexity of the underlying graph structure corresponding to the network. For self-containedness, we summarize the needed notions and results from the literature.

Definition 2.2.1 *A directed graph is said to be*

- weight balanced *if, at each node $i \in \mathcal{V}$, the out-degree and in-degree are equal; i.e., for each $i \in \mathcal{V}$, $d^{out}(i) = d^{in}(i)$;*

- complete *if every pair of distinct vertices is connected by a unique edge; that is $g_{ik} = 1$ for each $i, k \in \mathcal{V}$, $i \neq k$;*

- strongly connected *if and only if any two distinct nodes of the graph can be connected via a path that traverses the directed edges of the digraph.* □

- undirected *if the adjacency matrix is symmetric, i.e., $g_{ik} = g_{ki}$ for all $i, k \in \mathcal{V}$.*

Lemma 2.2.2 *([48]) Consider an $n \times n$ symmetric matrix $A = \{a_{ik}\}$ satisfying $\sum_{i=1}^{n} a_{ik} = 0$ for each $k \in \{1, 2, \ldots, n\}$. The following statements hold:*

(i) There exists an orthogonal matrix U such that

$$U^\top A U = \begin{bmatrix} 0 & 0 \\ 0 & \star \end{bmatrix} \tag{2.8}$$

where $\star$ represents any nonsingular matrix with an appropriate dimension and 0 represents any zero matrix with an appropriate dimension.

(ii) The matrix A has a zero eigenvalue with eigenvector $\mathbf{1}_n \in \mathbb{R}^n$.

Let the digraph be strongly connected and $\lambda_1 \leq \lambda_2 \leq \cdots \leq \lambda_N$ be the eigenvalues of $\mathcal{L}$.[1] Then, $\lambda_1 = 0$ is a simple eigenvalue of $\mathcal{L}$ associated with the eigenvector 1_N; $\mathcal{L}$ is positive semi-definite and, therefore, there exists an orthonormal matrix $\Psi \in \mathbb{R}^{N\times N}$ such that $\Psi\mathcal{L}\Psi^\top = \mathrm{diag}(\lambda_1, \lambda_2, \ldots, \lambda_N)$.

If the digraph is symmetric, let $\widetilde{\Psi} = (\psi_2, \psi_3, \ldots, \psi_N) \in \mathbb{R}^{N\times N-1}$ with $\psi_i = (\psi_{i1}, \psi_{i2}, \ldots, \psi_{iN})$ being the orthonormal eigenvector corresponding to the nonzero eigenvalue λ_i, $i \in \{2, 3, \ldots, N\}$, which satisfies $\sum_{k=1}^{N} \psi_{ik} = 0$. Moreover, $\widetilde{\Psi}$ satisfies the following:

$$\widetilde{\Psi}\widetilde{\Psi}^\top = \frac{1}{N}\begin{bmatrix} N-1 & -1 & \ldots & -1 \\ -1 & N-1 & \ldots & -1 \\ \vdots & \vdots & \ddots & \vdots \\ -1 & -1 & \ldots & N-1 \end{bmatrix} =: U \tag{2.9}$$

$\widetilde{\Psi}^\top\widetilde{\Psi} = I$, $U^2 = U$, $\Lambda := \widetilde{\Psi}^\top\mathcal{L}\widetilde{\Psi} = \mathrm{diag}(\lambda_2, \lambda_3, \ldots, \lambda_N)$. Note that $\widetilde{\Psi}$ has smaller dimension than Ψ, namely, $\widetilde{\Psi}$ does not contain the eigenvector associated to the zero eigenvalue of the Laplacian.

[1] See [48] for more information on algebraic graph theory.

Part I

Synchronization and Consensus in Networks with Intermittent Communication

Chapter 3

A Hybrid Consensus Protocol for Pointwise Exponential Stability

3.1 Introduction

This chapter deals with the problem of consensus of first-order integrator systems communicating at stochastically determined time instances over a network. The consensus problem studied here consists of designing a protocol guaranteeing that the state of each agent converges to a common value by only using intermittent information from their neighbors. To solve this problem, we design hybrid state-feedback protocols that undergo an instantaneous change in their states when new information is available, and evolves continuously between such events. Due to the combination of continuous and impulsive dynamics, we use hybrid systems theory to model the interconnected systems, the controller, and the network topologies as well as to design the protocols, for which, we apply a Lyapunov theorem for asymptotic stability of sets for hybrid systems. Aside from asymptotic stability, we specify the point to which the consensus states converge to and, when the communications graph is strongly connected and

weight balanced, write it as a function of their initial conditions. We show that a diagonal-like set is, in fact, partially pointwise globally exponentially stable, which is a stronger notion than typical notions of asymptotic stability due to the additional requirement that each point in the set is Lyapunov stable; see e.g. [29] and [30] for similar notions. Furthermore, we show that the consensus condition is robust to a class of perturbations on the information. Finally, we give some brief insight into modeling and an asymptotic stability result for the case when information may arrive at asynchronous events for each agent.

The remainder of this chapter is organized as follows. Section 3.2 introduces the consensus problem, impulsive network model, and the control structure. In Section 3.3, a hybrid protocol and the main results for the case of synchronous communication are presented.

3.2 Consensus using Intermittent Information

In this article, we consider a network of N agents, each of which has scalar integrator dynamics given by

$$\dot{x}_i = u_i \in \mathbb{R} \qquad i \in \mathcal{V} := \{1, 2, \ldots, N\} \tag{3.1}$$

and exchanges information over a digraph $\Gamma = (\mathcal{V}, \mathcal{E}, \mathcal{G})$, where x_i is the state and u_i is the control input of the i-th agent. Our goal is to design a control protocol (or feedback controller) assigning the input u_i to drive the solutions of each agent to a common constant value, i.e., reach consensus. In particular, we are interested in the following asymptotic convergence property of the states x_i converging to each other. Such a property is typically referred to as static consensus; see [6, 7].

Definition 3.2.1 (static consensus) *Given the agents in* (3.1) *over a digraph* Γ*, a control protocol* u_i *is said to solve the consensus problem if every resulting maximal solution with* $u =$

$(u_1, u_2, \ldots, u_N)$ is complete and $t \mapsto (x_1(t), x_2(t), \ldots, x_N(t))$ satisfies

$$\lim_{t\to\infty} |x_i(t) - x_k(t)| = 0$$

for each $i, k \in \mathcal{V}$, $i \neq k$. □

Under certain connectivity assumptions, when each agent can communicate to its neighbors continuously, the distributed control law given by

$$u_i = -\gamma \sum_{k\in\mathcal{N}(i)} (x_i - x_k) \tag{3.2}$$

drives each agent in (3.1) to the average of the agents' initial conditions, [10]. The closed-loop interconnection of (3.1) with (3.2) can be written in compact form as

$$\dot{x} = -\gamma\mathcal{L}x$$

where $x = (x_1, x_2, \ldots, x_N)$ is the state and $\mathcal{L}$ is the Laplacian matrix of Γ. However, we are interested in the case when communication between agents occur at possibly nonperiodic isolated time instances, i.e., intermittently. For such a case, the control law in (3.2) is not an appropriate choice since the neighboring states, x_k, to the i-th agent are not available when communication has not occurred. Next, we outline the specific intermittent communication scheme we consider in this paper.

We allow the state of each system to be available to its neighors only at isolated time instances. Each i-th agent accesses the state information from its k-th neighbors at time instances $t \in \{t_s^i\}_{s=1}^{\infty}$, where $s \in \mathbb{N} \setminus \{0\}$ is the communication event index. The sequence of times $\{t_s^i\}_{s=1}^{\infty}$ may not necessarily be known to the agents, however, it must satisfy some constraints. Namely, given positive numbers $T_2 \geq T_1$, we assume that the time elapsed between

such communication events for each i-th system satisfies

$$\begin{aligned} &T_1^i \leq t_{s+1}^i - t_s^i \leq T_2^i \qquad\qquad \forall\, s \in \{1, 2, \dots\} \\ &t_1^i \leq T_2^i \end{aligned} \tag{3.3}$$

where the positive scalars T_1^i and T_2^i define the lower and upper bounds, respectively, of the time allowed to elapse between consecutive transmission instances to agent i. Note that, for each $i \in \mathcal{V}$, the bounds T_1^i and T_2^i are assumed to be known, independently determined and uncorrelated, but not necessarily the same for each agent. Due to the nonperiodic arrival of information and impulsive dynamics, classical analysis tools (for continuous-time or discrete-time systems) do not apply to the design of the proposed controller. This motivates us to design the proposed controller by recasting the interconnected systems, the impulsive network, and such a control protocol in a hybrid system framework; specifically, the one given in [28].

Remark 3.2.2 *From the communication time law in* (3.3)*, it is possible that such times are stochastically driven. Namely, the sequences of time governing communications between the agents* $\{t_s^i\}_{s=1}^{\infty}$ *satisfying* (3.3) *can be governed by a bounded random variable. For example, a continuous uniform random variable* Ω_i *can be used where* Ω_i *takes values in the interval* $[T_1^i, T_2^i]$ *and* $t_{s+1}^i - t_s^i = \Omega_i$ *for each agent index* $i \in \mathcal{V}$ *and integer* $s > 1$.

In Section 3.3, we present sufficient conditions for the asymptotic convergence to synchronization for each agent when communication between agents occur asynchronously across the edges between them, namely, the scenario described above. Before that, in the next section, we present sufficient conditions for partial pointwise global exponential stability of the synchronization configuration when all agents communicate synchronously. Namely, the next section considers the case when the sequence of times $\{t_s^i\}_{s=1}^{\infty}$ satisfying (3.3) are equal for each $i \in \mathcal{V}$, i.e., there exists positive scalars T_1 and T_2 satisfying $T_1 \leq T_2$ such that the sequence of times $\{t_s\}_{s=1}^{\infty}$ satisfies $t_{s+1} - t_s \in [T_1, T_2]$ for each s and $t_1 \leq T_2$.

3.3 Pointwise Asymptotic Stability through Synchronous Communication

3.3.1 Hybrid Modeling

We propose a hybrid control algorithm for the consensus of agents with dynamics given by (3.1) over networks where information is synchronously transmitted between the agents satisfying (3.3). Namely, this section considers the sequence of times $\{t_s^i\}_{s=1}^{\infty}$ satisfying (3.3) to be equal for each $i \in \mathcal{V}$. Namely, there exists positive scalars T_1 and T_2 satisfying $0 < T_1 \leq T_2$ such that the sequence of times $\{t_s\}_{s=1}$ satisfies $t_{s+1} - t_s \in [T_1, T_2]$ and $t_1 \leq T_2$. To this end, a hybrid timer can be used to trigger the transmission between the agents in the network; namely, we consider a decreasing timer with state $\tau \in [0, T_2]$ that when reaching zero resets to a point in the interval $[T_1, T_2]$. More specifically, the timer τ can be defined by the following hybrid system

$$\begin{aligned} \dot{\tau} &= -1 & \tau &\in [0, T_2] \\ \tau^+ &\in [T_1, T_2] & \tau &= 0 \end{aligned} \tag{3.4}$$

For the i-th agent, the proposed control protocol assigns a value to u_i based on the measured output of the neighboring agents obtained at the isolated communication events.

Protocol 3.3.1 *Given parameter T_2 of the network, the i-th hybrid controller has state η_i with the following dynamics:*

$$\begin{aligned} u_i &= \eta_i \\ \dot{\eta}_i &= h\eta_i & \tau &\in [0, T_2] \\ \eta_i^+ &= -\gamma \sum_{k \in \mathcal{N}(i)} (x_i - x_k) & \tau &= 0 \end{aligned} \tag{3.5}$$

where $h \in \mathbb{R}$ and $\gamma > 0$ is the controller gain parameter.

Using Protocol 3.3.1, we consider the interconnected state-feedback networked system resulting from the agent dynamics in (3.1) and a nonperiodic decreasing timer to model the communication times. We denote such interconnection as $\mathcal{H}$. The state of $\mathcal{H}$ is given by $\xi = (x, \eta, \tau) \in \mathbb{R}^N \times \mathbb{R}^N \times [0, T_2] =: \mathcal{X}$, where $x = (x_1, x_2, \ldots, x_N)$ and $\eta = (\eta_1, \eta_2, \ldots, \eta_N)$ comprise the agents' system states and controller states, respectively. By combining the agents' continuous dynamics in (3.1), the timer's hybrid dynamics in (3.4), and the protocol in (3.5), we arrive to the hybrid system $\mathcal{H}$ given by

$$\begin{aligned} \dot{\xi} &= \begin{bmatrix} \eta \\ h\eta \\ -1 \end{bmatrix} =: f(\xi) \qquad && \xi \in C := \mathcal{X}, \\ \xi^+ &\in \begin{bmatrix} x \\ -\gamma \mathcal{L} x \\ [T_1, T_2] \end{bmatrix} =: G(\xi) \qquad && \xi \in D := \mathbb{R}^N \times \mathbb{R}^N \times \{0\}. \end{aligned} \tag{3.6}$$

3.3.2 Properties of maximal solutions

A solution ϕ to a general hybrid system $\mathcal{H}$ in (2.1) is parametrized by $(t, j) \in \mathbb{R}_{\geq 0} \times \mathbb{N}$, where t denotes ordinary time and j denotes jump time. The domain dom $\phi \subset \mathbb{R}_{\geq 0} \times \mathbb{N}$ is a hybrid time domain if for every $(T, J) \in$ dom ϕ, the set dom $\phi \cap ([0, T] \times \{0, 1, \ldots, J\})$ can be written as the union of sets $\bigcup_{j=0}^{J} (I_j \times \{j\})$, where $I_j := [t_j, t_{j+1}]$ for a time sequence $0 = t_0 \leq t_1 \leq t_2 \leq \cdots \leq t_{J+1}$. The t_j's with $j > 0$ define the time instants when the state of the hybrid system jumps and j counts the number of jumps. The set $\mathcal{S}_{\mathcal{H}}$ contains all maximal solutions to $\mathcal{H}$, and the set $\mathcal{S}_{\mathcal{H}}(\xi_0)$ contains all maximal solutions to $\mathcal{H}$ from ξ_0. A solution to $\mathcal{H}$ is called maximal if it cannot be extended, i.e., it is not a truncated version of another solution. It is called complete if its domain is unbounded. A solution is Zeno if it is complete and its domain is bounded in the t direction. A solution is precompact if it is complete and bounded.

With the definition of solutions above, we have the following results.

Lemma 3.3.2 *Let $0 < T_1 \leq T_2$ be given for all $i \in \mathcal{V}$. Every maximal solution $\phi \in \mathcal{S}_H$ satisfies the following:*

1. *ϕ is complete, i.e., $\operatorname{dom}\phi$ is unbounded.*

2. *for each $(t, j) \in \operatorname{dom}\phi$,*

$$(j-1)T_1 \leq t \leq (j+1)T_2 \tag{3.7}$$

for all $j \geq 1$.

Proof Given the hybrid system $\mathcal{H}$ with $0 < T_1 \leq T_2$, we first show completeness of solutions. Note that for any $\xi \in C \setminus D$, we have that the tangent cone[1] $\mathbb{T}_C(\xi) \cap f(\xi) \neq \emptyset$. Moreover, when $\xi \in C \cap D$, solutions cannot be extended via flow. Due to the fact that the flow map is linear, finite escape time during flows is impossible. Lastly, it is straightforward to check that $G(D) \subset C \cup D$. Therefore, by [28, Proposition 6.10], every maximal solution to $\mathcal{H}$ is complete.

Next, we will show item 2). Due to the dynamics of τ, the jump times satisfy (3.3). Therefore, it is straight forward to see that for every $(t, j) \in \operatorname{dom}\phi$, $(j-1)T_1 \leq t \leq (j+1)T_2$.

■

Our goal is to show that Protocol 3.3.1 not only guarantees the static consensus property in Definition 3.2.1 with an exponential decay rate, but also renders Lyapunov stable the set of points such that $x_i = x_k$ for all $i, k \in \mathcal{V}$. To this end, we define the set to exponentially stabilize as

$$\mathcal{A} := \{\xi \in \mathcal{X} : x_i = x_k, \eta_i = 0 \ \forall i, k \in \mathcal{V}, \tau \in [0, T_2]\}. \tag{3.8}$$

[1]The tangent cone to a set $S \subset \mathbb{R}^n$ at a point $x \in \mathbb{R}^N$, is the set of all vectors $w \in \mathbb{R}^N$ for which there exists $x_i \in S$, $\tau_i > 0$ with $x_i \to x$, $\tau_i \searrow 0$, and $w = \lim_{i\to\infty} \frac{x_i - x}{\tau_i}$; see [28, Definition 5.12] for more information.

3.3.3 Coordinate change

We establish exponential stability by changing to coordinates obtained through a key property of the Laplacian matrix. More precisely, let Γ be a strongly connected digraph. The associated Laplacian $\mathcal{L}$ is such that there exists a nonsingular matrix $U = [v_1, U_1]$ such that $U^\top \mathcal{L} U = \begin{bmatrix} 0 & 0 \\ 0 & \bar{\mathcal{L}} \end{bmatrix}$, which is a diagonal matrix containing the eigenvalues of $\mathcal{L}$, where $\bar{\mathcal{L}}$ is a diagonal matrix with diagonal elements $(\lambda_2, \lambda_3, \ldots, \lambda_N)$ with λ_i's being the positive eigenvalues of $\mathcal{L}$. Then, we change the coordinates ξ of $\mathcal{H}$ to the new coordinates χ defined using $\bar{x} = U^\top x$ and $\bar{\eta} = U^\top \eta$. By applying the transformation to both sides of the continuous dynamics of the state x and η of $\mathcal{H}$ in (3.6), we have

$$\begin{aligned} \dot{\bar{x}} &= U^\top \dot{x} = U^\top \eta = \bar{\eta} \\ \dot{\bar{\eta}} &= U^\top \dot{\eta} = 0. \end{aligned} \tag{3.9}$$

During jumps, the difference equations of the states x and η of $\mathcal{H}$ in (3.6) become

$$\begin{aligned} \bar{x}^+ &= U^\top x^+ = U^\top x = \bar{x} \\ \bar{\eta}^+ &= -\gamma U^\top \mathcal{L} x = -\gamma U^\top \mathcal{L} U \bar{x} = -\gamma \begin{bmatrix} 0 & 0 \\ 0 & \bar{\mathcal{L}} \end{bmatrix} \bar{x} \end{aligned}$$

Then, the new coordinates denoted by χ are defined by collecting the scalar states $\bar{x}_1$ and $\bar{\eta}_1$ into $\bar{z}_1 = (\bar{x}_1, \bar{\eta}_1)$ and the remaining states of $\bar{x}$ and $\bar{\eta}$ into $\bar{z}_2 = (\bar{x}_2, \bar{x}_3, \ldots, \bar{x}_N, \bar{\eta}_2, \bar{\eta}_3, \ldots, \bar{\eta}_N)$, so as to write χ as $\chi = (\bar{z}_1, \bar{z}_2, \tau) \in \mathcal{X}$. The new coordinates lead to a hybrid system denoted

as $\widetilde{\mathcal{H}}$ with the following data:

$$\begin{aligned} \tilde{f}(\chi) &:= \begin{bmatrix} A_{f1}\bar{z}_1 \\ A_{f2}\bar{z}_2 \\ -1 \end{bmatrix} \qquad \forall \chi \in \widetilde{C} := \mathcal{X} \\ \widetilde{G}(\chi) &:= \begin{bmatrix} A_{g1}\bar{z}_1 \\ A_{g2}\bar{z}_2 \\ [T_1, T_2] \end{bmatrix} \qquad \forall \chi \in \widetilde{D} := \{\chi \in \mathcal{X} : \tau = 0\} \end{aligned} \tag{3.10}$$

where

$$\begin{aligned} A_{f1} &= \begin{bmatrix} 0 & 1 \\ 0 & h \end{bmatrix}, A_{g1} = \begin{bmatrix} 1 & 0 \\ 0 & 0 \end{bmatrix}, \\ A_{f2} &= \begin{bmatrix} 0 & I \\ 0 & hI \end{bmatrix}, A_{g2} = \begin{bmatrix} I & 0 \\ -\gamma\bar{\mathcal{L}} & 0 \end{bmatrix} \end{aligned} \tag{3.11}$$

and $\gamma > 0$. Moreover, in the new coordinates, the set to stabilize for the hybrid system $\widetilde{\mathcal{H}}$ in (3.10) is defined as

$$\widetilde{\mathcal{A}} := \{(\bar{z}_1, \bar{z}_2, \tau) \in \mathcal{X} : \bar{z}_1 = (x^*, 0), x^* \in \mathbb{R}, \bar{z}_2 = 0\}. \tag{3.12}$$

3.3.4 Basic properties and equivalencies of $\mathcal{H}$ and $\widetilde{\mathcal{H}}$

Lemma 3.3.3 *The hybrid systems $\mathcal{H}$ and $\widetilde{\mathcal{H}}$ satisfy the hybrid basic conditions.*

Proof The jump and flow sets of both systems are closed. The flow maps $\widetilde{f}$ and f are continuous. The jump map $\widetilde{G}$ is outer semicontinuous since its graph $\{(x, y) : x \in \widetilde{D}, y \in \widetilde{G}(x)\}$ since the interval $[T_1, T_2]$ is closed. Furthermore, $\widetilde{G}$ is bounded and nonempty for each $x \in \widetilde{D}$. Similar arguments show the same property for G. ■

Next, we show that global exponential stability of $\widetilde{\mathcal{A}}$ for $\widetilde{\mathcal{H}}$ is a necessary and sufficient

condition for global exponential stability of $\mathcal{A}$ for $\mathcal{H}$.

Lemma 3.3.4 *Given $0 < T_1 \leq T_2$ and a strongly connected digraph, the set $\widetilde{\mathcal{A}}$ is GES for the hybrid system $\widetilde{\mathcal{H}}$ if and only if $\mathcal{A}$ is GES for the hybrid system $\mathcal{H}$.*

Proof First, we show the necessity of the claim. Pick a point $z^* = (\bar{x}_1^*, \bar{\eta}_1^*, \bar{x}^*, \bar{\eta}^*) \in \mathbb{R}^{2N}$, such that $(z^*, \tau^*) \in \widetilde{\mathcal{A}}$. Then, there exists $x^* \in \mathbb{R}$ such that $z^* = (x^*, 0, \mathbf{0}_{N-1}, \mathbf{0}_{N-1})$. In light of the properties of Laplacian matrices in Section 2.1 and with the assumption that the digraph is strongly connected, it follows that zero is a simple eigenvalue of the Laplacian with associated eigenvector $v_1 = \frac{1}{\sqrt{N}}\mathbf{1}_N$. Then, there exists a nonsingular matrix $U = [v_1 \ U_1]$ such that $U^\top \mathcal{L} U = \begin{bmatrix} 0 & 0 \\ 0 & \mathcal{L} \end{bmatrix}$ which leads to the coordinate change $\bar{x} = U^\top x$ and $\bar{\eta} = U^\top \eta$. From z^* above, premultiplying the aforementioned expressions by U leads to

$$x = U \begin{bmatrix} \bar{x}_1^* & \bar{x}^{*\top} \end{bmatrix}^\top = [v_1 \ U_1] \begin{bmatrix} x^* & \mathbf{0}_{N-1}^\top \end{bmatrix}^\top = x^* \mathbf{1}_N, \tag{3.13}$$

and

$$\eta = U \begin{bmatrix} \bar{\eta}_1^* & \bar{\eta}^{*\top} \end{bmatrix}^\top = [v_1 \ U_1] \begin{bmatrix} 0 & \mathbf{0}_{N-1}^\top \end{bmatrix}^\top = \mathbf{0}_N. \tag{3.14}$$

Since $x = x^* \mathbf{1}_N$ corresponds to $x_i = x^*$ for each $i \in \mathcal{V}$, we have $x_i = x_k$ for each $i, k \in \mathcal{V}$. Therefore, since τ^* does not change among the two coordinates, the point $(x, \eta, \tau) = (x^* \mathbf{1}_N, \mathbf{0}_N, \tau)$ belongs to the set $\mathcal{A}$.

To show sufficiency, pick a point $\tilde{z} = (\tilde{x}, \tilde{\eta}) \in \mathbb{R}^{2N}$ such that $\tilde{z}, \tilde{\tau}) \in \mathcal{A}$. For a point to be in $\mathcal{A}$ then it must satisfy $\tilde{x}_i = \tilde{x}_k = \tilde{x}^*$ and $\eta_i = 0$ for each $i, k \in \mathcal{V}$ for some $\tilde{x}^* \in \mathbb{R}$. Then, we have that $\tilde{z} = (x^* \mathbf{1}_N, \mathbf{0}_N)$. Then, in light of the equivalences (3.13), (3.14) we have that $x^* U^\top \mathbf{1}_N = \begin{bmatrix} x^* & \mathbf{0}_{N-1}^\top \end{bmatrix}^\top$, and naturally $\bar{\eta} = U \mathbf{0}_N = \mathbf{0}_N$. Therefore, the point $(x^*, 0, \mathbf{0}_{N-1}, \mathbf{0}_{N-1})$ belongs to $\widetilde{\mathcal{A}}$.

It remains to show the equivalence of $\mathcal{A}$ being globally exponentially stable for the

hybrid system $\mathcal{H}$ and $\widetilde{\mathcal{A}}$ being globally exponentially stable for $\widetilde{\mathcal{H}}$. This is no more than utilizing Definition 2.1.4 and the change of coordinates $\bar{x} = U^\top x$ and $\bar{\eta} = U^\top \eta$. Then, it is clear that if a solution to $\mathcal{H}$ is bounded by an exponential function then a change of coordinates would result in a similar exponential bound for a solution to $\widetilde{\mathcal{H}}$. The reverse direction can be proved similarly. ■

In this section, we consider the exponential stability of the set $\widetilde{\mathcal{A}}$ for the hybrid system $\widetilde{\mathcal{H}}$. Inspired by [49] and using Lemma 3.3.4, we have the following stability result for $\mathcal{H}$.

Proposition 3.3.5 *Let T_1 and T_2 be two positive scalars satisfying $T_1 \leq T_2$. Let the digraph be strongly connected. The set $\widetilde{\mathcal{A}}$ is globally exponentially stable for the hybrid system $\widetilde{\mathcal{H}}$ if there exist scalars $\gamma > 0$ and $h \in \mathbb{R}$, and a positive definite symmetric matrix P satisfying*

$$A_{g2}^\top \exp(A_{f2}^\top \nu) P \exp(A_{f2}\nu) A_{g2} - P < 0 \tag{3.15}$$

for all $\nu \in [T_1, T_2]$. Namely, every solution ϕ to $\widetilde{\mathcal{H}}$ satisfies

$$|\phi(t,j)|_{\widetilde{\mathcal{A}}} \leq \exp\left(\frac{R}{2}\right)\sqrt{\frac{\alpha_2}{\alpha_1}} \exp\left(-\frac{\alpha}{2}(t+j)\right) |\phi(0,0)|_{\widetilde{\mathcal{A}}} \tag{3.16}$$

for all $(t,j) \in \operatorname{dom}\phi$ where $\alpha \in \left(0, \frac{|\lambda_d|}{1+T_2}\right]$, $R \in \left[\frac{T_2|\lambda_d|}{1+T_2}, \infty\right)$, β can be chosen arbitrarily small such that $\lambda_d = \ln\left(1 - \frac{\beta}{\alpha_2}\right) < 0$, and

$$\begin{aligned} \alpha_1 &= \min_{s\in[0,T_2]} \left\{\exp(2hs),\ \lambda_{\min}\left(\exp(A_{f2}^\top s) P \exp(A_{f2} s)\right)\right\} \\ \alpha_2 &= \max_{s\in[0,T_2]} \left\{\exp(2hs),\ \lambda_{\max}\left(\exp(A_{f2}^\top s) P \exp(A_{f2} s)\right)\right\}. \end{aligned} \tag{3.17}$$

Proof Consider the condidate Lyapunov function

$$V(\chi) = V_1(\chi) + V_2(\chi) \tag{3.18}$$

where $V_1(\chi) = \exp(2h\tau)\bar{\eta}_1^2$, and $V_2(\chi) = \bar{z}_2^\top \exp(A_{f2}^\top \tau) P \exp(A_{f2}\tau)\bar{z}_2$ where the matrix P is symmetric and positive definite; i.e., $P = P^\top > 0$. Note that, for each $\chi \in \widetilde{\mathcal{A}}$, $V(\chi) = 0$ and

$V(\chi) > 0$ for each $\chi \in (\widetilde{C} \cup \widetilde{D}) \setminus \widetilde{\mathcal{A}}$. From the definition of $\widetilde{\mathcal{A}}$, we have $|\chi|^2_{\widetilde{\mathcal{A}}}$ reduces to $\bar{\eta}_1^2 + \bar{z}_2^\top \bar{z}_2$. Then, it follows that V satisfies

$$\alpha_1 |\chi|^2_{\widetilde{\mathcal{A}}} \leq V(\chi) \leq \alpha_2 |\chi|^2_{\widetilde{\mathcal{A}}} \tag{3.19}$$

for all $\chi \in \mathcal{X}$ where α_1 and α_2 are defined in (3.17).

Then, for each $\chi \in \widetilde{C}$, we have that

$$\langle \nabla V_1(\chi), \widetilde{f}(\chi) \rangle = 2h \exp(2h\tau)\bar{\eta}_1^2 - 2h \exp(2h\tau)\bar{\eta}_1^2 = 0$$

and

$$\langle \nabla V_2(\chi), \widetilde{f}(\chi) \rangle = 2\bar{z}_2^\top A_{f2}^\top \exp(A_{f2}^\top \tau) P \exp(A_{f2}\tau)\bar{z}_2 - 2\bar{z}_2^\top A_{f2}^\top \exp(A_{f2}^\top \tau) P \exp(A_{f2}\tau)\bar{z}_2 = 0$$

where we use the fact that the matrices A_{f2} and $\exp(A_{f2}\tau)$ commutes. Then, we have that V satisfies

$$\langle \nabla V(\chi), \widetilde{f}(\chi) \rangle = \langle \nabla V_1(\chi), \widetilde{f}(\chi) \rangle + \langle \nabla V_2(\chi), \widetilde{f}(\chi) \rangle = 0. \tag{3.20}$$

For each $\chi \in \widetilde{D}$ (i.e., $\tau = 0$), after the jump there exists a scalar $\nu \in [T_1, T_2]$ to which τ is updated to, at such points the states $\bar{\eta}_1$ and $\bar{z}_2$ are updated to 0 and $A_{g2}\bar{z}_2$, respectively. For each $\chi \in \widetilde{D}, g \in \widetilde{G}(\chi)$, the update in $\bar{\eta}_1$ at jumps to zero leads to $V_1(g) - V_1(\chi) = -\bar{\eta}_1^2 \leq 0$ which implies that at such points V is given by

$$V(g) - V(\chi) = V_1(g) + V_2(g) - V_1(\chi) - V_2(\chi) \leq V_2(g) - V_2(\chi).$$

It follows that, for each $\chi \in \widetilde{D}, g \in \widetilde{G}(\chi)$, we have

$$\begin{aligned} V_2(g) - V_2(\chi) &\leq \bar{z}_2^\top A_{g2} \exp(A_{f2}^\top \nu) P \exp(A_{f2}\nu) A_{g2}\bar{z}_2 - \bar{z}_2^\top P \bar{z}_2 \\ &\leq -\frac{\beta}{\alpha_2} V(\chi), \end{aligned}$$

where we used the definition of β in (3.17) and the bounds in (4.19). Then, we define $\lambda_d = \ln(1-\beta/\alpha_2)$ which is assumed to be negative since β can be chosen to be arbitrarily small and positive. Then, $V(g) \leq \exp(\lambda_d)V(\chi)$ for each $\chi \in \widetilde{D}$, $g \in \widetilde{G}(\chi)$.

With a little more abuse of notation, consider a maximal solution $\phi = (\phi_1, \phi_2, \phi_\tau)$ to $\widetilde{\mathcal{H}}$ where ϕ_1 and ϕ_2 correspond to states $\bar{z}_1$ and $\bar{z}_2$, respectively. As shown in the proof of [28, Proposition 3.29], direct integration of $(t,j) \mapsto V(\phi(t,j))$ over $\operatorname{dom}\phi$ leads to $V(\phi(t,j)) \leq \exp(\lambda_d j)V(\phi(0,0))$ for each $(t,j) \in \operatorname{dom}\phi$.

Pick $\alpha \in \left(0, \frac{|\lambda_d|}{1+T_2}\right]$ and $R \in \left[\frac{T_2|\lambda_d|}{1+T_2}, \infty\right)$. In light of Lemma 3.3.2, it follows that $\lambda_d j \leq R - \alpha(t+j)$ for all $(t,j) \in \operatorname{dom}\phi$ which leads to (3.16). Furthermore, since all maximal solutions are complete, we have that the set $\widetilde{\mathcal{A}}$ is GES for the system $\widetilde{\mathcal{H}}$ in (3.10) and from Lemma 3.3.4 $\mathcal{A}$ in (3.8) is GES for $\mathcal{H}$ in (3.6). ■

Corollary 3.3.6 *Let T_1 and T_2 be two positive scalars satisfying $T_1 \leq T_2$ be given and the digraph be completely connected. If there exist scalars $\gamma > 0$ and $h \in \mathbb{R}$, and a positive definite symmetric matrix P satisfying*

$$\tilde{A}_g^\top \exp(\tilde{A}_f^\top \nu) P \exp(\tilde{A}_f \nu) \tilde{A}_g - P < 0$$

for all $\nu \in [T_1, T_2]$ where

$$\tilde{A}_f = \begin{bmatrix} 0 & 1 \\ 0 & h \end{bmatrix}, \qquad \tilde{A}_g = \begin{bmatrix} 1 & 0 \\ -\gamma N & 0 \end{bmatrix}, \tag{3.21}$$

then the set $\widetilde{\mathcal{A}}$ is globally exponentially stable for $\widetilde{\mathcal{H}}$.

Proof Using the change of coordinates in (3.9), the result follows from the proof of Proposition 3.3.5, where, for a completely connected network $\bar{\mathcal{L}} = NI_{N-1}$. ■

Remark 3.3.7 *Proposition 3.3.5 holds under a weaker condition of existence of a spanning tree*

in the directed graph. Namely, a spanning tree exists if there exists a root agent in the graph such that all other agents are a child of the root. The root agent is commonly referred to as a leader, while its children are called followers.

Remark 3.3.8 *The condition* (3.15) *may be difficult to satisfy numerically. In fact, these conditions are not convex in* γ*,* h *and* P*, and need to be verified for infinitely many values of* ν*. In [50], the authors use a polytopic embedding strategy to arrive to a linear matrix inequality in which one needs to find some matrices* X_i *such that the exponential matrix is an element in the convex hull of the* X_i *matrices. Those results can be adapted to our setting.* □

Condition (3.15) has a form that is similar to the discrete Lyapunov equation $A^\top PA - P < 0$. Namely, if there exists a $P = P^\top > 0$ matrix such that $A^\top PA - P < 0$ is satisfied, then the eigenvalues of A are contained within the unit circle. Using this principle, the following result gives a sufficient condition to satisfy the matrix inequality in (3.15).

Proposition 3.3.9 *Given* $0 < T_1 \leq T_2$ *and a strongly connected digraph* Γ*, there exists* $\gamma > 0$ *and* $h \in \mathbb{R}$ *satisfying*

$$\left| \frac{\lambda_N \gamma(\exp(hT_2) - 1)}{h} - 1 \right| < 1 \tag{3.22}$$

where λ_N *is the largest eigenvalue of* $\mathcal{L}$*, if and only if there exists* $P = P^\top > 0$ *such that* (3.15) *holds.*

Proof Since P is positive definite and satisfies (3.15), then the spectral radius[2]. Due to the form of A_{f2} and A_{g2}, it follows that

$$\exp(A_{f2}\nu)A_{g2} = \begin{bmatrix} I - \frac{\gamma(\exp(h\nu)-1)}{h}\bar{\mathcal{L}} & 0 \\ -\frac{\gamma \exp(h\nu)}{h}\bar{\mathcal{L}} & 0 \end{bmatrix} =: \widetilde{A} \tag{3.23}$$

[2]The spectral radius of a matrix M is $\max\{|\lambda_1|, |\lambda_2|, \ldots, |\lambda_N|\}$ of $\exp(A_{f2}\nu)A_{g2}$ is less than 1 for each $\nu \in [0, T]$, where λ_i is the i-th eigenvalue of M.

which is a block diagonal matrix. Due the form of $\widetilde{A}$, its associated eigenvalues are $\{0\}$ with a multiplicity of $N-1$ and the eigenvalues of the $(1,1)$ block therein. Note that since Γ is strongly connected, the eigenvalues λ_i of the Laplacian are such that $0 = \lambda_1 < \lambda_2 < \lambda_3 < \cdots < \lambda_N$ and the diagonal matrix $\bar{\mathcal{L}} = \mathrm{diag}(\lambda_2, \lambda_2, \ldots, \lambda_N)$. Therefore, the $(1,1)$ block of $\widetilde{A}$ is diagonal which implies that the eigenvalues of this block matrix of $\widetilde{A}$ are $\mu_{i-1} = \frac{\gamma(\exp(h\tau)-1)}{h}\lambda_i - 1$ for each $i \in \{2, \ldots, N\}$. Therefore, we have that

$$\max_{i\in\{2,\ldots,N\}} |\mu_{i-1}| \leq \left| \frac{\lambda_i \gamma(\exp(h\nu) - 1)}{h} - 1 \right| \tag{3.24}$$

$$\leq \left| \frac{\lambda_N \gamma(\exp(hT_2) - 1)}{h} - 1 \right| < 1 \tag{3.25}$$

from (3.23) which concludes the proof. ■

Remark 3.3.10 *Moreover, if $h = 0$, and the digraph $\Gamma = (\mathcal{V}, \mathcal{E}, \mathcal{G})$ is strongly connected, if one picks γ such that $\gamma < 2/(\lambda_N T_2)$, then it is guaranteed that there exists a positive definite symmetric matrix P such that condition* (3.15) *is satisfied.* □

3.3.5 Consensus Convergent Point

The following result characterizes the point to which solutions to $\mathcal{H}$ converge to.

Proposition 3.3.11 *Let the scalars T_1 and T_2 satisfy $0 < T_1 \leq T_2$ and let the digraph Γ be strongly connected and weight balanced. If γ and h are chosen such that $\mathcal{A}$ is GES for $\mathcal{H}$, then every solution $\phi = (\phi_x, \phi_\eta, \phi_\tau) \in \mathcal{S}_{\mathcal{H}}(\phi(0,0))$ is complete and each i-th component of ϕ_x and ϕ_η, denoted as ϕ_{x_i} and ϕ_{η_i} for all $i \in \mathcal{V}$, respectively, satisfies $\lim_{t+j\to\infty} \phi_\eta(t,j) = 0$ and*

$$\lim_{t+j\to\infty} \phi_{x_i} = \frac{1}{N} \sum_{i=1}^{N} (\phi_{x_i}(0,0) + \phi_\tau(0,0)\phi_{\eta_i}(0,0)) \tag{3.26}$$

when $h = 0$, and when $h \neq 0$ it follows that

$$\lim_{t+j\to\infty} \phi_{x_i} = \frac{1}{N}\sum_{i=1}^{N}\left(\phi_{x_i}(0,0) + \frac{\exp(h\phi_\tau(0,0)) - 1}{h}\phi_{\eta_i}(0,0)\right). \tag{3.27}$$

Proof Let $\delta_x = \frac{1}{N}\sum_{i\in\mathcal{V}} x_i$ and $\delta_\eta = \sum_{i\in\mathcal{V}} \frac{1}{N}\eta_i$ be the average of the system states and controller states, respectively. For every $\tau \in [0, T_2]$, the dynamics of $(\delta_x, \delta_\eta, \tau)$ is given by

$$\dot{\delta}_x = \delta_\eta, \tag{3.28}$$

$$\dot{\delta}_\eta = h\delta_\eta, \tag{3.29}$$

$$\dot{\tau} = -1. \tag{3.30}$$

Since the digraph is weight balanced, we have $d^{in}(i) = d^{out}(i)$ for each $i \in \mathcal{V}$. At jumps, when $\tau = 0$, we have that $\delta_x^+ = \delta_x$ and δ_η is updated as follows:

$$\delta_\eta^+ = \frac{1}{N}\sum_{i\in\mathcal{V}}\left(-\gamma \sum_{k\in\mathcal{N}(i)}(x_i - x_k)\right) \tag{3.31}$$

$$= -\frac{\gamma}{N}\sum_{i\in\mathcal{V}}\left(\sum_{k\in\mathcal{N}(i)}(x_i - x_k)\right) = 0 \tag{3.32}$$

where we use the property of the strong connectivity and weight-balanced graph. Therefore, after the first jump δ_x remains constant and δ_η is reset to and stays at zero. Now, take a solution $\phi = (\phi_x, \phi_\eta, \phi_\tau) \in \mathcal{S}_\mathcal{H}(\phi_x(0,0), \phi_\eta(0,0), \phi_\tau(0,0))$ to $\mathcal{H}$. First, consider the case when $h = 0$. It follows that during flows for each component of ϕ_x and ϕ_η, denoted as ϕ_{x_i} and ϕ_{η_i} for each $i \in \mathcal{V}$, by direct integration of the x_i component is given as $\phi_{x_i}(t,0) = \phi_{x_i}(0,0) + \phi_{\eta_i}(0,0)t$ for each $t \in [0, t_1]$, where $t_1 = \phi_\tau(0,0)$. Due to the fact that the average value δ_x does not change after the first jump, we have that

$$\delta_x(\phi_\tau(0,0), 0) = \frac{1}{N}\sum_{i\in\mathcal{V}}\phi_{x_i}(\phi_\tau(0,0), 0) \tag{3.33}$$

$$= \frac{1}{N}\sum_{i\in\mathcal{V}}(\phi_{x_i}(0,0) + \phi_{\eta_i}(0,0)\phi_\tau(0,0)) \tag{3.34}$$

is also the average point for each $(t, j) \in \operatorname{dom}\phi$ such that $j \geq 1$. Furthermore, due to Lemma 3.3.4 and the Lyapunov analysis in the proof of Proposition 3.3.5, we know that $\mathcal{A}$ is GES for $\mathcal{H}$. Since δ_x is constant for all $j \geq 1$ and solutions to $\mathcal{H}$ converge to $\mathcal{A}$ exponentially, then we have that

$$\lim_{t+j\to\infty} \phi_{x_i}(t, j) = \frac{1}{N} \sum_{i\in\mathcal{V}} (\phi_{x_i}(0, 0) + \phi_{\eta_i}(0, 0)\phi_\tau(0, 0)) \tag{3.35}$$

for each $i \in \mathcal{V}$. Furthermore, at such points on $\mathcal{A}$, $\phi_\eta = \mathbf{0}_N$ which leads to the fact that $\lim_{t+j\to\infty} \phi_\eta(t, j) = \mathbf{0}_N$. For the case when $h \neq 0$, we have that direct integration of the continuous dynamics of (x_i, η_i) leads to $\phi_{x_i} = \phi_{x_i}(0, 0) + \frac{1}{h}(\exp(ht) - 1)\phi_{\eta_i}(0, 0)$ for each $t \in [0, t_1]$. Then, by following similar approach above, it follows that

$$\lim_{t+j\to\infty} \phi_{x_i}(t, j) = \left(\frac{1}{N} \sum_{i=1}^{N} \left(\phi_{x_i}(0, 0) + \frac{\exp(h\phi_\tau(0, 0)) - 1}{h} \phi_{\eta_i}(0, 0) \right) \right)$$

for each $i \in \mathcal{V}$ which concludes the proof. ■

3.3.6 Partial pointwise exponential stability for $\mathcal{H}$

Using the previous results, we can now give sufficient conditions for the set $\mathcal{A}$ to be partially pointwise globally exponentially stable with respect to (x, η) for $\mathcal{H}$. Namely, in addition to the set $\mathcal{A}$ begin exponentially attractive, each point in $\mathcal{A}$ is pointwise stable. The notion of partial pointwise exponential stability is given as follows.

Definition 3.3.12 *(partial pointwise global exponential stability) Consider a hybrid system $\mathcal{H}$ with state $\xi = (p, q) \in \mathbb{R}^n$. The closed set $\mathcal{A} \subset \mathbb{R}^r \times \mathbb{R}^{n-r}$ where $r \in \mathbb{N}$ and $0 < r \leq n$ is* partially pointwise global exponentially stable *with respect to the state component p for $\mathcal{H}$ if*

1) every maximal solution ϕ to $\mathcal{H}$ is complete and has a limit belonging to $\mathcal{A}$;

2) $\mathcal{A}$ is exponentially attractive for $\mathcal{H}$, namely, for each $\phi \in \mathcal{S}_\mathcal{H}$ there exist $\kappa, \alpha > 0$ such that

$|\phi(t,j)|_{\mathcal{A}} \leq \kappa e^{-\alpha(t+j)}|\phi(0,0)|_{\mathcal{A}}$ *for all* $(t,j) \in \operatorname{dom}\phi$*; and*

3) *for each* $p^* \in \mathbb{R}^r$ *such that there exists* $q \in \mathbb{R}^{n-r}$ *satisfying* $(p^*, q) \in \mathcal{A}$*, it follows that for each* $\varepsilon > 0$ *there exists* $\delta > 0$ *such that every solution* $\phi = (\phi_p, \phi_q)$ *to* $\mathcal{H}$ *with* $\phi_p(0,0) \in p^* + \delta\mathbb{B}$ *satisfies* $|\phi_p(t,j) - p^*| \leq \varepsilon$ *for all* $(t,j) \in \operatorname{dom}\phi$*.* □

Along with global exponential stability of $\mathcal{A}$ established in Proposition 3.3.5, partial pointwise global exponential stability requires that each point in the diagonal-like set $\mathcal{A}$ is stable with respect to (x, η).

Theorem 3.3.13 *Given* $0 < T_1 \leq T_2$ *and a weight balanced digraph* $\Gamma = (\mathcal{V}, \mathcal{E}, \mathcal{G})$*, suppose there exist scalars* $h \in \mathbb{R}$ *and* $\gamma > 0$ *and a positive definite symmetric matrix* P *such that* (3.15) *in Proposition 3.3.5 holds. Then, the set* $\mathcal{A}$ *is partially pointwise globally exponentially stable with respect to* (x, η) *for the hybrid system* $\mathcal{H}$*.*

Proof Items 1 and 2 in Definition 3.3.12 are satisfied according to Lemma 3.3.2 and Theorem 3.3.5, respectively. It remains to show item 3. Denote $\tilde{x} = x - x^*\mathbf{1}$ and $\tilde{\chi} = (\tilde{x}, \eta, \tau)$. We have

$$\begin{aligned} \dot{\tilde{\chi}} &= \begin{bmatrix} \eta \\ h\eta \\ -1 \end{bmatrix} && \tilde{\chi} \in \mathcal{X}, \\ \tilde{\chi}^+ &\in \begin{bmatrix} \tilde{x} \\ -\gamma\mathcal{L}\tilde{x} \\ [T_1, T_2] \end{bmatrix} && \tilde{\chi} \in \{\tilde{\chi} \in \mathcal{X} : \tau = 0\}. \end{aligned} \tag{3.36}$$

In these coordinates, the set to stabilize is $\widetilde{\mathcal{A}} = \{0_N\} \times \{0_N\} \times [T_1, T_2]$. Pick a function

$V(\tilde{\chi}) = \tilde{\chi}\exp(A_f^\top \tau)P\exp(A_f\tau)\tilde{\chi}$ where $A_f = \begin{bmatrix} 0 & I \\ 0 & hI \end{bmatrix}$ and $P = P^\top > 0$. Note that

$$\alpha_1|\tilde{\chi}|^2_{\tilde{\mathcal{A}}} \leq V(\tilde{\chi}) \leq \alpha_2|\tilde{\chi}|^2_{\tilde{\mathcal{A}}} \tag{3.37}$$

where $\alpha_1 = \min_{\tau\in[0,T_2]} \lambda_{\min}(\exp(A_f^\top \tau)P\exp(A_f\tau))$ and $\alpha_2 = \max_{\tau\in[0,T_2]} \lambda_{\max}(\exp(A_f^\top \tau)P\exp(A_f\tau))$. During flows, we have

$$\langle \nabla V(\tilde{\chi}), (\eta, h\eta, -1)\rangle = 0 \tag{3.38}$$

for all $\tilde{\chi} \in C$. Furthermore, for each $\tilde{\chi} \in D, g \in (\tilde{x}, -\gamma\mathcal{L}\tilde{x}, [T_1, T_2])$ we have that

$$V(g) - V(\tilde{\chi}) \leq 0, \tag{3.39}$$

namely, that $V(g) \leq V(\tilde{\chi})$. Pick a solution $\tilde{\phi} = (\tilde{\phi}_x, \tilde{\phi}_\eta, \tilde{\phi}_\tau)$ to $\mathcal{H}$ in (3.36). It follows from (3.38) and (3.39) that $V(\tilde{\phi}(t,j)) \leq V(\tilde{\phi}(0,0))$ for all $(t,j) \in \operatorname{dom}\phi$. It follows (3.37) that $\alpha_1|\tilde{\phi}(t,j)|^2_{\tilde{\mathcal{A}}} \leq V(\tilde{\phi}(t,j)) \leq V(\tilde{\phi}(0,0)) \leq \alpha_2|\tilde{\phi}(0,0)|^2_{\tilde{\mathcal{A}}}$. This implies that on the original coordinates, a solution $\phi = (\phi_x, \phi_\eta, \phi_\tau)$ to $\mathcal{H}$ in (3.6) is such that $\phi_x(t,j) = \tilde{\phi}_x(t,j) - x^*$ for all $(t,j)\operatorname{dom}\phi$ (note that $\operatorname{dom}\phi = \operatorname{dom}\tilde{\phi}$, $\tilde{\phi}_\eta = \phi_\eta$ and $\tilde{\phi}_\tau = \phi_\tau$) implying that

$$\begin{aligned}\left|\begin{bmatrix} \phi_x(t,j) - x^* \\ \phi_\eta(t,j) \\ \phi_\tau(t,j) \end{bmatrix}\right|_{\mathcal{A}} &= |\phi(t,j)|_{\tilde{\mathcal{A}}} \leq \sqrt{\frac{\alpha_2}{\alpha_1}}|\phi(0,0)|_{\mathcal{A}} \\ &= \sqrt{\frac{\alpha_2}{\alpha_1}}\left|\begin{bmatrix} \phi_x(0,0) - x^* \\ \phi_\eta(0,0) \\ \phi_\tau(0,0) \end{bmatrix}\right|_{\mathcal{A}}.\end{aligned}$$

Pick $\epsilon = \sqrt{\frac{\alpha_2}{\alpha_1}}\delta$. This implies that for $\left|\begin{bmatrix} \phi_x(0,0) - x^* \\ \phi_\eta(0,0) \\ \phi_\tau(0,0) \end{bmatrix}\right|_{\mathcal{A}} < \delta$ the solution is such that

$$\left|\begin{bmatrix} \phi_x(t,j) - x^* \\ \phi_\eta(t,j) \\ \phi_\tau(t,j) \end{bmatrix}\right|_{\mathcal{A}} \leq \sqrt{\frac{\alpha_2}{\alpha_1}} \left|\begin{bmatrix} \phi_x(0,0) - x^* \\ \phi_\eta(0,0) \\ \phi_\tau(0,0) \end{bmatrix}\right|_{\mathcal{A}} < \sqrt{\frac{\alpha_2}{\alpha_1}}\delta = \epsilon$$

for all $(t,j) \in \operatorname{dom}\phi$ which concludes the proof. ■

3.3.7 Robustness to Perturbations on Communication Noise

In a realistic setting, the information transmitted is affected by communication or channel noise. In this section, we consider the systems under the effect of communication noise m_i when agent i sends out information. Specifically, if the k-th agent receives information of the i-th agent perturbed by $m_i \in \mathbb{R}$, $i \in \mathcal{V}$, we have that when communication occurs, the output of each agent is given by $y_i = x_i + m_i$. In such a case, the controller from Protocol 3.3.1 with $h \equiv 0$ becomes

$$\begin{aligned} \dot{\eta}_i &= 0 && \tau \in [0, T_2] \\ \eta_i^+ &= -\gamma \sum_{k \in \mathcal{N}(i)} (y_i - y_k) && \tau = 0 \end{aligned}$$

which, different than (3.5), leads to an update law with communication noise given by

$$\eta_i^+ = -\gamma \sum_{k \in \mathcal{N}(i)} (x_i - x_k) - \gamma \sum_{k \in \mathcal{N}(i)} (m_i - m_k).$$

Then, by taking the stack of η_i for each $i \in \mathcal{V}$, i.e., $\eta = (\eta_1, \eta_2, \ldots, \eta_N)$, we have that

$$\eta^+ = -\gamma \mathcal{L} x - \gamma \mathcal{L} m,$$

where $m = (m_1, m_2, \ldots, m_N)$.

Using the change of coordinates involving U, as in Section 3.3.1, namely,

$$\bar{x} = U^\top x \qquad \bar{\eta} = U^\top \eta \qquad \bar{m} = U^\top m$$

it follows that at jumps the update of the new state $\bar{\eta}$ is given by

$$\bar{\eta}^+ = (0, -\gamma\bar{\mathcal{L}}\bar{x} - \gamma\bar{\mathcal{L}}\bar{m})).$$

Note that the first component of $\bar{\eta}^+$ does not depend on the communication noise. Defining the perturbed error hybrid system as $\widetilde{\mathcal{H}}_m$ and with states $\chi = (\bar{z}_1, \bar{z}_2, \tau)$, $\bar{z}_1 = (\bar{x}_1, \bar{\eta}_1)$, and $\bar{z}_2 = (\bar{x}_2, \bar{x}_3, \ldots, \bar{x}_N, \bar{\eta}_2, \bar{\eta}_3, \ldots, \bar{\eta}_N)$. Then, the data of $\widetilde{\mathcal{H}}_m$ is given by

$$\begin{aligned} F_m(\chi) =& (A_{f1}\bar{z}_1, A_{f2}\bar{z}_2, -1) \qquad \forall \chi \in C_m := \mathcal{X} \\ G_m(\chi, \bar{m}) =& \left(\widetilde{A}_g \bar{z}_1, \bar{A}_g \bar{z} - \begin{bmatrix} 0 \\ \gamma\bar{\mathcal{L}} \end{bmatrix} \bar{m}, -1 \right) \\ & \qquad \forall \chi \in D_m := \{\chi \in \mathcal{X} : \tau = 0\} \end{aligned} \tag{3.40}$$

Then, using the change of coordinates as in Section 3.3.1, we can show that global exponential stability of $\mathcal{A}$ in (3.12) for $\widetilde{\mathcal{H}}_m$ in (3.10) is robust to communication noise.

Theorem 3.3.14 *Let $0 < T_1 \leq T_2$ be given. Suppose the digraph $\Gamma = (\mathcal{E}, \mathcal{V}, \mathcal{G})$ is strongly connected. If there exists $\gamma > 0$ and a positive definite symmetric matrix P such that* (3.15) *holds for all $\nu \in [T_1, T_2]$, then the hybrid system $\widetilde{\mathcal{H}}_m$ with input $\bar{m}$ is ISS with respect to $\mathcal{A}$ as in* (3.12)*.*

Proof Consider the same Lyapunov function form the proof of Theorem 3.3.5, i.e., $V(\chi) = V_1(\chi) + V_2(\chi)$ as in (3.18). For the hybrid system defined by the states $\bar{z}$, the perturbation does not appear on the flow map. Therefore, the analysis on flows apply from the proof of

Theorem 3.3.5, namely, for each $\chi \in C_m$

$$\langle \nabla V(\chi), F_m(\chi) \rangle = 0. \tag{3.41}$$

When $\tau = 0$, a jump occurs mapping τ to some point $\nu \in [T_1, T_2]$. Defining $B_g = \begin{bmatrix} 0 & \gamma \bar{\mathcal{L}}^\top \end{bmatrix}^\top$, the state $\bar{z}$ is updated by $G_m(\chi, \bar{m})$ in (3.40) to $\bar{A}_g \bar{z} - B_g \bar{m}$. At jumps, we have that, for each $\chi \in D_m$ and $g \in G_m(\chi, \bar{m})$, the change in V is given by

$$\begin{aligned} V(g) - V(\chi) &= V_1(g) - V_1(\chi) + V_2(g) - V_2(\chi) \\ &\leq \bar{z}_2^\top \bar{A}_{g2}^\top e^{\bar{A}_{f2}^\top \nu} P e^{\bar{A}_{f2}\nu} \bar{A}_{g2} \bar{z} - 2\bar{m} B_{f2}^\top e^{\bar{A}_{f2}^\top \nu} P e^{\bar{A}_{f2}\nu} A_{g2} \bar{z}_2 \\ &\quad + \bar{m} B_{f2}^\top e^{\bar{A}_{f2}^\top \nu} P e^{\bar{A}_{f2}\nu} B_{f2} \bar{m} - \bar{z}_2^\top P \bar{z}_2 \end{aligned}$$

Following the steps in the proof of Theorem 3.3.5, from (3.15), there exists a scalar $\beta > 0$ such that $\bar{z}_2^\top (\bar{A}_{g2}^\top e^{\bar{A}_{f2}^\top \nu} P e^{\bar{A}_{f2}\nu} \bar{A}_{g2} - P) \bar{z}_2 < -\beta \bar{z}_2^\top \bar{z}_2$. Furthermore, the second term can be decomposed using Young's inequality $2a^\top b \leq ca^\top a + \frac{1}{c} b^\top b$. Let $a = \bar{z}$ and $b = \bar{m} B_f^\top e^{\bar{A}_f^\top \nu} P e^{\bar{A}_f \nu} \bar{A}_g$, and $c = \beta/2$. Then, we have that

$$V(g) - V(\chi) \leq -\frac{\beta}{2} \bar{z}^\top z + \mu \gamma^2 \lambda_N^2 \bar{m}^\top \bar{m} \tag{3.42}$$

where λ_N is the maximum eigenvalue of $\bar{\mathcal{L}}$, $\gamma > 0$ and $\kappa = \lambda_N^2 |P| (\frac{2}{\beta} + |P|) \max_{\nu \in [T_1, T_2]} |e^{\bar{A}_f \nu}|$. Then, from (3.41) and (3.42), we have that

$$V(g) \leq e^\theta V(\chi) + \gamma^2 \kappa |\bar{m}|^2 \tag{3.43}$$

for all $\chi \in \widetilde{D}, g \in \widetilde{G}(\chi, \bar{m})$ where $\theta = \ln(1 - \beta/\alpha_2)$ and α_2 is defined in (3.17). Therefore, given any maximal solution pair $(\phi, \bar{m})$ to $\mathcal{H}$ in (3.40), we have that during flows $V(\phi(t, 0)) = V(\phi(0, 0))$ for all $t \in [0, t_1]$ and with jumps of the solution given by (3.43), V over any maximal

solution is given by

$$V(\phi(t,j)) \leq e^{\theta j} V(\phi(0,0)) + \kappa\gamma^2 \sum_{i=0}^{j-1} e^{\sigma(j-1-i)} |m(t_{i+1}, i+1|^2$$

for all $(t,j) \in \operatorname{dom}\phi$, with $j \geq 1$.

Furthermore, with θ negative as in the proof of Theorem 3.3.5, for each $(t,j) \in \operatorname{dom}\phi$ such that $j \geq 1$, we have $V(\phi(t,j)) \leq e^{\theta j} V(\phi(0,0)) + \frac{\kappa e^{-\theta}\gamma^2}{e^{-\theta}-1}|m|^2_{(t,j)}$. By following similar arguments as in Theorem 3.3.5, we have

$$\begin{aligned} |\phi(t,j)|^2_{\mathcal{A}} &\leq \frac{\alpha_2}{\alpha_1} e^{\theta j} |\phi(0,0)|^2_{\mathcal{A}} + \frac{\kappa e^{-\theta}\gamma^2}{(e^{-\theta}-1)\alpha_1} |\bar{m}|^2_{(j,t)} \\ &\leq \frac{\alpha_2}{\alpha_1} e^{-\alpha(t+j)} e^{R} |\phi(0,0)|^2_{\mathcal{A}} + \frac{\kappa e^{-\theta}\gamma^2}{(e^{-\theta}-1)\alpha_1} |\bar{m}|^2_{(j,t)} \end{aligned}$$

where $\alpha \in \left(0, \frac{\lambda_d}{1+T_2}\right]$ and $R = \left[\frac{T_2\lambda_d}{1+T_2}, \infty\right)$ which leads to

$$|\phi(t,j)|_{\mathcal{A}} = \max\left\{ \sqrt{2\frac{\alpha_2}{\alpha_1}} e^{-\frac{\alpha(t+j)}{2}} e^{\frac{R}{2}} |\phi(0,0)|_{\widetilde{\mathcal{A}}}, \sqrt{2\frac{\kappa e^{-\theta}}{(e^{-\theta}-1)\alpha_1}} \gamma |\bar{m}|_{(j,t)} \right\}$$

which concludes the proof. ■

Remark 3.3.15 *From Lemma 3.3.3, $\mathcal{H}$ and $\widetilde{\mathcal{H}}$ satisfy the hybrid basic conditions. Due to the fact that all maximal solutions to these hybrid systems are complete, [28, Proposition 6.14] implies that solutions with perturbed initial conditions stay close to the unperturbed solutions. More precisely, for every $\tau' > 0$, $\varepsilon' \geq 0$ and compact set K, there exists $\delta > 0$ such that for every maximal solution $\phi_\delta \in \mathcal{S}_{\mathcal{H}}(K + \delta\mathbb{B})$ there exists a solution ϕ to $\mathcal{H}$ with $\phi(0,0) \in K$ such that ϕ_δ and ϕ are (τ', ε')-close.*[3] *In particular, given an unperturbed initial condition $\phi(0,0)$ for $\phi_\delta(0,0) \in \phi(0,0) + \delta$ where $\delta \in [-\delta'_x, \delta'_x] \times [-\delta'_\eta, \delta'_\eta] \times [-\delta'_\tau, \delta'_\tau]$ to $\widetilde{\mathcal{H}}$ with data in* (3.10) *where $\phi_\delta = (\phi_{\delta x}, \phi_{\delta\eta}, \phi_{\delta\tau})$, $\phi = (\phi_x, \phi_\eta, \eta_\tau)$ and $\delta = (\delta_x, \delta_\eta, \delta_\tau)$ is bounded, then by using Proposition 3.3.11 it follows that when $h = 0$ the limit point ϕ_{x_i} of the perturbed solutions are*

[3] Given $\tau', \varepsilon' > 0$, two hybrid arcs ϕ_1 and ϕ_2 are (τ', ε')-close if the following is satisfied: for all $(t,j) \in \operatorname{dom}\phi_1$ with $t + j \leq \tau'$ there exists s such that $(s,j) \in \operatorname{dom}\phi_2$, $|t - s| < \varepsilon'$, and $|\phi_1(t,j) - \phi_2(s,j)| < \varepsilon'$; for all $(t,j) \in \operatorname{dom}\phi_2$ with $t + j \leq \tau'$ there exists s such that $(s,j) \in \operatorname{dom}\phi_1$, $|t - s| < \varepsilon'$, and $|\phi_2(t,j) - \phi_1(s,j)| < \varepsilon'$.

given by

$$\lim_{t+j\to\infty} \phi_{x_i} = \frac{1}{N}\sum_{i=1}^{N} \left(\phi_{x_i}(0,0) + \phi_\tau(0,0)\phi_{\eta_i}(0,0)\right) \tag{3.44}$$

$$+ \frac{1}{N}\sum_{i=1}^{N} \left(\phi_{\delta_{x_i}}(0,0) + \phi_\tau(0,0)\phi_{\delta\eta_i}(0,0) + \phi_{\delta_\tau}\left(\phi_{\eta_i} + \phi_{\delta_{\eta_i}}\right)\right) \tag{3.45}$$

and when $h \neq 0$ it follows that the limit point of the perturbed solution is given by

$$\lim_{t+j\to\infty} \phi_{x_i} = \frac{1}{N}\sum_{i=1}^{N} \Big(\phi_{x_i}(0,0) + \phi_{\delta_{x_i}}(0,0) \tag{3.46}$$

$$+ \frac{1}{h}\exp(h(\phi_\tau(0,0) + \phi_{\delta_\tau}(0,0))) - 1(\phi_{\eta_i} + \phi_{\delta_{\eta_i}})(0,0)\Big). \tag{3.47}$$

In the next section, we will look at the case when information is transmitted between each agent asynchronously.

3.4 Numerical Examples

Example 3.4.1 *Consider five agents with dynamics as in* (3.1) *over the strongly connected graph with adjacency matrix*

$$\mathcal{G} = \begin{bmatrix} 0 & 1 & 1 & 0 & 1 \\ 1 & 0 & 1 & 0 & 0 \\ 1 & 0 & 0 & 1 & 0 \\ 0 & 0 & 1 & 0 & 1 \\ 1 & 0 & 1 & 1 & 0 \end{bmatrix}. \tag{3.48}$$

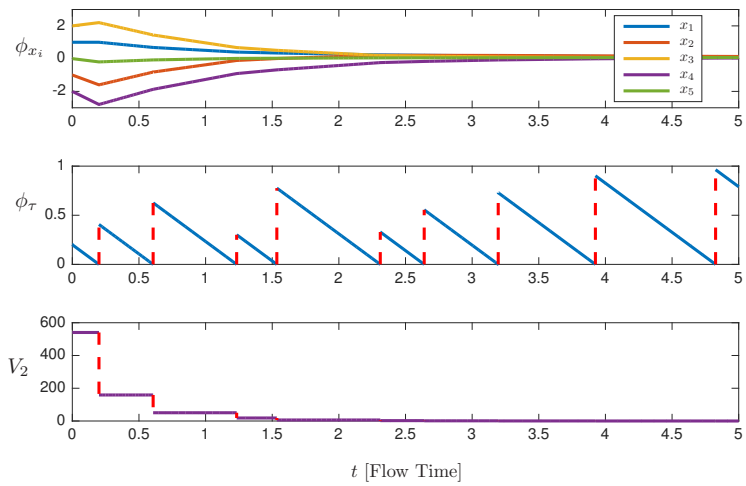

Figure 3.1: (top) The x and τ components of a solution $\phi = (\phi_x, \phi_\eta, \phi_\tau)$ to $\mathcal{H}$ with $\mathcal{G}$ in (3.48) using Protocol 3.3.1 which satisfies Proposition 3.3.5. (bottom) Note that since $V_2(\chi)$ for $\widetilde{\mathcal{H}}$ deceases to zero with respect to flow time, it indicates that the solution reaches consensus.

Let $T_1 = 0.5$ and $T_2 = 1.5$. Then, it can be found that the parameters

$$P \approx \begin{bmatrix} 35.48 & 0 & 0 & 0 & -1.26 & 0 & 0 & 0 \\ 0 & 26.69 & 0 & 0 & 0 & 4.06 & 0 & 0 \\ 0 & 0 & 19.20 & 0 & 0 & 0 & 3.25 & 0 \\ 0 & 0 & 0 & 26.69 & 0 & 0 & 0 & 4.06 \\ -1.26 & 0 & 0 & 0 & 1.69 & 0 & 0 & 0 \\ 0 & 4.06 & 0 & 0 & 0 & 9.19 & 0 & 0 \\ 0 & 0 & 3.25 & 0 & 0 & 0 & 12.13 & 0 \\ 0 & 0 & 0 & 4.06 & 0 & 0 & 0 & 9.18 \end{bmatrix}$$

and $\gamma = 0.3$ satisfy condition (3.15). Figure 3.1 shows the x_i components $i \in \{1, 2, 3, 4, 5\}$ of a solution $\phi = (\phi_x, \phi_\eta, \phi_\tau)$ from initial conditions given by $\phi_x(0, 0) = (1, -1, 2, -2, 0)$, $\phi_\eta(0, 0) = (0, -3, 1, -4, -1)$, and $\phi_\tau(0, 0) = 0.2$ as well as the the function $V_2(\chi)$ below Proposition 3.3.5 evaluated along ϕ projected onto the ordinary time domain.[4] $\triangle$

[4]Code at `https://github.com/HybridSystemsLab/ConsSyncTimes`

3.5 Summary

We showed that hybrid consensus protocols are viable algorithms for the consensus of first order systems with stochastically determined communication events over a general graph. Using a hybrid systems framework, we defined the communication events between the systems using a hybrid decreasing timer. Recasting consensus as a set stability problem, we took advantage of several properties of the graph structure and employed a Lyapunov based approach to certify that this set is partially pointwise globally exponentially stable. We further showed that global exponential stability of the consensus set is robust to communication noise. Lastly, we presented a protocol for reaching state consensus where agents receive local updates asynchronously. The results in this paper can be used to design large-scale networked systems that communicate at stochastic time instants over general communication graphs.

Chapter 4

Decentralized Synchronization of Linear Time-invariant Systems

4.1 Introduction

In this chapter, the consensus work in the pervious chapter is further developed where each agent has some internal linear dynamics. Namely, the problem of robustly synchronizing (in terms of both exponential attractivity and stability) $N > 1$ continuous-time agents with linear dynamics (under nominal conditions) from intermittent measurements of functions of their outputs over a network is considered. Each agent has dynamics given by the following differential equation modeling the evolution of the state of the i-th agent:

$$\dot{x}_i = Ax_i + Bu_i + \Delta_i(x_i, t) \tag{4.1}$$

where $A \in \mathbb{R}^{n\times n}$ is the nominal system matrix, $B \in \mathbb{R}^{n\times p}$ is the input matrix, u_i is the control input, $\Delta_i : \mathbb{R}^n \times \mathbb{R}_{\geq 0} \to \mathbb{R}^n$ models unknown and possibly heterogeneous dynamics, and $t \geq 0$ denotes ordinary time. The i-th agent in the network measures its local information y_i and

received information from its neighbors y_k at times $t \in \{t_s^i\}_{s=1}^{\infty}$. Moreover, at such event times, the output of each agent is given by

$$y_i = Hx_i + \varphi_i(x_i, t) \tag{4.2}$$

where H is the output matrix and φ_i is an unknown function modeling communication noise. The event times t_s^i are independently defined for each agent (as the index i denotes); the only restriction imposed on communication times is that they must satisfy

$$\begin{aligned} t_{s+1}^i - t_s^i \in [T_1^i, T_2^i] \qquad & \forall s \in \{1, 2, \dots\} \\ t_1^i \leq T_2^i \qquad & \end{aligned} \tag{4.3}$$

where, for each $i \in \mathcal{V}$, the positive scalars T_1^i and T_2^i satisfy $T_2^i \geq T_1^i$ and define the lower and upper bounds on the communication rate, respectively. Namely, these parameters (which are known but may be different for each agent) govern the amount of time allowed to elapse between consecutive communication events. The parameter T_2^i is often referred to as the *maximum allowable time interval* (MATI).

Motivated by the challenges outlined in Section 1.2.1, a distributed hybrid controller is proposed. Such a controller is capable of asymptotically synchronizing the state of each agent over the network, with stability and robustness, by only exchanging information among neighbors at independent communication events t_s^i. In the nominal case, the algorithm proposed here guarantees global exponential stability of the set characterizing synchronization, called the synchronization set, and when projected to the state space of all agents, the synchronization set is the set of points $x = (x_1, x_2, \dots, x_N)$ such that

$$x_1 = x_2 = \cdots = x_N.$$

Moreover, in the presence of small enough general perturbations, the proposed algorithm guar-

antees that the stability properties are preserved, semiglobally and practically. Under the perturbation effect of measurement noise, we also show that the system is input-to-state stable (in the hybrid sense).

The distributed hybrid controller has state variables which have hybrid dynamics; i.e., the internal states are updated both continuously and, at times, are impulsively updated. In general terms, the continuous dynamics of the controller state are given by a differential equation of the form

$$\dot{\eta}_i = f_{ci}(y_i, \eta_i), \tag{4.4}$$

when no new information is available, while when new information arrives, the internal states are updated according to

$$\eta_i^+ = \sum_{k=1}^{N} g_{ik} G_{ci}^k(\eta_i, \eta_k, y_i, y_k) \tag{4.5}$$

where $\mathcal{V} := \{1, 2, \ldots, N\}$ defines the set of all agents; g_{ik} models the connection between agents i and k, namely, $g_{ik} = 1$ if the k-th agent can share information to agent i and $g_{ik} = 0$ otherwise; the map f_{ci} defines the continuous evolution of the controller state and the map G_{ci}^k defines the impulsive update law when new information is collected from each connected agent. Then, η_i is injected into the continuous-time dynamics of the i-th agent's input u_i and, at communication events, updates its internal state impulsively. Following the hybrid systems framework in [51], the interconnected closed-loop model containing continuous dynamics of each agent, the communication events, and the distributed hybrid controller is modeled as a closed-loop hybrid model in Section 4.2.1.

The main contribution of this work lay on the establishment of sufficient conditions for nominal and robust synchronization over networks with intermittent information availability. In fact, the proposed design conditions guarantee the states of each agent converge to synchro-

nization with an exponential rate when information is only available at, possibly, asynchronous and non-periodic time instance. Precisely, as shown in Section 4.2.3 through an appropriate choice in coordinates we utilize Lyapunov arguments for hybrid systems to establish sufficient conditions that assure global exponential stability of the synchronization set. An in-depth robustness analysis and design procedure are presented in Section 4.2.5, wherein we establish several key robustness properties. In part, this is enabled by the proposed hybrid controller which is designed to satisfy certain regularity conditions that, under nominal conditions has uniform global asymptotic stability of the synchronization set, guarantees robustness to small enough perturbations. In Section 4.2.5.1, we provide results on robustness with respect to perturbations emerging from unmodeled dynamics, skewed clocks, as well as communication noise. In Section 4.2.5.2, results on robustness in the form of an input-to-state stability (ISS) property with respect to communication noise is provided, for which an explicit ISS bound is given.

In Section 4.3, numerical simulations to illustrate our results are provided. Wherein, the results are exemplified using the case of asynchronous update times where the dynamics of the agents have harmonic oscillator dynamics under different scenarios. Robustness to communication noise and packet dropout are also considered.

4.2 Robust Global Synchronization with Intermittent Information

4.2.1 Hybrid Modeling

Consider N agents with dynamics in (4.1) that are connected via a directed graph. Due to the impulsive nature of the communication structure outlined in (4.3), we define a decreasing timer to model such a communication scheme. Namely, for each $i \in \mathcal{V}$, let $\tau_i \in [0, T_2^i]$ be a timer

state that decreases with respect to continuous time and, upon reaching zero, is reset to a point within the interval $[T_1^i, T_2^i]$ and allows agent i to receive information from its connected agents. Namely, τ_i has the following hybrid dynamics:

$$\begin{aligned} \dot{\tau}_i &= -1 & \tau_i &\in [0, T_2^i], \\ \tau_i^+ &\in [T_1^i, T_2^i] & \tau_i &= 0. \end{aligned} \tag{4.6}$$

This hybrid system generates any possible sequence of time instances $\{t_s^i\}_{s=1}^{\infty}$ at which events occur and satisfy (4.3). Note that T_1^i and T_2^i may not be the same for each $i \in \mathcal{V}$, therefore, the interval which communication can occur may be vastly different.[1]

Consider the following definitions of the maps in (4.4) and (4.5), which yield the particular hybrid dynamics[2] for η_i therein. The map $f_{ci} : \mathbb{R}^n \times \mathbb{R}^p \to \mathbb{R}^p$ is defined as

$$f_{ci}(x_i, \eta_i) = E\eta_i \qquad \forall i \in \mathcal{V} \tag{4.7}$$

and the map $G_{ci}^k : \mathbb{R}^n \times \mathbb{R}^n \times \mathbb{R}^m \times \mathbb{R}^m \rightrightarrows \mathbb{R}^p$ as

$$\begin{aligned} G_{ci}^k(\eta_i, \eta_k, y_i, y_k) &= K(y_i - y_k) \\ &= KH(x_i - x_k) + K(\varphi_i(x_i) - \varphi_k(x_k)) \end{aligned} \tag{4.8}$$

for each $i, k \in \mathcal{V}$. The constants E and K define the tuning parameters of the control algorithm. For simplicity, for the remainder of this section, we will assume that $\Delta \equiv 0$ and $\varphi_i \equiv 0$ for all $i \in \mathcal{V}$, and consider the nominal case, i.e., perfect knowledge of the plant dynamics and its output maps. The scenario when these perturbations are nonzero is addressed in Section 4.2.5. Without such perturbations and with the map (4.8), the impulsive dynamics of η_i in (4.5) are

[1] For instance, consider the case of $N = 2$ with $T_1^2 = T_1^1$ and $T_2^2 = 2T_2^1$. At jumps, the timer states τ_1 and τ_2 are reset by $\tau_1 \in [T_1^1, T_2^1]$ when $\tau_1 = 0$ and $\tau_2^+ \in [T_1^1, 2T_2^1]$ when $\tau_2 = 0$; i.e., τ_1 could potentially jump twice as fast as τ_2.

[2] Other choices of the maps f_{ci} and G_{ci}^k might be possible to obtain different dynamics of the variable η_i. Although not pursued in this paper, one can potentially choose sliding mode-like dynamics as in [52].

given by

$$\eta_i^+ = KH \sum_{k \in \mathcal{N}(i)} (x_i - x_k). \tag{4.9}$$

For the design of our algorithm for synchronization under intermittent information, we employ the change in coordinates[3]

$$\theta_i = KH \sum_{k \in \mathcal{N}(i)} (x_i - x_k) - \eta_i. \tag{4.10}$$

which leads to

$$\theta = (\mathcal{L} \otimes KH)x - \eta \tag{4.11}$$

where $x = (x_1, x_2, \ldots, x_N)$, $\theta = (\theta_1, \theta_2, \ldots, \theta_N)$, $\eta = (\eta_1, \eta_2, \ldots, \eta_N)$, and $\mathcal{L}$ is the Laplacian matrix given by the directed graph Γ of the network. Let $\xi = (z, \tau) \in \mathcal{X} := \mathbb{R}^{(n+p)N} \times \mathcal{T}$ where $z = (x, \theta)$, $\tau = (\tau_1, \tau_2, \ldots, \tau_N)$, and $\mathcal{T} = [0, T_2^1] \times [0, T_2^2] \times \cdots \times [0, T_2^N]$. Then, a hybrid system $\mathcal{H}$ is defined as the collection of all agents with dynamics in (4.1) and controller states (4.4) and (4.5) with data (C, f, D, G) such that, for every $\xi \in C := \mathcal{X}$, we have that

$$\dot{\xi} = (A_f z, -1_N) =: f(\xi). \tag{4.12}$$

The state matrix A_f is given by

$$A_f = \begin{bmatrix} A_1 & -\widetilde{B} \\ \widetilde{K}A_1 - \widetilde{E}\widetilde{K} & \widetilde{E} - \widetilde{K}\widetilde{B} \end{bmatrix}$$

where $A_1 = I \otimes A + \widetilde{B}\widetilde{K}$, $\widetilde{B} = I \otimes B$, $\widetilde{K} = \mathcal{L} \otimes KH$, and $\widetilde{E} = I \otimes E$.[4] When $\tau_i = 0$, a jump of

[3]This change of coordinates was also found useful for the design of observers under intermittent information in [49, 53]. Therein, the authors proposed a continuous-time observer design to estimate the state of an LTI plant when its output is available only at intermittent time instances. The observer designed therein uses a memory state (akin to the hybrid controller in this work) that is reset when new measurements are available. Using a similar change of coordinates, sufficient conditions for asymptotic stability of the zero estimation error are derived. These results were extended to the network case in [54].

[4]Through the change of variables in (4.11), the $z = (x, \theta)$ components of the flow dynamics in (4.12) are given

the i-th agent occurs: the components θ and τ are mapped via $\theta_i^+ = 0$ and $\tau_i^+ \in [T_1^i, T_2^i]$ while x_i remains constant; moreover, for each $k \in \mathcal{V} \setminus \{i\}$ the state components x_k, θ_k and τ_k are held constant. Specifically, for each $\xi \in D := \cup_{i \in \mathcal{V}} D_i$ where $D_i := \{\xi \in \mathcal{X} : \tau_i = 0\}$, we have that

$$\xi^+ \in G(\xi) := \{G_i(\xi) : \xi \in D_i, i \in \mathcal{V}\} \tag{4.13}$$

where

$$G_i(\xi) = \begin{bmatrix} x \\ (\theta_1, \theta_2, \ldots, \theta_{i-1}, 0, \theta_{i+1}, \ldots, \theta_N) \\ (\tau_1, \tau_2, \ldots, \tau_{i-1}, [T_1^i, T_2^i], \tau_{i+1}, \ldots, \tau_N) \end{bmatrix}.$$

Lemma 4.2.1 *Given positive scalars T_1^i and T_2^i such that $T_1^i \leq T_2^i$, the hybrid system $\mathcal{H} = (C, f, D, G)$ with satisfies the hybrid basic conditions.*

Proof By construction, the sets C and D are closed. The flow map f in (4.12) is continuous. The jump map G is outer semicontinuous since its graph is closed; moreover, it is locally bounded on D.[5] ■

Remark 4.2.2 *Note that satisfying the hybrid basic conditions implies that the hybrid system $\mathcal{H}$ is well-posed and that asymptotic stability of a compact set as defined in [51, Definition 3.3] is robust to small enough perturbations. See Section 4.2.5.1 for more information on specific robustness results as a consequence of the hybrid basic conditions.*

4.2.2 Properties of Maximal Solutions to $\mathcal{H}$

As mentioned in Section 2.1, solutions to a general hybrid system $\mathcal{H}$ can evolve continuously and/or discretely according to the differential and difference equations/inclusions (and

by $\dot{x} = (I \otimes A)x + (I \otimes B)\eta = (I \otimes A)x + (I \otimes B)(\widetilde{K}x - \theta) = A_1 x - \widetilde{B}\theta$ and $\dot{\theta} = \tilde{K}\dot{x} - \dot{\eta} = \widetilde{K}(A_1 x - \tilde{B}\theta) - \widetilde{E}(\widetilde{K}x - \theta)$.

[5] The graph of a set-valued mapping $G : \mathbb{R}^n \to \mathbb{R}^n$ is defined as gph $G = \{(x, y) : x \in \mathbb{R}^n, y \in G(x)\}$.

the sets where those apply) that describe the hybrid dynamics. The following properties of the domain of maximal solutions are established by exploiting the fact that a timer variable being zero is the only trigger of jumps in the system.

Lemma 4.2.3 *([55, Lemma 3.5]) Let $0 < T_1^i \leq T_2^i$ be given for all $i \in \mathcal{V}$. Every maximal solution $\phi \in \mathcal{S}_{\mathcal{H}}$ satisfies the following:*

1. *ϕ is complete; i.e., $\operatorname{dom}\phi$ is unbounded;*
2. *for each $(t,j) \in \operatorname{dom}\phi$, $\left(\frac{j}{N} - 1\right)\underline{T} \leq t \leq \frac{j}{N}\overline{T}$, where $\underline{T} := \min_{i\in\mathcal{V}} T_1^i$ and $\overline{T} := \max_{i\in\mathcal{V}} T_2^i$;*
3. *for all $j \in \{1,2,3,\dots\}$ such that $(t_{(j+1)N},(j+1)N),(t_{jN},jN) \in \operatorname{dom}\phi$, $t_{(j+1)N} - t_{jN} \in [\underline{T},\overline{T}]$.*

4.2.3 Sufficient Conditions for Synchronization

In this section, we consider the following notion of asymptotic synchronization for hybrid system $\mathcal{H}$.

Definition 4.2.4 *Consider the hybrid system $\mathcal{H}$ in (2.1) with state $\xi = (\xi_1,\xi_2,\dots,\xi_N)$ where, for each $i \in \mathcal{V}$, ξ_i is partitioned as $\xi_i = (p_i,q_i)$, where $p_i \in \mathbb{R}^r$ and $q_i \in \mathbb{R}^{n-r}$ for each $i \in \mathcal{V}$ with integers n,r satisfying $1 \leq r \leq n$. The hybrid system $\mathcal{H}$ is said to have*

- stable synchronization with respect to p *if for every $\varepsilon > 0$, there exists $\delta > 0$ such that every maximal solution $\phi = (\phi_1,\phi_2,\dots,\phi_N)$ to $\mathcal{H}$, where $\phi_i = (\phi_{i,p},\phi_{i,q})$ from $|\phi_i(0,0) - \phi_k(0,0)| \leq \delta$ for each $i,k \in \mathcal{V}$ implies $|\phi_{i,p}(t,j) - \phi_{k,p}(t,j)| \leq \varepsilon$ for all $i,k \in \mathcal{V}$ and $(t,j) \in \operatorname{dom}\phi$.*
- globally attractive synchronization with respect to p *if every maximal solution to $\mathcal{H}$ is complete, and for each $i,k \in \mathcal{V}$, $\lim_{\substack{(t,j)\in\operatorname{dom}\phi \\ t+j\to\infty}} |\phi_{i,p}(t,j) - \phi_{k,p}(t,j)| = 0$*

- global asymptotic synchronization with respect to p *if it has both stable synchronization and global attractive synchronization with respect to* p.

Remark 4.2.5 *If $r = n$, then Definition 4.2.4 can be considered to be a full-state synchronization notion, while if $r < n$, it can be considered to be a partial state synchronization notion. Note that stable synchronization with respect to p requires solutions ϕ_i for each $i \in \mathcal{V}$ to start close to each other, while only the components $\phi_{i,p}$, $i \in \mathcal{V}$ remain close to each other over their solution domain of definition. Similarly, global attractive synchronization with respect to p only requires that the Euclidean distance between each ϕ_i approaches zero, while the other components are left unconstrained. Also, note that boundedness of the solution is not required.*

It is worth noting that the hybrid systems framework in [28] covers both purely continuous-time and purely discrete-time systems. Namely, continuous-time systems can be modeled in this framework by letting D be empty and G be any arbitrary function, and likewise, discrete-time systems are recovered by letting C be empty and f be any arbitrary function. In the following example, we showcase the notions in Definition 4.2.4 for the case of continuous-time systems for the synchronization of agents with integrator dynamics.

Example 4.2.6 *Consider the case of four completely connected agents, i.e., $\mathcal{V} := \{1, 2, 3, 4\}$ and $g_{ik} = 1$ for each $i, k \in \mathcal{V}$ such that $i \neq k$. Each agent has integrator dynamics $\dot{x}_i = u_i$ and is controlled by $u_i = -\gamma \sum_{k=1}^{4}(x_i - x_k)$ where $\gamma > 0$. Integrating the fully interconnected system $\dot{x} = -\gamma \mathcal{L} x$ from $\phi(0, 0)$ leads to the complete solution $\phi = (\phi_1, \phi_2, \phi_3, \phi_4)$ with domain $\operatorname{dom} \phi = \mathbb{R}_{\geq 0} \times \{0\}$ given by $\phi_i(t, 0) = \frac{1}{4}(\phi_i(0, 0)(3\exp(-4\gamma t) + 1) - \sum_{r \in \mathcal{V} \setminus \{i\}} \phi_r(0, 0)(\exp(-4\gamma t) - 1))$ for each $i \in \mathcal{V}$ and each $t \geq 0$. Stable synchronization can be seen by picking $\delta \in (0, \varepsilon)$ for any given $\varepsilon > 0$. For each $i, k \in \mathcal{V}$ such that $i \neq k$, it follows that $|\phi_i(t, 0) - \phi_k(t, 0)| = \exp(-4\gamma t)|\phi_i(0, 0) - \phi_k(0, 0)| \leq \exp(-4\gamma t)\delta < \epsilon$. Moreover, from the derivation above, attractive synchronization is*

guaranteed, for each $i, k \in \mathcal{V}$, by noting that $\lim_{t\to\infty} |\phi_i(t,0) - \phi_k(t,0)| = 0$. *Due to the fact that this system exhibits both stable synchronization and global attractive synchronization, it globally asymptotically synchronizes.* $\triangle$

Remark 4.2.7 *There are several notions of synchronization in the literature. A widely used notion of synchronization considers only attractive synchronization in the sense of limits; see, e.g., [20, 22, 23, 15]. Another common notion of synchronization is given as the convergence of all agents to a common solution, namely, that there exists a solution ϕ_s such that, for each $i \in \mathcal{V}$, ϕ_i converges to ϕ_s; see, e.g., [56, 25].*

Asymptotic synchronization as defined in Definition 4.2.4 can be reformulated as a set stability problem. In light of the partial notion of synchronization, our goal is to stabilize the set of points ξ such that each component of x and θ are synchronized. In particular, given a complete solution $\phi = (\phi_x, \phi_\theta, \phi_\tau)$ to the hybrid system $\mathcal{H}$, we want $\lim_{t+j\to\infty} |\phi_{x_i}(t,j) - \phi_{x_k}(t,j)| = 0$ and $\lim_{t+j\to\infty} |\phi_{\theta_i}(t,j) - \phi_{\theta_k}(t,j)| = 0$ for each $i, k \in \mathcal{V}$ where $\phi_x = (\phi_{x_1}, \phi_{x_2}, \ldots, \phi_{x_N})$ and $\phi_\theta = (\phi_{\theta_1}, \phi_{\theta_2}, \ldots, \phi_{\theta_N})$. To obtain such a property by solving a set stability problem, we define the synchronization set as

$$\mathcal{A} = \{\xi = (z, \tau) \in \mathcal{X} : x_1 = x_2 = \cdots = x_N, \theta_1 = \theta_2 = \cdots = \theta_N\}, \tag{4.14}$$

for the hybrid system $\mathcal{H}$ where $\mathcal{X} = \mathbb{R}^{N(n+p)} \times \mathcal{T}$ as defined in Section 4.2.1.

We consider the following global exponential stability notion of closed sets $\mathcal{A}$ for general hybrid systems $\mathcal{H}$, see [57] for more information.

Definition 4.2.8 *Let $\mathcal{A} \subset \mathbb{R}^n$ be closed. The set $\mathcal{A}$ is said to be* globally exponentially stable *for the hybrid system $\mathcal{H}$ if every maximal solution to $\mathcal{H}$ is complete and there exist strictly positive scalars κ and r such that for each solution ϕ to $\mathcal{H}$, $|\phi(t,j)|_\mathcal{A} \leq \kappa \exp(-r(t+j))|\phi(0,0)|_\mathcal{A}$ for all $(t,j) \in \operatorname{dom}\phi$.*

Next, we establish a sufficient condition that guarantees the synchronization property via stability analysis of $\mathcal{A}$ in (4.14). We establish such a result by using a Lyapunov function. An appropriate choice of V must satisfy $V(\xi) = 0$ for each $\xi \in \mathcal{A}$, while for any $\xi \in \mathcal{X} \setminus \mathcal{A}$, $V(\xi) > 0$. To simplify notation, we introduce the average of the timers of $\mathcal{H}$ given by $\bar{\tau} = \frac{1}{N}\sum_{i=1}^{N} \tau_i$. Inspired by [58], consider the following Lyapunov function candidate as

$$V(\xi) = z^\top \bar{\Psi} R(\tau) \bar{\Psi}^\top z, \tag{4.15}$$

where $\bar{\Psi} = \mathrm{diag}(\widetilde{\Psi} \otimes I_n, \widetilde{\Psi} \otimes I_p)$ with $\widetilde{\Psi}$ defined in Section 2.2, $R(\tau) = \mathrm{diag}(P, Q\exp(\sigma\bar{\tau}))$, $P = \mathrm{diag}(P_2, P_3, \ldots, P_N)$, $Q = \mathrm{diag}(Q_2, Q_3, \ldots, Q_N)$, $P_i = P_i^\top > 0$, and $Q_i = Q_i^\top > 0$ for each $i \in \{2, 3, \ldots, N\}$. The Lyapunov function V in (8.6) satisfies [28, Definition 3.16], which makes it a suitable Lyapunov function candidate for asymptotic stability of $\mathcal{A}$ in (4.14). The following result shows that, under certain conditions, for each $\xi \in C$, V decreases during flows, however, at jumps, may have a nonnegative change. Our previous work on distributed estimation with intermittent communication in [55] uses a similar construction of a Lyapunov function. However, such a Lyapunov function decreases during flows and has a non-positive change during jumps. To guarantee exponential stability of the synchronization set, the result [28, Proposition 3.29] is exploited, namely, [28, Proposition 3.29] uses a balancing condition between jumps and flows to guarantee that solutions converge to the desired set with an exponential rate.

Theorem 4.2.9 *Given $0 < T_1^i \leq T_2^i$ for each $i \in \mathcal{V}$ and an undirected connected graph Γ, the set $\mathcal{A}$ is globally exponentially stable for the hybrid system $\mathcal{H}$ with data in* (4.12) *and* (4.13) *if there exist scalars $\sigma > 0$, $\varepsilon \in (0, 1)$, matrices $K \in \mathbb{R}^{n\times p}$ and $E \in \mathbb{R}^{p\times p}$, and positive definite symmetric matrices P_i, Q_i for each $i \in \{2, 3, \ldots, N\}$, satisfying*

$$M(\nu) = \begin{bmatrix} \mathrm{He}(P\bar{A}) & -P\bar{B} + \exp(\sigma\nu)(\bar{K}\bar{A} - \bar{E}\bar{K})^\top Q \\ \star & \mathrm{He}(\exp(\sigma\nu)Q(\bar{E} - \bar{K}\bar{B} - \frac{\sigma}{2}I)) \end{bmatrix} < 0 \tag{4.16}$$

for each $\nu \in [0, \overline{T}]$*, where* $\bar{A} = I \otimes A + \Lambda \otimes BKH$*,* $\bar{B} = I \otimes B$*,* $\bar{E} = I \otimes E$*,* $\bar{K} = \Lambda \otimes KH$*,* $\Lambda = diag\lambda_2, \lambda_3, \ldots, \lambda_N$ *where* λ_i *are the nonzero eigenvalues of* $\mathcal{L}$*, and*

$$(1-\varepsilon)\underline{T} - \frac{\alpha_2 \sigma \overline{T}}{\beta} > 0. \tag{4.17}$$

where $\underline{T} := \min_{i \in \mathcal{V}} T_1^i$*,* $\overline{T} := \max_{i \in \mathcal{V}} T_2^i$*,*

$$\beta = -\max_{\nu \in [0, \overline{T}]} \bar{\lambda}(M(\nu))$$

$$\alpha_2 = \max\{\overline{\lambda}(P), \overline{\lambda}(Q)\exp(\sigma\overline{T})\}.$$

Moreover, every $\phi \in \mathcal{S}_{\mathcal{H}}$ *satisfies*

$$|\phi(t,j)|_{\mathcal{A}} \leq \kappa \exp\left(-r(t+j)\right) |\phi(0,0)|_{\mathcal{A}} \tag{4.18}$$

for all $(t,j) \in \operatorname{dom}\phi$*, where* $\kappa = \sqrt{\frac{\alpha_2}{\alpha_1}} \exp\left(\frac{\beta(1-\varepsilon)\underline{T}}{2\alpha_2}\right)$ *and* $r = \frac{\beta}{2\alpha_2 N} \min\left\{\varepsilon N, (1-\varepsilon)\underline{T} - \frac{\alpha_2 \sigma \overline{T}}{\beta}\right\}$*, and* $\alpha_1 = \min\{\underline{\lambda}(P), \underline{\lambda}(Q)\}$*.*

Proof Consider the Lyapunov function V in (8.6). Note that, due to the definition of $\bar{\Psi}$, the distance of ξ to the set $\mathcal{A}$ is equivalent to the distance of $\bar{\Psi}^\top z$ to the origin due to the domain of the timer states. More specifically, $|\xi|_{\mathcal{A}}^2 = |\bar{\Psi} z|^2$. Furthermore, from V it follows that

$$\alpha_1 |\xi|_{\mathcal{A}}^2 \leq V(\xi) \leq \alpha_2 |\xi|_{\mathcal{A}}^2 \tag{4.19}$$

where α_1 and α_2 are given below (4.16).[6] During flows, the change in V is given by $\langle \nabla V(\xi), f(\xi) \rangle$ for each $\xi \in C$. To compute such inner product, define $\tilde{R}(\tau) = \operatorname{diag}(0, Q\exp(\sigma\bar{\tau}))$ and note that

[6] Note that $\overline{\lambda}(\cdot)$ and $\underline{\lambda}(\cdot)$ are the maximum and minimum eigenvalues, respectively.

$\dot{\tilde{\tau}} = -1$. Then, it follows that

$$\begin{aligned}\langle \nabla V(\xi), f(\xi)\rangle &= 2z^\top \bar{\Psi} R(\tau)\bar{\Psi}^\top A_f z - \sigma z^\top \bar{\Psi}\tilde{R}(\tau)\bar{\Psi}^\top z \\ &= 2z^\top \bar{\Psi} R(\tau)\bar{\Psi}^\top A_f (I + \bar{\Psi}\bar{\Psi}^\top - \bar{\Psi}\bar{\Psi}^\top) z - \sigma z^\top \bar{\Psi}\tilde{R}(\tau)\bar{\Psi}^\top z \\ &= 2z^\top \bar{\Psi} R(\tau)\bar{\Psi}^\top A_f \bar{\Psi}\bar{\Psi}^\top z + 2z^\top \bar{\Psi} R(\tau)\bar{\Psi}^\top A_f (I - \bar{\Psi}\bar{\Psi}^\top) z - \sigma z^\top \bar{\Psi}\tilde{R}(\tau)\bar{\Psi}^\top z\end{aligned} \tag{4.20}$$

where we use the property that $\dot{z}^\top \bar{\Psi} R(\tau)\bar{\Psi}^\top z = z^\top \bar{\Psi} R(\tau)\bar{\Psi}^\top \dot{z}$. Recall from Section 2.2 that $\Psi\Psi^\top = U$, $U\mathcal{L} = \mathcal{L}U$ and $\Psi^\top 1 = 0_{N-1\times N}$, which leads to

$$\begin{aligned}\bar{\Psi} R(\tau)\bar{\Psi}^\top A_f (I - \bar{\Psi}\bar{\Psi}^\top) &= \bar{\Psi} P \bar{\Psi}^\top A_f (I \otimes I - U \otimes I) \\ &= \bar{\Psi} R(\tau)\bar{\Psi}^\top (I \otimes I - U \otimes I) A_f \\ &= \bar{\Psi} R(\tau)(\bar{\Psi}^\top - \bar{\Psi}^\top \bar{\Psi}\bar{\Psi}^\top) A_f \\ &= \bar{\Psi} R(\tau)(\bar{\Psi}^\top - \bar{\Psi}^\top) A_f = 0\end{aligned}$$

which reduces (4.20) to

$$\begin{aligned}\langle \nabla V(\xi), f(\xi)\rangle &= z^\top \bar{\Psi} R(\tau)\bar{\Psi}^\top A_f \bar{\Psi}\bar{\Psi}^\top z + z^\top \bar{\Psi}\bar{\Psi}^\top A_f^\top \bar{\Psi} R(\tau)\bar{\Psi}^\top z - \sigma z^\top \bar{\Psi}\tilde{R}(\tau)\bar{\Psi}^\top z \\ &= z^\top \bar{\Psi}(R(\tau)\bar{\Psi}^\top A_f \bar{\Psi} + \bar{\Psi}^\top A_f^\top \bar{\Psi} R(\tau) - \sigma\tilde{R}(\tau))\bar{\Psi}^\top z.\end{aligned} \tag{4.21}$$

Due to the definition of $\widetilde{\Psi}\mathcal{L}\widetilde{\Psi}^\top = \Lambda = \mathrm{diag}(\lambda_2, \lambda_3, \ldots, \lambda_N)$, we have that

$$\bar{\Psi}^\top A_f^\top \bar{\Psi} = \begin{bmatrix} \bar{A} & -\bar{B} \\ \bar{K}\bar{A} - \bar{E}\bar{K} & \bar{E} - \bar{K}\bar{B} \end{bmatrix} =: \bar{A}_f$$

where $\bar{A} = I \otimes A + \Lambda \otimes BKH$, $\bar{B} = I \otimes B$, $\bar{E} = I \otimes E$, and $\bar{K} = \Lambda \otimes KH$. Therefore, from (4.21), it follows that

$$\langle \nabla V(\xi), f(\xi)\rangle = z^\top \bar{\Psi}(R(\tau)\bar{A}_f + \bar{A}_f^\top R(\tau) - \sigma\tilde{R}(\tau))\bar{\Psi}^\top z z^\top \bar{\Psi} M(\tau)\bar{\Psi}^\top z$$

where M is defined in (4.16). From (4.16) it follows that

$$\langle \nabla V(\xi), f(\xi) \rangle = z^\top \bar{\Psi} M(\tau) \bar{\Psi}^\top z \leq -\beta |\xi|_{\mathcal{A}}^2 \leq -\frac{\beta}{\alpha_2} V(\xi) \tag{4.22}$$

where $\beta = -\max_{\nu \in \mathcal{T}} \overline{\lambda}(M(\nu))$ and α_2 is defined in (4.17).

Next, we consider the case $\xi \in D$ and $g \in G(\xi)$. In particular, if there exists at least one component of τ, say, the i-th component, such that $\tau_i = 0$. From the definition of G in (4.13), x is updated by its identity, $\theta_i^+ = 0$ and $\tau_i^+ \in [T_1^i, T_2^i]$. Moreover, for each $k \in \mathcal{V} \setminus \{i\}$, the k-th component of θ is updated by its identity, i.e., $\theta_k^+ = \theta_k$. Therefore, it follows that during jumps we have that $(\theta^+)^\top \theta^+ \leq \theta^\top \theta$ due to the i-th component being updated to zero when $\tau_i = 0$. Likewise, after the jump of the i-th timer τ_i, we have that τ_i^+ is reset to a point $\nu \in [T_1^i, T_2^i]$. It follows that $\exp(\sigma \bar{\tau}^+) = \exp(\sigma \bar{\tau}) \exp(\sigma \frac{\nu}{N})$. Then, the function V after a jump is given by

$$V(g) \leq \exp\left(\sigma \frac{\overline{T}}{N}\right) V(\xi). \tag{4.23}$$

$$\begin{aligned}
V(g) - V(\xi) &= (z^+)^\top \bar{\Psi} R(\tau^+) \bar{\Psi}^\top z^+ - z^\top \bar{\Psi} R(\tau) \bar{\Psi}^\top z \\
&= x^\top (\widetilde{\Psi}^\top \otimes I_n) P (\widetilde{\Psi}^\top \otimes I_n)^\top x - x^\top (\widetilde{\Psi} \otimes I_n) P (\widetilde{\Psi}^\top \otimes I_n) x \\
&\quad + \exp(\sigma \bar{\tau}^+) (\theta^+)^\top (\widetilde{\Psi} \otimes I_p) Q (\widetilde{\Psi}^\top \otimes I_p) \theta^+ - \exp(\sigma \bar{\tau}) \theta^\top (\widetilde{\Psi} \otimes I_p) Q (\widetilde{\Psi}^\top \otimes I_p) \theta \\
&\leq \exp(\sigma \bar{\tau}^+) (\theta^+)^\top (\widetilde{\Psi} \otimes I_p) Q (\widetilde{\Psi}^\top \otimes I_p) \theta^+ - \exp(\sigma \bar{\tau}) \theta^\top (\widetilde{\Psi} \otimes I_p) Q (\widetilde{\Psi}^\top \otimes I_p) \theta \\
&\leq \left(\exp\left(\sigma \frac{\nu}{N}\right) - 1\right) \exp(\sigma \bar{\tau}) \theta^\top (\widetilde{\Psi} \otimes I_p) Q (\widetilde{\Psi}^\top \otimes I_p) \theta \\
&\leq \left(\exp\left(\sigma \frac{\overline{T}}{N}\right) - 1\right) V(\xi).
\end{aligned} \tag{4.24}$$

due to $\bar{\tau} \leq \overline{T}$. Note that the quantity $\exp(\sigma \frac{\overline{T}}{N}) - 1$ may be positive.

Next, we evaluate V over a solution to ensure that the distance of the solution ϕ to the

set $\mathcal{A}$ converges to zero in the limit as $t+j$ approaches infinity. Pick $\phi \in \mathcal{S}_{\mathcal{H}}$ and any $(t,j) \in \operatorname{dom}\phi$. Let $0 = t_0 \leq t_1 \leq t_2 \leq \cdots \leq t_{j+1} \leq t$ satisfy $\operatorname{dom}\phi \bigcup ([0,t_{j+1}] \times \{0,1,2,\ldots,j\}) = \bigcup_{s=0}^{j}([t_s,t_{s+1}] \times \{s\})$ for each $s \in \{0,1,2,\ldots,j\}$ and almost all $r \in [t_s,t_{s+1}], \phi(r,s) \in C$. Then, (4.22) implies that, for each $s \in \{0,1,2,\ldots,j\}$ and for almost all $r \in [t_s,t_{s+1}]$,

$$\frac{d}{dr}V(\phi(r,s)) \leq -\frac{\beta}{\alpha_2}V(\phi(r,s)). \tag{4.25}$$

Integrating both sides of this inequality yields

$$V(\phi(t_{s+1},s)) \leq \exp\left(-\frac{\beta}{\alpha_2}(t_{s+1}-t_s)\right)V(\phi(t_s,s)) \tag{4.26}$$

for each $s \in \{0,1,\ldots,j\}$. Similarly, for each $s \in \{1,2,\ldots,j\}, \phi(t_s,s-1) \in D$, and using (4.24), we get

$$V(\phi(t_s,s)) \leq \exp\left(\sigma\frac{\overline{T}}{N}\right)V(\phi(t_s,s-1)). \tag{4.27}$$

It follows, from the previous two inequalities, for each $(t,j) \in \operatorname{dom}\phi$,

$$V(\phi(t,j)) \leq \exp\left(-\frac{\beta}{\alpha_2}t + \sigma\frac{\overline{T}}{N}j\right)V(\phi(0,0)) \tag{4.28}$$

By virtue of (4.19) and Lemma 4.2.3, it follows that (4.28) becomes

$$|\phi(t,j)|_{\mathcal{A}} \leq \sqrt{\frac{\alpha_2}{\alpha_1}}\exp\left(\frac{\beta(1-\varepsilon)\underline{T}}{2\alpha_2}\right)\exp\left(-\frac{\beta\varepsilon}{2\alpha_2}t + \left(\frac{\sigma\overline{T}}{2N} - \frac{\beta(1-\varepsilon)\underline{T}}{2\alpha_2 N}\right)j\right)|\phi(0,0)|_{\mathcal{A}}$$

where we used the property that there exists $\varepsilon \in (0,1)$ such that $t = \varepsilon t + (1-\varepsilon)t \geq \varepsilon t + (1-\varepsilon)\left(\frac{j}{N}-1\right)\underline{T}$. Moreover, from (4.17), and due to every maximal solution to $\mathcal{H}$ being complete, it follows that the bound on $|\phi(t,j)|_{\mathcal{A}}$ implies that $\mathcal{A}$ is globally exponentially stable for the hybrid system $\mathcal{H}$. ■

Remark 4.2.10 *The matrix inequality in* (4.16) *comes from the asymptotic stability analysis in the proposed new coordinates* $\xi = (x,\theta,\tau)$*, namely, the analysis during flows; see* (4.22)*. This*

approach introduces some conservativeness as the reset of θ_i to zero when $\tau_i = 0$ is not being exploited. This is due to the multiplication of θ by $\widetilde{\Psi} \otimes I_p$ in V. In fact, it is not straightforward to ensure a nonpositive change in V during jumps. If such a change could be guaranteed, then the conditions in Theorem 4.2.9 could be relaxed. Though it exists due to converse theorems, at this time we do not have a Lyapunov function that satisfies the decreasing properties on both jumps and flows.

Note that the matrix in (4.1) must be satisfied for an infinite number of points, i.e., $\nu \in [0, \overline{T}]$. Moreover, it can be noted that (4.16) may be a large matrix in general, which could make finding feasible solutions difficult. It turns out that (4.16) can be decomposed into $N-1$ matrices due to the fact that each block in the matrix is block diagonal. This leads to the following result.

Proposition 4.2.11 *Let $0 < T_1^i \leq T_2^i$ be given for all $i \in \mathcal{V}$. Inequality* (4.16) *holds if there exist a scalar $\sigma > 0$ and matrices $P_i = P_i^\top > 0$ and $Q_i = Q_i^\top > 0$ for each $i \in \{2, 3, \ldots, N\}$ satisfying $\overline{M}_i(0) < 0$ and $\overline{M}_i(\overline{T}) < 0$ where*

$$\overline{M}_i(\nu) := \begin{bmatrix} \mathrm{He}(P\bar{A}_i) & -PB + \exp(\sigma\nu)(\bar{K}_i\bar{A}_i - E\bar{K}_i)Q_i \\ \star & \mathrm{He}(\exp(\sigma\nu)Q_i(E - \bar{K}_iB - \frac{\sigma}{2}I)) \end{bmatrix} \tag{4.29}$$

for each $\lambda_i \in \lambda(\mathcal{L}) \setminus \{0\}$, where $\bar{A}_i = A + \lambda_i BKH$ and $K_i = \lambda_i KH$.

Proof By definitions of P, Q, Λ and the He operator, the matrix in (4.16) is a block diagonal matrix. Therefore, we can rearrange M in (4.16) as the diagonal of $N-1$ sub-matrices $\overline{M}(\nu) = \mathrm{diag}(\overline{M}_2(\nu), \overline{M}_3(\nu), \ldots, \overline{M}_N(\nu))$ where, for each $i \in \{2, 3, \ldots, N\}$, M_i is given by (4.29). Given $\nu \in [0, \overline{T}]$ and $\sigma > 0$, define the function $r : [0, \overline{T}] \to [0, 1]$ as $r(\nu) = \frac{\exp(\sigma\nu) - \exp(\sigma\overline{T})}{1 - \exp(\sigma\overline{T})}$ for each $\nu \in [0, \overline{T}]$. Then, it can be verified that for any $\nu \in [0, \overline{T}]$ $\exp(\sigma\nu) = r(\nu) + (1 - r(\nu))\exp(\sigma\overline{T})$. Therefore, for each $\nu \in [0, \overline{T}]$, the matrix $\overline{M}_i$ in (4.29) can be rewritten as $\overline{M}_i(\nu) = r(\nu)\overline{M}_i(0) +$

$(1-r(\nu))\overline{M}_i(\overline{T})$. By assumption $\overline{M}_i(0) < 0$ and $\overline{M}_i(\overline{T}) < 0$, for each $i \in \{2, \ldots, N\}$, and hence (4.16) holds for each $\nu \in [0, \overline{T}]$. ■

Remark 4.2.12 *Note that conditions $\overline{M}_i(0) < 0$ and $\overline{M}_i(\overline{T}) < 0$ are nonconvex in P, Q, K, E, and σ. At this time, there is no clear way to reduce the matrices in the conditions into a convex form. In fact, the matrices are bilinear in these variables; therefore, to solve* (4.29) *one should use a BMI solver such as YALMIP and BMILAB.*

Remark 4.2.13 *For the case of synchronous communication, a single timer $\tau \in [0, T_2]$ can be used to trigger the communication between all agents. Then, through the change of coordinates in* (4.10) *and following the approach in the proof of Theorem 4.2.9, it can be shown that if parameters, gains, and matrices exist such that* (4.16) *is satisfied for all $\tau \in [0, T_2]$ then the resulting hybrid system with a single timer has the corresponding synchronization set exponentially stable.*

4.2.4 Time to Synchronize

Due to its properties along solutions shown in Theorem 4.2.9, the proposed Lyapunov function can be further exploited to provide a bound on the time to converge to a neighborhood about the synchronization set $\mathcal{A}$. As expected, this time depends on the initial distance to the set $\mathcal{A}$ and the parameters of the hybrid system.

Proposition 4.2.14 *Given $0 < T_1^i \leq T_2^i$ for each $i \in \mathcal{V}$ and an undirected connected graph Γ, if there exist scalars $\sigma > 0$ and $\varepsilon \in (0, 1)$, matrices $K \in \mathbb{R}^{n \times p}$ and $E \in \mathbb{R}^{p \times p}$, and positive definite symmetric matrices P_i, Q_i for each $i \in \{2, 3, \ldots, N\}$,* (4.16) *and* (4.17)*, then for each $c_0 > c_1 > 0$ every maximal solution ϕ to $\mathcal{H}$ with initial condition*[7] *$\phi(0,0) \in \mathcal{X} \cap L_V(c_0)$ is such*

[7] A sublevel set of V, denoted as $L_V(\mu)$, is given by $L_V(\mu) := \{x \in \mathcal{X} : V(x) \leq \mu\}$.

that $\phi(t,j) \in L_V(c_1)$ *for each* $(t,j) \in \operatorname{dom}\phi$, $t+j \geq \bar{r}$, *where* $\bar{r} = (\frac{N}{\underline{T}}+1)\Omega+1$, $\Omega = \frac{\ln\left(\frac{c_1}{c_0}\right)-\sigma\frac{\overline{T}}{N}}{\frac{-\beta}{\alpha_2}+\frac{\sigma\overline{T}}{\underline{T}}}$, *and* $\underline{T}$, $\overline{T}$, β *and* α_2 *are given below* (4.17).

Proof Let $\phi_0 = \phi(0,0)$ and pick a maximal solution $\phi \in \mathcal{S}_{\mathcal{H}}(\phi_0)$. From the proof of Theorem 4.2.9, we have that, for each $(t,j) \in \operatorname{dom}\phi$, (4.28) holds. Namely, for each $(t,j) \in \operatorname{dom}\phi$, V satisfies $V(\phi(t,j)) \leq \exp\left(-\frac{\beta}{\alpha_2}t + \sigma\frac{\overline{T}}{N}j\right)V(\phi_0)$. We want to find $(T,J) \in \operatorname{dom}\phi$ such that $V(\phi(T,J)) \leq c_1$ when $\phi(0,0) \in L_V(c_0)$. Considering the worst case for $V(\phi_0)$, it follows that $c_1 \leq \exp\left(-\frac{\beta}{\alpha_2}T + \sigma\frac{\overline{T}}{N}J\right)c_0$ which implies that $\ln\left(\frac{c_1}{c_0}\right) \leq -\frac{\beta}{\alpha_2}T + \sigma\frac{\overline{T}}{N}J$. Then, from Lemma 4.2.3, we have that for $(T,J) \in \operatorname{dom}\phi$, it follows that $J \leq N\left(\frac{T}{\underline{T}}+1\right)$ which implies that $T \leq \Omega$ where $\Omega = \frac{\ln\left(\frac{c_1}{c_0}\right)-\sigma\frac{\overline{T}}{N}}{\frac{-\beta}{\alpha_2}+\frac{\sigma\overline{T}}{\underline{T}}}$. Then, after $t+j \geq T+J$, the solution is at least c_1 close to the set $\mathcal{A}$. Defining $\bar{r} = T+J$, we have that $\bar{r} = \left(\frac{N}{\underline{T}}+1\right)\Omega+1$. ■

4.2.4.1 Sufficient Conditions for Asymptotic Synchronization under Synchronous Communication

In this section, we consider the case of synchronization when communication times are synchronized for each agent. Namely, we consider agents with the dynamics in (4.1) and output in (4.2), whose inputs are assigned by a controller governed by η_i given by the flow and jump dynamics in (4.4) and (4.5), respectively. We propose two different designs of the maps defining the controllers. Moreover, we consider the case when the sequence of communication times $\{t_s^i\}_{s=1}^{\infty}$ governed by (4.3) are equal for each $i \in \mathcal{V}$ where T_1 and T_2 are now the bounds on the intervals between communication time. Following the timer construction in (4.6), we use a single timer $\tau \in [0,T_2]$ with dynamics

$$\begin{aligned} \dot{\tau} &= -1 & \tau &\in [0,T_2], \\ \tau^+ &\in [T_1,T_2] & \tau &= 0. \end{aligned} \tag{4.30}$$

Consider the controller with state η_i having continuous dynamics given by

$$\dot{\eta}_i = h_i \eta_i \tag{4.31}$$

when $\tau \in [0, T_2]$ and discrete dynamics given by

$$\eta_i^+ = K \sum_{i=1}^{N} g_{ik}(y_i - y_k) \tag{4.32}$$

when $\tau = 0$. With some abuse of notation, using the coordinate change θ_i in (4.10), we define the state of the resulting hybrid system, denoted by $\mathcal{H}_s$, as $\xi = (z, \tau)$, where $z = (x, \theta)$. Then, the resulting dynamics from given by interconnecting agents given by (4.1) with controller dynamics (4.7) and (4.8) is given by

$$\begin{array}{rcl} \dot{\xi} & = & (A_f z, -1) \qquad\qquad \tau \in [0, T_2] \\ \xi^+ & \in & (A_g z, [T_1, T_2]) \qquad\qquad \tau = 0 \end{array} \tag{4.33}$$

where

$$A_f = \begin{bmatrix} A_1 & -\widetilde{B} \\ \widetilde{K} A_1 - \widetilde{E}\widetilde{K} & \widetilde{E} - \widetilde{K}\widetilde{B} \end{bmatrix} \qquad A_g = \begin{bmatrix} I & 0 \\ 0 & 0 \end{bmatrix}$$

$A_1 = I \otimes A + \widetilde{B}\widetilde{K}$, $\widetilde{B} = I \otimes B$, $\widetilde{K} = \mathcal{L} \otimes KH$, and $\widetilde{E} = I \otimes E$.

Then, using the Lyapunov function V in (8.6), we have the following sufficient conditions for exponential stability of the synchronization set

$$\mathcal{A}_s := \{(x, \theta, \tau) \in \mathbb{R}^{N(n+p)} \times [0, T_2] : x_1 = x_2 = \cdots = x_N, \theta_1 = \theta_2 = \cdots = \theta_N\}. \tag{4.34}$$

associated to $\mathcal{H}_s$.

Proposition 4.2.15 *Given $0 < T_1 \leq T_2$ and an undirected connected graph Γ. The set $\mathcal{A}$ in (4.14) is globally exponentially stable for the hybrid system $\mathcal{H}_s$ in (4.62) if there exist scalars $\sigma > 0$ and $\varepsilon \in (0, 1)$, matrices $K \in \mathbb{R}^{n \times p}$ and $E \in \mathbb{R}^{p \times p}$ and positive definite symmetric*

matrices P_i, Q_i for each $i \in \{2, 3, \ldots, N\}$, satisfying $\bar{M}(0) < 0$ and $\bar{M}(T_2) < 0$ where $\bar{M}$ is given in (4.29)*. Moreover, every maximal solution ϕ to the hybrid system from $\phi(0,0)$ in* (4.62) *satisfies*

$$|\phi(t,j)|_{\mathcal{A}} \leq \kappa_s \exp\left(-r(t+j)\right) |\phi(0,0)|_{\mathcal{A}} \tag{4.35}$$

for all $(t,j) \in \operatorname{dom}\phi$, where $\kappa_s = \sqrt{\frac{\alpha_2}{\alpha_1}} \exp\left(\frac{\beta T_1}{2\alpha_2(T_1+1)}\right)$, $r = \frac{\beta}{2\alpha_2}\frac{T_1}{T_1+1}$, and α_1, α_2, and β are given below (4.17)*.*

Proof Consider the Lyapunov function V given by

$$V(\xi) = z^\top \bar{\Psi} R(\tau) \bar{\Psi}^\top z \tag{4.36}$$

where $R = \operatorname{diag}(P, Q\exp(\sigma\tau))$, $P = \operatorname{diag}(P_2, P_3, \ldots, P_N)$ and $Q = \operatorname{diag}(Q_2, Q_3, \ldots, Q_N)$. It follows that (4.19) holds for the set $\mathcal{A}_s$. Moreover, for each $\tau \in [0, T_2]$ the change in V is equivalent to (4.22) using similar arguments as in the proof of Theorem 4.2.9. During jumps, i.e., when $\tau = 0$, the jump map G updates each state as follows: $\tau^+ \in [T_1, T_2]$,and $x^+ = x$, and $\theta^+ = 0$, which implies that the difference in V at jumps is given by

$$V(G(\xi)) - V(\xi) = -\theta(\widetilde{\Phi} \otimes I_p) Q (\widetilde{\Phi}^\top \otimes I_p)\theta \leq 0. \tag{4.37}$$

Following the proof of Theorem 4.2.4, integrating both sides of (4.25) yields (4.26). From (4.37), we have that $V(\phi(t_s, s)) \leq V(\phi(t_s, s-1))$. By combining (4.26) with V during jumps with (4.19), we have that

$$|\phi(t,j)|_{\mathcal{A}} \leq \sqrt{\frac{\alpha_2}{\alpha_1}} \exp\left(-\frac{\beta}{2\alpha_2} t\right) |\phi(0,0)|_{\mathcal{A}}$$

which results in (4.35), where we use the property that, for each $(t,j) \operatorname{dom}\phi$, $t \geq (j-1)T_1$ and $t = \varepsilon t + (1-\varepsilon)t \geq \varepsilon t + (1-\varepsilon)T_1(j-1)$, where $\varepsilon = \frac{T_1}{T_1+1}$. Due to the fact that every maximal solution to $\mathcal{H}$ is complete, it follows that the bound on $|\phi(t,j)|_{\mathcal{A}}$ implies that $\mathcal{A}$ is

globally exponentially stable for the hybrid system $\mathcal{H}_s$ defined in (4.62). Due to $\overline{M}_i(0) < 0$ and $\overline{M}_i(\overline{T}) < 0$, the steps in Proposition 4.2.11 can be applied to conclude the proof. ■

Now, we consider a sample-and-hold controller which yields an alternative design condition than in Proposition 4.2.15. The functions f_{ci} and G_{ci}^k are now given by

$$f_{ci}(x_i, \eta_i) = 0 \tag{4.38}$$

for all $(x_i, \eta_i) \in \mathbb{R}^n \times \mathbb{R}^p$, and by

$$G_{ci}^k(\eta_i, \eta_k, y_i, y_k) = \frac{1}{d_i^{in}} K_i(y_i - y_k). \tag{4.39}$$

for all $(\eta_i, \eta_k, y_i, y_k) \in \mathbb{R}^n \times \mathbb{R}^n \times \mathbb{R}^m \times \mathbb{R}^m$.

Now, we consider the change of coordinates ε_i, where ε_i defines the local relative error of the i-th system. Namely, $\varepsilon_i = \frac{1}{d_{in}^i} \sum_{k \in \mathcal{J}_i} (x_i - x_k)$. Note that at jumps, i.e., when $\tau = 0$, $\varepsilon_i^+ = \varepsilon_i$ and $\eta_i^+ = K_i H \varepsilon_i$. Let $\xi = (z, \tau)$, $z = (z_1, z_2, \ldots, z_N)$, and $z_i = (\varepsilon_i, \eta_i)$. Then, the new coordinates lead to a closed loop hybrid system, denoted as $\mathcal{H}_\varepsilon$, with the following data

$$\begin{aligned} f_\varepsilon(\xi) &= \begin{bmatrix} \bar{A}_f z \\ -1 \end{bmatrix} \quad \forall \xi \in C_\varepsilon := \mathbb{R}^{N(n+p)} \times [0, T_2] \\ G_\varepsilon(\xi) &= \begin{bmatrix} \bar{A}_g z \\ [T_1, T_2] \end{bmatrix} \quad \forall \xi \in D_\varepsilon := \mathbb{R}^{N(n+p)} \times \{0\} \end{aligned} \tag{4.40}$$

where the matrices $\bar{A}_f = I \otimes A_f - (\mathcal{G}^\top D_{in}^{-1}) \otimes B_f$, $\bar{A}_g = \text{diag}(A_{g1}, A_{g2}, \ldots, A_{gN}$, $D_{in} = \text{diag}(d_1^{in}, d_2^{in}, \ldots, d_N^{in})$, $A_f = \begin{bmatrix} A & B \\ 0 & 0 \end{bmatrix}$, $B_f = \begin{bmatrix} 0 & B \\ 0 & 0 \end{bmatrix}$, and $A_{gi} = \begin{bmatrix} I & 0 \\ K_i H & 0 \end{bmatrix}$.

Moreover, due to the change in coordinates, to stabilize the set of points is given by

$$\mathcal{A}_\varepsilon := \{0\} \times [0, T_2] \tag{4.41}$$

which is compact. Next, we present sufficient conditions for exponential synchronization of the

set $\mathcal{A}_\varepsilon$ for the hybrid system with data as in (4.40).

Theorem 4.2.16 *Let T_1 and T_2 be positive scalars such that $T_1 \leq T_2$ and the digraph Γ be strongly connected. If there exist a nonnegative scalar σ, a positive definite symmetric matrix $P \in \mathbb{R}^{N(n+p)\times N(n+p)}$, and matrices $K_i \in \mathbb{R}^{p\times n}$ for each $i \in \mathcal{V}$ such that*

$$\exp(\sigma\nu)\bar{A}_g^\top \exp(\bar{A}_f^\top \nu)P \exp(\bar{A}_f\nu)\bar{A}_g - P < 0 \tag{4.42}$$

for all $\nu \in [T_1, T_2]$, then the set $\mathcal{A}_\varepsilon$ in (4.41) is globally exponentially stable for $\mathcal{H}_\varepsilon$ in (4.40). Moreover, every $\phi \in \mathcal{H}_\varepsilon$ is such that

$$|\phi(t,j)|_{\mathcal{A}_\varepsilon} \leq \sqrt{\frac{\alpha_2}{\alpha_1}} \exp\left(-\min\left\{\sigma, -\lambda_d\right\}(t+j)\right) |\phi(0,0)|_{\mathcal{A}_\varepsilon} \tag{4.43}$$

for every $(t,j) \in \operatorname{dom}\phi$ where $\varepsilon \in (0,1)$, $\lambda_d = \ln(1-\frac{\beta}{\alpha_2})$, with $\beta > 0$ small enough, and

$$\begin{aligned} \alpha_1 &= \underline{\lambda}\left(\min_{\tau\in[0,T_2]} \exp(\bar{A}_f^\top \tau)P\exp(\bar{A}_f\tau)\right) \\ \alpha_2 &= \exp(\sigma T_2)\overline{\lambda}\left(\max_{\tau\in[0,T_2]} \exp(\bar{A}_f^\top \tau)P\exp(\bar{A}_f\tau)\right) \end{aligned} \tag{4.44}$$

Proof Consider the Lyapunov function

$$V(\xi) = \exp(\sigma\tau)z^\top \exp(\bar{A}_f^\top \tau)P\exp(\bar{A}_f\tau)z \tag{4.45}$$

with P positive definite and σ nonnegative. Note that V is bounded by

$$\alpha_1|z|^2_{\mathcal{A}_\varepsilon} \leq V(\xi) \leq \alpha_2|z|^2_{\mathcal{A}_\varepsilon} \tag{4.46}$$

where α_1 and α_2 are given below (4.43).

During flows, for each $\xi \in C$, we have that the change in V is given by $\langle \nabla V(\xi), f(\xi)\rangle =$

$-V(\xi)$, namely,

$$\begin{aligned}\langle \nabla V(\xi), F(\xi)\rangle &= 2\exp((\sigma\tau)z^\top \exp(\bar{A}_f^\top \tau)P\exp(\bar{A}_f\tau)z - \sigma\exp(\sigma\tau)z^\top \exp(\bar{A}_f^\top\tau)P\exp(\bar{A}_f\tau)z \\ &\quad + \exp(\sigma\tau)z^\top \exp(\bar{A}_f^\top\tau)(\bar{A}_f^\top P + P\bar{A}_f)\exp(\bar{A}_f\tau)z \\ &= -\sigma\exp(\sigma\tau)z^\top \exp(\bar{A}_f^\top\tau)P\exp(\bar{A}_f\tau)z = -\sigma V(\xi). \end{aligned} \tag{4.47}$$

Next, we consider the case of $\xi \in D$, for such a case, we have that $\tau = 0$ and is mapped to a point ν in the interval $[T_1, T_2]$; likewise, the state z is mapped to $\bar{A}_g z$. In light of (4.42), there exists small enough $\beta > 0$ such that, for each $\xi \in D$, $g \in G(\xi)$, the change in V is given by

$$V(g) - V(\xi) \leq -\beta z^\top z = -\beta|z|_{\mathcal{A}_\varepsilon} \leq -\frac{\beta}{\alpha_2}V(\xi). \tag{4.48}$$

First, pick a maximal solution, ϕ to $\mathcal{H}$ with data as in (4.40), without loss of generality, from $\phi(0,0) \in C$. From direct integration of the change in V during flows, we have

$$V(\phi(t_{j+1}, j)) = \exp(-\sigma(t_{j+1} - t_j))V(\phi(t_j, j)) \tag{4.49}$$

where $(t_{j+1}, j), (t_j, j) \in \operatorname{dom}\phi$. The change in V during jumps leads to

$$V(\phi(t_j, j+1)) \leq \exp(\lambda_d)V(\phi(t_j, j)) \tag{4.50}$$

where $\lambda_d = \ln(1 - \frac{\beta}{\alpha_2}) < 0$ due to β being small. Then by combines (4.49) and (4.50), the function V over any maximal solution ϕ is given by

$$\begin{aligned} V(\phi(t,j)) &\leq V(\phi(0,0))\exp(-\sigma t + \lambda_d j) \\ &\leq V(\phi(0,0))\exp(-\min(\sigma, -\lambda_d)(t+j)) \end{aligned}$$

with $\sigma, -\lambda_d > 0$ for every $(t,j) \in \operatorname{dom}\phi$. From (4.46), we obtain the expression in (4.43) which implies that the set $\mathcal{A}_\varepsilon$ is GES for the hybrid system $\mathcal{H}$ with data as in (4.40). ■

Remark 4.2.17 *Note that condition* (4.42) *is akin to the discrete Lyapunov equation with sys-*

tem matrix $H(\nu) = e^{\sigma\nu/2} e^{\bar{A}_f \nu} \bar{A}_g$ *which implies that condition* (4.42) *is satisfied if, for each* $\nu \in [T_1, T_2]$*, the eigenvalues of* $H(\nu)$ *are contained with the unit circle.*

Remark 4.2.18 *Typically written in the literature, a directed tree is a directed graph, where every node, except a single root node, has exactly one parent. A directed spanning tree is a directed tree formed by graph edges that connect all the nodes of the graph [48]. Theorem 4.2.16 may be extended to the case when only a directed spanning tree is required, similar to that in [59, 60]. However, such a notion for an undirected graph is a subset of connected graphs, namely, a spanning tree for an undirected graph is connected, but not the reverse.*

Remark 4.2.19 *Proposition 4.2.15 and Theorem 4.2.16 require different matrix inequalities to be satisfied for exponential stability of the synchronization sets in their respective coordinates. The expression* (4.42) *in Proposition 4.2.15 is akin to a continuous-time Lyapunov condition, and, as mentioned in Remark 4.2.17, the expression* (4.42) *in Theorem 4.2.16 is similar to that of a discrete-time Lyapunov condition. However, due to the change in coordinates it is not analytically clear which one is tighter. To shed some light on this issue, Example 4.3.2 compares, under reasonable assumptions, how the gains* K *and* E *that can be chosen to satisfy both conditions. Moreover, in that example, we compare the convergence speed to the synchronization set.*

4.2.5 Robustness of Synchronization

In this section, we consider the effect of general perturbations and unmodeled dynamics on the agents in the network. In such a setting, the perturbed model of each agent is given in (4.1) and the output generated by each agent is given by (4.2), where the functions $\Delta_i : \mathbb{R}^n \times \mathbb{R}_{\geq 0} \to \mathbb{R}^n$ and $\varphi_i : \mathbb{R}^n \to \mathbb{R}^p$ are unknown functions that may capture the unmodeled

dynamics, as well as, the disturbances and communication noise, respectively. In particular, due to the disturbances on the output, the values of y_k transmitted to agent i at communication times $t = t_s$ from agent k (where $k \in \mathcal{N}(i)$) may be affected by some communication channel noise, specifically, $y_k(t_s) = Hx_k(t_s) + \varphi_k(x_k(t_s), t_s)$.

Adding the perturbations to (4.7) and (4.8), we have that the continuous dynamics of the distributed controllers do not change, but the discrete dynamics become

$$\eta_i^+ = KH \sum_{k \in \mathcal{N}(i)} (x_i - x_k) + K\tilde{\varphi}_i(x, t) \tag{4.51}$$

where $\tilde{\varphi}_i(x, t) = \sum_{k \in \mathcal{N}(i)} (\varphi_i(x_i, t) - \varphi_k(x_k, t))$. For simplicity, hence forth we will drop the arguments of some of the perturbations. We will consider the model in the θ coordinates in Section 4.2.1 for the study of robustness. Then, following the definition of θ_i in (4.10), the resulting perturbed hybrid system $\widetilde{\mathcal{H}}$ has data $(C, \widetilde{f}, D, \widetilde{G})$ and state $\xi = (z, \tau) \in \mathcal{X}$, $z = (x, \theta)$. The perturbed data is given by

$$\widetilde{f}(\xi) = f(\xi) + (\Delta(x, t), \widetilde{K}\Delta(x, t), 0) \quad \forall \xi \in C \tag{4.52}$$

where $\Delta(t, x) = (\Delta_1(x_1, t), \Delta_2(x_1, t), \ldots, \Delta_N(x_1, t))$ and $\widetilde{K} = (\mathcal{L} \otimes KH)$. Moreover, when $\xi \in D$,

$$\widetilde{G}(\xi, \varphi) := \{\widetilde{G}_i(\xi, \delta) : \xi \in \widetilde{D}_i, i \in \mathcal{V}\} \qquad \forall \xi \in D \tag{4.53}$$

and

$$\widetilde{G}(\xi, \varphi) := \begin{bmatrix} x \\ (\theta_1, \theta_2, \ldots, \theta_{i-1}, -K\tilde{\varphi}_i, \theta_{i+1}, \ldots, \theta_N) \\ (\tau_1, \tau_2, \ldots, \tau_{i-1}, [T_1^i, T_2^i], \tau_{i+1}, \ldots, \tau_N) \end{bmatrix}. \tag{4.54}$$

In the following sections, we will discuss the robustness of the hybrid system $\widetilde{\mathcal{H}}$ to different classes of perturbations. In particular, we will discuss its robustness to general pertur-

bations on compact set via the hybrid basic conditions and input-to-state stability relative to the synchronization set $\mathcal{A}$.

4.2.5.1 General Robustness on Compact Sets

In this section, we focus on the generic robustness property to small perturbations. To apply standard robustness results for hybrid systems, the set that is asymptotically stable must be compact. Note that the set $\mathcal{A}$ given by (4.14) is unbounded: the points $x_1 = x_2 = \cdots = x_N$ and $\theta_1 = \theta_2 = \cdots = \theta_N$ can be any value in $\mathbb{R}^n$ and $\mathbb{R}^p$, respectively. Therefore, we restrict the state space to the compact set $S \times \mathcal{T}$. While this set restricts the state space of the hybrid system, it can easily be considered to be arbitrarily large. The price to pay is that, due to the fact that the state space is now bounded, it is not guaranteed that maximal solutions to the hybrid system are complete. We consider the hybrid system $\widetilde{\mathcal{H}} = (C, \widetilde{f}, D, \widetilde{G})$ as in Section 4.2.1 with flow and jumps sets given by $\widetilde{C} = C \cap (S \times \mathcal{T})$ and $\widetilde{D} = D \cap (S \times \mathcal{T})$ where $S \subset \mathbb{R}^{N(n+p)}$ is compact. Moreover, the set of interest is given by $\widetilde{\mathcal{A}} = \mathcal{A} \cap (S \times \mathcal{T})$. We have the following result.

Theorem 4.2.20 *Let $0 < T_1^i \leq T_2^i$ be given for all $i \in \mathcal{V}$. Suppose that the hybrid system satisfies the conditions in Theorem 4.2.9 for the unperturbed hybrid system $\mathcal{H}$ with data in* (4.12) *and* (4.13)*. Then, there exists $\beta \in \mathcal{KL}$ such that, for every compact set $S \subset \mathbb{R}^{N(n+p)}$ and $\varepsilon > 0$, there exists $\rho^\star \geq 0$ such that if $\max\{\bar{\Delta}, \bar{\varphi}\} \leq \rho^\star$ where $\bar{\Delta} = \sup_{(x,t)\in\mathcal{X}\cap(S\times\mathcal{T})\times\mathbb{R}_{\geq 0}} |\Delta(x,t)|$ and $\bar{\varphi} = \sup_{(x,t)\in\mathcal{X}\cap(S\times\mathcal{T})\times\mathbb{R}_{\geq 0}} |\widetilde{\varphi}(x,t)|$ then, every $\phi \in \mathcal{S}_{\widetilde{\mathcal{H}}}(S \times \mathcal{T})$ satisfies $|\phi(t,j)|_{\widetilde{\mathcal{A}}} \leq \beta(|\phi(0,0)|_{\widetilde{\mathcal{A}}}, t + j) + \varepsilon$ for all $(t,j) \in \operatorname{dom}\phi$.*

Proof Consider the hybrid system $\widetilde{\mathcal{H}}$ and a continuous function $\rho : \mathbb{R}^{nN} \times \mathbb{R}^{pN} \times \mathcal{T} \to \mathbb{R}_{\geq 0}$,

the ρ-perturbation of $\widetilde{\mathcal{H}}$, denoted $\widetilde{\mathcal{H}}_\rho$, is the hybrid system

$$\begin{cases} \xi \in \widetilde{C}_\rho & \dot{\xi} \in F_\rho(\xi) \\ \xi \in \widetilde{D}_\rho & \xi^+ \in G_\rho(\xi) \end{cases} \tag{4.55}$$

where

$$\widetilde{C}_\rho = \{\xi \in \widetilde{C} \cup \widetilde{D} : (\xi + \rho(\xi)\mathbb{B}) \cap \widetilde{C} \neq 0\}$$

$$F_\rho(\xi) = \overline{\text{con}} f((\xi + \rho(\xi)\mathbb{B}) \cap C = +\rho(\xi)\mathbb{B} \quad \forall \xi \in \widetilde{C} \cap \widetilde{D}$$

$$\widetilde{D}_\rho = \{\xi \in \widetilde{C} \cup \widetilde{D} : (\xi + \rho(\xi)\mathbb{B}) \cap \widetilde{D} \neq 0\}$$

$$G_\rho(\xi) = \{v \in \widetilde{C} \cap \widetilde{D} : v \in g + \rho(g)\mathbb{B}, g \in G(\xi + \rho(\xi)) \cap \widetilde{D}\}$$

$$\forall \xi \in \widetilde{C} \cap \widetilde{D}$$

Since the set $\mathcal{A}$ is GES for $\mathcal{H}$, it is also UGAS for $\mathcal{H}$. Since ρ is continuous and $\mathcal{H}$ satisfies the hybrid basic conditions, by [28, Theorem 6.8], $\widetilde{\mathcal{H}}_\rho$ is nominally well-posed and, moreover, by [28, Proposition 6.28] is well-posed. Then, [28, Theorem 7.20] implies that $\mathcal{A}$ is semiglobally practically robustly $\mathcal{KL}$ pre-asymptotically stable for $\widetilde{\mathcal{H}}$. Namely, for every compact set $S \times \mathcal{T} \subset \mathbb{R}^{N(n+p)} \times \mathcal{T}$ and every $\varepsilon > 0$, there exists $\widetilde{\rho} \in (0,1)$ such that every maximal solution ϕ to $\mathcal{H}_{\widetilde{\rho}\rho}$ from $S \times \mathcal{T}$ satisfies $|\phi(t,j)|_{\mathcal{A}\cap(S\times\mathcal{T})} \leq \beta(|\phi(0,0)|_{\mathcal{A}\cap(S\times\mathcal{T})}, t+j) + \varepsilon$ for all $(t,j) \in \operatorname{dom}\phi$. Then, the result follows by picking $\rho^* > 0$ such that $\max\{1, |\widetilde{K}|, |K|\}\rho^* \leq \widetilde{\rho}$ and relating solutions to $\widetilde{\mathcal{H}}$ and solutions to $\mathcal{H}_{\widetilde{\rho}\rho}$. ■

4.2.5.2 Robustness to Communication Noise

In this section, we consider the hybrid system $\mathcal{H}$ in Section 4.2.5 when communication noise is present. Namely, φ_i reduces to a function $m_i(t) = \widetilde{\varphi}_i(x_i, t)$ for all $t \in \mathbb{R}_{\geq 0}$ and $i \in \mathcal{V}$. We have the following result.

Theorem 4.2.21 *Given $0 < T_1^i \leq T_2^i$ for each $i \in \mathcal{V}$ and an undirected connected graph Γ, if*

there exist scalars $\sigma > 0$, $\varepsilon \in (0,1)$ *and matrices* $K \in \mathbb{R}^{n\times p}$ *and* $H \in \mathbb{R}^{p\times p}$, *and positive definite symmetric matrices* P_i, Q_i *for each* $i \in \{2,3,\ldots,N\}$, *satisfying* (4.16) *for each* $\nu \in [0,\overline{T}]$ *and* (4.17) *holds, then the set* $\mathcal{A}$ *is input-to-state stable for the hybrid system* $\widetilde{\mathcal{H}}$ *in* (4.52) *and* (4.53) *with respect to communication noise* $m = (m_1, m_2, \ldots, m_N)$. *More specifically, for each* $\phi \in \mathcal{S}_{\widetilde{\mathcal{H}}}$ *and for any* $(t,j) \in \operatorname{dom}\phi$,

$$|\phi(t,j)|_{\mathcal{A}} \leq \max\left\{\kappa \exp\left(-r(t+j)\right)|\phi(0,0)|_{\mathcal{A}}, \gamma_m |m|_\infty\right\} \tag{4.56}$$

where $\underline{T}$, $\overline{T}$, α_2, *and* β *are given below* (4.17) *and* κ, r, α_1, *are given below* (4.18), $b = \exp(\sigma\overline{T}/N)\overline{\lambda}(Q)$, $\gamma_m = NS\sqrt{\frac{\alpha_1}{\alpha_2}}\exp(\sigma\overline{T})b|K|^2$ *and* $S = \frac{\exp(-\epsilon)}{\exp(-\epsilon)-1}$ *where* $\epsilon \in \left(0, \frac{\alpha_2\sigma\overline{T}}{\beta} - (1-\varepsilon)\underline{T}\right)$.

Proof Consider the Lyapunov function candidate $V : \mathcal{X} \to \mathbb{R}_{\geq 0}$ given by (8.6). It follows that V satisfies (4.19) for all $\xi \in C \cup D$ where α_1 and α_2 are given in the Proof of Theorem 4.2.9. Note that communication noise only occurs upon communication events, when $\xi \in D$. Therefore, for each $\xi \in C$, we have that

$$\langle \nabla V(\xi), \widetilde{f}(\xi)\rangle \leq -\beta|\xi|^2_{\mathcal{A}} \leq -\frac{\beta}{\alpha_2}V(\xi) \tag{4.57}$$

and $\beta = -\overline{\lambda}(M(\nu))$ for each $\nu \in [0,\overline{T}]$ where M is given by (4.16). Moreover, at jumps, we have that the state is updated by (4.54), with $m_i(t) = \widetilde{\varphi}_i(x,t)$. It follows that for each $\xi \in D$ and $g \in G(\xi)$, that there exists at least one timer reseting, i.e., $\tau_i = 0$, after the jump it follows that $\tau_i^+ = \nu$ where $\nu \in [T_1^i, T_2^i]$ and $\theta_i = -Km_i$. Then, if follows that

$$V(g) \leq \exp\left(\frac{\sigma\overline{T}}{N}\right)V(\xi) + b|K|^2|m|^2 \tag{4.58}$$

where $b = \exp(\sigma\overline{T}/N)\overline{\lambda}(Q)$ and we use the fact that $\exp(\sigma\bar{\tau}^+) = \exp(\sigma\bar{\tau})\exp(\sigma\nu/N)$.

Now pick $\phi \in \mathcal{S}_{\mathcal{H}}$, or any $(t,j) \in \operatorname{dom}\phi$ and let $0 = t_0 \leq t_1 \leq t_2 \leq \cdots \leq t_{j+1} \leq t$ satisfy $\operatorname{dom}\phi \cup ([0,t_{j+1}] \times \{0,1,\ldots,j\}) = \cup_{s=0}^{j}([t_s,t_{s+1}] \times \{s\})$. For each $s \in \{0,1,\ldots,j\}$ and almost all $r \in [t_s,t_{s+1}]$, $\phi(r,s) \in C$. Then, integrating both sides of (4.57) implies that for each $s \in$

$\{0, 1, \ldots, j\}$ and for almost all $r \in [t_s, t_{s+1}]$, we have that $V(\phi(r, s)) \leq \exp\left(-\frac{\beta}{\alpha_2}\right) V(\phi(t_s, s))$. Similarly, for each $s \in \{1, 2, \ldots, j\}$, $\phi(t_s, s-1) \in D$, and using (4.58), we get

$$V(\phi(t_s, s-1)) \leq \exp\left(\frac{\sigma\overline{T}}{N}\right) V(\phi(t_s, s-1) + b|K|^2|m|^2.$$

By using the previous two expressions, it follows that for each $(t, j) \in \operatorname{dom}\phi$

$$\begin{aligned} V(\phi(t, j)) \leq \exp\left(\frac{\sigma\overline{T}}{N} j - \frac{\beta}{\alpha_2} t\right) V(\phi(0, 0)) \\ + b|m|_\infty^2 \sum_{k=1}^{j} \left(\exp\left(\frac{\sigma\overline{T}}{N} k\right) \exp\left(-\frac{\beta}{\alpha_2}(t - t_k)\right)\right). \end{aligned}$$

and that the right summation of the above expression can be reduced. First, note that for $t \geq t_j$, then it follows that

$$\sum_{k=1}^{j} \exp\left(\frac{\sigma\overline{T}}{N} k\right) \exp\left(-\frac{\beta}{\alpha_2}(t - t_k)\right) \leq \sum_{k=1}^{j} \exp\left(\frac{\sigma\overline{T}}{N} k\right) \exp\left(-\frac{\beta}{\alpha_2}(t_j - t_k)\right).$$

Due to the increasing sequence of times $t_1 \leq t_2 \leq \cdots \leq t_j$, there must exist an integer $\tilde{j}$ which defines the maximum multiple of N, i.e., $\tilde{j} = \lfloor \frac{j}{N} \rfloor$. Then, the expression $\sum_{k=1}^{j} \left(\exp\left(\frac{\sigma\overline{T}}{N} k\right) \exp\left(-\frac{\beta}{\alpha_2}(t_j - t_k)\right)\right)$ can be grouped into a double sum as follows:

$$\begin{aligned} \sum_{k=1}^{j} \left(\exp \frac{\sigma\overline{T}}{N} k - \frac{\beta}{\alpha_2}(t_j - t_k)\right) = \sum_{s=0}^{\tilde{j}-1} \sum_{k=1}^{N} \exp\left(\frac{\sigma\overline{T}}{N}(sN + k) - \frac{\beta}{\alpha_2}(t_j - t_{sN+k})\right) \\ + \sum_{k=\tilde{j}N+1}^{j} \exp\left(\frac{\sigma\overline{T}}{N} k - \frac{\beta}{\alpha_2}(t_j - t_k)\right) \end{aligned}$$

Note that for each $s \in \{0, \ldots, \tilde{j} - 1\}$, it follows that

$$\begin{aligned} \max_{t_{sN+k}, k \in \{1, \ldots, N-1\}} \sum_{k=1}^{N} \exp\left(\frac{\sigma\overline{T}}{N}(sN + k) - \frac{\beta}{\alpha_2}(t_j - t_{sN+k})\right) \\ = \sum_{k=1}^{N} \exp\left(-\frac{\beta}{\alpha_2}(t_j - t_{(s+1)N}) + \sigma\overline{T}(s+1)\right) \\ = N \exp\left(-\frac{\beta}{\alpha_2}(t_j - t_{(s+1)N}) + \sigma\overline{T}(s+1)\right) \end{aligned}$$

which corresponds to the maximizer satisfying $t_{sN+k} = t_{(s+1)N}$ for all $k \in \{1, \ldots, N-1\}$.

Therefore, it follows that

$$
\begin{aligned}
&\sup_{\substack{\phi\in\mathcal{S}_{\mathcal{H}}\\(t_j,j)\in\operatorname{dom}\phi}}\sum_{k=1}^{j}\exp\left(\frac{\sigma\overline{T}}{N}k-\frac{\beta}{\alpha_2}(t_j-t_k)\right)\\
\leq&\sup_{\substack{\phi\in\mathcal{S}_{\mathcal{H}}\\(t_j,j)\in\operatorname{dom}\phi}}\sum_{s=1}^{\tilde{j}-1}\max_{\substack{t_{sN+k}\\k\in\{1,\dots,N-1\}}}\sum_{k=1}^{N}\exp\left(\frac{\sigma\overline{T}}{N}(sN+k)-\frac{\beta}{\alpha_2}(t_j-t_{sN+k})\right)\\
&\qquad+\sup_{\substack{\phi\in\mathcal{S}_{\mathcal{H}}\\(t_j,j)\in\operatorname{dom}\phi}}\sum_{k=\tilde{j}N+1}^{j}\exp\left(\frac{\sigma\overline{T}}{N}k-\frac{\beta}{\alpha_2}(t_j-t_k)\right)\\
\leq&\sup_{\substack{\phi\in\mathcal{S}_{\mathcal{H}}\\(t_j,j)\in\operatorname{dom}\phi}}\sum_{k=1}^{\tilde{j}-1}N\exp\left(-\frac{\beta}{\alpha_2}(t_{\tilde{j}N}-t_{(s+1)N})+\sigma\overline{T}(s+1)\right)+N\exp(\sigma\overline{T})
\end{aligned}
$$

where we use the property that $j-\tilde{j}N<N$. By item 3 in Lemma 4.2.3, we have that $t_{(j+1)N}-t_{jN}\in[\underline{T},\overline{T}]$ for all $j\geq 0$ such that $(t_{(j+1)N},(j+1)N),(t_{jN},jN)\in\operatorname{dom}\phi$ which implies that for each $s\in\{0,1,\dots,\tilde{j}-1\}$ $t_{\tilde{j}N}-t_{sN}\in[(\tilde{j}-s)\underline{T}),(\tilde{j}-s)\overline{T}]$. Therefore,

$$
\begin{aligned}
&\sup_{\substack{\phi\in\mathcal{S}_{\mathcal{H}}\\(t_j,j)\in\operatorname{dom}\phi}}\sum_{k=1}^{j}\exp\left(\frac{\sigma\overline{T}}{N}k-\frac{\beta}{\alpha_2}(t_j-t_k)\right)\\
&\qquad\leq N\exp(\sigma\overline{T})\sum_{s=1}^{\tilde{j}}\exp\left(\left(-\frac{\beta}{\alpha_2}\underline{T}+\sigma\overline{T}\right)s\right)+N\exp(\sigma\overline{T})\\
&\qquad=N\exp(\sigma\overline{T})\sum_{s=0}^{\tilde{j}}\exp\left(\left(-\frac{\beta}{\alpha_2}\underline{T}+\sigma\overline{T}\right)s\right)
\end{aligned}
$$

Then, it follows that

$$
\begin{aligned}
V(\phi(t,j))\leq&\exp\left(-\frac{\beta}{\alpha_2}t+\frac{\sigma\overline{T}}{N}j\right)\\
&+N\exp(\sigma\overline{T})b|K|^2|m|_\infty^2\sum_{s=0}^{\tilde{j}}\exp\left(\left(-\frac{\beta}{\alpha_2}\underline{T}+\sigma\overline{T}\right)s\right)
\end{aligned}
$$

where $\tilde{j}=\lfloor\frac{j}{N}\rfloor$. Note that by the continuity of (4.17), there exists small positive scalar ϵ such that $-\frac{\beta}{\alpha_2}\underline{T}+\sigma\overline{T}\leq-\epsilon$. Note that for each $n\in\mathbb{N}$, we have that

$$
\sum_{s=0}^{n}\exp\left(-\epsilon s\right)\leq\frac{\exp(-\epsilon)}{\exp(-\epsilon)-1}=:S. \tag{4.59}
$$

Then, it follows from (4.19), we have (4.56). We can conclude the proof using similar arguments as in the proof of Theorem 4.2.9. ■

4.2.5.3 Synchronous Communication Case

In this section, we consider the hybrid system $\mathcal{H}_\varepsilon$ in Section 4.2.4.1 when communication noise is present. Namely, we define a function $m_i(t) = \varphi_i(x_i, t)$ for all $t \in \mathbb{R}_{\geq 0}$ and $i \in \mathcal{V}$. In such a case, the update law (4.5) results in

$$\eta_i^+ = \frac{K_i}{d_i^{in}} \sum_{k \in \mathcal{N}(i)} H(x_i - x_k) - \frac{K_i}{d_i^{in}} \sum_{k \in \mathcal{N}(i)} (m_i - m_k). \tag{4.60}$$

during jumps, i.e., when $\tau = 0$.

This leads to a hybrid system $\widetilde{\mathcal{H}}_\varepsilon$ with data $(C_\varepsilon, f_\varepsilon, D_\varepsilon, \widetilde{G}_\varepsilon)$ with $\widetilde{G}_\varepsilon$ given by $\widetilde{G}_\varepsilon(\xi) = G_\varepsilon(\xi) + \begin{bmatrix} B_g \bar{m} \\ 0 \end{bmatrix} \forall D_\varepsilon$ where where C_ε, f_ε, D_ε and $\widetilde{G}_\varepsilon$ are given in (4.30), and $B_g = \operatorname{diag}\left(\begin{bmatrix} 0 \\ K_1 \end{bmatrix}, \begin{bmatrix} 0 \\ K_2 \end{bmatrix}, \ldots, \begin{bmatrix} 0 \\ K_N \end{bmatrix} \right)$, $\bar{m} = (\bar{m}_1, \bar{m}_2, \ldots, \bar{m}_N)$ and $\overline{M}_i = \sum_{k \in \mathcal{V} \setminus \{i\}} (m_i - m_k)$.

Theorem 4.2.22 *Let T_1 and T_2 be two positive scalars such that $T_1 \leq T_2$ and the digraph Γ be strongly connected. If there exist a positive scalar σ, a symmetric positive definite matrix $P \in \mathbb{R}^{(n+p)\times(n+p)}$ and matrices $K_i \in \mathbb{R}^{p \times n}$ for each $i \in \mathcal{V}$ satisfying* (4.42)*, then the hybrid system $\mathcal{H}$ is ISS with respect to $\bar{m} = (\bar{m}_1, \bar{m}_2, \ldots, \bar{m}_N)$ relative to the set $\mathcal{A}_\varepsilon$ in* (4.41)*. Moreover, given a solution ϕ from $\phi(0,0)$, we have that for each $(t,j) \in \operatorname{dom} \phi$,*

$$|\phi(t,j)|_{\mathcal{A}} \leq \max \left\{ \sqrt{2\frac{\alpha_2}{\alpha_1}} e^{\frac{R}{2}} e^{-\frac{r(t+j)}{2}} |\phi(0,0)|_{\mathcal{A}}, \sqrt{\frac{\rho e^{-\theta}}{e^{-\theta} - 1}} |K| |\bar{m}|_\infty \right\}$$

where $\theta = \ln\left(1 - \frac{\beta}{2\alpha_2}\right)$, α_1 and α_2 are given by (4.44)*, $r \in \left(0, \frac{\theta}{1+T_2}\right]$ and $R \in \left[\frac{T_2|\sigma|}{1+T_2}, \infty\right)$.*

Proof Consider the Lyapunov function in (4.45). Note that (4.46) holds where α_1 and α_2 are given in (4.44). Since measurement noise is not preset during flows, we have that (4.47) holds for all $\xi \in C_m$. We must consider the change in $V(\xi) = e^{\sigma\tau} z^\top e^{A_f^\top \tau} P e^{A_f \tau} z$ during jumps, namely,

$V(g) - V(\xi)$ for each $\xi \in D$, $g \in G_m(\xi)$. It follows that

$$\begin{aligned} V(g) - V(\xi) &= e^{\sigma\nu}(A_g z + B_g \bar{m})^\top e^{A_f^\top \nu} P e^{A_f \nu}(A_g z + B_g \bar{m}) - z^\top P z \\ &= e^{\sigma\nu} z^\top A_g^\top e^{A_f^\top \nu} P e^{A_f \nu} A_g z + e^{\sigma\nu} \bar{m}^\top B_g^\top e^{A_f^\top \nu} P e^{A_f \nu} B_g \bar{m} \\ &\quad + 2 e^{\sigma\nu} z^\top A_g^\top e^{A_f^\top \nu} P e^{A_f \nu} B_g \tilde{m} - z^\top P z \end{aligned}$$

From condition (4.42), there exists small enough $\beta > 0$ such that $z_i^\top (e^{\sigma\nu} A_g^\top e^{A_f^\top \nu} P e^{A_f \nu} A_g - P) z_i \leq -\beta z_i^\top z_i$ for each $\nu \in [T_1, T_2]$. Furthermore, by Young's Inequality $2a^\top b \leq \epsilon a^\top a + \frac{1}{\epsilon} b^\top b$ for every $\epsilon > 0$. Choosing $a = z_i$, $b = e^{\sigma\nu} A_g^\top e^{A_f^\top \nu} P e^{A_f^\top \nu} K_g \tilde{m}_i$ and $\epsilon = \frac{\beta}{2}$, we have that

$$\begin{aligned} V(g) - V(\xi) &= z^\top (A_g^\top e^{A_f^\top \nu} P e^{A_f \nu} A_g - P) z + 2 e^{\sigma\nu} z^\top A_g^\top e^{A_f^\top \nu} P e^{A_f \nu} B_g \bar{m} \\ &\quad + e^{\sigma\nu} \bar{m}^\top B_g^\top e^{A_f^\top \nu} P e^{A_f \nu} B_g \bar{m} \\ &\leq -\frac{\beta}{2} z^\top z + e^{\sigma\nu} \bar{m}^\top B_g^\top e^{A_f^\top \nu} P e^{A_f \nu} B_g \bar{m} + \frac{2}{\beta} e^{\sigma\nu} \bar{m}^\top B_g^\top e^{A_f^\top \nu} P P e^{A_f \nu} B_g \bar{m} \\ &\leq -\frac{\beta}{2} z^\top z + e^{\sigma\nu} \bar{m}^\top B_g^\top e^{A_f^\top \nu} P \left(1 + \frac{2}{\beta} P\right) e^{A_f \nu} B_g \bar{m} \\ &\leq -\frac{\beta}{2} z^\top z + e^{\sigma\nu} \rho \max_{i \in \mathcal{V}} |B_g|^2 \bar{m}^\top \bar{m} \\ &\leq -\frac{\beta}{2\alpha_2} V(\xi) + \rho |B_g|^2 |\bar{m}|^2 \end{aligned}$$

where $\rho = e^{\sigma T_2} |P| \left(\frac{2}{\beta}|P| + 1\right) \max_{\nu \in [T_1, T_2]} \left|e^{A_f \nu}\right|^2$ and we used the fact that from (4.42), $|e^{\frac{\sigma}{2}\nu} e^{A_f \nu} A_g| < 1$ for each $\nu \in [T_1, T_2]$.

Following the steps of the proof of [49, Theorem 2], it follows that solutions are bounded by

$$|\phi(t,j)|_{\mathcal{A}} \leq \max \left\{ \sqrt{2 \frac{\alpha_2}{\alpha_1}} e^{\frac{R}{2}} e^{-\frac{r(t+j)}{2}} |\phi(0,0)|_{\mathcal{A}}, \sqrt{\frac{\rho e^{-\theta}}{e^{-\theta} - 1}} |K| |\bar{m}|_\infty \right\}$$

where $\theta = \ln(1 - \frac{\beta}{2\alpha_2})$, $r \in \left(0, \frac{\theta}{1+T_2}\right]$ and $R \in \left[\frac{T_2|\sigma|}{1+T_2}, \infty\right)$ for all $(t,j) \in \operatorname{dom} \phi$. Thus, by [47], we have that the hybrid system $\widetilde{\mathcal{H}}_\varepsilon$ is ISS with respect to $\bar{m}$ and relative to the set $\mathcal{A}$ in (4.41).

■

4.2.6 Robustness to Information Loss

At each communication event, a packet containing a measurement y_k is received by agent i. In this section, we study the robustness of the exponential stability of the set $\mathcal{A}$ in (4.14) to the loss of such information, i.e., the situation when some of such data packets are lost. We assume the following properties on the packets.

Assumption 4.2.23 *A Bernoulli random variable b_k indicates whether the packet with is successfully received. If it is received successfully, then $b_k = 1$; otherwise $b_k = 0$. For each $k \in \mathcal{V}$, b_k is identically and independently distributed with $P(b_k = 1) = d_r$ and $P(b_k = 0) = 1 - d_r$ where $d_r \in (0, 1)$.*

This assumption is a common way to model packet losses in large-scale networks [61]. In Example 4.3.6, we consider the case of the proposed controller designed for exponential stability of the synchronization set, wherein, the communication between agents is subjected to such information loss.

However, if we can upper bound the number of packets lost in the network. Then, we can utilize the previous notions to design a controller that maintains stability of the synchronization set in spite of the dropouts. Then, the number of consecutive packets lost is less than $p^* \in \mathbb{N}$ then we can robustify the controller designed by Proposition 4.2.15 as follows.

Corollary 4.2.24 *Let $0 < T_1 \leq T_2$, an undirected connected graph Γ and $p^* \in \mathbb{N}$. The synchronization set $\mathcal{A}_s$ in (4.34) is GES for $\mathcal{H}_s$ in (4.62) if there exist scalar $\sigma > 0$, and matrices $P_i = P_i^\top > 0$ and $Q_i = Q_i^\top > 0$ for each $i \in \{2, 3, \ldots, N\}$ such that $\overline{M}_i(0) < 0$ and $\overline{M}_i(T_2(p^* + 1)) < 0$ where*

$$\overline{M}_i(\nu) := \begin{bmatrix} \mathrm{He}(P\bar{A}_i) & -PB + \exp(\sigma\nu)(\bar{K}_i\bar{A}_i - E\bar{K}_i)Q_i \\ \star & \mathrm{He}(\exp(\sigma\nu)Q_i, E - \bar{K}_iB - \frac{\sigma}{2}I) \end{bmatrix} \tag{4.61}$$

for each $\lambda_i \in \lambda(\mathcal{L}) \setminus \{0\}$ *where* $\bar{A}_i = A + \lambda_i BKH$, *and* $K_i = \lambda_i KH$.

Proof Due to the number of packet dropouts being upper bounded by $p^* \in \mathbb{N}$, the interval between two successfully received packets is between T_1 to $T_2 + p^* T_2$, where $p^* T_2$ is the additional maximum intervals of time. Therefore, we can model the packet dropouts by a timer given by

$$\begin{cases} \dot{\tau}_{p^*} = -1 & \tau_{p^*} \in [0, T_2(1+p^*)] \\ \tau_{p^*}^+ \in [T_1, T_2(1+p^*)] & \tau_{p^*} = 0. \end{cases}$$

Namely, if there are p^* possible packet dropouts, then the dynamics τ_{p^*} effectively model any possible sequence of times in (4.3) where T_2 therein, with a little abuse of notation, can be replaced with $T_2(1+p^*)$. Therefore, the hybrid system $\mathcal{H}_s$ can be defined using τ_{p^*}, namely, HS_s with state $\xi = (x, \theta, \tau_{p^*})$ and dynamics

$$\begin{cases} \dot{\xi} & = & (A_f z, -1) & \tau & \in & [0, T_2(1+p^*)] \\ \xi^+ & \in & (A_g z, [T_1, T_2(1+p^*)]) & \tau & = & 0 \end{cases} \tag{4.62}$$

Following the proof of Proposition 4.2.15 concludes the result. Namely, consider V in (4.36) where there exists $\alpha_1, \alpha_2 > 0$ satisfying $\alpha_1 |\xi|_{\mathcal{A}_s} \leq V(\xi) \leq \alpha_2 |\xi|_{\mathcal{A}_s}$. During flows, when $\tau \in [0, T_2(1+p^*)]$, and in light of (4.61), the function $\langle \nabla V(\xi), f(\xi) \rangle \leq \beta |\xi|_{\mathcal{A}_s}$. Moreover, by applying Proposition 4.2.11, with $\overline{M}_i(0) < 0$ and $\overline{M}_i < 0$, implies that For each $\xi \in D$, $g \in G(\xi)$, the change in V satisfies $V^+(g) - V(\xi) \leq 0$. Looking at the change in V over a typical solution ■

4.3 Numerical Examples

4.3.1 Synchronization under Nominal Conditions

Example 4.3.1 *Given $T_2^i = 0.7$ and $T_1^i = 0.9$ for each $i \in \mathcal{V}$, we apply Theorem 4.2.9 to a network of six harmonic oscillators, where each agent has dynamics given by*

$$\ddot{x}_i + x_i = u_i. \tag{4.63}$$

We consider the case where each agent is connected only to two neighbors in a cycle graph. Moreover, the output of each agent is both position x_1 and velocity x_2 information, i.e, $H = I$. In state space form, we have an LTI system of the form in (4.1) with state matrices $A = \begin{bmatrix} 0 & 1 \\ -1 & 0 \end{bmatrix}, B = \begin{bmatrix} 0 \\ 1 \end{bmatrix}$ and an adjacency matrix given by

$$\mathcal{G} = \begin{bmatrix} 0 & 1 & 0 & 0 & 0 & 1 \\ 1 & 0 & 1 & 0 & 0 & 0 \\ 0 & 1 & 0 & 1 & 0 & 0 \\ 0 & 0 & 1 & 0 & 1 & 0 \\ 0 & 0 & 0 & 1 & 0 & 1 \\ 1 & 0 & 0 & 0 & 1 & 0 \end{bmatrix}. \tag{4.64}$$

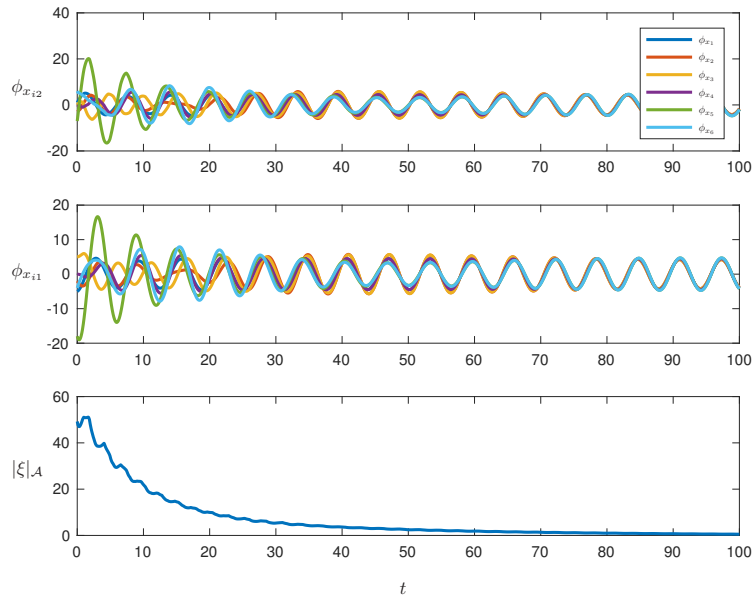

Figure 4.1: Numerical solutions of 6 interconnected linear oscillators communicating over a ring graph.

It can be shown that the following parameters $K = -\begin{bmatrix} 0.15 & 0.15 \end{bmatrix}$, $E = -1$, $\sigma = 0.9$ *and* P_i *and* Q_i *such that*

$$P_2 = P_3 = \begin{bmatrix} 0.1173 & -0.0025 \\ \star & 0.1132 \end{bmatrix} \qquad Q_2 = Q_3 = 0.2162$$

$$P_4 = P_5 = \begin{bmatrix} 0.1144 & 0.0092 \\ \star & 0.0963 \end{bmatrix} \qquad Q_4 = Q_5 = 0.2097$$

$$P_6 = \begin{bmatrix} 0.1116 & -0.0134 \\ \star & 0.0897 \end{bmatrix} \qquad Q_5 = 0.2023$$

satisfy the conditions in (4.16) *and* (4.17).[8] *In Figure 4.1, a numerical solution* $\phi = (\phi_x, \phi_\eta, \phi_\tau)$ *to the hybrid system* $\mathcal{H}$ *with the above parameters from initial conditions* $\phi_x(0,0) = (-5, 1, -2, -3, 5, 0, 0, 0, -18, -7, -$ $\phi_\eta = (0.5, 0, 10, -2, 5, -10)$ *and* $\phi_\tau(0,0) = (0.25, 0.5, 0.86, 0.87, 0.14, 0.1)$ *is shown.*

The convergence to the synchronization set $\mathcal{A}$ *is exponential in nature, and is guar-*

[8] Code at `github.com/HybridSystemsLab/LTIAsyncSync`

K	E	Theorem 4.2.9	t^*
$-\begin{bmatrix}0.1 & 0.1\end{bmatrix}$	-0.5	✓	165.38
$-\begin{bmatrix}0.15 & 0.15\end{bmatrix}$	-1	✓	120.2
$-\begin{bmatrix}0.5 & 0.5\end{bmatrix}$	-1.8	×	30.1
$-\begin{bmatrix}0.6 & 0.6\end{bmatrix}$	-0.1	×	27.05
$\begin{bmatrix}0.15 & -0.6\end{bmatrix}$	-0.1	×	30.66

Table 4.1: Comparison of convergence times for different gains K and E for the hybrid system $\mathcal{H}$ with asynchronous communication in Section 4.2.1. The ✓ indicates that the conditions are satisfied, and the × indicates that the conditions are not satisfied but solutions converge to the synchronization set.

anteed by the sufficient condition in Proposition 4.2.14. In Table 4.1, we compare the convergence time (in flow time, t) of solutions to $\mathcal{H}$ with different gains K and E in (4.7) *and* (4.8)*, respectively. Note the conditions in Theorem 4.2.9 are not necessary and it may be possible that gains can be found so that solutions still converge to the synchronization set. In Table 4.1, we indicate whether it is possible to satisfy the conditions in Theorem 4.2.9 for the gains chosen by placing a ✓ if the conditions are satisfied and by placing a × if it is not possible to satisfy the conditions for the selected gain. Moreover, in Table 4.1, we compare convergence times of solutions to the set $\mathcal{A}$ for different parameter choices. More specifically, we consider a solution ϕ such that $|\phi(0,0)|_{\mathcal{A}} \approx 50$ and find the time it takes for the solution to converge to and stay in a neighborhood near $\mathcal{A}$ in* (4.14)*, i.e., we find t^* such that $t^* = \{T \in \mathbb{R}_{\geq 0} : |\phi(t,j)|_{\mathcal{A}} \leq 0.1 \ \forall (t,j) \in \operatorname{dom}\phi \text{ s.t. } t \geq T\}$. Due to the nonuniqueness of solutions $\mathcal{H}$ in* (4.12) *and* (4.13) *when the network parameters are such that $T_1^i \neq T_2^i$, Table 4.1 provides an average t^* over 100 solutions.* △

In the next example, we consider the case of synchronization for three agents where communication occurs simultaneously, namely, the system outlined in Section 4.2.4.1 is employed.

Example 4.3.2 *Consider the case of a network of three harmonic oscillators in* (4.3.1) *con-*

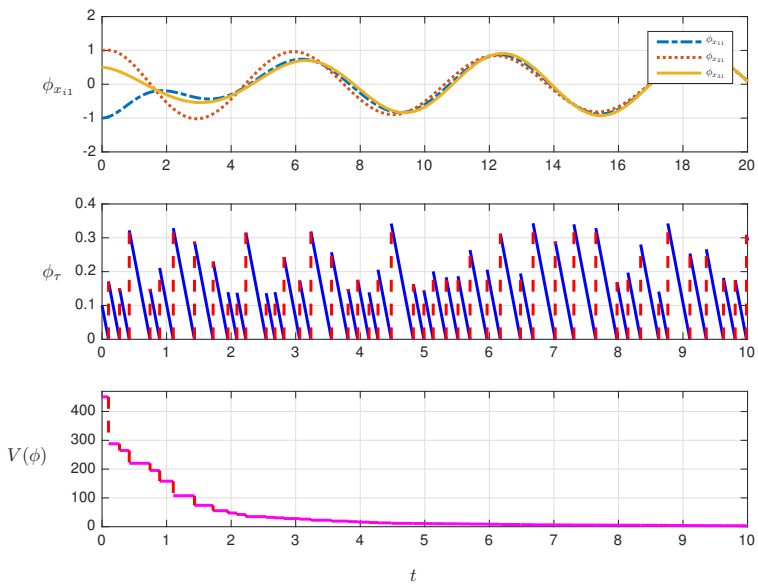

Figure 4.2: A numerical solution of the first component of the state ϕ_{x_i} for each $i \in \{1, 2, 3\}$ where $\phi_{x_i} = (\phi_{x_{i1}}, \phi_{x_{i2}})$ and ϕ_τ for Example 4.3.2. (top and middle, respectively) The Lyapunov function V in (4.45) evaluated along the solution to $\mathcal{H}_\varepsilon$ decreases to zero, indicating that the solution synchronizes over hybrid time. (bottom)

nected on a strongly connected graph with adjacency matrix $\mathcal{G} = \begin{bmatrix} 0 & 1 & 1 \\ 1 & 0 & 1 \\ 1 & 0 & 0 \end{bmatrix}$ *with network parameters* $T_1 = 0.13$ *and* $T_2 = 0.35$. *By applying Theorem 4.2.16 to this network, it follows that for parameters* $K_1 = \begin{bmatrix} -0.4 & -1 \end{bmatrix}$, $K_2 = \begin{bmatrix} -0.5 & -0.2 \end{bmatrix}$, $K_3 = \begin{bmatrix} -0.2 & -0.15 \end{bmatrix}$, $\sigma = 0.1$ *and* P

can be found to

$$P \approx \begin{bmatrix} 65.6 & 16.0 & 3.0 & -8.6 & 8.1 & -1.1 & -10.0 & 2.1 & -1.8 \\ 16.0 & 52.3 & 5.0 & -13.2 & -2.6 & -1.8 & -3.8 & -5.6 & -3.1 \\ 3.0 & 5.0 & 11.0 & -1.4 & -0.4 & -4.8 & -0.6 & -0.2 & -6.1 \\ -8.6 & -13.2 & -1.4 & 67.3 & 2.4 & 6.5 & -26.5 & -7.6 & -5.0 \\ 8.1 & -2.5 & -0.4 & 2.4 & 41.4 & 1.0 & 2.6 & -17.3 & -0.5 \\ -1.1 & -1.8 & -4.8 & 6.5 & 1.0 & 14.9 & -2.3 & -1.0 & -10.1 \\ -10.0 & -3.8 & -0.6 & -26.5 & 2.5 & -2.3 & 14.7 & 1.6 & 2.9 \\ 2.1 & -5.6 & -0.2 & -7.6 & -17.3 & -1.0 & 1.6 & 10.1 & 1.3 \\ -1.8 & -3.1 & -6.1 & -5.0 & -0.5 & -10.1 & 2.9 & 1.2 & 16.3 \end{bmatrix} \tag{4.65}$$

satisfy condition (4.42)*. Figure 4.2 shows a numerical solution* $\phi = (\phi_x, \phi_\eta, \phi_\tau)$ *for the hybrid system* $\mathcal{H}$ *from* $\phi_x(0,0) = (-1, 0, 1, 0, 0.5, 0)$*,* $\phi_\eta(0,0) = (1, 2, -1)$ *and* $\phi_\tau(0,0) = 0.1$*. In this figure, a plot of the first component of each* $x_i = (x_{i1}, x_{i2})$ *over flow time, the solution corresponding to the* τ *component and the Lyapunov function in* (4.45) *evaluated along the solution (in error coordinates). Note that the function* V *tends to zero exponentially over time, indicating that the solutions converge to synchronization.* [9] △

In the next example, we study the convergence time for the case when there is a single timer.

Example 4.3.3 *Consider the system in* (4.63) *with network in* (4.64) *for the case of a single timer where* $T_1 = 0.7$ *and* $T_2 = 0.9$*. In Table 4.2 and due to the nonuniqueness of solutions, we give the average time to converge to a neighborhood close to the synchronization set for the gains chosen, similar to Example 4.3.1. More specifically, this table characterizes the time to converge* t^* *to and stay within a neighborhood of the set* $\mathcal{A}$*. Moreover, Table 4.2 shows the tightness of the sufficient conditions provided in Proposition 4.2.15.* △

A small-world network is a type of sparse network known to model real-world settings such as the world wide web, electric power girds, and networks of brain neurons. In particular, a

[9] Code at `https://github.com/HybridSystemsLab/LTISyncStrong`

K	E	Proposition 4.2.15	$t^*\}$
$-\begin{bmatrix}0.1 & 0.1\end{bmatrix}$	0	✓	181.87
$-\begin{bmatrix}0.15 & 0.15\end{bmatrix}$	0	✓	119.36
$-\begin{bmatrix}0.2 & 0.2\end{bmatrix}$	0	✓	90.69
$-\begin{bmatrix}0.3 & 0.3\end{bmatrix}$	0	✓	59.62
$-\begin{bmatrix}0.5 & 0.5\end{bmatrix}$	0	×	33.70

Table 4.2: Comparison of convergence times and results for different choices of gains K and E for the hybrid system $\mathcal{H}_\varepsilon$ with synchronous communication. The ✓ indicates that the conditions are satisfied, and the × indicates that the conditions are not satisfied but solutions converge to the synchronization set.

small-world network is a graph structure in which most agents are, on average, a short geodesic distance[10] from any other node. In the following example, we use the random graph generator in [62] to generate the interconnection between 100 agents.

Example 4.3.4 *In this example, we consider the case of a network of 100 agents with dynamics as in* (4.63) *with* $T_1^i = 0.7$ *and* $T_2^i = 0.9$ *for each* $i \in \mathcal{V}$. *We generated a random graph using the small world generator in [62] for* $N = 100$, *the average degree* $k = 3$ *and special restructuring parameter* $\beta = 0.1$. *The resulting graph structure is depicted in the upper left of Figure 4.3. Furthermore, we use the parameters in Example 4.3.1, namely,* $K = -[0.15, 0.15]$ *and* $E = -1$. *The solutions* $\phi = (\phi_x, \phi_\eta, \phi_\tau)$ *were initialized randomly inside a bounded region, namely,* $\phi_{x_i}(0,0) \in [-5,5]^2$, $\phi_{\eta_i}(0,0) \in [-5,5]$ *and* $\phi_{\tau_i}(0,0) \in \mathcal{T}$ *for each* $i \in \mathcal{V}$[11] *The plots in the upper right section of Figure 4.3 show the evolution of the first component of the plant state* x_{1i} *for each* $i \in \mathcal{V}$. *It can be seen that solutions asymptotically converge to synchronization as time progresses: in fact, the bottom plot shows that, indeed, the error converges to zero.* △

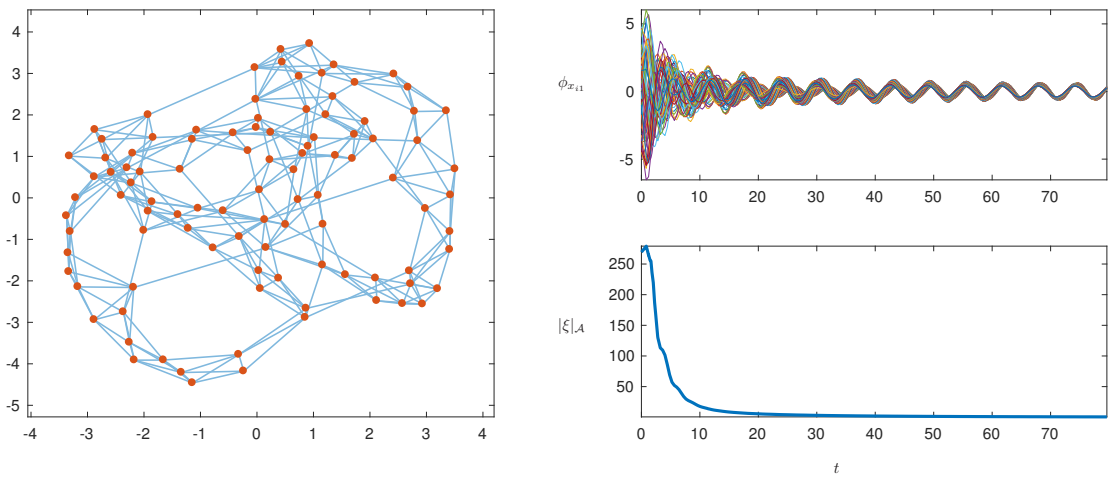

Figure 4.3: (left) Randomly generated undirected small-world network containing 100 agents. (upper right) The first component of the states of each agent in the network. Note that over time all agents converge to synchrony. (bottom right) The norm of the relative error over ordinary time converges to zero.

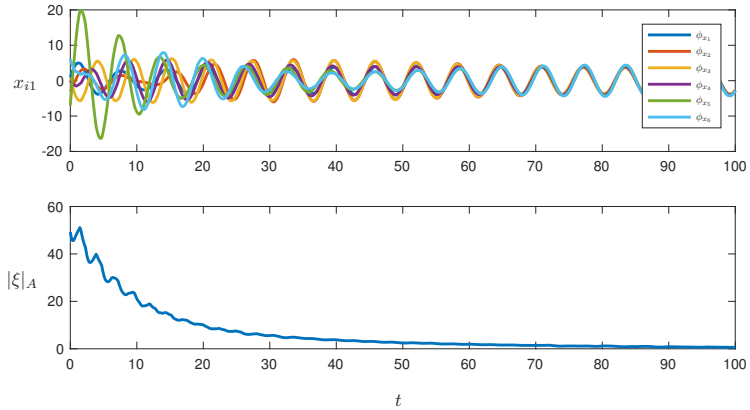

Figure 4.4: When communication noise is present, solutions converge to a neighborhood about the synchronization set as indicated by the norm of the relative error converging to an average value of 0.1147.

4.3.2 Synchronization under Perturbations and Information Loss

Example 4.3.5 *In this example, we consider the case of $\mathcal{H}$ with measurement noise. Let the system be given by the dynamics in Example 4.3.1 connected by a network with adjacency matrix in* (4.64) *where $T_1^i = 0.7$ and $T_2^i = 0.9$ for each $i \in \mathcal{V}$. Let the output y_i in* (4.2) *be given by a constant bias, i.e., $\varphi_i(x_i, t) \equiv m_i$ for each $i \in \mathcal{V}$, where $m_1 = (0.1, 0.1)$, $m_2 = (-0.1, -0.1)$, $m_3 = (0, 0)$, $m_4 = (0.2, 0.2)$, $m_5 = (-0.15, -0.15)$, and $m_6 = (0.3, 0.3)$. Moreover, let $K = -\begin{bmatrix} 0.15 & 0.15 \end{bmatrix}$ and $E = -1$, which, as was shown in Example 4.3.1, satisfy Theorem 4.2.9 therefore the resulting hybrid system $\mathcal{H}$ with data given by* (4.12) *and* (4.13) *has $\mathcal{A}$ exponentially stable. In Figure 4.4, we show a numerical solution to the hybrid system from the initial conditions in Example 4.3.1. In this figure, it can be seen that solutions converge to a neighborhood around the synchronization set $\mathcal{A}$. Namely, it can be seen that after the transient period, the norm of the relative error $|\varepsilon|$ of the solution converges to an average value of* 0.1147 *for this case.* △

Example 4.3.6 *At each communication event, a packet containing a measurement y_k is received by agent i. In this example, we study the robustness of the exponential stability of the set $\mathcal{A}$ in* (4.14) *to the loss of such information, i.e., the situation when some data packets are lost. We assume that the packet arrival is given by Bernoulli random variables. Namely, a Bernoulli random variable b_k indicates whether the packet is successfully received. If it is received successfully, then $b_k = 1$; otherwise $b_k = 0$. For each $k \in \mathcal{V}$, b_k is identically and independently distributed with $P(b_k = 1) = d_r$ and $P(b_k = 0) = 1 - d_r$, where $d_r \in (0, 1)$.*

Consider the system in Example 4.3.1 with a graph as in (4.64)*. Under the same initial conditions as in Example 4.3.1, Figure 4.5 shows the norm of the average relative error*

[10] A geodesic distance is defined by the minimum number of edges traversed to get from the starting node to the end node.

[11] Code at `github.com/HybridSystemsLab/LTISyncSmallWorld`

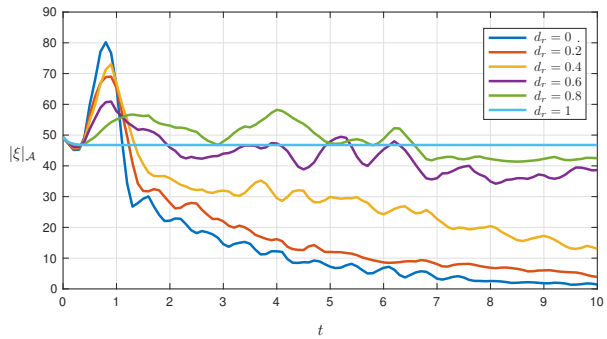

Figure 4.5: The norm of the average relative error ε_i for 10 averaged trajectories for each dropout rate $d_r = \{0, 0.2, 0.4, 0.6, 0.8, 1\}$

$|\varepsilon|$ over the average of 10 *trajectories projected onto the t domain for each dropout rate $d_r \in \{0, 0.2, 0.4, 0.6, 0.8, 1\}$. Note that for larger dropout rates, the convergence degrades. Moreover, for dropout rate larger than $d_r = 0.6$, the norm of the relative error ε does not appear to converge to zero.* △

4.4 Summary

The problem of synchronization of multiple continuous-time linear time-invariant systems connected over an intermittent network was studied. Communications across the network occurs at isolated time events, which, using the hybrid systems framework was modeled using a decreasing timer. Recasting synchronization as a set stability problem, we took advantage of several properties of the graph structure and employed a Lyapunov based approach to certify exponential stability of the synchronization set. Then, in part, as a consequence of the regularity of the hybrid systems data and the aforementioned stability properties, robustness to communication noise, and unmodeled dynamics was characterized in terms of semi-global practical stability. When communication noise was affecting the dynamics, the Lyapunov function candidate chosen certified ISS stability for the synchronization set and relative to such noise.

Chapter 5

On Synchronization in General Hybrid Systems

5.1 Introduction

Due to its broad applications, synchronization of dynamical systems has received a significant amount of attention recently. Specifically, synchronization is a key property to study in spiking neurons and control of chaotic systems [63, 64], formation control and flocking maneuvers [7], and many others applications.

Synchronization of networked systems has been studied using different approaches and methodologies. Namely, synchronization in both continuous and discrete-time domains has been investigated in [20, 65], and for both linear and nonlinear systems [66]. The network structure in such systems is typically studied using graph theory. Graph theory provides a solid understanding of the connectivity of the network and its effect on the individual dynamics of the systems [67]. On the other hand, the study of stability and attractivity of synchronization is typically done using systems theory tools, like Lyapunov functions [15], contraction theory [17],

and incremental input-to-state stability [18], for instance. To the best of our knowledge, there is a distinct lack in the synchronization literature for the case where each agent may contain states that evolve both continuously and discretely.

In this chapter, the synchronization of multi-agent hybrid systems is considered. The agents considered here are allowed to have states that evolve continuously and, at times, discretely. A general framework for the study of synchronization in interconnected hybrid systems is presented to allow for complex interactions between the agents in the network. Namely, the interconnected model presented allows for states that evolve continuously and, at times, jump; such actions allow information to be transferred across a network to affect the states of a neighboring agent. For such general models, asymptotic synchronization notions for hybrid systems are presented, these notions require both stable and convergent behavior (in the uniform and nonuniform sense). Using tools for analysis of asymptotic stability of set in hybrid systems, we present results for asymptotic synchronization of interconnected hybrid systems. Namely, this chapter is meant to begin the discussion on the implications of asymptotic stability of a set to the asymptotic synchronization.

The remainder of this paper is organized as follows. Section 5.2 introduces the class of interconnected hybrid systems considered, the notion of asymptotic synchronization, and the main results.

5.2 Interconnected Agents with Hybrid Dynamics

5.2.1 Hybrid Modeling and General Properties

Consider a network of N agents connected through a graph. For each $i \in \mathcal{V} := \{1, 2, \ldots, N\}$, the i-th agent is modeled as a hybrid inclusion in (2.1). Let $x_i \in \mathbb{R}^n$ be the state of each agent, $u_i \in \mathbb{R}^p$ the input to each agent, and $y_i \in \mathbb{R}^m$ the output, which is given by

$y_i = h(x_i)$. The output y_i may be measured by the agent itself and its neighbors. Moreover, we define the information available to each i-th agent, denoted as $\tilde{y}_i$, as a sequence collecting all neighboring outputs y_k, where $k \in \mathcal{N}(i) \cup \{i\}$, namely, we define $\tilde{y}_i = \{y_k\}_{k \in \mathcal{N}_i \cup \{i\}} \in \mathbb{R}^{m(d_i+1)}$. Then, each i-th agent may evolve continuously by

$$\dot{x}_i \in \widetilde{F}(x_i, u_i) \tag{5.1}$$

for every $x_i \in \widetilde{C}$, where $\widetilde{C}$ is a subset of $\mathbb{R}^n$. Furthermore, when the state x_i is in a set $\widetilde{D} \subset \mathbb{R}^n$ a self-induced jump in the state of the i-th agent may occur such jump is modeled by the difference inclusion

$$x_i^+ \in \widetilde{G}_{in}(x_i, u_i) \tag{5.2}$$

Such an event may trigger an abrupt change in the state of its neighbors, in which, for each $i, k \in \mathcal{V}$ $i \neq k$, we have

$$x_k^+ \in (1 - g_{ik})x_k + g_{ik}G_{ex}(x_k, u_k) =: \widetilde{G}_{ex}^{ik}(x_k, u_k). \tag{5.3}$$

where g_{ik} is the adjacency matrix. Note that when there is a connection between agents i and k the element in the adjacency matrix is $g_{ik} = 1$ which leads to $\widetilde{G}_{ex}^{ik}(x_k, u_k) = G_{ex}(x_k, u_k)$. Moreover, when there is no connection between such agents, we have that $g_{ik} = 0$ which results in the lack of communication between agents implying that $\widetilde{G}_{ex}^{ik}(x_k, u_k) = x_k$; specifically, there is no change in the state of agent k induced by the jumps of agent i.

We consider state-feedback laws for the control of each agent; the dynamic case can be treated similarly. We define static output feedback controllers by $\kappa_c^i : \mathbb{R}^{m(d_i+1)} \to \mathbb{R}^p$ during the continuous evolution of the state. Depending on the scenario, events due to measurements of information from the neighbors and self-induced jumps may only be available to the agents at different time instances. When there is an instantaneous change in x_i due to a self-induced

update, i.e., $x_i \in \widetilde{D}$, we denote the feedback controller by $\kappa^i_{d,in} : \mathbb{R}^m \to \mathbb{R}^p$, which depends on the measured y_i only. When a neighboring system jumps, i.e., when $x_k \in \widetilde{D}$, $k \in \mathcal{N}(i)$, we denote the controller by $\kappa^i_{d,ex} : \mathbb{R}^m \to \mathbb{R}^p$ which depends on the measured y_k which jumped.

A complete model of the network can be obtained by, stacking the agents' states with dynamics as in (5.1)-(5.3). The resulting interconnected hybrid system, denoted $\mathcal{H}$, with state $x = (x_1, x_2, \ldots, x_N)$ is given by

$$\begin{aligned} \dot{x} &\in (\widetilde{F}(x_1, \kappa^1_c(\tilde{y}_1)), \widetilde{F}(x_2, \kappa^2_c(\tilde{y}_2)), \ldots, \widetilde{F}(x_N, \kappa^N_c(\tilde{y}_N))) =: F(x) \\ x &\in C := \widetilde{C} \times \widetilde{C} \times \cdots \times \widetilde{C} \\ x^+ &\in \{\widetilde{G}_i(x) : x_i \in \widetilde{D}, i \in \mathcal{V}\} =: G(x) \\ x &\in D := \{x \in \mathbb{R}^{Nn} : \exists i \in \mathcal{V}, \text{ s.t. } x_i \in \widetilde{D}\}. \end{aligned} \tag{5.4}$$

The jump map $\widetilde{G}_i$ updates the i-th entry of the full state x, via $\widetilde{G}_{in}$ when $x_i \in \widetilde{D}$, and maps all other $k \in \mathcal{V} \setminus \{i\}$ components by $\widetilde{G}^{ik}_{ex}$, namely,

$$\begin{aligned} \widetilde{G}_i(x) := (&\widetilde{G}^{i1}_{ex}(x_1, \kappa^1_{d,ex}(y_i)), \ldots, \widetilde{G}_{in}(x_i, \kappa^i_{d,in}(y_i)), \\ &\ldots, \widetilde{G}^{iN}_{ex}(x_N, \kappa^N_{d,ex}(y_i))). \end{aligned} \tag{5.5}$$

Note that when multiple components of x are in $\widetilde{D}$ then G is the union of more than one jump map $\widetilde{G}_i$.

Remark 5.2.1 *Due to the structure of $\mathcal{H}$, this framework covers the cases of synchronization and consensus protocols for both continuous-time systems and discrete time systems. For example, using the above hybrid model, a purely continuous-time model can be recovered by considering $\widetilde{D} = \emptyset$ and with $\widetilde{G}_{in}$, $\widetilde{G}_{ex}$ arbitrary, and, likewise, a discrete-time model can be obtained using $\mathcal{H}$ by letting $\widetilde{C} = \emptyset$ and with $\widetilde{F}$ arbitrary.*

5.2.2 Partial Synchronization Notions

We introduce an asymptotic synchronization notion that requires both the synchronization error between the components of solutions on hybrid time domains to converge to zero, as well as stable behavior. We call this notion *asymptotic synchronization* and we define it as follows:

Definition 5.2.2 (asymptotic synchronization for $\mathcal{H}$) *Consider the hybrid system $\mathcal{H}$ in* (5.4)*. For each $i \in \mathcal{V}$, $x_i = (p_i, q_i)$, where $p_i \in \mathbb{R}^r$ and $q_i \in \mathbb{R}^{n-r}$ with integers $n \geq r \geq 1$. The hybrid system $\mathcal{H}$ is said to have*

- stable synchronization *with respect to p if for every $\varepsilon > 0$ there exists $\delta > 0$ such that, every solution $\phi = (\phi_1, \phi_2, \ldots, \phi_N)$ to $\mathcal{H}$ where $\phi_i = (\phi_i^p, \phi_i^q)$ is such that*

$$|\phi_i(0,0) - \phi_k(0,0)| \leq \delta \implies \begin{cases} |\phi_i^p(t,j) - \phi_k^p(t,j)| \leq \varepsilon \\ \qquad \forall (t,j) \in \operatorname{dom} \phi \end{cases}$$

  for all $i, k \in \mathcal{V}$.

- locally attractive synchronization *with respect to p if there exists $\mu > 0$ such that every maximal solution ϕ to $\mathcal{H}$ is complete and $|\phi_i(0,0) - \phi_k(0,0)| \leq \mu$ implies*

$$\lim_{\substack{(t,j) \in \operatorname{dom} \phi \\ t+j \to \infty}} |\phi_i^p(t,j) - \phi_k^p(t,j)| = 0. \tag{5.6}$$

  for all $i, k \in \mathcal{V}$.

- global attractive synchronization *with respect to p if every maximal solution ϕ to $\mathcal{H}$ is complete and satisfies* (5.6) *for all $i, k \in \mathcal{V}$.*

- local asymptotic synchronization *with respect to p if it has both stable and local attractive synchronization with respect to p.*

- global asymptotic synchronization *with respect to p if it has both stable and global attractive synchronization with respect to p.* $\square$

Next, we define synchronization in the uniform sense.

Definition 5.2.3 (uniform global asymptotic synchronization for $\mathcal{H}$): *Consider the hybrid system $\mathcal{H}$ in* (5.4). *For each $i \in \mathcal{V}$, let $x_i = (p_i, q_i)$, where $p_i \in \mathbb{R}^r$ and $q_i \in \mathbb{R}^{n-r}$ with integers $n \geq r \geq 1$. The hybrid system $\mathcal{H}$ is said to have*

- uniform stable synchronization *with respect to p if there exists a class-$\mathcal{K}_\infty$ function α such that any solution $\phi = (\phi_1, \phi_2, \ldots, \phi_N)$ to $\mathcal{H}$ where $\phi_i = (\phi_i^p, \phi_i^q)$ satisfies $|\phi_i^p(t,j) - \phi_k^p(t,j)| \leq \alpha(|\phi_i(0,0) - \phi_k(0,0)|)$ for all $(t,j) \in \operatorname{dom}\phi$ and for all $i, k \in \mathcal{V}$.*

- uniform global attractive synchronization *with respect to p if every maximal solution to $\mathcal{H}$ is complete and for each $\varepsilon > 0$ and $r > 0$ there exists $T > 0$ such that for any solution ϕ to $\mathcal{H}$ with $|\phi_i(0,0) - \phi_k(0,0)| \leq r$, for each $i, k \in \mathcal{V}$, $(t,j) \in \operatorname{dom}\phi$ satisfying $t + j \geq T$ imply $|\phi_i^p(t,j) - \phi_k^p(t,j)| \leq \varepsilon$ for each $i, k \in \mathcal{V}$.*

- uniform global asymptotic synchronization *if it has both uniform stable and uniform global attractive synchronization.*

Remark 5.2.4 *If $r = n$, then the notions in Definitions 5.2.2 and 5.2.3 can be considered as full-state notions, while if $r < n$ it can be considered to be a partial state notions. Note that stable synchronization requires solutions ϕ_i, for each $i \in \mathcal{V}$, to start close; while, only the components ϕ_i^p, $i \in \mathcal{V}$ remain close over their solution domain. Similarly, local attractive synchronization with respect to p only requires the distance between each ϕ_i^p to approach zero, while the other component is left unconstrained.*

5.2.3 Results for Partial Synchronization

Our first observation is that stable synchronization with respect to p in a hybrid system leads to uniqueness in the p components of solutions to $\mathcal{H}$.

Lemma 5.2.5 *If the hybrid system $\mathcal{H}$ as in* (5.4) *has stable synchronization with respect to p, then the p component in the t direction*[1] *of every maximal solution $\phi = (\phi_1, \phi_2, \ldots, \phi_N)$ from $\phi(0,0) \in \mathcal{A}$, with $\mathcal{A}$ as in* (5.7)*, is unique.*

Proof We proceed by contradiction. Assume $\mathcal{H}$ has stable synchronization with respect to p and consider two maximal solutions $\phi_i = (\phi_{i,1}, \phi_{i,2}, \ldots, \phi_{i,N}), \phi_{i,k} = (\phi^p_{i,k}, \phi^q_{i,k})$ where $\phi_1(0,0) = \phi_2(0,0) \in \mathcal{A}$. Suppose that the projections of the p components of these solutions in the t direction are not unique, namely, there exists $t^* > 0$ such that $\phi^p_{t,1}(t^*) \neq \phi^p_{t,2}(t^*)$ and $(t^*, j) \in \operatorname{dom} \phi_i$. Pick $\varepsilon > 0$ such that $\varepsilon < |\phi^p_{t,1}(t^*) - \phi^p_{t,2}(t^*)|$. Then, using this ε in the stable synchronization notion, no matter how small $\delta > 0$ is chosen, we have that solutions from $\phi_1(0,0) = \phi_2(0,0)$ satisfy $|\phi^p_{t,1}(t) - \phi^p_{t,2}(t)| > \varepsilon$ when $t = t^*$, which contracts the definition of stable synchronization.

■

Next, we recast synchronization as a set stabilization problem with $x_i = (p_i, q_i)$ for each $i \in \mathcal{V}$. We define the synchronization set as

$$\mathcal{A} = \{x = (x_1, x_2, \ldots, x_N) \in \mathbb{R}^{Nn} : p_1 = p_2 = \ldots = p_N\} \tag{5.7}$$

Note that when $r = n$, the synchronization set $\mathcal{A}$ reduces to the diagonal set $\{x \in \mathbb{R}^{nN} : x_1 = x_2 = \ldots = x_N\}$.

By using the properties of solutions ϕ for the hybrid system $\mathcal{H}$ in (5.4), we levy the fact that given a solution, the distance of ϕ to the set $\mathcal{A}$ results in $|\phi(t,j)|^2_{\mathcal{A}} = \sum_{i=1}^{N} |\phi^p(t,j) - \bar{\phi}^p(t,j)|$

[1] The projection of the p component in the t direction is defined as $t \mapsto \phi^p(t) := \lim_{h \searrow 0, (t+h,j) \in \operatorname{dom} \phi} \phi^p(t+h, j)$.

where $\bar{\phi}^p$ is the average value of ϕ_k^p for each $k \in \mathcal{V}$, i.e., $\bar{\phi}^p = \sum_{k=1}^N \phi_k^p$. Using this equivalence and the triangle inequality with the definition of global asymptotic stability in Definition [28, Definition 7.1] leads to the implication that $\mathcal{H}$ has global asymptotic synchronization. Next, we present our sufficient conditions for global asymptotic synchronization with respect to p for $\mathcal{H}$.

Theorem 5.2.6 *Given a hybrid system $\mathcal{H}$ as in* (5.4) *with data* (C, F, D, G)*, if the set $\mathcal{A}$ in* (5.7) *is globally asymptotically stable for $\mathcal{H}$, then $\mathcal{H}$ has global asymptotic synchronization with respect to p.*

Proof Given a solution ϕ to the interconnected hybrid system $\mathcal{H}$ in (5.4), we partition ϕ as $(\phi_1, \phi_2, \ldots, \phi_N)$, where each i-th component corresponds to the i-th component of x in (5.4). Let $\phi_i = (\phi_i^p, \phi_i^q)$ and $\phi^p = (\phi_1^p, \phi_2^p, \ldots, \phi_N^p)$ be the stack of ϕ_i^p components of the solution. Then, by virtue of the definition of the distance to the set $\mathcal{A}$ it follows that

$$\begin{aligned} |\phi|_{\mathcal{A}}^2 &= \left| \phi^p - \frac{1}{N} \sum_{i=1}^N \phi_k^p \mathbf{1} \right|^2 = |(\Pi \otimes I)\phi^p|^2 \\ &= (\phi^p)^\top (\Pi \otimes I_r)^\top (\Pi \otimes I_r)\phi^p \\ &= \sum_{i=1}^N \left| \phi_i^p - \frac{1}{N} \sum_{k=1}^N \phi_k^p \right|^2 = \sum_{i=1}^N \left| \phi_i^p - \bar{\phi}^p \right|^2 \end{aligned} \tag{5.8}$$

where $\bar{\phi}^p = \frac{1}{N} \sum_{k=1}^N \phi_k^p$. First, we show that $\mathcal{A}$ being stable for $\mathcal{H}$ implies that $\mathcal{H}$ has stable synchronization. Given $\varepsilon > 0$, pick $\delta > 0$ such that $|\phi(0,0)|_{\mathcal{A}} \leq \delta$ implies $|\phi(t,j)|_{\mathcal{A}} \leq \sqrt{\varepsilon}$ for all $(t,j) \in \operatorname{dom} \phi$ and $|\phi_i(0,0) - \phi_k(0,0)| \leq \delta$. Therefore, by virtue of (5.8), it follows that

$$\begin{aligned} |\phi_i^p(t,j) - \phi_k^p(t,j)|^2 &= |\phi_i^p(t,j) - \phi_k^p(t,j) + \bar{\phi}^p(t,j) - \bar{\phi}^p(t,j)|^2 \\ &\leq |\phi_i^p(t,j) - \bar{\phi}^p(t,j)|^2 + |\phi_k^p(t,j) - \bar{\phi}^p(t,j)|^2 \\ &\leq \sum_{i=1}^N \left| \phi_i^p(t,j) - \bar{\phi}^p(t,j) \right|^2 = |\phi(t,j)|_{\mathcal{A}}^2 \leq \varepsilon \end{aligned}$$

for all $(t,j) \in \operatorname{dom} \phi$ and hence $\mathcal{H}$ has stable synchronization. Next, we show that $\mathcal{H}$ has globally

attractive synchronization. Assume that $\mathcal{A}$ is globally attractive for $\mathcal{H}$, then for any complete solution to $\mathcal{H}$, if follows that

$$\lim_{\substack{(t,j)\in \operatorname{dom}\phi \\ t+j\to\infty}} |\phi(t,j)|_{\mathcal{A}} = 0$$

which implies that

$$\lim_{\substack{(t,j)\in \operatorname{dom}\phi \\ t+j\to\infty}} \sum_{i=1}^{N} \left|\phi_i^p(t,j) - \bar{\phi}^p(t,j)\right| = 0.$$

It follows that, for each $i, k \in \mathcal{V}$,

$$\lim_{\substack{(t,j)\in \operatorname{dom}\phi \\ t+j\to\infty}} |\phi_i^p(t,j) - \phi_k^p(t,j)| = 0, \tag{5.9}$$

implying that $\mathcal{H}$ has globally attractive synchronization. Due to the fact that $\mathcal{H}$ has both stable and attractive synchronization it follows that $\mathcal{H}$ has global asymptotic synchronization. ■

Remark 5.2.7 *The local case of the result in Theorem 5.2.6 can be considered similarly, specifically, if the hybrid system $\mathcal{H}$ has the set $\mathcal{A}$ locally asymptotically stable then $\mathcal{H}$ has local asymptotic synchronization with respect to p.*

The next result establishes the sufficient conditions for uniform global attractive synchronization with respect to p.

Theorem 5.2.8 *Given a hybrid system $\mathcal{H}$ as in* (5.4) *with data* (C, F, D, G)*, if the set $\mathcal{A}$ in* (5.7) *is uniformly globally attractive for $\mathcal{H}$, then $\mathcal{H}$ has uniform global attractive synchronization with respect to p.*

Proof Let $\mathcal{A}$ being uniformly globally attractive for $\mathcal{H}$ implies that $\mathcal{H}$ has uniform global attractive synchronization. Given $\varepsilon > 0$ and $r > 0$, let $|\phi(0,0)|_{\mathcal{A}} < r$ and $|\phi_i(0,0) - \phi_k(0,0)| < r$ for each $i, k \in \mathcal{V}$ then there exists $T > 0$ such that for $t + j \geq T$, implies $|\phi(t,j)|_{\mathcal{A}} \leq \varepsilon$. It follows

that,

$$
\begin{aligned}
|\phi_i^p(t,j) - \phi_k^p(t,j)|^2 &= |\phi_i^p(t,j) - \phi_k^p(t,j) + \bar{\phi}^p(t,j) - \bar{\phi}^p(t,j)|^2 \\
&\leq |\phi_i^p(t,j) - \bar{\phi}^p(t,j)|^2 + |\phi_k^p(t,j) - \bar{\phi}^p(t,j)|^2 \\
&\leq \sum_{i=1}^{N} \left|\phi_i^p(t,j) - \bar{\phi}^p(t,j)\right|^2 \leq \varepsilon
\end{aligned}
$$

which implies that $\mathcal{H}$ has uniform global synchronization with respect to p. ■

Remark 5.2.9 *Note that we cannot achieve uniform stable synchronization for the hybrid system $\mathcal{H}$ from uniform global asymptotic stability of the synchronization set $\mathcal{A}$ for $\mathcal{H}$. At this time, it is not evident how to recover the $\mathcal{K}_\infty$ function in terms of the synchronization error on the right-hand side of the inequality in the definition of uniform stable synchronization in Definition 5.2.3.*

Our final result establishes a $\mathcal{KL}$ characterization for uniform global asymptotic synchronization.

Theorem 5.2.10 *A hybrid system $\mathcal{H}$ as in* (5.4) *has uniform global asymptotic synchronization with respect to p if and only if there exists a function $\beta \in \mathcal{KL}$ such that any maximal solution $\phi = (\phi_1, \phi_2, \ldots, \phi_N)$ where $\phi_i = (\phi_i^p, \phi_i^q)$, satisfies*

$$
|\phi_i^p(t,j) - \phi_k^p(t,j)| \leq \beta(|\phi_i(0,0) - \phi_k(0,0)|, t+j) \tag{5.10}
$$

for all $(t,j) \in \operatorname{dom}\phi$ and for all $i,k \in \mathcal{V}$.

Proof The sufficient direction is immediate by definition of class-$\mathcal{KL}$ functions. To show necessity, assume $\mathcal{H}$ has uniform global asymptotic synchronization with respect to p. Define a

function $\beta_0 : \mathbb{R}_{\geq 0} \times \mathbb{R}_{\geq 0} \rightrightarrows [-\infty, \infty)$ by

$$\beta_0(r,s) = \sup\{|\phi_i^p(t,j) - \phi_i^q(t,j)| : \phi \in \mathcal{S}_{\mathcal{H}}(\phi(0,0)), \\ |\phi_i(0,0) - \phi_k(0,0)| < r, t+j \geq s, i,k \in \mathcal{V}\} \tag{5.11}$$

which implies that the bound

$$|\phi_i^p(t,j) - \phi_k^p(t,j)| \leq \beta_0(|\phi_i(0,0) - \phi_k(0,0), t+j)$$

for all $(t,j) \in \operatorname{dom}\phi$ and $i,k \in \mathcal{V}$ holds for all solutions to ϕ to $\mathcal{H}$. The definition further implies that $\beta_0(r,s)$ is nondecreasing in r and nonincreasing in s. One also has $\beta_0(r,s) \leq \alpha(r)$ for all $r,s \geq 0$, where α comes from the definition of uniform stable synchronization. Now define $\beta : \mathbb{R}_{\geq 0} \times \mathbb{R}_{\geq 0} \to \mathbb{R}_{\geq 0}$ by

$$\beta(r,s) = \max\{0, \beta_0(r,s)\}.$$

Then, $\beta(r,s)$ is non decreasing in r and nonincreasing in s, $\lim_{r\to 0^+} \beta(r,s) = 0$ for each $s \in \mathbb{R}_{\geq 0}$ since $\beta(r,s)$, and the bound in (5.10) holds for each solution ϕ. Finally, uniform global asymptotic attractivity of $\mathcal{A}$ implies that $\lim_{s\to\infty} \beta(r,s) = 0$ for each $r \geq 0$. Hence, β is a class-$\mathcal{KL}$ function. ■

Remark 5.2.11 *With global asymptotic stability, synchronization can be studied using (nonuniform and uniform) asymptotic stability tools for hybrid systems. Namely, sufficient conditions for such notions can be formulated in terms of an appropriately defined Lyapunov function $V : \mathbb{R}^n \to \mathbb{R}$ satisfying the conditions in [28, Definition 3.16] for $\mathcal{A}$. Such conditions require V to satisfy a bound of the form $\langle \nabla V(x), f\rangle < 0$ for all $x \in C \setminus \mathcal{A}$ and $f \in F(x)$, and $V(g) - V(x) < 0$ for all $x \in D \setminus \mathcal{A}$ and $g \in G(x)$. Then, integration of V over a solution ϕ leads to a strict decrease in V for all points in the flow and jump set, respectively. At times, however,*

strict inequalities might be hard to obtain. For such cases, when the system $\mathcal{H}$ in (5.4) *satisfies the hybrid basic conditions, we get stability and, via the invariance principle in [28, Theorem 8.2], if every maximal solution is complete to $\mathcal{H}$ converges to the largest weakly invariant subset where V does not change. Furthermore, at times, V may not necessarily decrease during flows but strictly decreases at jumps, or vice versa, in which case we can utilize the relaxed conditions in [28, Proposition 3.24, Proposition 3.27, Proposition 3.29, and Proposition 3.30].*

5.3 Summary

In this chapter, a brief discussion of asymptotic synchronization for generic interconnected agents with hybrid dynamics is presented. This chapter presents both uniform and nonuniform notions of partial state asymptotic synchronization in the sense of both stable and attractive synchronization which leads to an asymptotic synchronization property. Sufficient conditions for synchronization through the stability of a synchronization set were presented Lyapunov based tools for hybrid systems to certify asymptotic synchronization for two applications.

Part II

Impulse-Coupled Oscillators

Chapter 6

Desynchronization in Impulse-Coupled Oscillators

6.1 Introduction

Impulse-coupled oscillators are multi-agent systems with state variables consisting of timers that evolve continuously until a state-dependent event triggers an instantaneous update of their values. Networks of such oscillators have been employed to model the dynamics of a wide range of biological and engineering systems. In fact, impulse-coupled oscillators have been used to model groups of fireflies [31], spiking neurons [32, 33], muscle cells [34], wireless networks [35], and sensor networks [36]. With synchronization being a property of particular interest, such complex networks have been found to coordinate the values of their state variables by sharing information only at the times the events/impulses occur [31, 37].

The opposite of synchronization is *desynchronization*. In simple words, desynchronization in such systems is the notion that the agents' event times are separated "as far apart" as possible in time. Desynchronization is similar to phase-shifting or splay-state configurations,

and is sometimes referred in the literature as an inhibited behavior [38, 39]. For impulse-coupled oscillators, desynchronization is given as the behavior in which the separation between all of the timers impulses is equal [40]. This behavior has been found to be present in communication schemes in fish [41] and in networks of spiking neurons [42, 43]. Desynchronization of oscillators has recently been shown to be of importance in the understanding of Parkinson's disease [44, 45], in the design of algorithms that limit the amount of overlapping data transfer and data loss in wireless digital networks [35], and in the design of round-robin scheduling schemes for sensor networks [36].

Motivated by the applications mentioned above and the lack of a full understanding of desynchronization in multi-agent systems, this paper pertains to the study of the dynamical properties of desynchronization in a network of impulse-coupled oscillators with a completely connected communication graph. The uniqueness of the approach emerges from the use of hybrid systems tools, which not only conveniently capture the continuous and impulsive behavior in the networks of interest, but also are suitable for analytical study of asymptotic stability and robustness to perturbations.

More precisely, the dynamics of the proposed hybrid system capture the (linear) continuous evolution of the states as well their impulsive/discontinuous behavior due to state triggered events. Analysis of the asymptotic behavior of the trajectories (or solutions) to these systems is performed using the framework of hybrid systems introduced in [28, 27]. To this end, we recast the study of desynchronization as a set stabilization problem. Unlike synchronization, for which the set of points to stabilize is obvious, the complexity of desynchronization requires first to determine such a collection of points, which we refer to as the *desynchronization set*. We propose an algorithm to compute such set of points. Then, using Lyapunov stability theory for hybrid systems, we prove that the desynchronization set is asymptotically stable by defining a Lyapunov-like function as the distance between the state and (an inflated version of) the desyn-

chronization set. In our context, asymptotic stability of the desynchronization set implies that the distance between the state and the desynchronization set converges to zero as the amount of time and the number of jumps get large. Using the proposed Lyapunov-like function and invoking an invariance principle, the basin of attraction is characterized and shown to be the entire state space minus a set of measure zero, which turns out to actually be an exact estimate of the basin of attraction. Furthermore, also exploiting the availability of a Lyapunov-like function, we analytically characterize the time for the solutions to reach a neighborhood of the desynchronization set. In particular, this characterization provides key insight for the design of algorithms used in applications in which desynchronization is crucial, such as wireless digital networks and sensor networks.

The asymptotic stability property of the desynchronization configuration is shown to be robust to several types of perturbations. The perturbations studied here include a generic perturbation in the form of an inflation of the dynamics of the proposed hybrid system model of the network of interest and several kinds of perturbations on the timer rates. Using the tools presented in [28, 27], we analytically characterize the effect of these perturbations on the already established asymptotic stability property of the desynchronization set. In particular, these perturbations capture situations where the agents in the network are heterogeneous due to having differing timer rates, threshold values, and update laws. To verify the analytical results, we simulate networks of impulse-coupled oscillators under several classes of perturbations. Specifically, we show numerical results when perturbations affect the update laws and the timer rates.

The remainder of this paper is organized as follows. Section 6.2 is devoted to hybrid modeling of networks of impulse-coupled oscillators. Section 6.3.1 introduces an algorithm to determine the desynchronization set. Section 6.3.2 presents the stability results while the time to convergence is characterized in Section 6.3.3. The robustness results are in Section 6.3.4.

Section 6.4 presents numerical results illustrating our results. Final remarks are given in Section 6.5.

6.2 Hybrid System Model of Impulse-Coupled Oscillators

6.2.1 Mathematical Model

In this paper, we consider a model of N impulse-coupled oscillators. Each impulse-coupled oscillator has a continuous state (τ_i for the i-th oscillator) defining its internal timer. Once the timer of any oscillator reaches a threshold ($\bar{\tau}$), it triggers an impulse and is reset to zero. At such an event, all the other impulse-coupled oscillators rescale their timer by a factor given by $(1+\varepsilon)$ times the value of their timer, where $\varepsilon \in (-1, 0)$.[1] Figure 6.1 shows a trajectory of two impulse-coupled oscillators with states τ_1 and τ_2. In this figure, the dark red circles indicate when a timer state has reached the threshold and, thus, resets to zero. The light green circles indicate when an oscillator is externally reset and, hence, decreases its timer by $(1+\varepsilon)$ times its current state.

According to this outline of the model, the dynamics of the impulse-coupled oscillators involve impulses and timer resets, which are treated as true discrete events and instantaneous updates, while the smooth evolution of the timers before/after these events define the continuous dynamics. We follow the hybrid formalism of [28, 27], where a hybrid system is given by four objects (C, f, D, G) defining its *data*.

A hybrid system capturing the dynamics of the impulse-coupled oscillators is denoted as $\mathcal{H}_N := (C, f, D, G)$ and can be written in the compact form

$$\mathcal{H}_N : \qquad \tau \in \mathbb{R}^N \qquad \begin{cases} \dot{\tau} & = & f(\tau) & \tau \in C \\ \tau^+ & \in & G(\tau) & \tau \in D \end{cases}, \tag{6.1}$$

[1] Cf. the model for synchronization in [31] where $\varepsilon > 0$.

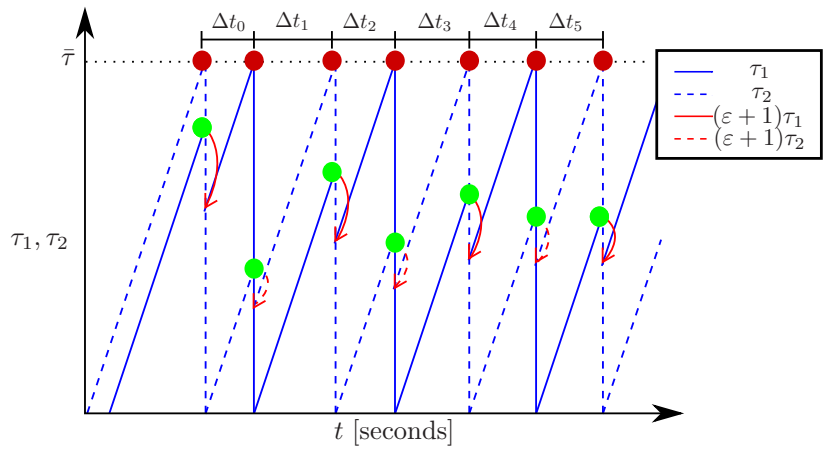

Figure 6.1: An example of two impulse-coupled oscillators reaching desynchronization (as Δt_i converges to a constant.) The internal resets (dark red circles) map the timers to zero. The external resets (light green circles) map the timers to a fraction $(1+\varepsilon)$ of their current value.

where $N \in \mathbb{N} \setminus \{0, 1\}$ is the number of impulse-coupled oscillators. The state of $\mathcal{H}_N$ is given by

$$\tau := [\tau_1 \quad \tau_2 \quad \dots \quad \tau_N]^\top \in P_N := [0, \bar{\tau}]^N.$$

The flow and jump sets are defined to constrain the evolution of the timers. The flow set is defined by

$$C := P_N, \tag{6.2}$$

where $I := \{1, 2, \dots, N\}$ and $\bar{\tau} > 0$ is the threshold. During flows, an internal clock gradually increases based on the homogeneous rate, ω. Then, the flow map is defined as

$$f(\tau) := \omega \mathbf{1} \qquad \forall \tau \in C$$

with $\omega > 0$ defining the natural frequency of each impulse-coupled oscillator. The impulsive events are captured by a jump set D and a jump map G. Jumps occur when the state is in the jump set D defined as

$$D := \{\tau \in P_N : \ \exists i \in I \text{ s.t. } \tau_i = \bar{\tau}\}. \tag{6.3}$$

From such points, the i-th timer is reset to zero and forces a jump of all other timers. Such discrete dynamics are captured by the following jump map: for each $\tau \in D$ define $G(\tau) = [g_1(\tau) \;\; g_2(\tau) \;\; \dots \;\; g_N(\tau)]^\top$, where, for each $i \in I$,

$$g_i(\tau) = \begin{cases} 0 & \text{if } \tau_i = \bar{\tau}, \tau_r < \bar{\tau} \;\; \forall r \in I \setminus \{i\} \\ \{0, \tau_i(1+\varepsilon)\} & \text{if } \tau_i = \bar{\tau} \; \exists r \in I \setminus \{i\} \text{ s.t. } \tau_r = \bar{\tau} \\ (1+\varepsilon)\tau_i & \text{if } \tau_i < \bar{\tau} \; \exists r \in I \setminus \{i\} \text{ s.t. } \tau_r = \bar{\tau} \end{cases} \tag{6.4}$$

with parameters $\varepsilon \in (-1, 0)$ and $\bar{\tau} > 0$; for $\tau \in D$, g_i is not empty. When a jump is triggered, the state τ_i jumps according to the i-th component of the jump map g_i. When a state reaches the threshold $\bar{\tau}$, it is reset to zero only when all other states are less than that threshold; otherwise, if multiple timers reach the threshold simultaneously, the jump map is set valued to indicate that either $g_i(\tau) = 0$ or $g_i(\tau) = (1+\varepsilon)\tau_i$ is possible. This is to ensure that the jump map satisfies the regularity conditions outlined in Section 8.2.2.[2]

6.2.2 Basic Properties of $\mathcal{H}_N$

6.2.2.1 Hybrid Basic Conditions

First, note that the hybrid system $\mathcal{H}_N$ satisfies the hybrid basic conditions as in Definition 2.1.8.

Lemma 6.2.1 *$\mathcal{H}_N$ satisfies the hybrid basic conditions.*

Proof Condition (a) is satisfied since C and D are closed. The function f is constant and therefore continuous on C, satisfying (b). With G as in (6.4), the graph of each g_i outer

[2] In [38], a more general flow map and a jump map incrementing τ_i by $\varepsilon > 0$ are considered.

semicontinious since its graph given by

$$\begin{aligned}\text{gph}(g_i) &= \{(x,y) : y \in g_i(x), x \in D\} \\ &= \{(x,y) : y = 0, x_i = \bar{\tau}, x_r \leq \bar{\tau}\ \forall r \neq i, x \in D\} \cup \{(x,y) : y = (1+\varepsilon)x_i, x_i \leq \bar{\tau}\ \exists x_r = \bar{\tau}, x \in D\}\end{aligned}$$

is closed. Then the set-valued mapping G is outer semicontinuous. By definition, G is bounded and nonempty for each $\tau \in D$, and hence it satisfies (c). ■

Note that satisfying the hybrid basic conditions implies that $\mathcal{H}_N$ is well-posed [28, Theorem 6.30], which, with asymptotic stability of a compact set, gives robustness to vanishing state disturbances; see [28, 27]. Section 6.3.4 considers different types of perturbations that $\mathcal{H}_N$ can withstand.

6.2.2.2 Solutions to $\mathcal{H}_N$

Namely, due to the nature of the flow and jump map, the solutions exhibit natural tendencies outlined in the following results.

Lemma 6.2.2 *From every point in $C \cup D$, there exists a solution and every maximal solution to $\mathcal{H}_N$ is complete and bounded.*

Proof The result follows from Proposition 2.10 in [28] using the following properties. For each point such that $\tau \in C$, the components of the flow map f are positive and induce solutions that flow towards D. For each $\tau \in D$, the jump map satisfies $G(\tau) \subset C$. Since it is impossible for solutions with initial conditions $\tau(0,0) \in C \cup D$ to escape $C \cup D$, all maximal solutions are complete and bounded. ■

Due to the jump map G, if the elements of the solution are initially equal (denote this set as $\mathcal{S} := \{\tau \in P_N : \exists i, r \in I, i \neq r, \tau_i = \tau_r\}$) it is possible for them to remain equal for all time. Furthermore, it is also possible for solutions to be initialized on the jump set such that

one element is at the threshold and another is equal to zero then after the jump they will be equal, e.g. let $\tau_1 = \bar{\tau}$, $\tau_2 = 0$ then $\tau_1^+ = \tau_2^+ = 0$. We denote this set as $\mathcal{G} := \{\tau \in D \setminus \mathcal{S} : \exists i, r \in I, i \neq r, \tau_i = 0, \tau_r = \bar{\tau}\}$. The next result considers solutions initialized on the set $\mathcal{X} := \mathcal{S} \cup \mathcal{G}$.

Lemma 6.2.3 *For each $\tau(0,0) \in \mathcal{X}_N$, there exists a solution τ to $\mathcal{H}_N$ from $\tau(0,0)$ such that, for some $M \in \{0,1\}$, $\tau(t,j) \in \mathcal{S}$ for all $t + j \geq M$, $(t,j) \in \operatorname{dom}\tau$.*

Proof Consider a solution τ to the hybrid system $\mathcal{H}_N$ with initial condition $\tau(0,0) \in \mathcal{S}$. Due to the flow map for each state being equal, τ remains in $\mathcal{S}$ during flows. Furthermore, at points $\tau \in \mathcal{S} \cap D$, the jump map G is set valued by the definition of g_i in (6.4). From these points, $G(\tau) \cap \mathcal{S} \neq \emptyset$. In fact, for each $\tau(0,0) \in \mathcal{S}$, there exists at least one solution such that $\tau(t,j) \in \mathcal{S}$ for all $t+j \geq 0$, with $(t,j) \in \operatorname{dom}\tau$. Consider the case of solutions initialized at $\tau(0,0) \in \mathcal{G}$ (Note that $\tau(0,0) \in D$). It follows that for some $r \in I$, $\tau_r(0,0) = \bar{\tau}$ and $g_r(\tau(0,0)) = 0$. Therefore, after the initial jump, we have that $G(\tau(0,0)) \cap \mathcal{S} \neq \emptyset$, by which using previous arguments implies that $\tau(t,j) \in \mathcal{S}$ for all $t + j \geq 1$. ■

Furthermore, there is a distinct ordering to the jumps. If τ is such that $\tau_i \neq \tau_r$ for all $i \neq r$ then the ordering of each τ_i is preserved after N jumps. More specifically, we have the following result.

Lemma 6.2.4 *For every solution τ to $\mathcal{H}_N$ with $\tau(0,0) \notin \mathcal{X}$, if at $(t_j, j) \in \operatorname{dom}\tau$ we have $0 \leq \tau_{i_1}(t_j,j) < \tau_{i_2}(t_j,j) < ... < \tau_{i_N}(t_j,j) \leq \bar{\tau}$ for some sequence of non-repeated elements $\{i_m\}_{m=1}^N$ of I (that is, a reordering of the elements of the set $I = \{1, 2, \ldots, N\}$) then, after N jumps, it follows that $0 \leq \tau_{i_1}(t_{j+N}, j+N) < \tau_{i_2}(t_{j+N}, j+N) < ... < \tau_{i_N}(t_{j+N}, j+N) \leq \bar{\tau}$.*

Proof Let τ be a solution to $\mathcal{H}_N$ from $P_N \setminus \mathcal{X}$. There exists a sequence i_k of distinct elements with $i_k \in I$ for each $k \in I$, such that $0 \leq \tau_{i_1}(t,j) < \tau_{i_2}(t,j) < \ldots < \tau_{i_N}(t,j) \leq \bar{\tau}$ over $[t_0, t_1] \times \{0\}$. After the jump at $(t,j) = (t_1, 0)$ we have $0 = \tau_{i_N}(t, j+1) < \tau_{i_1}(t, j+1) < \tau_{i_2}(t, j+$

$1) < \ldots < \tau_{i_{N-1}}(t, j+1) < \bar{\tau}$. Continuing this way for each jump, it follows that after $N-1$ more jumps, the solution is such that $0 \leq \tau_{i_1}(t_N, j+N) < \tau_{i_2}(t_N, j+N) < \ldots < \tau_{i_N}(t_N, j+N) \leq \bar{\tau}$ and the order at time (t, j) is preserved. ■

Using these properties of solutions to $\mathcal{H}_N$, the next section defines the set to which these solutions converge and establishes its stability properties.

6.3 Dynamical Properties of $\mathcal{H}_N$

The set of points from where the attractivity property holds called the basin of attraction and excludes all points where the system trajectories may never converge to $\mathcal{A}$. In fact, it will be established in Section 6.3.2 that the basin of attraction for asymptotic stability of desynchronization of $\mathcal{H}_N$ does not include any point τ such that any two or more timers are equal or become equal after a jump, which is the set $\mathcal{X}_N$ defined in Lemma 6.2.3. For this purpose, a Lyapunov-like function be constructed in Section 6.3.2 to show that a compact set denoted $\mathcal{A}$, defining the desynchronization condition, is asymptotically stable and weakly globally asymptotically stable.

6.3.1 Construction of the set $\mathcal{A}$ for $\mathcal{H}_N$

In this section, we identify the set of points corresponding to the impulse-coupled oscillators being desynchronized, namely, we define the *desynchronization set*. We define desynchronization as the behavior in which the separation between all of the timers' impulses is equal (and nonzero), see Figure 6.1. More specifically desynchronization is defined as follows:

Definition 6.3.1 *A solution τ to $\mathcal{H}_N$ is desynchronized if there exists $\Delta > 0$ and a sequence of non-repeated elements $\{i_m\}_{m=1}^N$ of I (that is, a reordering of the elements of the set $I =$*

$\{1, 2, \ldots, N\}$) *such that* $\lim_{j\to\infty}(t_j^{i_m} - t_j^{i_{m+1}}) = \Delta$ *for all* $m \in \{1, 2, \ldots, N-1\}$ *and* $\lim_{j\to\infty}(t_j^N - t_j^{i_1}) = \Delta$, *where* $\{t_j^{i_m}\}_{j=0}^{\infty}$ *is the sequence of jump times of the state* τ_{i_m}.

In fact, this separation between impulses leads to an ordered sequence of impulse times with equal separation. The desynchronization set $\mathcal{A}$ for the hybrid system $\mathcal{H}_N$ captures such a behavior and is parameterized by ε, the threshold $\bar{\tau}$, and the number of impulse-coupled oscillators N.

To define this set, first we provide some basic intuition about the dynamics of $\mathcal{H}_N$ when desynchronized. The set $\mathcal{A}$ must be forward invariant and such that trajectories staying in it satisfy the property in Definition 6.3.1. Due to the definition of the flow map f, there exist sets in the form of "lines" ℓ_k, each of them in the direction $\mathbf{1}$, which is the direction of the flow map, intersecting the jump set at a point which, for the k-th line, we denote as $\widetilde{\tau}^k$. We define the desynchronization set as the union of sets ℓ_k collecting points $\tau = \widetilde{\tau}^k + \mathbf{1}s \in P_N$ parameterized by $s \in \mathbb{R}$.

To identify $\widetilde{\tau}^k$, consider a point $\widetilde{\tau}^k \in D \setminus \mathcal{X}$ with components satisfying $\widetilde{\tau}_1^k = \bar{\tau} > \widetilde{\tau}_2^k > \widetilde{\tau}_3^k > \ldots > \widetilde{\tau}_N^k$. Due to Definition 6.3.1, it must be true that the difference between jump times are constant. This means that there must be some correlation between Δ and the difference between, in this case, τ_1^k and τ_2^k. Moreover, there must be a correlation between τ_1^k and all other states at jumps. It follows that this point belongs to $\mathcal{A}$ only if the distance between the expiring timer ($\widetilde{\tau}_1^k$) and each of its other components ($\widetilde{\tau}_i^k$, $i \in I \setminus \{1\}$) is equal to the distance between the value after the jump of the timer expiring next ($\widetilde{\tau}_2^{k+}$) and the value after the jump of its other components ($\widetilde{\tau}_i^{k+}$, $i \in I \setminus \{2\}$), respectively. This property ensures that, when in the desynchronization set, the relative distance between the leading timer and each of the other timers is equal, before and after jumps. More precisely,

$$\widetilde{\tau}_1^k - \widetilde{\tau}_i^k = \widetilde{\tau}_2^{k+} - \widetilde{\tau}_{\mathrm{next}(i)}^{k\,+} \qquad \forall\, i \in I \setminus \{1\}, \tag{6.5}$$

where $\widetilde{\tau}^{k+} = G(\widetilde{\tau}^k)$ and $\text{next}(i) = i+1$ if $i+1 \leq N$ and 1 otherwise.[3] Since $\mathcal{X}$ contains all points such that at least two or more timers are the same, we can consider the case when one component of $\widetilde{\tau}^k$ is equal to $\bar{\tau}$ at a time. For each such case, we have $(N-1)!$ possible permutations of the other components and N possible timer components equal to $\bar{\tau}$, leading to $N!$ total possible sets ℓ_k.

To illustrate computation of $\widetilde{\tau}^k$ in (6.5) and the construction of $\mathcal{A}$, consider the case of $N = 2$ and $\widetilde{\tau}_1^1 = \bar{\tau} > \widetilde{\tau}_2^1$. For $i = 2$, (6.5) becomes

$$\bar{\tau} - \widetilde{\tau}_2^1 = \widetilde{\tau}_2^1(\varepsilon + 1)$$

which leads to $\widetilde{\tau}_2^1 = \frac{\bar{\tau}}{\varepsilon+2}$. It follows that $\widetilde{\tau}^1 = [\bar{\tau}, \frac{\bar{\tau}}{\varepsilon+2}]^\top$. Similarly for $\widetilde{\tau}_2^1 = \bar{\tau} > \widetilde{\tau}_1^1$, we get from (6.5) the equation $\bar{\tau} - \widetilde{\tau}_1^1 = \widetilde{\tau}_2^1(\varepsilon + 1)$, which implies $\widetilde{\tau}^2 = [\frac{\bar{\tau}}{\varepsilon+2}, \bar{\tau}]^\top$. A glimpse at the case for $N = 3$ with $\widetilde{\tau}_1^1 = \bar{\tau} > \widetilde{\tau}_2^1 > \widetilde{\tau}_3^1$ indicates that (6.5) leads to

$$\bar{\tau} - \widetilde{\tau}_2^1 = \widetilde{\tau}_2^1(1+\varepsilon) - \widetilde{\tau}_3^1(1+\varepsilon), \qquad \bar{\tau} - \widetilde{\tau}_3^1 = \widetilde{\tau}_2^1(1+\varepsilon) - 0.$$

The solution to these equations is $\widetilde{\tau}^1 = [\bar{\tau}, \bar{\tau}(\varepsilon+2)/(\varepsilon^2+3\varepsilon+3), \bar{\tau}/(\varepsilon^2+3\varepsilon+3)]^\top$.

For the N case, the algorithm above results in the system of equations $\Gamma\tau_s = b$, where

$$\Gamma = \begin{bmatrix} 1 & 0 & 0 & 0 & \dots & 0 \\ 0 & (2+\varepsilon) & -(1+\varepsilon) & 0 & \dots & 0 \\ 0 & (1+\varepsilon) & 1 & -(1+\varepsilon) & \ddots & \vdots \\ 0 & (1+\varepsilon) & 0 & 1 & \ddots & 0 \\ \vdots & \vdots & \vdots & 0 & \ddots & -(1+\varepsilon) \\ 0 & (1+\varepsilon) & 0 & 0 & \dots & 1 \end{bmatrix} \tag{6.6}$$

and $b = \bar{\tau}\mathbf{1}$, where τ_s is the state $\widetilde{\tau}^k$ sorted into decreasing order. For example, if $\widetilde{\tau}^k$ is such that $\widetilde{\tau}_2^k = \bar{\tau} > \widetilde{\tau}_1^k > \widetilde{\tau}_3^k$, then τ_s is given as $[\widetilde{\tau}_2^k, \widetilde{\tau}_1^k, \widetilde{\tau}_3^k]^\top$. It can be shown that for any $\varepsilon \in (-1, 0)$,

[3] Note that G is single valued at each $\widetilde{\tau}^k \notin \mathcal{X}$.

a solution τ_s exists (see Lemma 6.2.2). Then, τ_s needs to be unsorted and becomes $\widetilde{\tau}^k$ in the definition of the set ℓ_k.

The solution to $\Gamma\tau_s = b$ is the result of a single case of $\tau \in D \setminus \mathcal{X}$. As indicated above, to get a full definition of the set $\mathcal{A}$, the $N!$ sets ℓ_k should be computed. For arbitrary N, the set $\mathcal{A}$ is given as a collection of sets ℓ_k given by

$$\mathcal{A} = \bigcup_{k=1}^{N!} \ell_k, \tag{6.7}$$

where, for each $k \in \{1, 2, \ldots, N!\}$, $\ell_k := \{\tau : \tau = \widetilde{\tau}^k + \mathbf{1}s \in P_N, s \in \mathbb{R}\}$.

6.3.2 Lyapunov Stability

Lyapunov theory for hybrid systems is employed to show that the set of points $\mathcal{A}$ is asymptotically stable. Our candidate Lyapunov-like function, which is defined below and uses the distance function, is built by observing that there exist points where the distance to $\mathcal{A}$ may increase during flows. This is due to the sets ℓ_k being a subset P_N. To avoid this issue, we define

$$\widetilde{\mathcal{A}} = \bigcup_{k=1}^{N!} \widetilde{\ell}_k \supset \mathcal{A}$$

where $\widetilde{\ell}_k$ is the extension of ℓ_k given by

$$\widetilde{\ell}_k = \left\{\tau \in \mathbb{R}^N : \tau = \widetilde{\tau}^k + \mathbf{1}s, s \in \mathbb{R}\right\}. \tag{6.8}$$

Then, with this extended version of $\mathcal{A}$, the proposed candidate Lyapunov-like function for asymptotic stability of $\mathcal{A}$ for $\mathcal{H}_N$ is given by the locally Lipschitz function

$$V(\tau) = \min\{|\tau|_{\widetilde{\ell}_1}, |\tau|_{\widetilde{\ell}_2}, \ldots, |\tau|_{\widetilde{\ell}_k}, \ldots, |\tau|_{\widetilde{\ell}_{N!}}\} \quad \forall\, \tau \in P_N \setminus \mathcal{X} \tag{6.9}$$

where, for some k, $|\tau|_{\widetilde{\ell}_k}$ is the distance between the point τ and the set $\widetilde{\ell}_k$.[4] The following theorem establishes asymptotic stability of $\mathcal{A}$ for $\mathcal{H}_N$. We show that the change in V during flows is zero and that at jumps we have a strict decrease of V; namely, $V(G(\tau)) - V(\tau) = -|\varepsilon|V(\tau)$. A key step in the proof is in using [28, Theorem 8.2] on a restricted version of $\mathcal{H}_N$.

Theorem 6.3.2 *For every $N \in \mathbb{N}, N > 1$, $\bar{\tau} > 0, \omega > 0$, and $\varepsilon \in (-1, 0)$, the hybrid system $\mathcal{H}_N$ is such that the compact set $\mathcal{A}$ is*

1. *asymptotically stable with basin of attraction given by $\mathcal{B}_{\mathcal{A}} := P_N \setminus \mathcal{X}$.*

2. *Furthermore, $\mathcal{A}$ weakly globally asymptotically stable.*

Proof Let the set $\mathcal{X}_{N,v}$ define the v-inflation of $\mathcal{X}_N$ (defined in Lemma 6.2.3), that is, the open set[5] $\mathcal{X}_{N,v} := \{\tau \in \mathbb{R}^N : |\tau|_{\mathcal{X}} < v\}$, where $v \in (0, v^*)$ and $v^* = \min_{x \in \mathcal{X}, y \in \widetilde{\mathcal{A}}} |x - y|$. Given any $v \in (0, v^*)$, we now consider a restricted hybrid system $\widetilde{\mathcal{H}}_N = (f, \widetilde{C}, G, \widetilde{D})$, where $\widetilde{C} := C \setminus \mathcal{X}_{N,v}$ and $\widetilde{D} := D \setminus \mathcal{X}_{N,v}$, which are closed. We establish that $\widetilde{\mathcal{A}}$ is an asymptotically stable set for $\widetilde{\mathcal{H}}_N$.

Note that the continuous function V, given by (6.9), is defined as the minimum distance from τ to $\widetilde{\mathcal{A}}$, where $\widetilde{\mathcal{A}}$ is the union of $N!$ sets $\widetilde{\ell}_k$ in (6.8). To determine the change of V during flows[6], we consider the relationship between the flow map and the sets $\widetilde{\ell}_k$. The inner product between a vector pointing in the direction of the set $\widetilde{\ell}_k$ and the flow map on $\widetilde{C}$ satisfies

$$\mathbf{1}^\top f(\tau) = \mathbf{1}^\top(\omega \mathbf{1}) = \omega N = |\mathbf{1}||\omega \mathbf{1}| = |\mathbf{1}||f(\tau)| \cos\theta$$

, which is only true if θ is zero. Therefore, the direction of the flow map and of the vector defining $\widetilde{\ell}_k$ are parallel, implying that the distance to the set $\widetilde{\mathcal{A}}$ is constant during flows.

[4] The set $\widetilde{\ell}_k$ can be described as a straight line in $\mathbb{R}^n$ passing through a point $\widetilde{\tau}^k$ and with slope $\mathbf{1}$. Then, $|\tau|_{\widetilde{\ell}_k}$ can be written as the general point-to-line distance $|(\widetilde{\tau}^k - \tau) - 1/N((\widetilde{\tau}^k - \tau)^\top \mathbf{1})\mathbf{1}|$.

[5] The set $\mathcal{X}_{N,v}$ is open since every point $\tau \in \mathcal{X}_v$ is an interior point of $\mathcal{X}_{N,}$.

[6] Its derivative can be computed using Clarke's generalized gradient [68].

The change in V during jumps is given by $V(G(\tau))-V(\tau)$ for $\tau \in \widetilde{D}\backslash\widetilde{\mathcal{A}}$. Due to the fact that we can rearrange the components of $\tau \in P_N \setminus \mathcal{X}_N$, without loss of generality, we consider a single jump condition, namely, we consider τ such that $\bar{\tau} = \tau_1 > \tau_2 > \ldots > \tau_{N-1} > \tau_N$. Using the formulation in Section 6.3.1 and [69, Lemma A.1], the elements of the vector $\widetilde{\tau}^k$ associated with $\widetilde{\ell}_k$ for this case of τ are given by $\widetilde{\tau}_i^k = \frac{\sum_{p=0}^{N-i}(\varepsilon+1)^p}{\sum_{p=0}^{N-1}(\varepsilon+1)^p}\bar{\tau}$, which by [69, Lemma A.2] is equal to $\frac{(\varepsilon+1)^{N-i+1}-1}{(\varepsilon+1)^N-1}\bar{\tau}$. After the jump, $G(\tau)$ is single valued and is such that its elements are ordered as follows: $g_2(\tau) > g_3(\tau) > \ldots > g_N(\tau) > g_1(\tau) = 0$. Specifically, the jump map is $G(\tau) = [0, (1+\varepsilon)\tau_2, \ldots, (1+\varepsilon)\tau_N]^\top$. Then, the formulation in Section 6.3.1 and Lemma 6.2.2 leads to a case of $\widetilde{\tau}^k$ denoted as $\widetilde{\tau}^{k'}$. By [69, Lemma A.2], the elements of the vector $\widetilde{\tau}^{k'}$ are given by $\widetilde{\tau}_1^{k'} = \frac{\varepsilon}{(\varepsilon+1)^N-1}\bar{\tau}$ and $\widetilde{\tau}_i^{k'} = \frac{(\varepsilon+1)^{N-i+2}-1}{(\varepsilon+1)^N-1}\bar{\tau}$ for $i > 1$. Due to the ordering of τ and $G(\tau)$, $\widetilde{\tau}^{k'}$ is a one-element shifted (to the right) version of $\widetilde{\tau}^k$.

From the definition of $\widetilde{\tau}^k$ above, V at τ reduces to

$$V(\tau) = |\tau|_{\widetilde{\ell}_k} = \left|(\widetilde{\tau}^k - \tau) - \frac{1}{N}((\widetilde{\tau}^k - \tau)^\top \mathbf{1})\mathbf{1}\right|$$

for some k. Note that

$$(\widetilde{\tau}^k - \tau)^\top \mathbf{1} = \sum_{i=1}^{N} \widetilde{\tau}_i^k - \sum_{i=1}^{N} \tau_i$$

reduces to $\sum_{i=2}^{N} \widetilde{\tau}_i^k - \sum_{i=2}^{N} \tau_i$ since $\tau_1 = \widetilde{\tau}_1^k = \bar{\tau}$. Using [69, Lemma A.2] and [69, Lemma A.3], it follows that

$$\sum_{i=2}^{N} \widetilde{\tau}_i^k = \frac{\sum_{i=2}^{N}\sum_{p=0}^{N-i}(\varepsilon+1)^p}{\sum_{p=0}^{N-1}(\varepsilon+1)^p}\bar{\tau} = \frac{((\varepsilon+1)^N - 1) - N\varepsilon}{\varepsilon((\varepsilon+1)^N - 1)}\bar{\tau}.$$

Then, the first element of the vector inside the norm in the expression of $V(\tau)$ is given as

$$(\widetilde{\tau}_1^k - \tau_1) - \frac{1}{N}\left(\frac{((\varepsilon+1)^N - 1) - N\varepsilon}{\varepsilon((\varepsilon+1)^N - 1)}\bar{\tau} - \sum_{i=2}^{N}\tau_i\right) = -\frac{((\varepsilon+1)^N - 1) - N\varepsilon}{\varepsilon N((\varepsilon+1)^N - 1)}\bar{\tau} + \frac{1}{N}\sum_{i=2}^{N}\tau_i,$$

while the elements with $m \in \{2, 3, \ldots, N\}$ are given by

$$
\begin{aligned}
(\widetilde{\tau}_m^k - \tau_m) - \frac{1}{N}\left(\frac{((\varepsilon+1)^N - 1) - N\varepsilon}{\varepsilon((\varepsilon+1)^N - 1)}\bar{\tau} - \sum_{i=2}^{N}\tau_i\right) \\
= \left(\frac{(\varepsilon+1)^{N-m+1} - 1}{(\varepsilon+1)^N - 1}\bar{\tau} - \tau_m\right) - \frac{1}{N}\left(\frac{((\varepsilon+1)^N - 1) - N\varepsilon}{\varepsilon((\varepsilon+1)^N - 1)}\bar{\tau} - \sum_{i=2}^{N}\tau_i\right) \\
= \frac{\varepsilon N(\varepsilon+1)^{N-m+1} - ((\varepsilon+1)^N - 1)}{\varepsilon N((\varepsilon+1)^N - 1)}\bar{\tau} - \frac{N-1}{N}\tau_m + \frac{1}{N}\sum_{i=2, i\neq m}^{N}\tau_i.
\end{aligned}
$$

After the jump at τ, since $G(\tau)$ is single valued, $V(G(\tau))$ is given by

$$
|G(\tau)|_{\widetilde{\ell}_{k'}} = \left|(\widetilde{\tau}^{k'} - G(\tau)) - \frac{1}{N}((\widetilde{\tau}^{k'} - G(\tau))^\top \mathbf{1})\mathbf{1}\right|.
$$

Note that $(\widetilde{\tau}^{k'} - G(\tau))^\top \mathbf{1} = \sum_{i=1}^{N}\widetilde{\tau}_i^{k'} - \sum_{i=1}^{N} g_i(\tau)$ reduces to $\sum_{i=1}^{N}\widetilde{\tau}_i^{k'} - \sum_{i=2}^{N}(1+\varepsilon)\tau_i$, since $g_1(\tau) = 0$ and $g_i(\tau) = (1+\varepsilon)\tau_i$ for $i > 1$. Using [69, Lemma A.2] and [69, Lemma A.3], it follows that

$$
\sum_{i=1}^{N}\widetilde{\tau}_i^{k'} = \frac{\sum_{i=1}^{N}\sum_{p=0}^{N-i}(\varepsilon+1)^p}{\sum_{p=0}^{N-1}(\varepsilon+1)^p}\bar{\tau} = \frac{(\varepsilon+1)((\varepsilon+1)^N - 1) - N\varepsilon}{\varepsilon((\varepsilon+1)^N - 1)}\bar{\tau}
$$

which leads to

$$
(\widetilde{\tau}^{k'} - G(\tau))^\top \mathbf{1} = \frac{(\varepsilon+1)((\varepsilon+1)^N - 1) - N\varepsilon}{\varepsilon((\varepsilon+1)^N - 1)}\bar{\tau} - \sum_{i=2}^{N}(1+\varepsilon)\tau_i.
$$

The first element inside the norm in $V(G(\tau))$ is given by

$$
\begin{aligned}
(\widetilde{\tau}_1^{k'} - g_1(\tau)) - \frac{1}{N}\left(\frac{(\varepsilon+1)((\varepsilon+1)^N - 1) - N\varepsilon}{\varepsilon((\varepsilon+1)^N - 1)}\bar{\tau} - \sum_{i=2}^{N}(1+\varepsilon)\tau_i\right) \\
= \frac{\varepsilon}{(\varepsilon+1)^N - 1}\bar{\tau} - \frac{(\varepsilon+1)((\varepsilon+1)^N - 1) - N\varepsilon}{\varepsilon N((\varepsilon+1)^N - 1)}\bar{\tau} + \frac{1}{N}\sum_{i=2}^{N}(1+\varepsilon)\tau_i \\
= (1+\varepsilon)\left(-\frac{((\varepsilon+1)^N - 1) - N\varepsilon}{\varepsilon N((\varepsilon+1)^N - 1)}\bar{\tau} + \frac{1}{N}\sum_{i=2}^{N}\tau_i\right).
\end{aligned}
$$

For each element $m > 1$, it follows that

$$
\begin{aligned}
(\widetilde{\tau}_m^{k'} - g_m(\tau)) - \frac{1}{N}\left(\frac{(\varepsilon+1)((\varepsilon+1)^N-1) - N\varepsilon}{\varepsilon((\varepsilon+1)^N-1)}\bar{\tau} - \sum_{i=2}^{N}(1+\varepsilon)\tau_i\right) \\
= \frac{(\varepsilon+1)^{N-m+2}-1}{(\varepsilon+1)^N-1}\bar{\tau} - (1+\varepsilon)\frac{N-1}{N}\tau_m \\
- \frac{(\varepsilon+1)((\varepsilon+1)^N-1) - N\varepsilon}{\varepsilon N((\varepsilon+1)^N-1)}\bar{\tau} + \frac{1}{N}\sum_{i=2, i\neq m}^{N}(1+\varepsilon)\tau_i \\
= (1+\varepsilon)\left(\frac{\varepsilon N(\varepsilon+1)^{N-m+1} - ((\varepsilon+1)^N-1)}{\varepsilon N((\varepsilon+1)^N-1)}\bar{\tau}\right. \\
\left. - \frac{N-1}{N}\tau_m + \frac{1}{N}\sum_{i=2, i\neq m}^{N}\tau_i\right).
\end{aligned}
$$

Combining the expressions for each of the elements inside the norm of $V(G(\tau))$, it follows that $V(G(\tau)) = (1+\varepsilon)V(\tau)$.

Then, the change during jumps is given by $V(G(\tau)) - V(\tau) = \varepsilon V(\tau)$ where $\varepsilon \in (-1, 0)$. With the property of V during flows established above, the change of V along solutions is bounded during flows and jumps by the nonpositive functions $u_{\widetilde{C}}$ and $u_{\widetilde{D}}$, respectively, defined as follows: $u_{\widetilde{C}}(z) = 0$ for each $z \in \widetilde{C}$ and $u_{\widetilde{C}}(z) = -\infty$ otherwise; $u_{\widetilde{D}}(z) = \varepsilon V(z)$ for each $z \in \widetilde{D}$ and $u_{\widetilde{D}}(z) = -\infty$ otherwise. Using Lemma 6.2.1, the fact that $\widetilde{C}$ and $\widetilde{D}$ are closed, and the fact that every maximal solution to $\widetilde{\mathcal{H}}$ is bounded and complete, by [28, Theorem 8.2], every maximal solution to $\widetilde{\mathcal{H}}_N$ approaches the largest weakly invariant subset of $L_V(r') \cap \widetilde{C} \cap [L_{u_{\widetilde{C}}}(0) \cup (L_{u_{\widetilde{D}}}(0) \cap G(L_{u_{\widetilde{C}}}(0)))] = L_V(r') \cap \widetilde{C}$ for $r' \in V(\widetilde{C})$. Since every maximal solution jumps an infinite number of times, the largest invariant set is given for $r' = 0$ due to the fact that $V(G(\tau)) - V(\tau) = \varepsilon V(\tau) < 0$ if $r' > 0$. Then, the largest invariant set is given by $L_V(0) \cap \widetilde{C} = \widetilde{\mathcal{A}} \cap \widetilde{C}$ which is identically equal to $\mathcal{A}$. Hence, the set $\mathcal{A}$ is attractive. Stability is guaranteed from the fact that V is nonincreasing during flows and strictly decreasing during jumps. Then, the set $\widetilde{\mathcal{A}}$ is asymptotically stable for the hybrid system $\widetilde{\mathcal{H}}_N$. We have that $\mathcal{A}$ is (strongly) forward invariant and from Theorem 6.3.3 we know that $\mathcal{A}$ is uniformly attractive

from a neighborhood of itself. Then by Proposition 7.5 in [28], it follows that $\mathcal{A}$ is asymptotically stable.

Due to the set of solutions to $\widetilde{\mathcal{H}}_N$ coinciding with the set of solutions to $\mathcal{H}_N$ from $P_N \setminus \mathcal{X}_{N,v}$, the set $\mathcal{A}$ is asymptotically stable for $\mathcal{H}_N$ with basin of attraction $\mathcal{B}_{\mathcal{A}} = P_N \setminus \mathcal{X}_{N,v}$. Since v is arbitrary, it follows that the basin of attraction is equal to $P_N \setminus \mathcal{X}_N$.

For all $\tau \in \mathcal{X}_N$, the jump map G is set valued by definition of g_i in (6.4). From these points there exist solutions to $\mathcal{H}_N$ that jump out of $\mathcal{X}$. In fact, consider the case $\tau \in \mathcal{X}_N$. We have that $\tau_i = \tau_r$ for some $i, r \in I$. Then, after the jump it follows that $g_i(\tau) \in \{0, (1+\varepsilon)\bar{\tau}\}$ and $g_r(\tau) \in \{0, (1+\varepsilon)\bar{\tau}\}$, and there exist g_i and g_r such that $g_i = g_r$ or $g_i \neq g_r$. Since for every point in $\mathcal{X}_N$ there exists a solution that converges to $\mathcal{A}$ and also a solution that stays in $\mathcal{X}_N$, $\mathcal{X}_N$ is weakly forward invariant.[7] ■

6.3.3 Characterization of Time of Convergence

In this section, we characterize the time to converge to a neighborhood of $\mathcal{A}$. The proposed (upper bound) of the time to converge depends on the initial distance to the set $\widetilde{\mathcal{A}}$ and the parameters of the hybrid system $(\varepsilon, \bar{\tau})$.

Theorem 6.3.3 *For every $N \in \mathbb{N}$, $N > 1$, and every c_1, c_2 such that $\overline{c} > c_2 > c_1 > 0$ with $\overline{c} = \max_{x \in \mathcal{X}} |x|_{\widetilde{\mathcal{A}}}$, every maximal solution to $\mathcal{H}_N$ with initial condition $\tau(0,0) \in (P_N \setminus \mathcal{X}) \cap \widetilde{L}_V(c_2)$ is such that $\tau(t,j) \in \widetilde{L}_V(c_1)$ for each $(t,j) \in \operatorname{dom}\tau, t+j \geq M$, where $M = \left(\frac{\bar{\tau}}{\omega} + 1\right) \frac{\log \frac{c_2}{c_1}}{\log \frac{1}{1+\varepsilon}}$ and $\widetilde{L}_V(\mu) := \{\tau \in C \cup D : V(\tau) \leq \mu\}$.*

Proof Let $\tau_0 = \tau(0,0)$ and pick a maximal solution τ to $\mathcal{H}_N$ from τ_0. At every jump time

[7] For example, consider the case $N = 2$. If $\tau(0,0) = [\bar{\tau}, \bar{\tau}]^\top \in D$, then there are nonunique solutions due to the jump map begin set valued. It follows that after the jump, each τ_i can be mapped to any point in $\{0, \tau_i(1+\varepsilon)\}$, which leads to any of the following four options of the states (τ_1, τ_2) after such a jump: $(0,0), (0, \bar{\tau}(1+\varepsilon)), (\bar{\tau}(1+\varepsilon), 0)$ or $(\bar{\tau}(1+\varepsilon), \bar{\tau}(1+\varepsilon))$. If the state is mapped to either $(0,0)$ or $(\bar{\tau}(1+\varepsilon), \bar{\tau}(1+\varepsilon))$, then it remains in $\mathcal{X}_2$. Conversely, if any of the other options are chosen, then (τ_1, τ_2) leaves $\mathcal{X}_2$ and converges to $\mathcal{A}$ asymptotically.

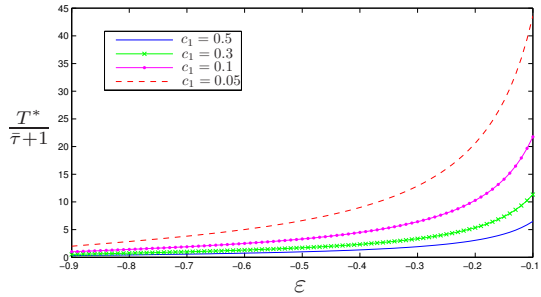

Figure 6.2: Time to converge (over $\bar{\tau}+1$) as a function of $\varepsilon \in [-0.9, -0.1]$, with $c_2 = 0.99\bar{\tau}$ and $c_1 \in \{0.5\bar{\tau}, 0.3\bar{\tau}, 0.1\bar{\tau}, 0.05\bar{\tau}\}$

$(t_j, j) \in \operatorname{dom}\tau$, define $\bar{g}_1 = \tau(t_1, 1)$, $\bar{g}_2 = \tau(t_2, 2), \ldots, \bar{g}_J = \tau(t_J, J)$, for some $J \in \mathbb{N}$. From Theorem 6.3.2, we have that there is no change in the Lyapunov function during flows. Furthermore, we have that for each $\tau \in D \setminus \mathcal{A}$ the difference $V(G(\tau)) - V(\tau) = \varepsilon V(\tau)$ with $\varepsilon \in (-1, 0)$. Since, for every j, $\tau(t_j, j) \in D$, we have $V(\bar{g}_1) - V(\tau_0) = \varepsilon V(\tau_0)$, which implies $V(\bar{g}_1) = (1+\varepsilon)V(\tau_0)$. At the next jump, we have $V(\bar{g}_2) = (1+\varepsilon)V(\bar{g}_1) = (1+\varepsilon)^2 V(\tau_0)$. Proceeding in this way, after J jumps we have $V(\bar{g}_J) = (1+\varepsilon)V(g_{J-1}) = (1+\varepsilon)^J V(\tau_0)$. From $V(\bar{g}_J) = (1+\varepsilon)^J V(\tau_0)$, we want to find J so that $V(\bar{g}_J) \leq c_1$ when $V(\tau_0) \leq c_2$. Considering the worst cast for $V(\tau_0)$, we want $(1+\varepsilon)^J c_2 \leq c_1$, which implies $\frac{c_2}{c_1} \leq \left(\frac{1}{1+\varepsilon}\right)^J$, and therefore $J = \left\lceil \frac{\log \frac{c_2}{c_1}}{\log \frac{1}{1+\varepsilon}} \right\rceil > 0$. For each j, the time between jumps satisfies $t_1 - t_0 \leq \frac{\bar{\tau}}{\omega}, t_2 - t_1 \leq \frac{\bar{\tau}}{\omega}, \ldots, t_j - t_{j-1} \leq \frac{\bar{\tau}}{\omega}$. Then, we have that after J jumps, $\sum_{j=1}^{J} t_j - t_{j-1} \leq J\frac{\bar{\tau}}{\omega}$. With $t_0 = 0$, the expression reduces to $t_J \leq J\frac{\bar{\tau}}{\omega} = \left\lceil \frac{\log \frac{c_2}{c_1}}{\log \frac{1}{1+\varepsilon}} \right\rceil \frac{\bar{\tau}}{\omega}$. Then, after $t + j \geq t_J + J$, the solution is at least c_1 close to the set $\widetilde{\mathcal{A}}$. Defining $M = t_J + J$, we then have $M = \left(\frac{\bar{\tau}}{\omega} + 1\right) \frac{\log \frac{c_2}{c_1}}{\log \frac{1}{1+\varepsilon}}$. ■

Figure 6.2 shows the time to converge (divided by $\frac{\bar{\tau}}{\omega} + 1$) versus ε with constant $c_2 = 0.99\bar{\tau}$ and varying values of c_1. As the figure indicates, the time to converge decreases as $|\varepsilon|$ increases, which confirms the intuition that the larger the jump the faster oscillators desynchronize.

6.3.4 Robustness Analysis

Lemma 6.2.1 establishes that the hybrid model of N impulse-coupled oscillators satisfies the hybrid basic conditions. In light of this property, the asymptotic stability property of $\mathcal{A}$ for $\mathcal{H}_N$ is preserved under certain perturbations; i.e., asymptotic stability is robust [28]. In the next sections, we consider a perturbed version of $\mathcal{H}_N$ and present robust stability results. In particular, we consider generic perturbations to $\mathcal{H}_N$, and two different cases of perturbations only on the timer rates to allow for heterogeneous timers.

6.3.4.1 Robustness to Generic Perturbations

We start by revisiting the definition of perturbed hybrid systems in [28].

Definition 6.3.4 (perturbed hybrid system [28, Definition 6.27]) *Given a hybrid system $\mathcal{H}$ and a function $\rho : \mathbb{R}^N \to \mathbb{R}_{\geq 0}$, the ρ-perturbation of $\mathcal{H}$, denoted $\mathcal{H}_\rho$, is the hybrid system*

$$\begin{cases} x \in C_\rho & \dot{x} \in F_\rho(x) \\ x \in D_\rho & x^+ \in G_\rho(x) \end{cases}$$

where

$$\begin{aligned} C_\rho &= \{x \in \mathbb{R}^n : (x + \rho(x)\mathbb{B}) \cap C \neq \emptyset\}, \\ F_\rho(x) &= \overline{\text{con}} F((x + \rho(x)\mathbb{B}) \cap C) + \rho(x)\mathbb{B} \quad \forall x \in \mathbb{R}^n, \\ D_\rho &= \{x \in \mathbb{R}^n : (x + \rho(x)\mathbb{B}) \cap D \neq \emptyset\}, \\ G_\rho(x) &= \{v \in \mathbb{R}^n : v \in g + \rho(g)\mathbb{B}, g \in G((x + \rho(x)\mathbb{B}) \cap D)\} \quad \forall x \in \mathbb{R}^n. \end{aligned}$$

Using this definition, we can deduce a generic perturbed hybrid system modeling N impulse-coupled oscillators. Then, for the hybrid system $\mathcal{H}_N$, we denote $\mathcal{H}_{N,\rho}$ as the ρ-perturbation of $\mathcal{H}_N$. Given the perturbation function $\rho : \mathbb{R}^N \to \mathbb{R}_{\geq 0}$, the perturbed flow map is given by $F_\rho(\tau) = \omega\mathbf{1} + \rho(\tau)\mathbb{B}$ for all $\tau \in C_\rho$, where the perturbed flow set C_ρ is given by $C_\rho = \{\tau \in \mathbb{R}^N :$

$(\tau + \rho(\tau)\mathbb{B}) \cap P_N \neq \emptyset\}$. For example, if $N = 2$ and $\rho(\tau) = \bar{\rho} > 0$ for all $\tau \in \mathbb{R}^N$, which would correspond to constant perturbations on the lower value and threshold, then $C_\rho = C + \rho\mathbb{B}$. The perturbed jump map and jump set are defined as $D_\rho = \{\tau \in \mathbb{R}^N : (\tau + \rho(\tau)\mathbb{B}) \cap D \neq \emptyset\}$, $G_\rho = [g_{1,\rho}(\tau), \ldots, g_{N,\rho}(\tau)]^\top$, where $g_{i,\rho}$ is the i-th component of G_ρ. The following result establishes that the hybrid system $\mathcal{H}_N$ is robust to small perturbations.

Theorem 6.3.5 *(robustness of asymptotic stability) If $\rho : \mathbb{R}^N \to \mathbb{R}_{\geq 0}$ is continuous and positive on $\mathbb{R}^N \setminus \mathcal{A}$, then $\mathcal{A}$ is semiglobally practically robustly $\mathcal{KL}$ asymptotically stable with basin of attraction $B_\mathcal{A} = P_N \setminus \mathcal{X}$, i.e., for every compact set $K \subset B_\mathcal{A}$ and every $\alpha > 0$, there exists $\delta \in (0, 1)$ such that every maximal solution τ to $\mathcal{H}_{N,\delta\rho}$ from K satisfies $|\tau(t, j)|_\mathcal{A} \leq \beta(|\tau(0, 0)|_\mathcal{A}, t + j) + \alpha$ for all $(t, j) \in \operatorname{dom} \tau$.*

Proof From Lemma 6.2.1, the hybrid system $\mathcal{H}_N$ satisfies the hybrid basic conditions. Therefore, by [28, Theorem 6.8] $\mathcal{H}_N$ is nominally well-posed and, moreover, by [28, Proposition 6.28] is well-posed. From the proof of Theorem 6.3.2, we know that the set $\mathcal{A}$ is an asymptotically stable compact set for the hybrid system $\mathcal{H}_N$ with basin of attraction $B_\mathcal{A}$. Since by Lemma 6.2.2, every maximal solution is complete, then [28, Theorem 7.20] implies that $\mathcal{A}$ is semiglobally practically robustly $\mathcal{KL}$ asymptotically stable. ■

Section 6.4.2.1 showcases several simulations of $\mathcal{H}_N$ with ρ-perturbations on the jump map.

6.3.4.2 Robustness to Heterogeneous Timer Rates

We consider the case when the continuous dynamic rates are perturbed in the form of

$$\frac{d}{dt}|\tau(t, j)|_{\tilde{\mathcal{A}}} = c(t, j)$$

for a given solution τ. For example, consider the perturbation of the flow map given by

$$f(\tau) = \omega\mathbf{1} + \Delta\omega \tag{6.10}$$

where $\Delta\omega \in \mathbb{R}^n$ is a constant defining a perturbation from the natural frequencies of the impulse-coupled oscillators. Then for some k, during flows, along a solution τ such that over $[t_j, t_{j+1}] \times \{j\}$ satisfies $V(\tau(t,j)) = |\tau(t,j)|_{\widetilde{\ell}_k}$, it follows that c reduces to $c(t,j) = \left(\frac{r_{\ell_k}^\top(\tau(t,j))(\frac{1}{N}\underline{\mathbf{1}}-\mathbf{I})}{|\tau(t,j)|_{\ell_k}}\right)\Delta\omega$.[8] Furthermore, the norm of the hybrid arc c can be bounded by a constant $\bar{c}$ given by

$$\bar{c} = \left|\left(\frac{1}{N}\underline{\mathbf{1}} - \mathbf{I}\right)\Delta\omega\right|. \tag{6.11}$$

Building from this example, the following result provides properties of the distance to $\widetilde{\mathcal{A}}$ from solutions τ to $\mathcal{H}_N$ under generic perturbations on f (not necessarily as in (6.10)).

Theorem 6.3.6 *Suppose that the perturbation on the flow map of $\mathcal{H}_N$ is such that a perturbed solution τ satisfies, for each j such that $\{t : (t,j) \in \operatorname{dom}\tau\}$ has more than one point, $\frac{d}{dt}|\tau(t,j)|_{\widetilde{\mathcal{A}}} = c(t,j)$ for all $t \in \{t : (t,j) \in \operatorname{dom}\tau\}$ and $\tau(t,j) \in P_N \setminus \mathcal{X}$ for all $(t,j) \in \operatorname{dom}\tau$, for some hybrid arc c with $\operatorname{dom} c = \operatorname{dom}\tau$. Then, the following hold:*

- *The asymptotic value of $|\tau(t,j)|_{\widetilde{\mathcal{A}}}$ satisfies*

$$\lim_{t+j\to\infty} |\tau(t,j)|_{\widetilde{\mathcal{A}}} \leq \lim_{t+j\to\infty} \sum_{i=0}^{j} (1+\varepsilon)^{j-i} \int_{t_i}^{t_{i+1}} c(t,j)dt \tag{6.12}$$

- *If there exists $\bar{c} > 0$ such that $|c(t,j)| \leq \bar{c}$ for each $(t,j) \in \operatorname{dom}\tau$ then*

$$\lim_{t+j\to\infty} |\tau(t,j)|_{\widetilde{\mathcal{A}}} \leq \frac{\bar{c}\bar{\tau}}{|\varepsilon|\omega}. \tag{6.13}$$

- *If $\widetilde{j} : \mathbb{R}_{\geq 0} \to \mathbb{N}$ is a function that chooses the appropriate minimum j such that $(t,j) \in$*

[8] Let $r_{\ell_k}(\tau)$ be the vector defined by the minimum distance from τ to the line ℓ_k. Then, it follows that $V(\tau) = (r_{\ell_k}^\top(\tau) r_{\ell_k}(\tau))^{\frac{1}{2}}$. To determine its change during flows, note that on $C \setminus (\mathcal{X} \cup \mathcal{A})$ the gradient is given by $\nabla V(\tau) = \frac{\partial}{\partial\tau}\left(r_{\ell_k}^\top(\tau) r_{\ell_k}(\tau)\right)^{\frac{1}{2}} = \frac{\left(r_{\ell_k}^\top(\tau)\frac{\partial}{\partial\tau} r_{\ell_k}(\tau)\right)}{|\tau|_{\ell_k}}$ where each j-th entry of $\frac{\partial}{\partial\tau} r_{\ell_k}(\tau)$ is given by $\frac{\partial}{\partial\tau} r_{\ell_k}^j(\tau) = \frac{\partial}{\partial\tau}\left((\widetilde{\tau}_j^k - \tau_j) - \frac{1}{N}\sum_{i=1}^N (\widetilde{\tau}_i^k - \tau_i)^\top\right) = \left[\frac{1}{N}, \frac{1}{N}, \ldots, \frac{1}{N}, -1+\frac{1}{N}, \frac{1}{N}, \ldots, \frac{1}{N}\right]$ – the term $-1+\frac{1}{N}$ corresponds to the j-th element of the vector. It follows that $\frac{\partial}{\partial\tau} r_{\ell_k}(\tau) = \frac{1}{N}\underline{\mathbf{1}} - \mathbf{I}$. Then, for each $\tau \in C \setminus \mathcal{X}$, $\langle \nabla V(\tau), f(\tau)\rangle = \left(\frac{r_{\ell_k}^\top(\tau)(\frac{1}{N}\underline{\mathbf{1}}-\mathbf{I})}{|\tau|_{\ell_k}}\right) f(\tau)$.

$\operatorname{dom}\tau$ *for each time* t *and* $t \mapsto c(t, \widetilde{j}(t))$ *is absolutely integrable, i.e.,* $\exists B$ *such that*

$$\int_0^\infty |c(t, \widetilde{j}(t))| dt \leq B, \tag{6.14}$$

then

$$\lim_{t+j\to\infty} |\tau(t,j)|_{\widetilde{\mathcal{A}}} \leq \frac{B}{\varepsilon}. \tag{6.15}$$

Proof Consider a maximal solution τ to $\mathcal{H}_N$ with initial condition $\tau(0,0) \in P_N \setminus \mathcal{X}$. This proof uses the function V from the proof of Theorem 6.3.2. With V equal to the distance from τ to the set $\widetilde{\mathcal{A}}$, then, for each $\tau \in D \setminus \mathcal{X}$, we have that $V(G(\tau)) - V(\tau) = \varepsilon V(\tau)$. Using the fact that $V(\tau) = |\tau|_{\widetilde{\mathcal{A}}}$ and the fact that, G along the solution is single valued, it follows that $|\tau|_{\widetilde{\mathcal{A}}}$ after a jump can be equivalently written as $|\tau(t_j, j+1)|_{\widetilde{\mathcal{A}}} = (1+\varepsilon)|\tau(t_j, j)|_{\widetilde{\mathcal{A}}}$. By assumption, in between jumps, the distance to the set $\widetilde{\mathcal{A}}$ is such that $\frac{d}{dt}|\tau(t,j)|_{\widetilde{\mathcal{A}}} = c(t,j)$, which implies that at t_{j+1} the distance to the desynchronization set is given by

$$|\tau(t_{j+1}, j)|_{\widetilde{\mathcal{A}}} = \int_{t_j}^{t_{j+1}} c(s,j) ds + |\tau(t_j, j)|_{\widetilde{\mathcal{A}}}.$$

It follows that

$$\begin{aligned}
|\tau(t_1, 0)|_{\widetilde{\mathcal{A}}} &= \int_0^{t_1} c(s,0) ds + |\tau(0,0)|_{\widetilde{\mathcal{A}}} \\
|\tau(t_1, 1)|_{\widetilde{\mathcal{A}}} &= (1+\varepsilon)\left(\int_0^{t_1} c(s,0) ds + |\tau(0,0)|_{\widetilde{\mathcal{A}}}\right) = (1+\varepsilon)\int_0^{t_1} c(s,0) ds + (1+\varepsilon)|\tau(0,0)|_{\widetilde{\mathcal{A}}} \\
|\tau(t_2, 1)|_{\widetilde{\mathcal{A}}} &= \int_{t_1}^{t_2} c(s,1) ds + (1+\varepsilon)\int_0^{t_1} c(s,0) ds + (1+\varepsilon)|\tau(0,0)|_{\widetilde{\mathcal{A}}} \\
|\tau(t_2, 2)|_{\widetilde{\mathcal{A}}} &= (1+\varepsilon)\left(\int_{t_1}^{t_2} c(s,1) ds + (1+\varepsilon)\int_0^{t_1} c(s,0) ds + (1+\varepsilon)|\tau(0,0)|_{\widetilde{\mathcal{A}}}\right).
\end{aligned}$$

Then, proceeding in this way, we obtain

$$|\tau(t_j, j)|_{\widetilde{\mathcal{A}}} = (1+\varepsilon)^j |\tau(0,0)|_{\widetilde{\mathcal{A}}} + \sum_{i=0}^{j-1} (1+\varepsilon)^{j-i} \int_{t_i}^{t_{i+1}} c(s,i) ds.$$

For the case of generic $t_{j+1} \geq t \geq t_j$, we have that

$$|\tau(t,j)|_{\widetilde{\mathcal{A}}} = (1+\varepsilon)^j |\tau(0,0)|_{\widetilde{\mathcal{A}}} + \sum_{i=0}^{j} (1+\varepsilon)^{j-i} \int_{t_i}^{t} c(s,i)ds.$$

Since, we know that as either t or j goes to infinity, j or t go to infinity as well, respectively. The expression reduces to $\lim_{t+j\to\infty} |\tau(t,j)|_{\widetilde{\mathcal{A}}} = \lim_{j\to\infty}(1+\varepsilon)^j|\tau(0,0)|_{\widetilde{\mathcal{A}}} + \lim_{t+j\to\infty}\sum_{i=0}^{j}(1+\varepsilon)^{j-i}\int_{t_i}^{t} c(s,i)ds = \lim_{t+j\to\infty}\sum_{i=0}^{j}(1+\varepsilon)^{j-i}\int_{t_i}^{t} c(s,i)ds$. If $c(t,j) \leq \bar{c}$, it follows that $\lim_{t+j\to\infty} |\tau(t,j)|_{\widetilde{\mathcal{A}}} = \lim_{t+j\to\infty}\sum_{i=0}^{j}(1+\varepsilon)^{j-i}\int_{t_i}^{t} c(s,i)ds \leq \frac{\bar{c}\bar{\tau}}{|\varepsilon|\omega}$.

Lastly, since this hybrid system has the property that for any maximal solution τ with $(t,j) \in \operatorname{dom}\tau$, if t approaches ∞ then the parameter j also approaches ∞, the expression given by $\lim_{t+j\to\infty} |\tau(t,j)|_{\widetilde{\mathcal{A}}}$ can be simplified. To do this, we know that the series $\sum_{i=0}^{j}(1+\varepsilon)^{j-i} = \frac{(1+\varepsilon)^{j+1}-1}{\varepsilon}$ approaches $\frac{1}{|\varepsilon|}$ as $j \to \infty$. Since $1+\varepsilon > 0$ for $\varepsilon \in (-1,0)$, the series is absolutely convergent and its partial sum $s_j = \sum_{i=0}^{j}(1+\varepsilon)^{j-i}$ is such that $\{s_j\}_{j=m}^{\infty}$ is a nondecreasing sequence (for each m). This implies that $s_j \leq 1/|\varepsilon|$ for all j and for each m. Then, it follows that $(1+\varepsilon)^{j-i} \leq \frac{1}{|\varepsilon|}$ for every $j,i \in \mathbb{N}$. Since the expression is a function of j only and, for complete solutions, t is such that as $t \to \infty$, then $j \to \infty$, we obtain

$$\begin{aligned}
\lim_{t+j\to\infty}\sum_{i=0}^{j}(1+\varepsilon)^{j-i}\int_{t_i}^{t} c(s,i)ds &= \lim_{j\to\infty}\sum_{i=0}^{j}(1+\varepsilon)^{j-i}\int_{t_i}^{t} c(s,i)ds \\
&\leq \lim_{j\to\infty}\sum_{i=0}^{j}(1+\varepsilon)^{j-i}\int_{t_i}^{t} |c(s,i)|ds \\
&\leq \left(\sum_{i=0}^{\infty}(1+\varepsilon)^{j-i}\right)\int_{0}^{\infty} |c(s,i)|ds \\
&\leq \frac{1}{|\varepsilon|}\int_{0}^{\infty} |c(s,\widetilde{j}(s))|ds.
\end{aligned}$$

■

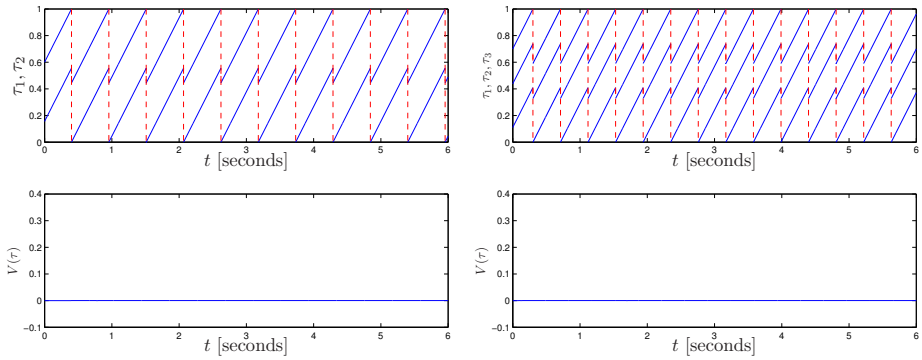

(a) Solutions to $\mathcal{H}_2$ with $\tau(0,0) \in \mathcal{A}$ (b) Solutions to $\mathcal{H}_3$ with $\tau(0,0) \in \mathcal{A}_3$

Figure 6.3: Solutions to $\mathcal{H}_N$ with $N \in \{2,3\}$ that are initially in the set $\mathcal{A}$.

6.4 Numerical Analysis

This section presents numerical results obtained from simulating $\mathcal{H}_N$. First, results on the nominal case of $\mathcal{H}_N$ given by (6.1) are presented. Then, under specific perturbations, the results for $\mathcal{H}_N$ are considered. The Hybrid Equations (HyEQ) Toolbox in [70] was used to compute the trajectories.

6.4.1 Nominal Case

The possible solutions to the hybrid system $\mathcal{H}_N$ fall into four categories: always desynchronized, asymptotically desynchronized, never desynchronized, and initially synchronized. The following simulation results show the evolution of solutions for each category. The parameters used in these simulations are $\bar{\tau} = 1$ and $\varepsilon = -0.2$.

6.4.1.1 Always desynchronized ($N \in \{2,3\}$)

A solution to $\mathcal{H}_N$ that has initial condition $\tau(0,0) \in \mathcal{A}$ stays desynchronized. Figure 6.3 shows the evolution of such a solution for systems $\mathcal{H}_2$ and $\mathcal{H}_3$. Furthermore, as also shown in the figures, for these same solutions, the Lyapunov function is initially zero and stays equal to

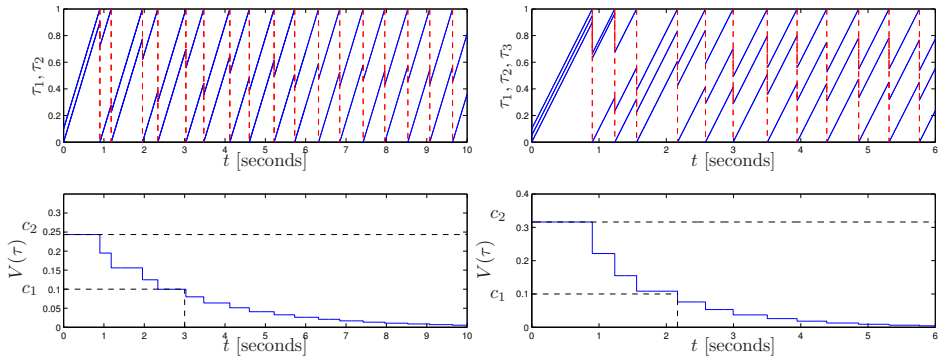

(a) Solutions to $\mathcal{H}_2$ with $c_2 = 0.24$ and $\tau(0,0) = [0, 0.1]^\top \in P_2 \setminus \mathcal{X}_2$.

(b) Solutions to $\mathcal{H}_3$ with $c_2 = 0.32$ and $\tau(0,0) = [0, 0.1, 0.2]^\top \in P_3 \setminus \mathcal{X}_3$.

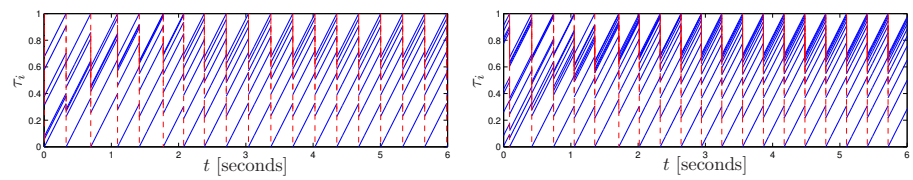

(c) A solutions to $\mathcal{H}_7$ with randomly chosen initial conditions $\tau(0,0) \in P_7 \setminus \mathcal{X}_7$.

(d) A solution to $\mathcal{H}_{10}$ with randomly chosen initial conditions $\tau(0,0) \in P_10 \setminus \mathcal{X}_10$.

Figure 6.4: Solutions to $\mathcal{H}_N$ that asymptotically converge to the desynchronization set $\mathcal{A}$ for $N \in \{2, 3, 7, 10\}$.

zero as hybrid time goes on.

6.4.1.2 Asymptotically desynchronized ($N \in \{2, 3, 7, 10\}$)

A solution of $\mathcal{H}_N$ that starts in $P_N \setminus (\mathcal{X} \cup \mathcal{A})$ asymptotically converges to $\mathcal{A}$, as Theorem 6.3.3 indicates. Figure 6.4(a) and Figure 6.4(b) show solutions to both $\mathcal{H}_2$ and $\mathcal{H}_3$ converging to their respective desynchronization sets.

For $\mathcal{H}_2$, if $\tau(0,0) = [0, 0.1]^\top$, then the initial sublevel set is $\widetilde{L}_V(c_2)$ with $c_2 = 0.24$. Using Theorem 6.3.3, the time to converge to the sublevel set $\widetilde{L}_V(c_1)$ with $c_1 = 0.1$ leads to $M = 7.84$. Figure 6.4(a) shows a solution to the system for 10 seconds of flow time. From the figure, it can be seen that $V(\tau(t,j)) \approx 0.1$ at $(t,j) = (3,4)$. Then, the property guaranteed by Theorem 6.3.3, namely, $V(\tau(t,j)) \leq c_1$ for each (t,j) such that $t + j \geq M$, is satisfied. Figure 6.4(b), shows a solution and the distance of this solution to $\mathcal{A}$. Notice that the initial

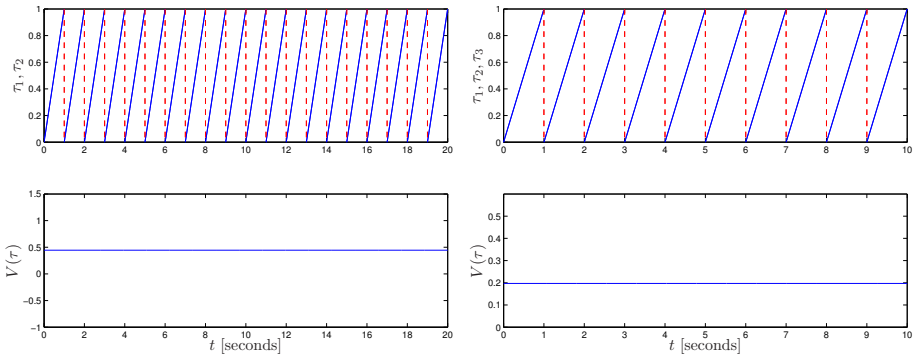

(a) Solutions to $\mathcal{H}_2$ with $\tau(0,0) \in \mathcal{X}_2$. (b) Solutions to $\mathcal{H}_3$ with $\tau(0,0) \in \mathcal{X}_3$.

Figure 6.5: Solutions to $\mathcal{H}_N$ initialized in $\mathcal{X}_N$ is outside the basin of attraction $\mathcal{B}_\mathcal{A}$ and, therefore, never converge to the set $\mathcal{A}$

sub level set is $\widetilde{L}_V(c_2)$ with $c_2 = 0.32$. From Theorem 6.3.3 it follows that the time to converge to $\widetilde{L}_V(c_1)$ with $c_1 = 0.1$ is given by $M = 10.14$, which is actually already satisfied at $(t, j) = (2.2, 4)$. Figure 6.4 show solutions to $\mathcal{H}_N$ that asymptotically desynchronize for $N \in \{7, 10\}$.

6.4.1.3 Always Synchronized

When the impulse-coupled oscillators start from an initial condition $\tau(0,0) \in \mathcal{X}_N$, a solution remains in $\mathcal{X}_N$. Since $\mathcal{X}_N$ is weakly forward invariant, there exist solutions $\tau(t,j) \in \mathcal{X}_N$ for all $(t,j) \in \operatorname{dom}\tau$. For such solutions it can be seen that V remains constant, seen Figure 6.5 for the case of $\mathcal{H}_2$ and $\mathcal{H}_3$.

6.4.1.4 Initially Synchronized

As mentioned in the proof of Theorem 6.3.2, there exist solutions that are initialized in $\mathcal{X}$ and eventually become desynchronized. This is due to the set-valuedness of the jump map at such points. Figure 6.6 shows two different solutions to $\mathcal{H}_2$ and $\mathcal{H}_3$ from the same initial conditions $\tau(0,0) = [0,0,0]^\top$. Furthermore, notice that, for each (t,j), the that Lyapunov function along solutions does not decrease to zero until all states are non-equal. Recall that

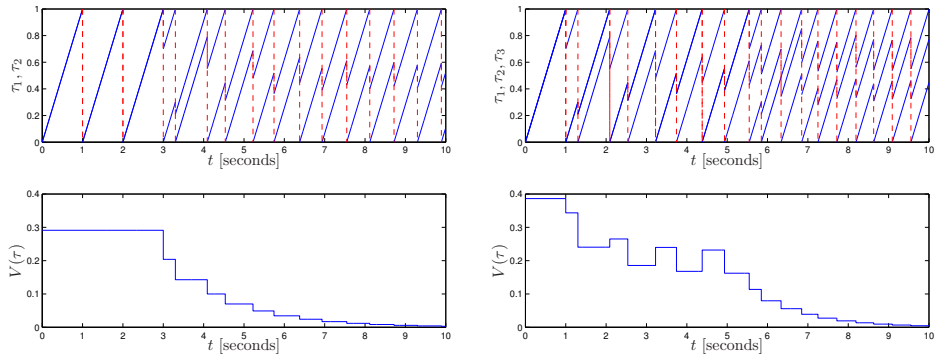

(a) Solutions to $\mathcal{H}_2$ with $\tau(0,0) \in \mathcal{X}_2$. Notice that the solution jumps out of $\mathcal{X}_2$ at $(t,j) = (3,3)$ and the function V begins to decrease after that jump.

(b) Solutions to $\mathcal{H}_3$ with $\tau(0,0) \in \mathcal{X}_3$. At hybrid time $(t,j) = (1,0)$ the timer state τ_1 jumps away from the other two and begin to desynchronize. At approximately $(t,j) = (4.5,8)$, all of the states are not equal and V begins to decrease.

Figure 6.6: Solutions to $\mathcal{H}_N$ for $N \in \{2,3\}$ that initially evolve in $\mathcal{X}$ and eventually become desynchronized due to the set-valuedness of the jump map.

from the analysis in Section 6.3.2, when states are equal, the issued solutions are outside of the basin of attraction.

6.4.2 Perturbed Case

In this section, we present numerical results to validate the statements in Section 6.3.4.

6.4.2.1 Simulations of $\mathcal{H}_N$ with perturbed jumps

In this section, we consider a class of perturbations on the jump map and jump set.

• **Perturbation of the threshold in the jump set:** We replace the jump set D by $D_\rho := \{\tau : \exists i \in I \ s.t. \ \tau_i = \bar{\tau} + \rho_i\}$ where $\rho_i \in [0, \bar{\rho}_i]$, $\bar{\rho}_i > 0$ for each $i \in I$. To avoid maximal solutions that are not complete, the flow set C is replaced by $C_\rho := [0, \bar{\tau} + \rho_1] \times [0, \bar{\tau} + \rho_2] \times$

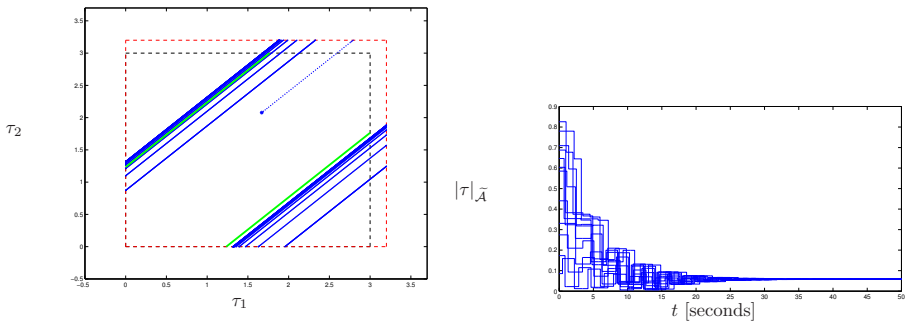

(a) Solution to $\mathcal{H}_2$ on the (τ_1, τ_2)-plane with initial condition $\tau(0,0) = [1.6, 2.1]^\top$.

(b) Distance to the set $\widetilde{\mathcal{A}}$ for 10 solutions with initial conditions randomly chosen from $[0, \bar{\tau} + \rho_1] \times [0, \bar{\tau} + \rho_2]$. The solutions have a distance that converges to a steady state value of approximately 0.08 at approximately 28 seconds of flow time.

Figure 6.7: Solutions to the hybrid system with perturbed threshold, namely, with $D_\rho = \{\tau : \exists i \in \{1,2\} \text{ s.t. } \tau_i = \bar{\tau} + \rho_i\}$ for $\rho_1 = \rho_2 = 0.2$.

$\ldots \times [0, \bar{\tau} + \rho_N]$. Furthermore, the components of the jump map are also replaced by

$$g_{\rho_i}(\tau) = \begin{cases} 0 & \text{if } \tau_i = \bar{\tau} + \rho_i, \tau_r < \bar{\tau} + \rho_j \quad \forall j \in I \setminus \{i\} \\ \{0, \tau_i(1+\varepsilon)\} & \text{if } \tau_i = \bar{\tau} + \rho_i \ \exists j \in I \setminus \{i\} \text{ s.t. } \tau_r = \bar{\tau} + \rho_j \\ (1+\varepsilon)\tau_i & \text{if } \tau_i < \bar{\tau} + \rho_i \ \exists j \in I \setminus \{i\} \text{ s.t. } \tau_r = \bar{\tau} + \rho_j \end{cases} . \tag{6.16}$$

This case of perturbations is an example of Theorem 6.3.5 with ρ affecting only the jump map. The trajectories of the perturbed version of $\mathcal{H}_N$ will converge to a region around the set $\widetilde{\mathcal{A}}$. Simulations are presented in Figures 6.7 and 6.8 for $N = 2$, $\omega = 1$, $\bar{\tau} = 3$, and $\varepsilon = -0.3$.

Figure 6.7 shows numerical results for the case when each ρ_i are equal, i.e., $\rho_1 = \rho_2 = 0.02$. Figure 6.7(a) shows a solution (solid blue) to the perturbed $\mathcal{H}_2$ with initial condition $\tau(0,0) = [1.6, 2.1]^\top$ (blue asterisk) on the (τ_1, τ_2)-plane with C (black dashed line), the perturbed flow set C_ρ (red dashed line), and the desynchronization set $\mathcal{A}$ (solid green line). From this figure, notice that the solution extends beyond the set C and resets at $\tau_i = 3 + 0.2$. The solution converges to a region near the desynchronization set, as Theorem 6.3.5 guarantees. To further clarify the response of $\mathcal{H}_2$ to this type of perturbation, Figure 6.7(b) shows the distance to the

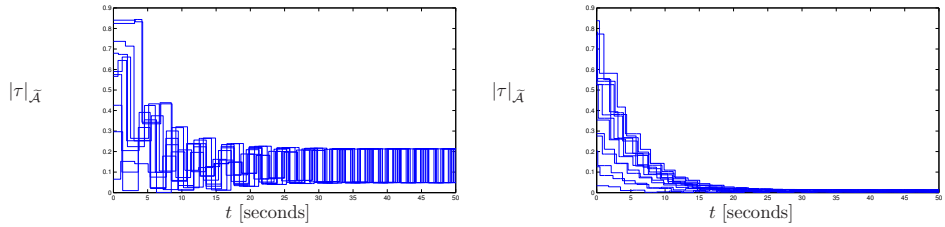

(a) Distance to the set $\widetilde{\mathcal{A}}$ for 10 solutions with random initial conditions $\tau(0,0) \in [0, \bar{\tau} + \rho_1] \times [0, \bar{\tau} + \rho_2]$ with $\rho_1 = 0.5$ and $\rho_2 = 0.4$.

(b) Distance to the set $\widetilde{\mathcal{A}}$ for 15 solutions with random initial conditions $\tau(0,0) \in [0, \bar{\tau} + \rho_1] \times [0, \bar{\tau} + \rho_2]$ with $\rho_1 = 0.02$ and $\rho_2 = 0.01$.

Figure 6.8: Numerical simulations of the perturbed version of $\mathcal{H}_2$ with jump set given by $D_\rho = \{\tau : \exists i \in \{1,2\} \text{ s.t. } \tau_i = \bar{\tau} + \rho_i\}$ for different values of ρ_i.

set $\widetilde{\mathcal{A}}$ for 10 solutions with randomly chosen initial conditions $\tau(0,0) \in C_\rho$. Notice that for the initial conditions chosen, all solutions converge to a distance of approximately 0.08 by $t \approx 28$ seconds.

Figure 6.8 shows the numerical results for the case when each ρ_i are not equal, i.e., $\rho_1 \neq \rho_2$. Figure 6.8(a) shows 10 solutions from random initial conditions $\tau(0,0) \in C_\rho$ with $\rho_1 = 0.5$ and $\rho_2 = 0.4$. For this case, the solutions converge to a region near $\widetilde{\mathcal{A}}$, in that, $|\tau(t,j)|_{\widetilde{\mathcal{A}}} \leq 0.22$ after approximately 0.28 seconds of flow time. Figure 6.8(b) shows 15 solutions when $\rho_1 = 0.02$ and $\rho_2 = 0.01$. For this set of simulations, the solutions converge to a distance of approximately 0.04 around $\widetilde{\mathcal{A}}$ after approximately 26 seconds of flow time. These simulations validate Theorem 6.3.5 with ρ affecting only the jump map, verifying that the smaller the size of the perturbation the smaller the steady-state value of the distance to $\widetilde{\mathcal{A}}$.

• **Perturbations on the reset component of the jump map:** Under the effect of the perturbations considered in this case, instead of reseting τ_i to zero, the perturbed jump resets τ_i to a value $\rho_i \in \mathbb{R}_{\geq 0}$, for each $i \in I$. The perturbed hybrid system has the following data:

$$f(\tau) = \omega \mathbf{1} \qquad \forall \tau \in C_\rho := C$$

and

$$G_\rho(\tau) = [g_{\rho_1}(\tau), \ldots, g_{\rho_1}(\tau)]^\top \qquad \forall \tau \in D_\rho = D$$

where, for each $i \in I$, the perturbed jump map is given by

$$g_i(\tau) = \begin{cases} \rho_i & \text{if } \tau_i = \bar{\tau}, \tau_r < \bar{\tau} \;\; \forall j \in I \setminus \{i\} \\ \{\rho_i, \tau_i(1+\varepsilon)\} & \text{if } \tau_i = \bar{\tau} \; \exists j \in I \setminus \{i\} \text{ s.t. } \tau_r = \bar{\tau} \\ (1+\varepsilon)\tau_i & \text{if } \tau_i < \bar{\tau} \; \exists j \in I \setminus \{i\} \text{ s.t. } \tau_r = \bar{\tau} \end{cases} . \tag{6.17}$$

This case of perturbations exemplifies Theorem 6.3.5 with ρ affecting only the jump map of $\mathcal{H}_N$. Figures 6.9 and 6.10 show several simulations to this perturbation of $\mathcal{H}_N$. All of the simulations in this section use parameters $\omega = 1$, $\bar{\tau} = 3$, $\varepsilon = -0.3$, and $N = 2$.

The first case of the perturbed jump map G_ρ considered is for $\rho_1 = \rho_2 = 0.02$. Figure 6.9(a) shows a solution to the perturbed $\mathcal{H}_2$ from the initial condition $\tau(0,0) = [2.4, 2.3]^\top$ on the (τ_1, τ_2)-plane. Notice that for $\tau \in D$ such that $\tau_i = \bar{\tau}$ the jump map resets τ_i to ρ_i (red dashed line) and not to 0 as in the unperturbed case. The solution for this case approaches a region around $\widetilde{\mathcal{A}}$, as Theorem 6.3.5 guarantees. Figure 6.9(b) shows the distance to the set $\widetilde{\mathcal{A}}$ over time for 10 solutions of the perturbed system $\mathcal{H}_2$ with initial conditions $\tau(0,0) \in P_2 \setminus \mathcal{X}_2$. This figure shows that solutions approach a distance of about 0.12 after 25 seconds.

Now, consider the case where $\rho_1 \neq \rho_2$. Figure 6.10 shows the distance to $\widetilde{\mathcal{A}}$ for two sets of solutions with different values for ρ_1 and ρ_2. More specifically, Figure 6.10(a) shows the case of $\rho_1 = 0.15$ and $\rho_2 = 0.25$. For this case, it can be seen that the solutions converge after ≈ 28 seconds of flow time and, after that time, satisfy $|\tau(t,j)|_{\widetilde{\mathcal{A}}} \leq 0.25$. Figure 6.10(b) shows the case of $\rho_1 = 0.02$ and $\rho_2 = 0.01$. For this case, this figure shows that, after ≈ 28 seconds of flow time, the solutions satisfy $|\tau(t,j)|_{\widetilde{\mathcal{A}}} \leq 0.04$. These simulations validate Theorem 6.3.5 with ρ affecting only the jump map, verifying that the smaller the size of the perturbation the

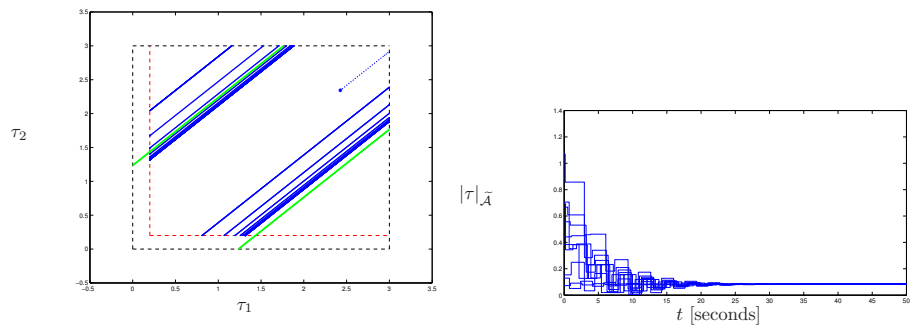

(a) Solution to $\mathcal{H}_2$ on the (τ_1, τ_2)-plane with initial condition $\tau(0,0) = [2.4, 2.3]^\top$.

(b) Distance to the set $\widetilde{\mathcal{A}}$ for 10 solutions to $\mathcal{H}_2$ with initial conditions randomly chosen from C. Most of the solutions have a distance that converges to a steady state value of approximately 0.12 at about 25 seconds

Figure 6.9: Solutions to the hybrid system $\mathcal{H}_2$ with the perturbed jump in (6.17) map with $\rho_1 = \rho_2 = 0.2$.

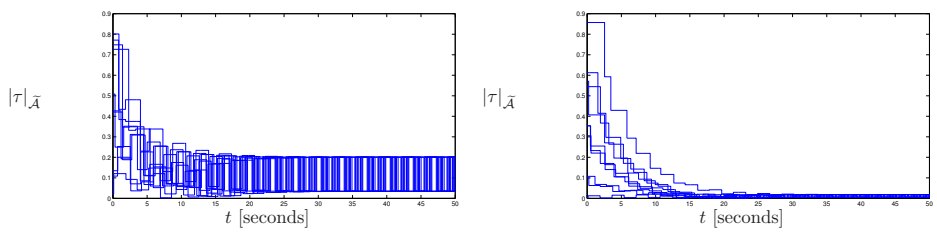

(a) Distance to the set $\widetilde{\mathcal{A}}$ for 10 solutions with random initial conditions $\tau(0,0) \in C$ with $\rho_1 = 0.15$ and $\rho_2 = 0.25$.

(b) Distance to the set $\widetilde{\mathcal{A}}$ for 10 solutions with random initial conditions $\tau(0,0) \in C$ with $\rho_1 = 0.02$ and $\rho_2 = 0.01$.

Figure 6.10: Solutions to the hybrid system $\mathcal{H}_2$ with the perturbed jump map with $\rho_1 \neq \rho_2$.

smaller the steady-state value of the distance to $\widetilde{\mathcal{A}}$.

• **Perturbations on the "bump" component of the jump map:** In this case, the component $(1+\varepsilon)\tau_i$ of the jump map is perturbed, namely, we use $\tau_i^+ = (1+\varepsilon)\tau_i + \rho_i(\tau_i)$, where $\rho_i : \mathbb{R}_{\geq 0} \to P_N \setminus \mathcal{X}$ is a continuous function. The perturbed jump map G_ρ has components $g_{\rho i}$ that are given as g_i in (6.4) but with $\tau_i(1+\varepsilon) + \rho_i(\tau_i)$ replacing $\tau_i(1+\varepsilon)$.

Consider the case $\rho_i(\tau_i) = \widetilde{\rho}_i \tau_i$ with $\widetilde{\rho}_i \in (0, |\varepsilon|)$ and let $\widetilde{\varepsilon}_i = \varepsilon + \widetilde{\rho}_i \in (-1, 0)$. Then τ_i^+ reduces to $\tau_i^+ = (1+\widetilde{\varepsilon}_i)\tau_i$ and the jump map $g_{\rho i}$ is given by (6.4) with $\widetilde{\varepsilon}_i$ in place of ε. This type of perturbation is used to verify Theorem 6.3.5 with ρ affecting only the "bump" portion

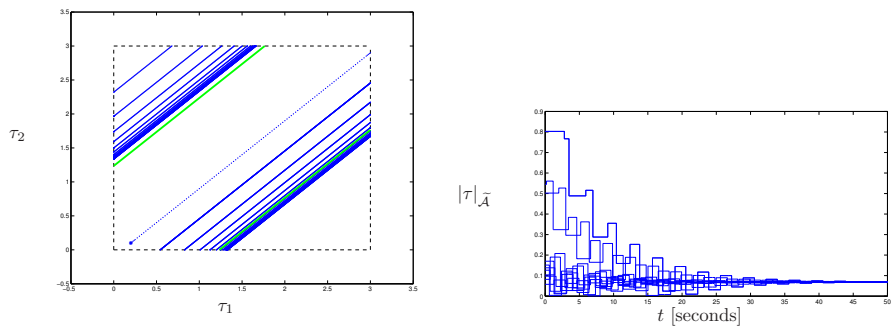

(a) Solution $\mathcal{H}_2$ on the (τ_1, τ_2)-plane with initial condition $\tau(0,0) = [0.1, 0.2]^\top$.

(b) Distance to the set $\widetilde{\mathcal{A}}$ for 10 solutions to $\mathcal{H}_2$ with initial conditions randomly chosen from C. These solutions have a distance that converges to a steady state value of approximately 0.08 at about 45 seconds.

Figure 6.11: Solutions to the hybrid system with perturbed "bump" on the jump map, with $\widetilde{\rho}_1 = \widetilde{\rho}_2 = 0.1$.

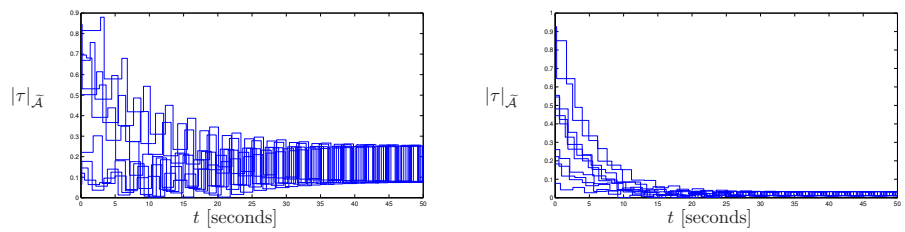

(a) Distance to the set $\widetilde{\mathcal{A}}$ for 10 solutions with random initial conditions $\tau(0,0) \in C$ with $\widetilde{\rho}_1 = 0.15$ and $\widetilde{\rho}_2 = 0.1$.

(b) Distance to the set $\widetilde{\mathcal{A}}$ for 10 solutions with random initial conditions $\tau(0,0) \in C$ with $\widetilde{\rho}_1 = 0.02$ and $\widetilde{\rho}_2 = 0.01$.

Figure 6.12: Numerical simulations of the perturbed version of $\mathcal{H}_2$ with the perturbed "bump" on the jump map with $\widetilde{\rho}_1 \neq \widetilde{\rho}_2$.

of the jump map. Figures 6.11 and 6.12 show simulations to $\mathcal{H}_N$ with the parameters $\omega = 1$, $\bar{\tau} = 3$, $\varepsilon = -0.3$, and $N = 2$.

Consider the case of $\mathcal{H}_2$ with G_ρ when $\widetilde{\rho}_1 = \widetilde{\rho}_2 = 0.1$, leading to $\widetilde{\varepsilon}_1 = \widetilde{\varepsilon}_2 = 0.2$. Figure 6.11 shows a solution on the (τ_1, τ_2)-plane for this case with initial condition $\tau(0,0) = [0.1, 0.2]^\top$. Notice that the solution approaches a region around $\mathcal{A}$ (green line), as Theorem 6.3.5 guarantees. Figure 6.11(b) shows the distance to the set $\widetilde{\mathcal{A}}$ over time for 10 solutions with initial conditions $\tau(0,0) \in C$. It shows that solutions approach a distance to $\widetilde{\mathcal{A}}$ of ≈ 0.09 after ≈ 40 seconds of flow time.

Next, the case of G_ρ with $\widetilde{\varepsilon}_1 \neq \widetilde{\varepsilon}_2$ is considered. Figure 6.12(a) shows the distance to $\widetilde{\mathcal{A}}$ for 10 solutions with perturbations given by $\widetilde{\rho}_1 = 0.15$ and $\widetilde{\rho}_2 = 0.1$. For this case, the distance to $\widetilde{\mathcal{A}}$ satisfies $|\tau(t,j)|_{\widetilde{\mathcal{A}}} \leq 0.3$ after ≈ 40 seconds of flow time. Figure 6.12(b) shows simulation results with $\widetilde{\rho}_1 = 0.02$ and $\widetilde{\rho}_2 = 0.01$. Notice that the smaller the value of the perturbation is, the closer the solutions get to the set $\widetilde{\mathcal{A}}$. For this case, after ≈ 30 seconds of flow time, the distance to $\widetilde{\mathcal{A}}$ satisfies $|\tau(t,j)|_{\widetilde{\mathcal{A}}} \leq 0.06$. These simulations validate Theorem 6.3.5 with ρ affecting only the jump map, verifying that the smaller the size of the perturbation the smaller the steady-state value of the distance to $\widetilde{\mathcal{A}}$ would be.

6.4.2.2 Perturbations on the Flow Map

This section considers a class of perturbations on the flow map, namely, the case when there exists a function $(t,j) \mapsto c(t,j)$ such that $c(t,j) \leq \bar{c}$ with $\bar{c}$ as in (6.11). Then, from Theorem 6.3.6 with (6.10), we know that

$$\lim_{t+j\to\infty} |\tau(t,j)|_{\widetilde{\mathcal{A}}} \leq \left|\frac{\bar{c}\bar{\tau}}{\varepsilon\omega}\right| \leq \left|\frac{\left|(\frac{1}{N}\underline{\mathbf{1}} - \mathbf{I})\Delta\omega\right|\bar{\tau}}{\varepsilon\omega}\right|. \tag{6.18}$$

Figure 6.13 shows a simulation so as to verify this property. The parameters of this simulation are $N = 2$, $\omega = 1$, $\varepsilon = -0.3$, $\bar{\tau} = 4$, and $\Delta\omega = [0.120, 0.134]^\top$. It follows from (6.11) that $\overline{c} = 0.0105$. Then, from (6.13), it follows that $\lim_{t+j\to\infty} |\tau(t,j)|_{\widetilde{\mathcal{A}}} \leq 0.1047$. Specifically, Figure 6.13(a) shows a solution on the (τ_1, τ_2)-plane of the perturbed hybrid system $\mathcal{H}_2$ with initial condition $\tau(0,0) = [0, 0.01]^\top$. This figure shows the solution (blue line) converging to a region around $\widetilde{\mathcal{A}}$ (between dash-dotted lines about $\mathcal{A}$ in green). Figure 6.13(b) shows the distance to the set $\widetilde{\mathcal{A}}$ of 10 solutions with initial conditions $\tau(0,0) \in C$ with a dashed line denoting the upper bound on the distance in (6.18). Notice that all solutions are within this bound after approximately 15 seconds of flow time and stay within this region afterwards.

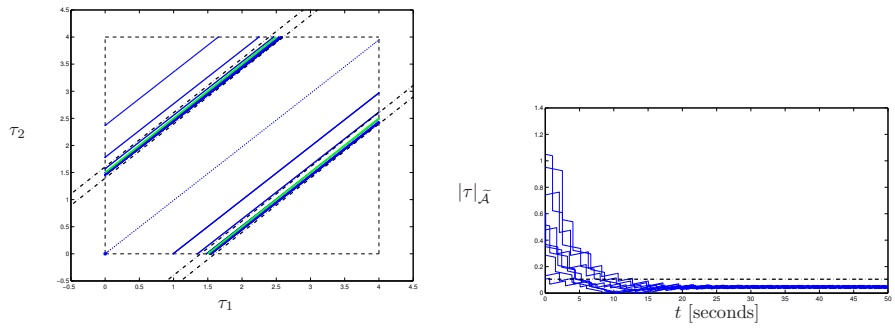

(a) Initial condition $\tau(0,0) = [0, 0.01]^\top$.

(b) Distance to the set $\widetilde{\mathcal{A}}$ for 10 solutions of the perturbed $\mathcal{H}_2$ with random initial conditions $\tau(0,0) \in C$.

Figure 6.13: Solutions to the hybrid system $\mathcal{H}_2$ with perturbed flow map given by the cases covered in Section 6.4.2.2. Figures (a) and (b) show solutions given by the flow perturbation $\Delta\omega = [0.120, 0.134]^\top$ given in Section 6.4.2.2. Note that these figures have a dashed black line denoting the calculated distance from $\widetilde{\mathcal{A}}$ in (6.18).

6.5 Summary

We have shown that desynchronization in a class of impulse-coupled oscillators is an asymptotically stable and robust property. These properties are established within a solid framework for modeling and analysis of hybrid systems, which is amenable for the study of synchronization and desynchronization in other impulse-coupled oscillators in the literature. The main difficulty in applying these tools lies on the construction of a Lyapunov-like quantity certifying asymptotic stability. As we show here, invariance principles can be exploited to relax the conditions that those functions have to satisfy, so as to characterize convergence, stability, and robustness in the class of systems under study. Future directions of research include the study of nonlinear reset maps, such as those capturing the phase-response curve of spiking neurons, as well as impulse-coupled oscillators connected via general graphs.

Chapter 7

Synchronization and Desynchronization in Interconnected Neurons

7.1 Introduction

Neuron models are commonly regarded as a typical non-smooth/impulsive system. The literature proposes many different frameworks for analysis of such systems, including compartmental models [71], phase plane models [72, 73], integrate-and-fire and impulsive differential equations [73, 74, 75], and large populations of interconnected neurons (neuron population models) [76, 73, 33]. Furthermore, being a natural process, these interconnections between neurons are inherently noisy [77, 78]. Unfortunately, there is a distinct lack of systematic methods for analysis of robustness of such interconnections.

Due to the impulsive nature of spiking neurons, hybrid systems provide a very promising platform for their study. This chapter models spiking neurons as hybrid systems and studies their dynamical properties in terms of asymptotic stability and robustness. The proposed hybrid framework captures the continuous evolution of the phase dynamics of the neurons as well

as their spiking/discontinuous behavior due to internal and external stimuli. The study of the asymptotic stability properties of these systems is performed using the tools in [27, 28].

This paper is organized as follows. In Section 7.2 we introduce the general framework and specific models under consideration then, in Section 7.3.1, we characterize the sets where solutions converge for several well-known neuron models. In particular, within the proposed framework, we consider the simplified Hodgkin-Huxley model [73, 79]; an inhibitory version of the Hodgkin-Huxley model; a "saddle-node on a periodic orbit" model, known as the SNIPER model [72]; and the Hopf model proposed in [80]. In Sections 7.3.2 - 7.3.5, details of the stability analysis for the case of two neurons and for each one of the phase response curves associated with the models just listed are given.

7.2 A Framework For Analysis for Spiking Neurons

7.2.1 Introduction to Neuron Models

A single neuron can be expressed by the general N-order, conductance based model given by

$$\dot{x} = I(x) + I^g(x,t), \tag{7.1}$$

where $x = (v, w) \in \mathbb{R}^N$, $v \in \mathbb{R}$ is the voltage difference across the membrane, w is the $(N-1)$-dimensional vector comprising the gating variables, I is the baseline vector field, and I^g is the stimulus effect; see, e.g., [73, 72, 81].

Using changes variables/parameters and model reduction techniques as in [73, 76, 82]), the evolution of the phase of the single neuron can be captured by the first order differential

equation

$$\frac{d\theta}{dt} = \omega + z(\theta)I^{\theta}(t), \tag{7.2}$$

with the natural frequency $\omega = \frac{2\pi}{T} > 0$. The period T is the time between the spiking and reset events of the singular neuron model in (7.1), while z is the phase response curve (PRC) characterizing the neurons sensitivity to the given stimulus, which is captured by I^{θ}. PRCs can be calculated from experimental, numerical, and analytical studies [81, 39].

7.2.2 Hybrid Modeling

Due to its impulsive nature, the neuron model presented in Section 7.2.1 can be modeled as a hybrid system. Specifically, the phase angle θ will flow continuously according to the natural frequency and jump when the neuron spiking condition is met. Utilizing the formulation of hybrid systems in [27, 28], we propose a hybrid system for modeling neurons given by $\mathcal{H}$ with data as in (C, f, D, G) with state $\theta = [\theta_1, \ldots, \theta_n]^\top \in [0, 2\pi]^n$. For each $i \in n$, $\theta_i \in [0, 2\pi]$ denotes the phase of each i-th neuron.

The continuous dynamics of each neuron are represented by a natural frequency ω_i, i.e., $\dot{\theta}_i = \omega_i$, which leads to $f(\theta) := [\omega_1, \ldots, \omega_n]^\top$. From the neuron model (7.2), the natural frequency is related to the spiking period T, in that, when the phase angle reaches 2π, the neuron activates the PRC. Then, the flow set is given by $C := [0, 2\pi]^n$ while jumps occur when θ is in the jump set given by $D := \{\theta \in C : \exists\ i \text{ s.t. } \theta_i = 2\pi\}$. Lastly, as previously described, each neuron jumps impulsively once any i-th neuron reaches a full period, i.e., $\theta_i = 2\pi$ from some i. At such an event, the neuron resets itself to zero and induces a reset on all other neurons by instantaneously changing their phase angles according to the PRC, namely, θ_i is reset to $\gamma(\theta_i) = \theta_i + hz(\theta_i)$, where $h > 0$ is the synapse coupling strength. In this way, the jump map is

given as $G(\theta) = [g(\gamma(\theta_i)), \ldots, g(\gamma(\theta_n))]^\top + G^u(\theta)$, where

$$g(s) = \begin{cases} 0 & \text{if } s > 2\pi \text{ or } s \leq 0 \\ \{0, s\} & \text{if } s = 2\pi \\ s & \text{if } s < 2\pi \text{ and } s > 0 \end{cases} \tag{7.3}$$

and $G^u : \mathbb{R}^n \rightrightarrows \mathbb{R}^n$ is a set-valued map representing an external stimuli. Note that g is set valued when the state is such that, after the jump, it is exactly 2π. By defining it set valued, (rather than just discontinuous) robust stability results for hybrid systems can be applied.

This general framework for neurons can be used to study the stability of different PRCs (synchronizing and desynchronizing) as well as their robustness. In our study of dynamical properties of neurons, we consider the following PRCs:

1. Simplified Hodgkin-Huxley model: $z(\theta) = -\sin(\theta)$;
2. Inhibited simplified Hodgkin-Huxley model: $z(\theta) = \sin(\theta)$;
3. SNIPER model: $z(\theta) = 1 - \cos(\theta)$;
4. Hopf model: $z(\theta) = -\sin(\theta - \theta_0)$.

7.2.3 Basic Properties of $\mathcal{H}$

To apply the stability analysis tools for hybrid systems outlined in [28], the hybrid system $\mathcal{H}$ must satisfy certain conditions, namely, the *hybrid basic conditions*.

Lemma 7.2.1 *Let z be continuous and G^u be outer semicontinuous. Then, the hybrid system $\mathcal{H}$ with data (C, f, D, G) defined in Section 7.2.2 satisfies the hybrid basic conditions.*

Proof Since both sets C and D are closed by construction, the condition (a) is satisfied. Condition (b) is satisfied since the flow set f is constant and thus continuous. Each i-th element of

the jump map G is given as $g(\theta_i + h_i z(\theta_i))$, where z is continuous, each h_i is constant and G^u is outer semicontinuous. Since, a vector with outer semicontinuous elements is outer semicontinuous and the sum of two outer semicontinuous set-valued map is also outer semicontinuous, it suffices to show that g is outer semicontinuous. To check the outer semicontinuity of g,

$$\begin{aligned}\text{gph}(g) = \{(x,y) : x \in \mathbb{R}, y \in g(x)\} = \{(x,y) : y = x, x \in [0, 2\pi]\} \\ \cup \{(x,y) : y = 0, x \in [\underline{x}, 0] \vee x \in [2\pi, \overline{x}]\},\end{aligned}$$

is closed as long as $\underline{x}$ and $\overline{x}$ exist, for every z in this paper, this is the case. Furthermore, since $G(\theta)$ is non empty and bounded for every $\theta \in D$ then (c) is satisfied and $\mathcal{H}$ with data (C, f, D, G) defined in Section 7.2.2 satisfies the hybrid basic conditions. ■

With these conditions being satisfied, asymptotic stability of a compact set automatically implies that it is robust to vanishing state disturbances as well as other types of small perturbations [28].

7.3 Stability Analysis of Synchronization and Desynchronization with Zero Inputs

7.3.1 Proposed Approach

Our goal is to characterize the set of points, denoted $\mathcal{A}$, that, for each of the considered PRC cases, is asymptotically stable. Asymptotic stability for hybrid systems is defined as the property of a set being both and attractive [27, 28] as defined in Section 2.1.

The basin of attraction for asymptotic stability, denoted $\mathcal{B}_{\mathcal{A}}$, is the set of points where the attractivity property holds. It excludes points from where solutions may never converge to $\mathcal{A}$. We denote this set as $\mathcal{X}$. Since, in this paper, we will analyze neuron model with PRCs, and

each case is inherently different, we will characterize this specific set for each case.

For example, for the study of synchronization in neuron models, the set $\mathcal{A}$ for $n = 2$ is given by the points in the jump set and away from $\mathcal{A}$ where $|\theta_1 - \theta_2|$ remains constant before and after the jump. Namely, it is defined by the values of θ satisfying

$$|\theta_1 - \theta_2| = |\theta_1^+ - \theta_2^+|. \tag{7.4}$$

To solve (7.4), let $h_1 = h_2 = h$, $\theta \in D \setminus \mathcal{A}$ with $\theta_1 = 2\pi$ and $\theta_2 = \theta^*$ such that $\theta^* + hz(\theta^*) \in (0, 2\pi)$. After the jump, $\theta_1^+ = 0$ and $\theta_2^+ = \theta^* + hz(\theta^*)$. Then

$$|2\pi - \theta^*| = |0 - (\theta^* + hz(\theta^*))| \quad \Longrightarrow \quad 2\pi - 2\theta^* = hz(\theta^*). \tag{7.5}$$

Similar results hold if $\theta_1 = \theta^*$ and $\theta_2 = 2\pi$. Then, the set $\mathcal{X}$ is given by $\mathcal{X} := \{\theta \in [0, 2\pi]^2 : |\theta_1 - \theta_2| = 2\pi - \theta^*, 2\pi - 2\theta^* = hz(\theta^*)\}$.

The approach in this paper is to employ Lyapunov stability results for hybrid systems in [27, 28] to establish that the set $\mathcal{A}$ is asymptotically stable for the hybrid system $\mathcal{H}$. To establish this property, a definition of a Lyapunov function candidate for hybrid systems and sufficient conditions for asymptotic stability are needed. Sufficient conditions for asymptotic stability in terms of Lyapunov functions can be found in [28, 27].

7.3.2 Simplified Hodgkin-Huxley (HH) Model ($n = 2$)

From [73], the simplified Hodgkin-Huxley model has a PRC function z given by $z(\theta) = -\sin(\theta)$. The associated neuron model with $n = 2$, $\omega_1 = \omega_2 = \omega > 0$, $h \in (0, \pi)$ and no external

stimuli ($G^u = 0$) can is given as follows

$$\mathcal{H}_{HH} := \begin{cases} C := [0, 2\pi] \times [0, 2\pi] \\ f(\theta) = [\omega, \omega]^\top \qquad \forall \theta \in C \\ D := \{(\theta_1, \theta_2) \in C : \exists i \in \{1, 2\} \text{ s.t. } \theta_i = 2\pi\} \\ G(\theta) = [g(\gamma(\theta_1)), g(\gamma(\theta_2))]^\top \qquad \forall \theta \in D \end{cases} \tag{7.6}$$

and the PRC given by $z(\theta) = -\sin(\theta)$. The function g in the jump map G is defined as in (7.3) with $\gamma(\theta_i) = \theta_i - h\sin(\theta_i)$, for each $i \in \{1, 2\}$. Note that when $\theta \in D$ is such that $\theta_i + h\sin(\theta_i) = 2\pi$, the function $g(\theta_i + h\sin(\theta_i))$ is set valued.

The simplified Hodgkin-Huxley model is known to synchronize the phases of the neurons, i.e., $|\theta_1 - \theta_2|$ approaches zero. For this system, the set to be stabilized is denoted $\mathcal{A}_{HH}$. It is defined as $\mathcal{A}_{HH} = \{(\theta_1, \theta_2) \in [0, 2\pi]^2 : |\theta_1 - \theta_2| = 0\}$ and represents a synchronization condition. To determine the set of points ($\mathcal{X}$ in Section 7.3) from where solutions to $\mathcal{H}_{HH}$ never converge to $\mathcal{A}_{HH}$, we follow the computation to arrive to (7.5). With $z(\theta) = -\sin(\theta)$, (7.5) becomes $2\pi = 2\theta^* - h\sin\theta^*$. The only solution to this expression is $\theta^* = \pi$, for any $h \in (0, \pi)$. Then, the set $\mathcal{X}_{HH}$ for $\mathcal{H}_{HH}$ is defined by $\mathcal{X}_{HH} := \{(\theta_1, \theta_2) : |\theta_1 - \theta_2| = \pi\}$.

Now, to establish that $\mathcal{A}_{HH}$ is asymptotically stable, consider the function defined on C as in (7.6) as

$$V_{HH}(\theta) = \min\{|\theta_1 - \theta_2|, 2\pi - |\theta_1 - \theta_2|\}. \tag{7.7}$$

This function satisfies the conditions for it to be a candidate Lyapunov function on $(C \cup D) \setminus \mathcal{X}_{HH}$ (see Definition 2.1.9). In fact, it is continuous everywhere, continuously differentiable away from $\mathcal{X}_{HH}$, positive for all $\theta \in (C \cup D) \setminus (\mathcal{A}_{HH} \cup \mathcal{X}_{HH})$, and $V_{HH}(\theta) = 0$ for all $\theta \in \mathcal{A}_{HH}$. In fact, we have the following result.

Lemma 7.3.1 *The function V_{HH} in (7.7) is a Lyapunov function candidate for $\mathcal{H}_{HH}$ on $\{\theta \in$*

$[0, 2\pi]^2 : V(\theta) < \pi\}$.

Proof To be a Lyapunov candidate, the function V in (7.7) must satisfy the conditions given in Definition 2.1.9. Both $|\theta_1 - \theta_2|$ and $2\pi - |\theta_1 - \theta_2|$ are continuous and nonnegative, $|\theta_1 - \theta_2| \geq 0$ by definition, and $2\pi - |\theta_1 - \theta_2| \geq 0$ for $\theta \in [0, 2\pi]^2$. It follows that, V_{HH} is nonnegative and continuous since the minimum of two nonnegative continuous functions is also nonnegative and continuous, satisfying condition *i*). For $\theta \in \mathcal{A}$ it follows that $\theta_1 = \theta_2$ leads to $V_{HH} = \min\{|\theta_1 - \theta_2|, 2\pi - |\theta_1 - \theta_2|\} = \min\{0, 2\pi\} = 0$, thus condition *iii*) is satisfied. Lastly, we must satisfy condition *ii*). Note that on $\theta \in [0, 2\pi]^2 \setminus \mathcal{A}$, V_{HH} is not continuously differentiable on $\mathcal{X}_{HH}$. It follows that, V_{HH} is a Lyapunov function for $\mathcal{H}_{HH}$ if we exclude the set $\mathcal{X}_{HH}$ from the analysis. At these points $\theta \in \mathcal{X}_{HH}$, the function $V(\theta) = \pi$. It follows that V_{HH} is a Lyapunov function for $\mathcal{H}_{HH}$ if we exclude these points such that $\{\theta \in [0, 2\pi]^2 : V(\theta) < \pi\}$. ■

It can be shown that for $\theta \in C$, we have $\dot{V} = 0$ while, for points $\theta \in D \setminus (\mathcal{X}_{HH} \cup \mathcal{A}_{HH})$, we have that $V(G(\theta)) - V(\theta) < 0$. These properties lead to the following result.

Theorem 7.3.2 *The hybrid system* (7.6) *with* $z(\theta) = -\sin(\theta)$ *has the set* $\mathcal{A}_{HH}$ *asymptotically stable with the basin of attraction given by* $(C \cup D) \setminus \mathcal{X}_{HH}$.

Proof From Lemma 7.3.1, V_{HH} is a Lyapunov function for $\mathcal{H}_{HH}$ on the set $\{\theta \in [0, 2\pi]^2 : V(\theta) < \pi\}$. To use the results of hybrid systems, we must satisfy the hybrid basic conditions and simply removing $\mathcal{X}_{HH}$ removes the property of having closed sets C and D. To alleviate this and regain the hybrid basic conditions, this analysis will consider a hybrid system $\widetilde{\mathcal{H}}_{HH}$ augmented by $v \in (0, \pi)$ with data $(\widetilde{C}, f, \widetilde{D}, G)$ such that $\widetilde{C} = C \cap K_v$ and $\widetilde{D} = D \cap K_v$ with $K_v = \{\theta \in [0, 2\pi]^2 : V(\theta) \leq v\}$. We have that the sets $\widetilde{C}$ and $\widetilde{D}$ are closed and the rest of the properties for the basic assumptions.

The remaining of this proof will follow from the sufficient conditions presented in

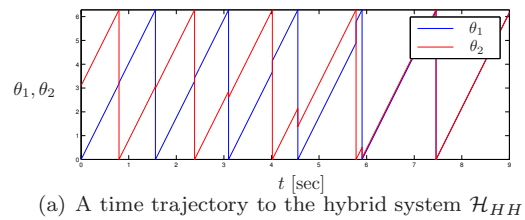

(a) A time trajectory to the hybrid system $\mathcal{H}_{HH}$

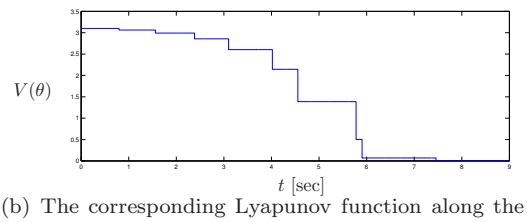

(b) The corresponding Lyapunov function along the solution to $\mathcal{H}_{HH}$.

Figure 7.1: A solution θ to the simplified Hodgkin-Huxley hybrid system $\mathcal{H}_{HH}$ with $\theta(0,0) = [0, 3.1]^\top$. Note that solutions become synchronized ($\theta_1(t,j) = \theta_2(t,j)$) and $V(\theta(t,j)) = 0$ at $(t,j) = (7.5, 9)$.

[27, Theorem 23]. First, note that $|\theta|_{\mathcal{A}_{HH}} = \frac{1}{\sqrt{2}}|\theta_1 - \theta_2|$ for each $\theta \in \widetilde{C} \cup \widetilde{D}$. For each $\theta \in \widetilde{C}$ the Lyapunov function V_{HH} must satisfy the condition $\langle \nabla V_{HH}(\theta), f(\theta) \rangle \leq 0$. Since $\nabla V_{HH} = \alpha[1 \ \ -1]^\top$ where $\alpha \in \{-1, 1\}$ and $f(\theta) = \omega \mathbf{1}$ for all $\theta \in \widetilde{C}$, the inner product is given by $\langle \nabla V_{HH}(\theta), f(\theta) \rangle = \alpha\omega - \alpha\omega = 0$ for each $\theta \in \widetilde{C}$. Without loss in generality due to the symmetry of the problem, we can consider the case of $\theta \in \widetilde{D}$ such that $\theta_1 = 2\pi$ and θ_2 is free and extend the results to the case when $\theta_2 = 2\pi$ and θ_1 is free. Each case of θ_2 is considered as follows.

- Consider the case of $\theta \in \widetilde{D}$ such that

$$\theta_1 = 2\pi, \qquad \theta_2 \in \{\theta_2 \in (\pi, 2\pi) : \theta_2 - h\sin(\theta_2) < 2\pi\}$$

  for which $V_{HH}(\theta) = 2\pi - \theta_2$. After the jump, we have and after the jump $\theta^+ = G(\theta)$ given by $\theta_1^+ = 2\pi$ and $\theta_2^+ = \theta_2 - h\sin(\theta_2)$ and V is given byt

$$\begin{aligned} V_{HH}(\theta^+) &= \min\{|0 - \theta_2 + h\sin\theta_2|, 2\pi - |0 - \theta_2 + h\sin\theta_2|\} \\ &= \min\{|-\theta_2 + h\sin\theta_2|, 2\pi - |-\theta_2 + h\sin\theta_2|\} \end{aligned}$$

Since $h \in (0, \pi)$, we have $\theta_2 - h\sin\theta_2 > 0$. Then, $V_{HH}(\theta^+) = \min\{\theta_2 - h\sin\theta_2, 2\pi - (\theta_2 - h\sin\theta_2)\}$. If $\theta_2 - h\sin\theta_2 > \pi$, then $V_{HH}(\theta^+) = 2\pi - (\theta_2 - h\sin\theta_2)$ and $V_{HH}(\theta^+) - V_{HH}(\theta) = 2\pi - (\theta_2 - h\sin\theta_2) - (2\pi - \theta_2) = -h|\sin\theta_2|$ which is negative since $\sin\theta_2 < 0$ for $\theta_2 \in (\pi, 2\pi)$. Furthermore, consider the case that $\theta_2 - h\sin\theta_2 < \pi$. Since $\theta_2 \in (\pi, 2\pi)$, this case is not possible.

- Next consider the case of $\theta \in \widetilde{D}$ such that

$$\theta_1 = 2\pi, \qquad \theta_2 \in \{\theta_2 \in (\pi, 2\pi) : \theta_2 - h\sin(\theta_2) > 2\pi\}$$

then $V_{HH}(\theta) = 2\pi - \theta_2$ as before . Although, after the jump we have $g_2(\theta_2) = 0$ and $V_{HH}(\theta^+) = \min\{|\theta_1^+ - \theta_2^+)|, 2\pi - |\theta_1^+ - \theta_2^+|\} = 0$. Then for this case of θ_1 and θ_2, we have that $V_{HH}(\theta^+) - V_{HH}(\theta) = -V_{HH}(\theta)$.

- Consider the case of $\theta \in \widetilde{D}$ such that θ^+ is set valued, for example let

$$\theta_1 = 2\pi \qquad \theta_2 \in \{\theta_2 \in (\pi, 2\pi) : \theta_2 - h\sin(\theta_2) = 2\pi\}.$$

which leads to $V_{HH}(\theta) = 2\pi - \theta_2$ as before. After the jump, we have that θ_2 is set valued, that is $\theta_2^+ = \{0, 2\pi\}$. This results in

$$\begin{aligned} V_{HH}(\theta^+) &= \min\{|0 - \{0, 2\pi\}|, 2\pi - |0 - \{0, 2\}|\} \\ &= \min\{\{0, 2\pi\}, 2\pi - \{0, 2\pi\}\} \\ &= \min\{\{0, 2\pi\}, \{2\pi, 0\}\} \end{aligned}$$

which, for either choice of θ_2^+, we have that $V_{HH}(\theta^+) = 0$. It follows that $V_{HH}(\theta^+) - V_{HH}(\theta) = -V_{HH}(\theta)$ is negative since $\theta_2 \in (\pi, 2\pi)$.

- Consider the other case of $\theta \in \widetilde{D}$ such that

$$\theta_1 = 2\pi, \qquad \theta_2 \in \{\theta_2 \in (0, \pi) : \theta_2 - h\sin(\theta_2) > 0\}$$

which implies

$$\begin{aligned} V_{HH}(\theta) &= \min\{|2\pi - \theta_2|, 2\pi - |2\pi - \theta_2|\} \\ &= \min\{2\pi - \theta_2, \theta_2\} \\ &= \theta_2. \end{aligned}$$

After the jump, it follows that

$$\begin{aligned} V_{HH}(\theta^+) = &= \min\{|0 - g_2(\theta_2)|, 2\pi - |0 - g_2(\theta_2)|\} \\ &= \min\{|-(\theta_2 - h\sin\theta_2)|, 2\pi - |-(\theta_2 - h\sin\theta_2)|\} \\ &= \min\{\theta_2 - h\sin\theta_2, 2\pi - (\theta_2 - h\sin\theta_2)\} \\ &= \theta_2 - h\sin\theta_2 \end{aligned}$$

since $h\sin\theta_2 > 0$ for $\theta_2 \in (0, \pi)$. This implies that

$$V_{HH}(\theta^+) - V_{HH}(\theta) = \theta - h\sin\theta_2 - \theta_2 = -h\sin\theta_2 = -h|\sin\theta_2|$$

which is negative for $h \in (0, \pi)$ and $\theta_2 \in (0, \pi)$.

- Lastly, consider the case when $\theta_1 = 2\pi$, and $\theta_2 \in \{\theta_2 \in (0, \pi) : \theta_2 - h\sin(\theta_2) \leq 0\}$. Then it follows that $V_{HH}(\theta) = \theta_2$ as before and $V_{HH}(\theta^+) = 0$ since $\theta_2^+ = 0$. Then difference is given by $V_{HH}(\theta^+) - V_{HH}(\theta) = -V_{HH}(\theta)$ and the system is in $\mathcal{A}_{HH}$ after this jump.

From the above analysis, we have that the difference of V_{HH} for different cases of $\theta \in \widetilde{D}$ is given by

$$\Delta V_{HH}(\theta) = \begin{cases} -h|\sin\theta_2| & \text{if } \theta_i = 2\pi \text{ and } \theta_j \in \{\theta_j \in (0, 2\pi) : \theta_j^+ \in (0, 2\pi)\} \\ -V_{HH}(\theta) & \text{otherwise} \end{cases}. \tag{7.8}$$

Furthermore, complete solutions that only flow are impossible. In fact, all complete solutions have at least $2\pi/\omega$ time between jumps. Since every maximal solution to $\widetilde{\mathcal{H}}_{HH}$ is

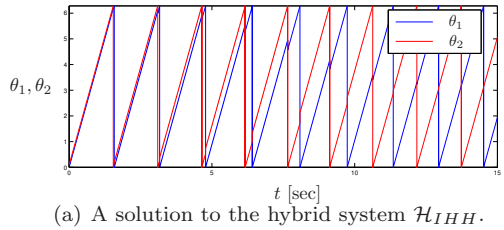

(a) A solution to the hybrid system $\mathcal{H}_{IHH}$.

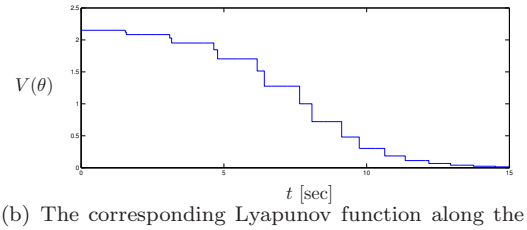

(b) The corresponding Lyapunov function along the solution to $\mathcal{H}_{IHH}$.

Figure 7.2: A solution θ to the simplified Inverse Hodgkin-Huxley hybrid system $\mathcal{H}_{IHH}$ with $\theta(0,0) = [0, 0.1]^\top$.

complete it follows that from [27, Theorem 23] the set $\mathcal{A}_{HH}$ is asymptotically stable for $\widetilde{\mathcal{H}}_{HH}$. Since $v \in (0, v^*)$ used in the definition of $\widetilde{\mathcal{H}}_{HH}$ is arbitrary, and the set K_v is compact and forward invariant, the basin of attraction of $\mathcal{A}_{HH}$ for the system $\mathcal{H}_{HH}$ contains the set $\{\theta \in [0, 2\pi]^2 : V_{HH}(\theta) < \pi\}$. In fact, if there exists $i \neq j$, $(i, j) \in \{1, 2\}$ and consider the case $\theta_i = 2\pi$ and $\theta_j = \pi$, then it follows that $V_{HH}(\theta) = \pi$, $V_{HH}(G(\theta)) = \pi - \sin\pi$ confirming that $V_{HH}(G(\theta)) - V_{HH}(\theta) = 0$. Then any solution that starts in $\mathcal{X}_{HH}$ will stay in this set, since $V_{HH}(\theta^+) = V_{HH}(\theta)$ for these points. It follows that $\mathcal{A}_{HH}$ is asymptotically stable for $\mathcal{H}_{HH}$ on the basin of attraction $\{\theta \in [0, 2\pi]^2 : V_{HH}(\theta) < \pi\}$. ■

Figure 7.1 is a solution to $\mathcal{H}_{HH}$ with $h = 0.9$ and initial condition $\theta(0,0) = [0, 3.1]^\top$; this solution starts just outside of the set $\mathcal{X}_{HH}$.

7.3.3 Inhibited Simplified Hodgkin-Huxley (IHH) Model ($n = 2$)

In this section, we consider the inhibited simplified Hodgkin-Huxley model. The PRC for this case is given by $z(\theta) = \sin(\theta)$. The positive sign on the sine function of the PRC has an inhibitory effect (compared to the excitatory response of the case in Section 7.3.2): after every

jump, the distance between the phases grows until they are a maximum distance apart. The resulting hybrid system is denoted as $\mathcal{H}_{IHH}$, which has the same data as in (7.6) except that $\gamma(\theta_i) = \theta_i + h\sin(\theta_i)$ with $h \in (0, \pi)$.

The set $\mathcal{X}_{IHH}$ is given by the points θ such that $\theta_1 = \theta_2$ and the points from where there could be a jump to $\theta_1 = \theta_2$. This set is given by $\mathcal{X}_{IHH} := \{\theta \in C : \theta_1 = \theta_2\} \cup \{(0, 2\pi), (0, 2\pi)\}$.

We define the set $\mathcal{A}$ for $\mathcal{H}_{IHH}$ as $\mathcal{A}_{IHH} := \ell_1 \cup \ell_2$ where $\ell_1 := \{\theta \in \mathbb{R}^2 : \theta = \widetilde{\theta}_1 + \mathbf{1}s, s \in \mathbb{R}\}$ and $\ell_2 := \{\theta \in \mathbb{R}^2 : \theta = \widetilde{\theta}_2 + \mathbf{1}s, s \in \mathbb{R}\}$ with $\widetilde{\theta}_1 = \begin{bmatrix} 2\pi \\ \pi \end{bmatrix}$ and $\widetilde{\theta}_2 = \begin{bmatrix} \pi \\ 2\pi \end{bmatrix}$. The sets ℓ_i represent lines in $\mathbb{R}^2$. Following [83], a Lyapunov function V_{IHH} can be defined as the distance from θ to the set $\mathcal{A}_{IHH}$. More specifically, $V_{IHH}(\theta) = d(\theta, \mathcal{A}_{IHH})$ for each $\theta \in [0, 2\pi]^2 \setminus \mathcal{X}_{IHH}$. The expression of the function V_{IHH} can be further reduced to the minimum distance to each set ℓ_i, namely $V_{IHH}(\theta) = \min\{d(\theta, \ell_1), d(\theta, \ell_2)\}$ while the distance $d(\theta, \ell_i)$ can be rewritten as $d(\theta, \ell_i) = \left|(\theta - \widetilde{\theta}_i) - \frac{1}{2}((\theta - \widetilde{\theta}_i)^\top \mathbf{1})\mathbf{1}\right|$, where $\widetilde{\theta}_i$ is defined for each ℓ_i as above. We have the following result.

Lemma 7.3.3 *The function V_{IHH} is a Lyapunov function candidate for $\mathcal{H}_{IHH}$ on $\{\theta \in [0, 2\pi]^2 : V(\theta) < \frac{\pi}{\sqrt{2}}\}$.*

Proof To show that V_{IHH} is a Lyapunov candidate function, each condition in Definition 2.1.9 must be satisfied. Condition *i*) is satisfied, since the minimum of two continuous nonnegative functions is continuous and nonnegative every on $(C \cup D) \setminus \mathcal{A}$. The function V_{IHH} is not continuously differentiable everywhere on $(C \cup D) \setminus \mathcal{X}_{IHH}$, in fact for the case of $\theta \in \mathcal{X}_{IHH}$ it follows that $V(\theta) = \frac{\pi}{\sqrt{2}}$. Then condition *ii*) is satisfied if we consider the case of $\theta \in \{\theta \in [0, 2\pi]^2 : V(\theta) < \frac{\pi}{\sqrt{2}}\}$. Lastly, condition *iii*) is satisfied by the definition of the distance functions, if $\theta \in \mathcal{A}_{IHH}$ there exists $i \in \{1, 2\}$ such that $\theta \in \ell_i$ and $d(\theta, \ell_i) = 0$. ■

Similar to $\mathcal{H}_{HH}$, we can use a Lyapunov stability argument to show the stability of $\mathcal{A}_{IHH}$ for

$\mathcal{H}_{IHH}$. The proof of this theorem follows closely that of the one for $\mathcal{H}_{HH}$, in that, during flows we have that $\dot{V} = 0$ everywhere, during jumps the difference is strictly decreasing for every point in the basin of attraction, i.e., $V(G(\theta)) - V(\theta) < 0$ for each $\theta \in D \setminus (\mathcal{X}_{IHH} \cup \mathcal{A}_{IHH})$.

Theorem 7.3.4 *The hybrid system $\mathcal{H}_{IHH}$ with the PRC $z(\theta) = \sin(\theta)$ has the set $\mathcal{A}_{IHH}$ asymptotically stable with basin of attraction $(C \cup D) \setminus \mathcal{X}_{IHH}$.*

Proof This proof follows similarly to the proof of Theorem 7.3.2 with the Lyapunov function as in (7.7) and sets $\mathcal{A}_{IHH}$ and $\mathcal{X}_{IHH}$. Note that the function $V_{IHH}(\theta) = \min\{d(\theta, \ell_i), d(\theta, \ell_2)\}$ is continuously differentiable on the open set $\mathcal{S} \setminus \mathcal{A}_{IHH}$, where $\mathcal{S} = \left\{\theta \in \mathbb{R}^2 : V(\theta) < \frac{\pi}{\sqrt{2}}\right\}$. We then define $v \in (0, \pi)$, and $K_v = \{x \in [0, 2\pi]^2 : V(\theta) \leq v\}$. As in Theorem 7.3.2, we define a hybrid system with flow and jump set constrained by K_v, namely $\mathcal{H}_{IHH}$ with data $(\widetilde{C}, f, \widetilde{D}, G)$. During flows, $\langle \nabla V(\theta), f(\theta) \rangle = 0$ for every $\theta \in \widetilde{C}$ due to the definition of f being perpendicular to the gradient of V. During jumps, the difference $V(\theta^+) - V(\theta)$ must be computed for every $\theta \in \widetilde{D}$. Without loss of generality we consider the isolated case of $\theta_1 = 2\pi$ and $\theta_2 \in (0, 2\pi)$ and extend it to the case of $\theta_1 \in (0, 2\pi)$ and $\theta_2 = 2\pi$. For the case of points during jumps it follows that due to the symmetry of the problem we can consider a single case of the jump set and extend this case to all cases of the jump set. For this analysis, we will use the case of $\theta \in D$ where $\theta_1 = 2\pi$ and $\theta_2 < 2\pi$ which implies that after the jump $G(\theta)$ leads to $\theta_1^+ = 0$, $\theta_2^+ = \theta_2 + h\sin(\theta_2)$, respectively. Before the jump, the function $V(\theta)$ for this case of $\theta \in \widetilde{D}$ is given by $V(\theta) = \min(d(\theta, \ell_1), d(\theta, \ell_2)) = d(\theta, \ell_1)$ using the point $\widetilde{\theta}_1 \in [2\pi, \pi]^\top$, the distance θ to ℓ_1 reduces to the following expression such that

$$V(\theta) = \left\| \begin{bmatrix} \frac{\theta_2}{2} - \frac{\pi}{2} \\ -\frac{\theta_2}{2} + \frac{\pi}{2} \end{bmatrix} \right\| = \frac{1}{\sqrt{2}} |\theta_2 - \pi|$$

and after the jump it follows that

$$V(G(\theta)) = \left| \begin{bmatrix} -\frac{\pi}{2} + \frac{\theta_2}{2} + \frac{h\sin(\theta_2)}{2} \\ \frac{\pi}{2} - \frac{\theta_2}{2} - \frac{h\sin(\theta_2)}{2} \end{bmatrix} \right| = \frac{1}{\sqrt{2}}|\theta_2 + h\sin(\theta_2) - \pi|$$

and the difference $V(G(\theta)) - V(\theta)$ leads to

$$\begin{aligned} V(G(\theta)) - V(\theta) &= \left| \begin{bmatrix} -\frac{\pi}{2} + \frac{\theta_2}{2} + \frac{h\sin(\theta_2)}{2} \\ \frac{\pi}{2} - \frac{\theta_2}{2} - \frac{h\sin(\theta_2)}{2} \end{bmatrix} \right| - \left| \begin{bmatrix} \frac{\theta_2}{2} - \frac{\pi}{2} \\ -\frac{\theta_2}{2} + \frac{\pi}{2} \end{bmatrix} \right| \\ &= \frac{1}{\sqrt{2}}(|\theta_2 + h\sin(\theta_2) - \pi| - |\theta_2 - \pi|) \end{aligned}$$

consider the case of $\theta_2 \in (0, \pi)$ then $V(G(\theta)) - V(\theta) = -\frac{1}{\sqrt{2}}h\sin(\theta_2) = -\frac{h}{\sqrt{2}}|\sin(\theta_2)|$ for $h \in (0, \pi)$ and $\sin(\theta_2) > 0$ for $\theta_2 \in (0, \pi)$. Furthermore, for the case of $\theta_2 \in (\pi, 2\pi)$, it follows that $V(G(\theta)) - V(\theta) = h\sin(\theta_2) = -\frac{h}{\sqrt{2}}|\sin(\theta_2)|$ implies asymptotic stability for every point $\theta \in [0, 2\pi]^2 \setminus \mathcal{X}$ for the $\widetilde{\mathcal{H}}_{IHH}$ system. It follows that from [27, Theorem 23], that $\mathcal{A}_{IHH}$ is asymptotically stable for the system $\widetilde{\mathcal{H}}_{IHH}$. Furthermore, complete solutions that only flow are impossible. Since $v \in (0, \pi)$ used in the definition $\widetilde{\mathcal{H}}_{IHH}$ is arbitrary, and the set K_v is compact and forward invariant, the basin of attraction of $\mathcal{A}_{IHH}$ for the system $\mathcal{H}_{IHH}$ contains $\mathcal{S}$. Furthermore, solutions initialized in $\mathcal{X}_{IHH}$ never converge to $\mathcal{A}_{IHH}$. In fact, consider $\theta \in D \cap \mathcal{X}_{IHH}$ such that $\theta = [2\pi, \pi]^\top$. For this case, note that $V(\theta^+) = V(\theta)$. It then follows that $\mathcal{S}$ is the basin of attraction for $\mathcal{A}_{IHH}$. ■

Figure 7.2 shows a solution to $\mathcal{H}_{IHH}$ with $h = 1$ and $\theta(0, 0) = [0, 0.1]^\top$, and the values of the corresponding Lyapunov function along the solutions.

7.3.4 SNIPER (S) Model ($n = 2$)

The SNIPER model has the PRC given by $z(\theta) = (1 - \cos(\theta))$. The resulting hybrid system with this PRC is denoted as $\mathcal{H}_S$. It has the same data as in (7.6) except that $\gamma(\theta_i) =$

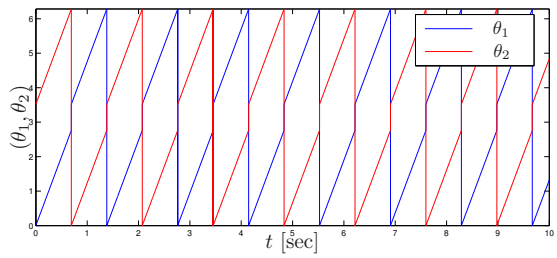

Figure 7.3: A solution to $\mathcal{H}_S$ that never converges to $\mathcal{A}_S$ with $z(\theta) = 1 - \cos(\theta)$, $h = \pi/8$, and initial condition $\theta(0,0) = [0, 2\pi - \theta^*]^\top \in \mathcal{X}$.

$\theta_i + h(1 - \cos(\theta_i))$ with $h > 0$. The solutions to the SNIPER system converge to the set

$$\mathcal{A}_S := \{(\theta_1, \theta_2) \in [0, 2\pi]^2 : |\theta_1 - \theta_2| = 0\} \tag{7.9}$$

which represents a synchronization condition. To determine the set of points ($\mathcal{X}$ in Section 7.3) from where solutions to $\mathcal{H}_S$ never converge to $\mathcal{A}_S$, we follow the computation to (7.5), leading to

$$2\pi - 2\theta^* = h(1 - \cos(\theta^*)), \tag{7.10}$$

which is an implicit expression on θ^*. As h increases, the right-hand side of (7.10) increases, and θ^* decreases. It follows that for $h > 0$, we have $\theta^* \in (0, \pi)$ and from (7.10), we obtain $\mathcal{X}_S := \{(\theta_1, \theta_2) \in [0, 2\pi]^2 : |\theta_1 - \theta_2| = 2\pi - \theta^*,$
$2\pi - 2\theta^* = h(1 - \cos(\theta^*))\}$. Figure 7.3 shows a specific example of a solution to $\mathcal{H}_S$ with initial conditions $\theta(0,0) = [0, 3.52] \in \mathcal{X}$, and$h = \pi/8$.

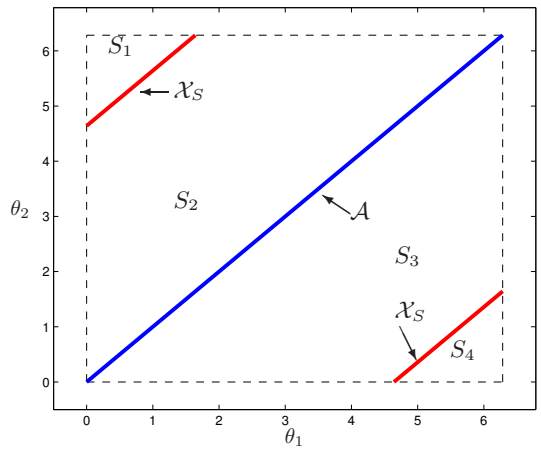

Figure 7.4: The (θ_1, θ_2)-plane for the hybrid system $\mathcal{H}_S$ with $h = 2.67$.

To prove that $\mathcal{A}_S$ is asymptotically stable for $\mathcal{H}_S$, define the sets S_i as

$$S_1 = \{(\theta_1, \theta_2) \in [0, 2\pi]^2 : \theta_2 - \theta_1 > 2\pi - \theta^*\} \tag{7.11}$$

$$S_2 = \{(\theta_1, \theta_2) \in [0, 2\pi]^2 : 0 < \theta_2 - \theta_1 < 2\pi - \theta^*\} \tag{7.12}$$

$$S_3 = \{(\theta_1, \theta_2) \in [0, 2\pi]^2 : 0 < \theta_1 - \theta_2 < 2\pi - \theta^*\} \tag{7.13}$$

$$S_4 = \{(\theta_1, \theta_2) \in [0, 2\pi]^2 : \theta_1 - \theta_2 > 2\pi - \theta^*\}. \tag{7.14}$$

Figure 7.4 indicates each of the sets S_i, $\mathcal{A}_S$ and $\mathcal{X}_S$. Note that solutions to $\mathcal{H}_S$ that do not jump into $\mathcal{A}_S$ will jump between two S_i sets cyclicly. More precisely, we have the following result.

Lemma 7.3.5 *Given the sets S_1, S_2, S_3, and S_4 in* (7.11)-(7.14)*, if $\theta \in D \cap S_i$ and $\theta^+ \in G(\theta) \setminus (\mathcal{A}_S \cup \mathcal{X}_S)$, then:*

(1) If $\theta \in S_1$, then $\theta^+ \in S_3$;

(2) If $\theta \in S_2$, then $\theta^+ \in S_4$;

(3) If $\theta \in S_3$, then $\theta^+ \in S_1$;

(4) If $\theta \in S_4$, then $\theta^+ \in S_2$.

Proof This proof is split in to 4 cases of $\theta \in D$. For each case there exist $i, j \in \{1, 2\}$, $i \neq j$ such that $\theta_i = 2\pi$ and $\theta_j \in (0, \theta^*) \vee (\theta^*, 2\pi)$. After the jump, $\theta^+ = G(\theta)$ where we have that $\theta_i^+ = 0$

and θ_j is left to be characterized. The following analysis will characterize the range of θ_j^+ for each case of θ on the sets given in (7.11) - (7.14) using the expression defining θ^* in (7.10).

1. Consider, $\theta \in D \cap S_1$, it follows that $\theta_2 = 2\pi$, $\theta_1 \in (0, \theta^*)$. After the jump, we have that $\theta_2^+ = 0$ and $\theta_1^+ = \theta_1 + (1 - \cos(\theta_1))$. Along the range of θ_1 it follows that $\theta_1^+ \in (0 + (1 - \cos(0)), \theta^* + (1 - \cos(\theta^*)) = (0, \theta^* + (1 - \cos(\theta^*))$. From (7.10), we have that $\theta_1^+ \in (0, 2\pi - \theta^*)$ which leads to $\theta^+ \in S_3$.

2. Consider, $\theta \in D \cap S_2$, it follows that $\theta_2 = 2\pi$, $\theta_1 \in (\theta^*, 2\pi)$. After the jump, we have that $\theta_2^+ = 0$ and $\theta_1^+ = \theta_1 + (1 - \cos(\theta_1))$. Along the range of θ_1, it follows that $\theta_1^+ \in (\theta^* + (1 - \cos(\theta^*)), 2\pi + (1 - \cos(2\pi))) = (\theta^* + (1 - \cos(\theta^*)), 2\pi)$. From (7.10), we have that $\theta_1^+ \in (2\pi - \theta^*, 2\pi)$ which leads to $\theta^+ \in S_4$.

3. These last two cases follow exactly like the first two. In fact, for the case of $\theta \in D \cap S_3$ it follows that $\theta_1 = 2\pi$ and $\theta_2 \in (\theta^*, 2\pi)$. After the jump, $\theta_1^+ = 0$ and $\theta_2 \in (2\pi - \theta^*, 2\pi)$ and $\theta^+ \in S_1$.

4. For the case of $\theta \in D \cap S_4$ it follows that $\theta_1 = 2\pi$ and $\theta_2 \in (0, \theta^*)$ leads to $\theta_1^+ = 0$ and $\theta_2 \in (0, 2\pi - \theta^*)$. For this case, we have that $\theta^+ \in S_2$

■

Using a trajectory-based approach, we establish that $\mathcal{A}_S$ is attractive for $\mathcal{H}_S$.

Theorem 7.3.6 *The hybrid system $\mathcal{H}_S$ with h satisfying $\cos(\theta_o - h(1 - \cos(\theta_o)) > \cos(\theta_o)$ for all $\theta_o \in (0, 2\pi - \theta^*)$, where θ^* satisfies (7.10), is such that the set $\mathcal{A}_S$ is attractive with basin of attraction $(C \cup D) \setminus \mathcal{X}_S$.*

Proof From Lemma 7.3.5, it follows that all solutions evolve cyclically. In that, any solution that hits a point $\theta \in S_1 \cap D$ gets mapped to S_3 since $G(\theta) \subset S_3$. Likewise, any solution that

hits a point $\theta \in S_3 \cap D$ gets mapped to S_1 since $G(\theta) \subset S_1$. Similarly, any solution that hits a point $\theta \in S_2 \cap D$ gets mapped to S_4 and any solution that hits a points $\theta \in S_4 \cap D$, get mapped to S_2.

Note that if θ^o is the value of the state after a jump at $(t_j, j) \in \operatorname{dom}\theta$ we have that the solution from that point flows (for $t > t_j$) and is given by $\theta(t, j) = \omega(t - t_j) + \theta^o$. Let $\theta : \operatorname{dom}\theta \to [0, 2\pi]^2$ be a solution to $\mathcal{H}_S$ and let $\{(0, 0), (t_1, 0), (t_1, 1), (t_2, 1), (t_2, 2), \ldots\} \in \operatorname{dom}\theta$. Then, at the jump times, the solutions evolve as follows:

$$\theta(0, 0) = (0, \theta_2^o) \tag{7.15}$$

$$\theta(t_1, 0) = (2\pi - \theta_2^o, 2\pi) \tag{7.16}$$

$$\theta(t_1, 1) = (2\pi - \theta_2^o + h(1 - \cos(2\pi - \theta_2^o)), 0) \tag{7.17}$$

$$= (2\pi - \theta_2^o + h(1 - \cos(\theta_2^o)), 0) \tag{7.18}$$

$$\theta(t_2, 1) = (2\pi, 2\pi - (2\pi - \theta_2^o + h(1 - \cos(\theta_2^o)))) \tag{7.19}$$

$$= (2\pi, \theta_2^o - h(1 - \cos(\theta_2^o)))) \tag{7.20}$$

$$\theta(t_2, 2) = (0, \theta_2^o - h(1 - \cos(\theta_2^o)) + h(1 - \cos(\theta_2^o - h(1 - \cos(\theta_2^o))))) \tag{7.21}$$

Without loss of generality, consider $\widetilde{\theta}_0 \in S_2$. After a full cycle, the solution reaches S_2, which leads to

$$\theta_0^+ = (0, \widetilde{\theta}_0 - h(1 - \cos(\widetilde{\theta}_0)) + h(1 - \cos(\widetilde{\theta}_0 - h(1 - \cos(\widetilde{\theta}_0)))).$$

Note that the distance to the set $\mathcal{A}_S$ can be defined as $V(\theta) := |\theta_1 - \theta_2|$, satisfying $V(\theta) = 0$ for each $\theta \in \mathcal{A}_S$, $V > 0$ for $\theta \notin \mathcal{A}_S$ and is continuously differentiable on the open set $\mathbb{R}^2 \setminus \mathcal{X}_S$. Furthermore, $\dot{V}(\theta) = 0$ for every $\theta \in C \cup D$. During jumps, we have that the difference at the

initial point in S_2 and after the full cycle is given by

$$V(\widetilde{\theta}_0^+) - V(\widetilde{\theta}_0) = |0 - (\widetilde{\theta}_0 - h(1-\cos(\widetilde{\theta}_0)) + h(1-\cos(\widetilde{\theta}_0 - h(1-\cos(\widetilde{\theta}_0)))))| - |0 - \widetilde{\theta}_0| \tag{7.22}$$

$$= \widetilde{\theta}_0 - h(1-\cos(\widetilde{\theta}_0)) + h(1-\cos(\widetilde{\theta}_0 - h(1-\cos(\widetilde{\theta}_0)))) - \widetilde{\theta}_0 \tag{7.23}$$

$$= -h(1-\cos(\widetilde{\theta}_0)) + h(1-\cos(\widetilde{\theta}_0 - h(1-\cos(\widetilde{\theta}_0)))). \tag{7.24}$$

When the condition

$$\cos(\widetilde{\theta}_0 - h(1-\cos(\widetilde{\theta}_0))) > \cos(\widetilde{\theta}_0) \tag{7.25}$$

holds, we have $V(\widetilde{\theta}_0^+) - V(\widetilde{\theta}_0) < 0$ for every $\theta_0 \in S_2$.

Furthermore, following the above full cycle analysis for solutions starting in S_4 and making a full cycle yields the same result as (7.24) with $\widetilde{\theta}_0 \in (2\pi - \theta^*, 2\pi)$ but has a difference given by $V(\widetilde{\theta}_0^+) - V(\widetilde{\theta}_0) > 0$ with the condition (7.25). This leads to solutions jumping further from $\mathcal{A}_S$, but closer to the point $\{2\pi, 0\}$.

Due to the symmetry of $\mathcal{H}_S$, it follows that every solution to $\mathcal{H}_S$ starting away from $\mathcal{X}_S$ has a distance V that decreases to zero after the full loop $S_2 \to S_4 \to S_2$ and has distance V that increases to $\{0, 2\pi\}$ after a full loop $S_4 \to S_2 \to S_4$. This suggests that every solution can only converge to the set $\mathcal{A}_S \cup \{(0, 2\pi), (2\pi, 0)\}$. On the other hand, since every solution to $\mathcal{H}_S$ is complete and bounded, by [84, Lemma 3.3], its ω-limit set is weakly invariant. Note that the set $\mathcal{A}_S$ is strongly forward invariant, but it is not weakly backward invariant. In fact, the points $\{(0, 2\pi), (2\pi, 0)\} \subset D$ get mapped to $G(\theta) = (0, 0) \in \mathcal{A}_S$ and once in $\mathcal{A}_S$ solutions cannot reach $\{(0, 2\pi), (2\pi, 0)\}$. The largest weakly invariant set in $\mathcal{A}_S \cup \{(0, 2\pi), (2\pi, 0)\}$ is $\mathcal{A}_S$. This shows that $\mathcal{A}_S$ is attractive for $\mathcal{H}_S$. ■

Remark 7.3.7 *It can be determined numerically, that the condition in Theorem 7.3.6 holds for*

$h \in (0, 2.67)$. *However, simulations show that solutions converge to* $\mathcal{A}_S$ *for larger values of* h. *In fact, since* h *proportionally affects the size of the 'impulse,' the larger the value of* h *is the sooner solutions converge to* $\mathcal{A}_S$.

7.3.5 Hopf (H) Model ($n = 2$)

The Hopf model has a PRC given by $z(\theta_i) = -\sin(\theta_i - \theta_0)$, where $\theta_0 \in (-\frac{\pi}{2}, \frac{\pi}{2})$ and $h \in (0, \pi)$, see, e.g., [85]. This PRC is similar to that of $\mathcal{H}_{HH}$ with a phase shift θ_0. The resulting hybrid system is denoted $\mathcal{H}_H$. It has the same data as in (7.6) except that $\gamma_i(\theta_i) = \theta_i + h\sin(\theta_i - \theta_0)$. For the range of $\theta_0 \in (-\frac{\pi}{2}, \frac{\pi}{2})$, solutions to this system approach the set $\mathcal{A}_H := \{(\theta_1, \theta_2) \in [0, 2\pi]^2 : |\theta_1 - \theta_2| = 0\}$. To determine the set from where solutions never converge to the set $\mathcal{A}_H$, namely to determine the set $\mathcal{X}_H$, from the computation in (7.5) with z given above, we obtain

$$2\pi - 2\theta^* = -h\sin(\theta^* - \theta_0) \tag{7.26}$$

which is an implicit equation parameterized by both h and θ_0. Then, the set $\mathcal{X}_H$ is defined by $\mathcal{X}_H := \{(\theta_1, \theta_2) : |\theta_1 - \theta_2| = 2\pi - \theta^*, 2\pi - 2\theta^* = -h\sin(\theta^* - \theta_0)\}$.

The function γ in the jump map can be rewritten as $\gamma(\theta_i) = \theta_i - h\sin(\theta_i)\cos(\theta_0) + h\cos(\theta_i)\sin(\theta_0)$. If we let $\rho(\theta_i, \theta_0) = h\cos(\theta_i)\sin(\theta_0)$ and $\tilde{h} = h\cos(\theta_0)$ then γ can be rewritten as

$$\gamma(\theta_i) = \theta_i - \tilde{h}\sin(\theta_i) + \rho(\theta_i, \theta_0) \tag{7.27}$$

We can now consider the offset θ_0 as a perturbation of the jump map in the simplified Hodgkin-Huxley model in Section 7.3.2. This perturbation satisfies $|\rho(\theta_i, \theta_0)| \leq h|\sin(\theta_0)|$ for all $\theta_i \in [0, 2\pi]$. In this way, $\mathcal{H}_{HH}$ can be considered to be the unperturbed version of $\mathcal{H}_H$. Since $\mathcal{H}_{HH}$ satisfies the hybrid basic conditions from Lemma 7.2.1 and with $\mathcal{A}_{HH}$ being asymptotically

stable for $\mathcal{H}_{HH}$, then using [28, Theorem 7.20], we have the following result.

Theorem 7.3.8 *The hybrid system $\mathcal{H}_H$ has the set $\mathcal{A}_H$ practically asymptotically stable in the parameter $\theta_0 \in (\frac{-\pi}{2}, \frac{\pi}{2})$, i.e., for each $\varepsilon > 0$ there exists $\theta_0^* > 0$ and a $\mathcal{KL}$ function β such that, for each $|\theta_0| \in [0, \theta_0^*)$, every solution θ to $\mathcal{H}_H$ from $[0, 2\pi]^2 \setminus \mathcal{X}_H$ satisfies $|\theta(t,j)|_{\mathcal{A}_H} \leq \beta(|\theta(t,j)|_{\mathcal{A}_H}, t+j) + \varepsilon$ for all $(t,j) \in \operatorname{dom}\theta$.*

Proof Since $\mathcal{H}_{HH}$ is well-posed and $\mathcal{A}_{HH}$ is an asymptotically stable, compact set from Theorem 7.3.2 on $[0, 2\pi] \setminus \mathcal{X}_{HH}$. Since $\mathcal{A}_H = \mathcal{A}_{HH}$ and ρ is given by (7.27), from [28, Lemma 7.20], that $\mathcal{A}_H$ is semiglobally practically stable. Given $\varepsilon > 0$ there exists a maximum size of the perturbation function ρ, which leads to a maximum value $\theta_0^* > 0$ for $|\theta_0|$, i.e. $|\theta_0| \in [0, \theta_0^*)$. Furthermore, with parameters θ_0 and ε satisfying the said conditions, there exists a $\mathcal{KL}$ function β such that for any solution ϕ_H from $[0, 2\pi] \setminus \mathcal{X}_H$ we have $|\phi_H(t,j)|_{A_H} \leq \beta(|\phi_H(t,j)|_{\mathcal{A}_H}, t+j) + \varepsilon$. for all $(t,j) \in \operatorname{dom}\phi_H$. ■

Figure 7.5 shows numerical results for large values of θ_0. The red regions correspond to points from where solutions converge to $\mathcal{A}_H$ (dashed cyan line), while the blue regions correspond to the points from where solutions "get stuck" due to the dynamics of the jump map. Moreover, the figure shows that as $|\theta_0|$ increases the blue regions get larger.

7.4 Summary

A framework for modeling and analyzing groups of spiking neurons was introduced. Within the hybrid system framework, several well-known neuron models were studied, including the excitatory and inhibitory Hodgkin-Huxley model, the saddle-point node on a periodic orbit model (SNIPER), and the Hopf model. For each model, we characterized the sets to which their respective solutions converge. Using Lyapunov stability tools for hybrid systems, asymptotic

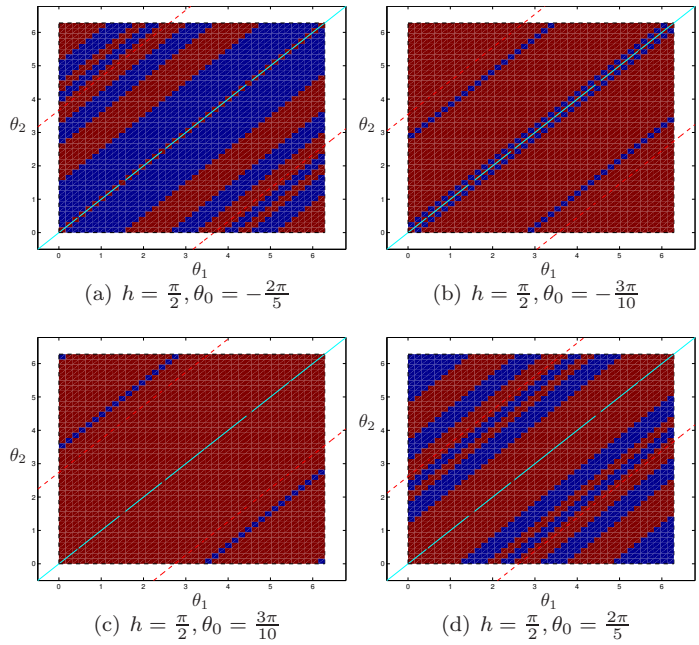

(a) $h = \frac{\pi}{2}, \theta_0 = -\frac{2\pi}{5}$ (b) $h = \frac{\pi}{2}, \theta_0 = -\frac{3\pi}{10}$

(c) $h = \frac{\pi}{2}, \theta_0 = \frac{3\pi}{10}$ (d) $h = \frac{\pi}{2}, \theta_0 = \frac{2\pi}{5}$

Figure 7.5: Numerical solutions to $\mathcal{H}_H$ with initial conditions $\theta(0,0) \in [0, 2\pi]^2$. The red regions correspond to the points that converge to $\mathcal{A}_H$ (dashed cyan) while the blue region corresponds to the points that "get stuck" near $\mathcal{A}_H$ due to the offset θ_0.

stability properties were established for each system for the case of $n = 2$. The introduction of an external stimulation in the Hodgkin-Huxley neuron model is paramount in achieving global asymptotic stability. Since the data of the hybrid systems satisfies certain regularity properties, the stability of these systems is robust to small perturbations.

Chapter 8

Frequency Hopping Rendezvous

8.1 Introduction

In this chapter, synchronization properties of pulse-coupled oscillators communicating over two bidirectional channels is considered. Bidirectional communication channels allow for both transmission and reception of information on the same channel. These channels are available to each oscillator. In such a setting, the packets transmitted by each oscillator on the currently chosen channel generate an event in the other oscillator only if they are on same communication channel.

The study of this problem stems from the control of networked reconfigurable systems, in particular, cognitive radio systems in space applications, in which system parameters, such as communication channel, transmission power, and direction of transmission or reception, can be updated in real time to react to a changing environment. In space applications, two-agent communication scenarios are key as they capture the scenario consisting of a ground station establishing a link with a satellite. Cognitive radio is a form of software defined radio. It is an agile communication system capable of dynamically changing its protocols with the rapid changes

of the environment, due to (but not limited to) adversarial jammers, managing communication with a primary user, and rendezvousing with other users in a decentralized network. In this context, the impulsive oscillators represent agents or radios that, through dynamic selection of the communication channel parameters, synchronize channel access with minimal information using feedback-based protocols. This feature could be advantageous in preventing adversaries from disrupting agent-to-agent communication since no pre-specified channel selection is made. In fact, traditional algorithms for establishing communication between nodes rely on a fixed channel selection sequence, such as the so-called *frequency hopping algorithm* which assigns to each agent a frequency-hopping pattern specifying the sequence (or code) of frequencies at which transmission is allowed [86]; see related work in [87], [88] and [89]. Compared with such works, a key feature of the algorithm emerging from the impulsive synchronization problem studied in this paper is that it does not require pilot tones on a pre-specified channel and that the channel selection patterns are determined in real time and based on feedback control.

The approach taken in this paper consists of modeling the pulse-coupled oscillators as a hybrid dynamical system, with continuous dynamics capturing the evolution of the oscillator's state in between impulses and discrete dynamics modeling self- and externally-triggered impulses. The resulting hybrid system contains continuous states, which are timers corresponding to the oscillator's variables, and discrete states, which are variables denoting the channel selected by each oscillator. Synchronization is recast as a compact set stabilization problem. Asymptotic stability of this set implies that the difference between the states of the oscillators and of the logic variables representing the selected channels converge to zero. Analysis is performed using the framework of hybrid systems and tools to assert asymptotic stability in [28, 27]. We construct a Lyapunov function to show synchronization for the case of two oscillators on two channels. Performance and robustness to loss of information are characterized numerically. Simulations show that synchronization is reached from initial conditions in a basin of attraction

containing almost every point in the state space. Experimental results validate the findings in a realistic environment.

The remainder of this paper is organized as follows. Section 8.2 is devoted to modeling. Section 8.3 presents the main tools for analysis as well as the main result. Numerical simulations are presented in Section 8.4. Experimental results are presented in Section 8.5.

8.2 Modeling Impulsive Oscillators with Channel Dependency

The pulse-coupled oscillator system of study consists of oscillators defining the agents with continuous states given by timers (τ_1, τ_2) and discrete states (q_1, q_2) denoting the current channel selection. These states are discretely updated when they reach a threshold and are externally reset when information is received. Information arrives to each agents from predefined channels. The agents can listen to one channel at a time.

Consider the case of two agents communicating over two channels via the following mechanism:

A) Each agent listens on the currently selected channel until its timer expires. Under such an event, the agent transmits a signal (or packet) on the current channel, resets its timer to zero, and switches to the other channel. Figure 8.1(a) shows that situation for a single pulse-coupled oscillator.

B) If an agent receives a packet while listening on the currently chosen channel, its timer is reset via an update law that reduces the listening time on that channel for the receiving agent. Figure 8.1(b) demonstrates the interaction between two pulse-coupled oscillators.

This mechanism can be thought as a control algorithm. It is inspired by synchronization

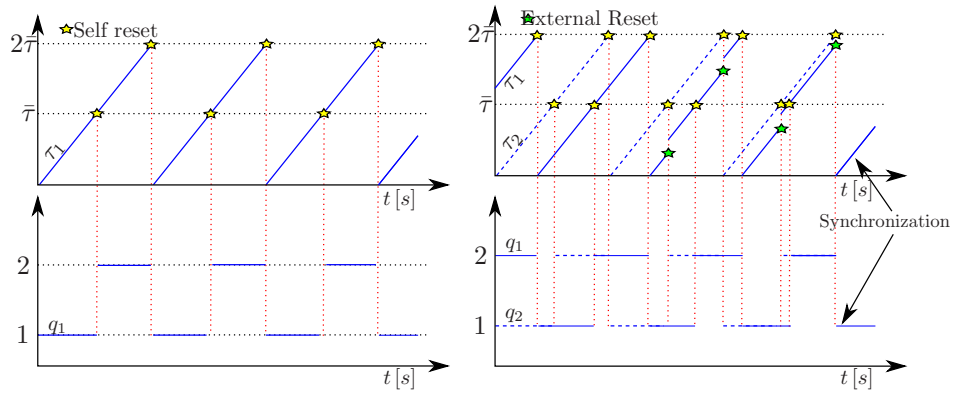

(a) A single pulse-coupled oscillator. (b) Two pulse-coupled oscillators.

Figure 8.1: (a) Trajectories (τ_1, q_1) of a single pulse-coupled oscillator over two channels. (b) Trajectories (τ_1, q_1) and (τ_2, q_2) of two pulse-coupled oscillators over two channels.

of biological systems in [34, 31], where agents can "listen" all the time. In fact, the main difference between the mechanism above and the synchronization mechanism studied in [31] is that here there is a constraint on data reception, which depends on the channel currently chosen by the agents and does not guarantee that information sent is always received. In the case of a common channel and no information loss, the agents will synchronize as in the work of [31].

8.2.1 Hybrid Modeling

From the outline in A) and B) above a two agent/two channel mechanism can be modeled as a hybrid system in (6.1). We denote it as $\mathcal{H}_{2,2}$. For each $i \in \{1, 2\}$, the i-th agent has a timer state τ_i and a channel state $q_i \in Q := \{1, 2\}$. The timer state takes value in the set $[0, 2\bar{\tau}]$, where $\bar{\tau} > 0$ is a parameter defining the threshold for jumps. Then, the state of the two agent/two channel system is given by $x = (\tau_1, q_1, \tau_2, q_2) \in P$ where $PP := [0, 2\bar{\tau}] \times Q \times [0, 2\bar{\tau}] \times Q$.

The flow and jump sets are defined to constrain the evolution of the timers (τ_1, τ_2) and the channel state (q_1, q_2). For example, when agent 1 is listening to channel one, that is, $q_1 = 1$, the timer τ_1 takes value in the set $[0, \bar{\tau}]$, while when agent 1 is listening to channel two, $q_1 = 2$, and τ_1 takes value in $[\bar{\tau}, 2\bar{\tau}]$. Then, flows are allowed when each of the agent's timers are within

the range corresponding to the current channel on which they are listening. This is captured via the flow set

$$C := \{x \in P : (\tau_1, q_1) \in C_1, (\tau_2, q_2) \in C_2\}, \tag{8.1}$$

where, for each $i \in Q$,

$$C_i := \{(\tau_i, q_i) \in [0, 2\bar{\tau}] \times Q : (q_i - 1)\bar{\tau} \leq \tau_i \leq q_i\bar{\tau}\}.$$

During flows, the timers count ordinary time and the channel state remains constant, i.e.,

$$f(x) := \begin{bmatrix} 1 & 0 & 1 & 0 \end{bmatrix}^\top \qquad \forall\, x \in C. \tag{8.2}$$

The discrete events described in A) and B) above are modeled by a jump set D and a jump map G. The events or jumps are triggered when a timer expires, i.e., the jump set D captures timer resets and packet reception events. These events correspond to either timer reaching its threshold. More precisely:

$$D := \{x \in C : (\tau_1, q_1) \in D_1\} \cup \{x \in C : (\tau_2, q_2) \in D_2\}, \tag{8.3}$$

where $D_i := \{(\tau_i, q_i) \in [0, 2\bar{\tau}] \times Q : \tau_i = q_i\bar{\tau}\}$. In such a case, the agent whose timer expired transmits a packet on its current channel and changes channel by updating its channel state and timer state appropriately. If the other agent is in the same channel, then its timer is incremented by a timer advance constant, $\varepsilon \in (0, 2\bar{\tau}]$, as to reduce the listening time on that channel. This

is captured via the jump map

$$G(x) = \begin{cases} g_1(x) & \text{if} \quad \tau_1 = q_1\bar{\tau},\, \tau_2 < q_2\bar{\tau},\, q_1 = q_2 \\ g_2(x) & \text{if} \quad \tau_1 < q_1\bar{\tau},\, \tau_2 = q_2\bar{\tau},\, q_1 = q_2 \\ g_3(x) & \text{if} \quad \tau_1 = q_1\bar{\tau},\, \tau_2 < q_2\bar{\tau},\, q_1 \neq q_2 \\ g_4(x) & \text{if} \quad \tau_1 < q_1\bar{\tau},\, \tau_2 = q_2\bar{\tau},\, q_1 \neq q_2 \\ g_5(x) & \text{if} \quad \tau_1 = q_1\bar{\tau},\, \tau_2 = q_2\bar{\tau},\, q_1 = q_2 \\ g_6(x) & \text{if} \quad \tau_1 = q_1\bar{\tau},\, \tau_2 = q_2\bar{\tau},\, q_1 \neq q_2. \end{cases} \qquad \forall\, x \in D \tag{8.4}$$

The first case (g_1) of G corresponds to the case when agent 1's timer reaches a threshold, which means that it is about to transmit a packet, agent 2's timer is not at a threshold, which means that it is listening, while both agents are on the same channel. In this way, g_1 is defined as

$$g_1(x) = \begin{bmatrix} (2-q_1)\bar{\tau} \\ 3-q_1 \\ n_2(x) \end{bmatrix}, \qquad n_2(x) \quad = \begin{cases} \begin{bmatrix} \tau_2+\varepsilon \\ q_2 \end{bmatrix} & \text{if} \quad \tau_2+\varepsilon < q_2\bar{\tau} \\ \begin{bmatrix} (2-q_2)\bar{\tau} \\ 3-q_2 \end{bmatrix} & \text{if} \quad \tau_2+\varepsilon > q_2\bar{\tau} \\ \left\{ \begin{bmatrix} \tau_2+\varepsilon \\ q_2 \end{bmatrix}, \begin{bmatrix} (2-q_2)\bar{\tau} \\ 3-q_2 \end{bmatrix} \right\} & \text{if} \quad \tau_2+\varepsilon = q_2\bar{\tau} \end{cases},$$

The function n_2 describes how agent 2 reacts to incoming information, allowing for timer resetting and channel switching if the jump pushes the timer past the threshold. More precisely, if the new value of the timer τ_2, which after the reset is $\tau_2 + \varepsilon$, is below the current threshold, then update τ_2 to $\tau_2 + \varepsilon$, but if it is above the current threshold, then reset it as if it expired and switch channels. When $\tau_2 + \varepsilon = q_2\bar{\tau}$ then the jump set is within a set of values and will do either.

The definition of the function g_2 in G is as g_1, but with reverse roles. More precisely,

it is given as

$$g_2(x) = \begin{bmatrix} n_1(x) \\ (2-q_2)\bar{\tau} \\ 3-q_2 \end{bmatrix}, \qquad n_1(x) \quad = \begin{cases} \begin{bmatrix} \tau_1+\varepsilon \\ q_1 \end{bmatrix} & \text{if} \quad \tau_1+\varepsilon < q_1\bar{\tau} \\ \begin{bmatrix} (2-q_1)\bar{\tau} \\ 3-q_1 \end{bmatrix} & \text{if} \quad \tau_1+\varepsilon > q_1\bar{\tau} \\ \left\{ \begin{bmatrix} \tau_1+\varepsilon \\ q_1 \end{bmatrix}, \begin{bmatrix} (2-q_1)\bar{\tau} \\ 3-q_1 \end{bmatrix} \right\} & \text{if} \quad \tau_1+\varepsilon = q_1\bar{\tau} \end{cases}.$$

Functions g_3 and g_4 capture the cases when the agents are in different channels. They are given by

$$g_3(x) = \begin{bmatrix} (2-q_1)\bar{\tau} \\ 3-q_1 \\ \tau_2 \\ q_2 \end{bmatrix}, \quad g_4(x) = \begin{bmatrix} \tau_1 \\ q_1 \\ (2-q_2)\bar{\tau} \\ 3-q_2 \end{bmatrix}.$$

When both agents reach their threshold at the same time neither are listening, so they both change channels and reset their timers. Functions g_5 and g_6 correspond to such a case, where g_5 corresponds to the case that the agents are in the same channel while g_6 to the case when they are not. Then

$$g_5(x) = g_6(x) = \begin{bmatrix} (2-q_1)\bar{\tau} \\ 3-q_1 \\ (2-q_2)\bar{\tau} \\ 3-q_2 \end{bmatrix}.$$

8.2.2 Basic Properties of $\mathcal{H}_{2,2}$

To apply analysis tools for hybrid systems, which will be presented in Section 8.3, the data of the hybrid system $\mathcal{H}_{2,2}$ must satisfy the hybrid basic conditions given in Definition 2.1.8.

Lemma 8.2.1 *The data of $\mathcal{H}_{2,2}$ satisfies the Hybrid Basic Conditions in Definition 2.1.8.*

Proof The function f is continuous since it is constant. The sets C and D are closed by design. The set valued map G is satisfies A3. Since x is such that $\tau_2 = \bar{\tau} - \varepsilon$, $q_2 = 1$, which is where g_1 is set valued for all x^i converging to x $\lim_{x^i \to x} g_1(x^i) \in g_1(x)$ This follows by the fact that $g_1(x^i)$ is either given by $((2-q_1)\bar{\tau}, 3-q_1, \tau_2+\varepsilon, q_2)$ or $((2-q_1)\bar{\tau}, 3-q_1, (2-q_2)\bar{\tau}, 3-q_2)$. which define the two points in $g_1(x)$. It follows that a similar proof can be performed for g_2. ■

8.3 Synchronization Properties of the Hybrid System Model for Two Impulsive Oscillators with Channel Dependency

The goal of this section is to show that solutions $x = (\tau_1, q_1, \tau_2, q_2)$ (with some abuse of notation) to $\mathcal{H}_{2,2}$ are such that

$$\tau_1(t,j) - \tau_2(t,j) \to 0 \qquad \text{and} \qquad q_1(t,j) - q_2(t,j) \to 0$$

as $t + j \to \infty$, and that if the initial conditions $\tau_1(0,0)$, $q_1(0,0)$ and $\tau_2(0,0)$, $q_2(0,0)$ are close, then the solutions stay close. In other words, our goal is to show that the compact set

$$\mathcal{A} := \{x \in C \cup D : \tau_1 = \tau_2, q_1 = q_2\} \tag{8.5}$$

is asymptotically stable for the hybrid system $\mathcal{H}_{2,2}$. Due to the evolution of the timers being periodic when in $\mathcal{A}$, asymptotic stability of $\mathcal{A}$ is a synchronization property for the agent timers. The set of points from where the attractivity property holds is the basin of attraction, denoted as $\mathcal{B}$.

A Lyapunov function as defined in Definition 2.1.9 is employed to show that the compact set in (8.5) is asymptotically stable. For a function V to be considered a Lyapunov candidate it must meet the following requirements. The following result from [27, Theorem 23] states the conditions on V for asymptotic stability of a compact set. Below, a level set $L_V(\mu)$ refers to the set of all points in $C \cup D$ such that $V(x) = \mu$, i.e., $L_V(\mu) := \{x \in C \cup D : V(x) = \mu\}$.

8.3.1 Asymptotic Stability Analysis of $\mathcal{H}_{2,2}$

The overall goal of this section is to determine the stability and attractivity properties of the set of points (8.5). We consider the function $V : \mathbb{R}^4 \to \mathbb{R}$ given by

$$V(x) = (1 - \rho(x))V_1(x) + \rho(x)V_2(x) \qquad \forall x \in C \cup D, \tag{8.6}$$

where V_1 is a piecewise function given by

$$V_1(x) = \begin{cases} \frac{1}{\varepsilon}(\tau_1 - \tau_2)^2 + \frac{\varepsilon}{4} & \text{if } |\tau_1 - \tau_2| \leq \frac{\varepsilon}{2} \\ \frac{1}{\varepsilon}(\tau_1 - \tau_2 - 2\bar{\tau})^2 + \frac{\varepsilon}{4} & \text{if } \tau_1 - \tau_2 \geq 2\bar{\tau} - \frac{\varepsilon}{2} \\ \frac{1}{\varepsilon}(\tau_1 - \tau_2 + 2\bar{\tau})^2 + \frac{\varepsilon}{4} & \text{if } \tau_1 - \tau_2 \leq -2\bar{\tau} + \frac{\varepsilon}{2} \\ V_2(x) & \text{if } |\tau_1 - \tau_2| \in \left(\frac{\varepsilon}{2}, 2\bar{\tau} - \frac{\varepsilon}{2}\right) \end{cases},$$

where $\varepsilon \in (0, 2\bar{\tau}]$, V_2 is given by

$$V_2(x) = \min\{|\tau_1 - \tau_2|, 2\bar{\tau} - |\tau_1 - \tau_2|\},$$

and, ρ is a C^1 function satisfying

$$\rho(x) = \begin{cases} 0 & \text{if } q_1 \neq q_2,\ q_1, q_2 \in \{1,2\} \\ 1 & \text{if } q_1 = q_2 \in \{1,2\} \end{cases}$$

and, for all $x \in C$,

$$\nabla_{\tau_1}\rho(x) = 0 \qquad \text{and} \qquad \nabla_{\tau_2}\rho(x) = 0.$$

For points not in $C \cup D$, the Lyapunov function V is given by any positive and continuous function that is continuously differentiable (almost everywhere). Furthermore, it can be verified that the Lyapunov function satisfies the conditions in Definition 2.1.9, namely, we have the following result.

Lemma 8.3.1 *The function $V : \mathbb{R}^4 \to \mathbb{R}$ given in* (8.6) *is a Lyapunov function candidate for* $(\widetilde{\mathcal{H}}_{2,2}, \mathcal{A})$*, where $\mathcal{A}$ is the compact set*

$$\mathcal{A} = \{x \in C \cup D : \tau_1 = \tau_2, q_1 = q_2\}.$$

Proof We prove that properties i)-iii) in Definition 2.1.9 hold for V in (8.6) when $\operatorname{dom} \mathrm{V} = \mathbb{R}^4$.

I) We first show that V is continuous on $(C \cup D)$, and hence on $(\widetilde{C} \cup \widetilde{D})$. For parameters $\bar{\tau}$ and ε such that $\bar{\tau} \geq \frac{\varepsilon}{2}$, continuity of V follows directly from the evaluation of the continuous functions

$$\begin{aligned} V_{1a}(x) &:= \tfrac{1}{\varepsilon}(\tau_1 - \tau_2)^2 + \tfrac{\varepsilon}{4}, \\ V_{1b}(x) &:= \tfrac{1}{\varepsilon}(\tau_1 - \tau_2 - 2\bar{\tau})^2 + \tfrac{\varepsilon}{4}, \\ V_{1c}(x) &:= \tfrac{1}{\varepsilon}(\tau_1 - \tau_2 + 2\bar{\tau})^2 + \tfrac{\varepsilon}{4}, \\ V_{2a}(x) &:= |\tau_1 - \tau_2|, \\ V_{2b}(x) &:= 2\bar{\tau} - |\tau_1 - \tau_2| \end{aligned} \tag{8.7}$$

at the boundaries of the pieces on which V is defined. To show that V is nonnegative on

$(C \cup D)$, note that V_{1a}, V_{1b}, V_{1c}, and V_{2a} are always nonnegative. The function V_{2b} is also nonnegative on $C \cup D$. Then, since all of the functions defining V are nonnegative on $(C \cup D)$, V is also nonnegative on that set. Then, in particular, property i) in Definition 2.1.9 holds.

II) We show that V is continuously differentiable on

$$\begin{aligned} \mathcal{O} &:= \{x \in P : 0 < V(x) < \bar{\tau}\} \\ &= \{x \in P : |\tau_1 - \tau_2| \neq \bar{\tau}, |\tau_1 - \tau_2| \neq 2\bar{\tau}, \\ &\qquad\qquad |\tau_1 - \tau_2| \neq 0\}, \end{aligned}$$

which satisfies $\widetilde{C} \setminus \mathcal{A} \subset \mathcal{O} \subset \mathbb{R}^4$. Note that the functions $V_{1a}, V_{1b}, V_{1c}, V_{2a}, V_{2b}$ are C^1 on this set (the points at which V_{2a}, V_{2b} are non-differentiable do not belong to this set). The points $(\tau_1, q_1, \tau_2, q_2)$ at which the definition of V switches between pieces are: for $q_1 \neq q_2$, $(\tau_1 - \tau_2) = \pm\frac{\varepsilon}{2}$, $(\tau_1 - \tau_2) = \pm(2\bar{\tau} - \frac{\varepsilon}{2})$ or $|\tau_1 - \tau_2| = \bar{\tau}$; for $q_1 = q_2$, $|\tau_1 - \tau_2| = \bar{\tau}$ or $\tau_1 = \tau_2$. The latter points (for $q_1 = q_2$) do not belong to $\mathcal{O}$. For points with $q_1 \neq q_2$, we have that the gradients evaluated at the boundary points of the respective functions coincide, from where differentiability of V follows.

III) The property $\lim_{\{x \to \mathcal{A},\, x \in \widetilde{C} \cup \widetilde{D}\}} V(x) = 0$ follows from the continuity of V shown in I) and the fact that $V(\mathcal{A}) = 0$. In fact, for each $x \in \mathcal{A}$ we have $q_1 = q_2$, then $V(x) = V_2(x)$, and for such points we have

$$V_2(x) = \min\{|\tau_1 - \tau_1|, 2\bar{\tau} - |\tau_1 - \tau_1|\} = \min\{0, 2\bar{\tau}\} = 0.$$

■

Lemma 8.3.2 *The function V given as in* (8.6) *satisfies*

$$V(x) > 0 \qquad \forall \;\; x \in (C \cup D) \setminus \mathcal{A}.$$

Proof Since by item i) of Definition 2.1.9, we have that V is nonnegative on $(C \cup D) \setminus \mathcal{A}$, we show that $V(x) \neq 0$ on such set. If $q_1 = q_2$ then $V(x) = V_2(x)$. The function V_2 is zero when $\tau_1 = \tau_2$, which is in $\mathcal{A}$, or when $|\tau_1 - \tau_2| = 2\bar{\tau}$. The latter case is outside $C \cup D$. Therefore, if $q_1 = q_2$ then $V(x) > 0$. If $q_1 \neq q_2$ then $V(x) = V_1(x)$, which depends on $V_{1a}, V_{1b}, V_{1c}, V_{2a}, V_{2b}$. By construction, since V_{1a}, V_{1b}, V_{1c} are lower bounded by $\frac{\varepsilon}{4}$, V is positive on the set $(C \cup D) \setminus \mathcal{A}$.

■

Then, by Lemma 8.3.1 and Lemma 8.3.2, function V in (8.6) is a Lyapunov function candidate for $(\mathcal{H}_{2,2}, \mathcal{A})$. Next, note that $G(\mathcal{A}) \subset \mathcal{A}$ since for each $x \in \mathcal{A}$, the jump map satisfies

$$G(x) = g_5(x) = \begin{bmatrix} (2-q_1)\bar{\tau} \\ 3-q_1 \\ (2-q_2)\bar{\tau} \\ 3-q_2 \end{bmatrix} = \begin{bmatrix} (2-q_1)\bar{\tau} \\ 3-q_1 \\ (2-q_1)\bar{\tau} \\ 3-q_1 \end{bmatrix} \in \mathcal{A}.$$

It follows that to establish that $\mathcal{A}$ is asymptotically stable, we have to check that

$$\langle \nabla V(x), f \rangle \leq 0 \quad \text{for all } x \in \widetilde{C} \setminus \mathcal{A}, f \in F(x), \tag{8.8}$$

$$V(g) - V(x) \leq 0 \quad \text{for all } x \in \widetilde{D} \setminus \mathcal{A}, g \in G(x) \setminus \mathcal{A} \tag{8.9}$$

according to Theorem 2.1.10. This analysis will be divided into the following lemmas to establish the flow and jumps conditions for asymptotic stability in Theorem 2.1.10.

Lemma 8.3.3 *For all $x \in \widetilde{C}$, with V in* (8.6)*,*

$$\langle \nabla V(x), F(x) \rangle = 0.$$

Proof Consider the possibilities of the candidate function (8.6) on $\widetilde{C} \setminus \mathcal{A}$. For points $x \in \widetilde{C} \setminus \mathcal{A}$ such that $q_1 \neq q_2$, we have $V(x) = V_1(x)$. When $V_1(x) \neq V_2(x)$ then $\langle \nabla V(x), F(x) \rangle$ can fall into the following three possibilities:

$$\langle \nabla V_{1a}(x), F(x) \rangle = \begin{bmatrix} \frac{2}{\varepsilon}(\tau_1 - \tau_2) & 0 & -\frac{2}{\varepsilon}(\tau_1 - \tau_2) & 0 \end{bmatrix} \begin{bmatrix} 1 \\ 0 \\ 1 \\ 0 \end{bmatrix} = 0 \qquad \text{if } |\tau_1 - \tau_2| \leq \frac{\varepsilon}{2}$$

$$\langle \nabla V_{1b}(x), F(x) \rangle = \begin{bmatrix} \frac{2}{\varepsilon}(\tau_1 - \tau_2 - 2\bar{\tau}) & 0 & -\frac{2}{\varepsilon}(\tau_1 - \tau_2 - 2\bar{\tau}) & 0 \end{bmatrix} \begin{bmatrix} 1 \\ 0 \\ 1 \\ 0 \end{bmatrix} = 0 \qquad \text{if } \tau_1 - \tau_2 \leq 2\bar{\tau} - \frac{\varepsilon}{2}$$

$$\langle \nabla V_{1c}(x), F(x) \rangle = \begin{bmatrix} \frac{2}{\varepsilon}(\tau_1 - \tau_2 + 2\bar{\tau}) & 0 & -\frac{2}{\varepsilon}(\tau_1 - \tau_2 + 2\bar{\tau}) & 0 \end{bmatrix} \begin{bmatrix} 1 \\ 0 \\ 1 \\ 0 \end{bmatrix} = 0 \qquad \text{if } \tau_1 - \tau_2 \leq -2\bar{\tau} + \frac{\varepsilon}{2}.$$

For points $x \in \widetilde{C}$ such that $q_1 = q_2$, then we have $V(x) = V_2(x)$. If $\tau_1 > \tau_2$, then the possible

expressions of $\langle \nabla V(x), F(x) \rangle$ are

$$\langle \nabla V_{2a}(x), F(x) \rangle = [1 \;\; 0 \;\; -1 \;\; 0] \begin{bmatrix} 1 \\ 0 \\ 1 \\ 0 \end{bmatrix} = 0 \qquad \text{if } \tau_1 - \tau_2 < 2\bar{\tau} - \tau_1 + \tau_2$$

$$\langle \nabla V_{2b}(x), F(x) \rangle = [-1 \;\; 0 \;\; 1 \;\; 0] \begin{bmatrix} 1 \\ 0 \\ 1 \\ 0 \end{bmatrix} = 0 \qquad \text{if } \tau_1 - \tau_2 > 2\bar{\tau} - \tau_1 + \tau_2 \;;$$

if $\tau_1 < \tau_2$, then

$$\langle \nabla V_{2a}(x), F(x) \rangle = [-1 \;\; 0 \;\; 1 \;\; 0] \begin{bmatrix} 1 \\ 0 \\ 1 \\ 0 \end{bmatrix} = 0 \qquad \text{if } \tau_2 - \tau_1 < 2\bar{\tau} - \tau_2 + \tau_1$$

$$\langle \nabla V_{2b}(x), F(x) \rangle = [1 \;\; 0 \;\; -1 \;\; 0] \begin{bmatrix} 1 \\ 0 \\ 1 \\ 0 \end{bmatrix} = 0 \qquad \text{if } \tau_2 - \tau_1 > 2\bar{\tau} - \tau_2 + \tau_1 \;.$$

So, we have that (8.8) holds. ■

Using symmetry between g_1, g_2 and g_3, g_4, and without loss of generality on $\widetilde{D}$, we can consider $\tau_1 = q_1\bar{\tau}$ and (τ_2, q_2) such that $(\tau_1, q_1, \tau_2, q_2) \in \widetilde{C} \cup \widetilde{D}$. Then, the set $\widetilde{D}$ will be

split accordingly to evaluate all possibilities of the jump map outside of $x \in g_5, g_6$. We will not consider the cases when $x \in g_5, g_6$. This is because when $x \in g_5$ then by definition $\tau_1 = \tau_2$ and $q_1 = q_2$ which means that these points are when $x \in \mathcal{A}$. Next looking at when $x \in g_6$ the conditions $\tau_1 = q_1\bar{\tau}$, $\tau_2 = q_2\bar{\tau}$ and $q_1 \neq q_2$ are outside the basin of attraction for $\widetilde{\mathcal{H}}_{2,2}$ because $|\tau_1 - \tau_2| = \bar{\tau}$.

Lemma 8.3.4 *For all* $x \in D_a := \{x \in \widetilde{D} : |\tau_1 - \tau_2| < \bar{\tau}, q_1 = q_2\}$,

$$\max_{g \in G(x)} V(g) - V(x) = \begin{cases} V_{2a}(g) - V_{2a}(x) & \textit{if} \quad q_1 = 1, \tau_1 = \bar{\tau}, \tau_2 \in \left[0, \bar{\tau} - \frac{3\varepsilon}{2}\right] \\ V_{1a}(g) - V_{2a}(x) & \textit{if} \quad q_1 = 1, \tau_1 = \bar{\tau}, \tau_2 \in \left[\bar{\tau} - \frac{3\varepsilon}{2}, \bar{\tau} - \varepsilon\right] \\ V_{2b}(g) - V_{2a}(x) & \textit{if} \quad q_1 = 2, \tau_1 = 2\bar{\tau}, \tau_2 \in \left[\bar{\tau}, 2\bar{\tau} - \frac{3\varepsilon}{2}\right] \\ V_{1c}(g) - V_{2a}(x) & \textit{if} \quad q_1 = 2, \tau_1 = 2\bar{\tau}, \tau_2 \in \left[2\bar{\tau} - \frac{3\varepsilon}{2}, 2\bar{\tau} - \varepsilon\right] \end{cases}$$

Proof Since $|\tau_1 - \tau_2| < \bar{\tau}$ for all $x \in D_a$, it follows from the definition of V in (8.6) and its components in (8.7) that

$$V(x) = V_2(x) = V_{2a}(x). \tag{8.10}$$

Note, that since $x \in D_a$ with the conditions above, x can only jump via g_1 given in (8.4). There are three options for the value of x after the jump, which we denote x^+. These possibilities are

captured by the following functions:

$$g_{11}(x) = \begin{bmatrix} (2-q_1)\bar{\tau} \\ 3-q_1 \\ \tau_2+\varepsilon \\ q_2 \end{bmatrix} \quad \text{if } \tau_2+\varepsilon < q_2\bar{\tau}, \qquad g_{12}(x) = \begin{bmatrix} (2-q_1)\bar{\tau} \\ 3-q_1 \\ (2-q_2)\bar{\tau} \\ 3-q_2 \end{bmatrix} \quad \text{if } \tau_2+\varepsilon > q_2\bar{\tau}$$

$$g_{13}(x) \in \{g_{11}(x), g_{12}(x)\} \qquad \text{if } \tau_2+\varepsilon = q_2\bar{\tau}$$

Note that, for every such x where $\tau_2+\varepsilon > q_2\bar{\tau}$, the jump is such that $x^+ = g_{12}(x) \in \mathcal{A}$. Furthermore, when x is such that $\tau_2+\varepsilon = q_2\bar{\tau}$, then x^+ can be either g_{11} or g_{12}. If x is such that $g_{13} = g_{12}$ then, according to (8.9), g_{13} does not need to be evaluated since $g_{12}(x) \in \mathcal{A}$. Now, analyzing the other situation, when $x^+ = g_{11}$, we have

$$x^+ = \begin{bmatrix} (2-q_1)\bar{\tau} \\ 3-q_1 \\ \tau_2+\varepsilon \\ q_2 \end{bmatrix}.$$

Using the definition of V in (8.6), the possible values of V at $x^+ = g_{11}(x)$ are analyzed for the cases when $q_1 = 1$ and when $q_1 = 2$.

- When $q_1 = 1$, we have

$$\tau_1 = \bar{\tau}, \qquad q_2 = 1, \qquad \tau_2 \in [0, \bar{\tau}-\varepsilon)\,. \tag{8.11}$$

  It follows that

$$q_1^+ = 2, \qquad \tau_1^+ = \bar{\tau}, \qquad q_2^+ = 1, \qquad \tau_2^+ \in [\varepsilon, \bar{\tau}). \tag{8.12}$$

Since, $\tau_1^+ - \tau_2^+ \in (0, \bar{\tau} - \varepsilon]$ with $q_1^+ \neq q_2^+$, it follows that $V(x^+) = V_1(x^+)$. From the piecewise definition of the function V_1, for $|\tau_1^+ - \tau_2^+| \leq \frac{\varepsilon}{2}$ we have $V_1(x^+) = V_{1a}(x^+)$. Then using $\tau_2^+ = \tau_2 + \varepsilon$

$$\begin{aligned} |\tau_1^+ - \tau_2^+| &\leq \tfrac{\varepsilon}{2} \\ \bar{\tau} - \tau_2 - \varepsilon &\leq \tfrac{\varepsilon}{2} \\ \implies \tau_2 &\geq \bar{\tau} - \tfrac{3\varepsilon}{2} \ . \end{aligned}$$

It follows that

$$V(x^+) = V_1(x^+) = V_{1a}(x^+) \quad \text{if } q_1 = 1, \tau_1 = \bar{\tau}, \tau_2 \in \left[\bar{\tau} - \frac{3\varepsilon}{2}, \bar{\tau} - \varepsilon\right) \tag{8.13}$$

Now consider the case $|\tau_1^+ - \tau_2^+| > \frac{\varepsilon}{2}$, $x \in D_a$. Then the function $V_1(x^+) = V_2(x^+)$. Using the fact that $\tau_2^+ = \tau_2 + \varepsilon$,

$$|\tau_1^+ - \tau_2^+| = |\bar{\tau} - \tau_2 - \varepsilon| < |\bar{\tau} - \varepsilon|.$$

It follows that $V(x^+)$ is given by

$$V(x^+) = V_1(x^+) = V_{2a}(x^+) \quad \text{if } q_1 = 1, \tau_1 = \bar{\tau}, \tau_2 \in \left[0, \bar{\tau} - \frac{3\varepsilon}{2}\right]. \tag{8.14}$$

- When $q_1 = 2$, we have

$$\tau_1 = 2\bar{\tau}, \qquad q_2 = 2, \qquad \tau_2 \in [\bar{\tau}, 2\bar{\tau} - \varepsilon)\,.$$

If follows that

$$q_1^+ = 1, \qquad \tau_1^+ = 0, \qquad q_2^+ = 2, \qquad \tau_2^+ \in [\bar{\tau} + \varepsilon, 2\bar{\tau})$$

Since $\tau_1^+ - \tau_2^+ \in (-2\bar{\tau}, -\bar{\tau} - \varepsilon]$ and $q_1^+ \neq q_2^+$, it follows that $V(x^+) = V_1(x^+)$. From the piecewise definition of the function V_1, for $\tau_1^+ - \tau_2^+ \leq -2\bar{\tau} + \frac{\varepsilon}{2}$ we have $V_1(x^+) = V_{1c}(x^+)$.

Then using $\tau_1^+ = 0$ and $\tau_2^+ = \tau_2 + \varepsilon$,

$$\begin{aligned} \tau_1^+ - \tau_2^+ &\leq -2\bar{\tau} + \tfrac{\varepsilon}{2} \\ 0 - \tau_2 - \varepsilon &\leq -2\bar{\tau} + \tfrac{\varepsilon}{2} \\ \Longrightarrow \tau_2 &\geq 2\bar{\tau} - \tfrac{3\varepsilon}{2}. \end{aligned}$$

It follows that

$$V(x^+) = V_1(x^+) = V_{1c}(x^+) \quad \text{if } q_1 = 2, \tau_1 = 2\bar{\tau}, \tau_2 \in \left[2\bar{\tau} - \frac{3\varepsilon}{2}, 2\bar{\tau} - \varepsilon\right) \tag{8.15}$$

Similar to the previous analysis, if we take the case when $\tau_1^+ - \tau_2^+ \geq -2\bar{\tau} + \frac{\varepsilon}{2}$, then $V_1 = V_2$. Using the fact that $\tau_2^+ = \tau_2 + \varepsilon$ then,

$$|\tau_1^+ - \tau_2^+| = |0 - \tau_2 - \varepsilon| > 2\bar{\tau} - |0 - \tau_2 - \varepsilon|$$

It follows that

$$V(x^+) = V_1(x^+) = V_{2b}(x^+) \quad \text{if } q_1 = 2, \tau_1 = 2\bar{\tau}, \tau_2 \in \left[\bar{\tau}, 2\bar{\tau} - \frac{3\varepsilon}{2}\right] . \tag{8.16}$$

■

Lemma 8.3.5 *For every $x \in D_a$*

$$\max_{g \in G(x)} V(g) - V(x) \leq -\varepsilon$$

Proof Now, we determine all of the possible differences $V(x^+) - V(x)$ as in (8.9). Using $V(x)$ as in (8.10), we consider $V(x^+) = V_{1a}(x^+)$ as in (8.13). We have

$$\begin{aligned} V(x) &= |\tau_1 - \tau_2| , \\ V(x^+) &= \tfrac{1}{\varepsilon}\left(\tau_1^+ - \tau_2^+\right)^2 + \tfrac{\varepsilon}{4} . \end{aligned}$$

Since $\tau_1 = \bar{\tau}$ and $\tau_2 \in \left[\bar{\tau} - \frac{3\varepsilon}{2}, \bar{\tau} - \varepsilon\right)$, then $\tau_1^+ = \bar{\tau}$ and $\tau_2^+ \in \left[\bar{\tau} - \frac{\varepsilon}{2}, \bar{\tau}\right)$. Then, using these

conditions:

$$\begin{aligned} V(x^+) - V(x) &= \tfrac{1}{\varepsilon}\left(\tau_1^+ - \tau_2^+\right)^2 + \tfrac{\varepsilon}{4} - |\tau_1 - \tau_2| \tfrac{1}{\varepsilon}\left(\bar{\tau} - \tau_2^+\right)^2 + \tfrac{\varepsilon}{4} - |\bar{\tau} + \tau_2| \\ &\leq \tfrac{1}{\varepsilon}\left(\bar{\tau} - \left(\bar{\tau} - \tfrac{\varepsilon}{2}\right)\right)^2 + \tfrac{\varepsilon}{4} - |\bar{\tau} + \bar{\tau} - \tfrac{3\varepsilon}{2}| \leq \tfrac{1}{\varepsilon}\left(\tfrac{\varepsilon}{2}\right)^2 + \tfrac{\varepsilon}{4} - \tfrac{3\varepsilon}{2} \leq -\varepsilon \ . \end{aligned} \tag{8.17}$$

Next, we consider $V(x^+) - V(x)$ with $V(x^+)$ as in (8.14) and $V(x)$ as in (8.10), then it follows that $V(x) = |\tau_1 - \tau_2|$ and $V(x^+) = |\tau_1^+ - \tau_2^+|$, respectively. Since $\tau_1 = \bar{\tau}$ and $\tau_2 \in \left[0, \bar{\tau} - \frac{3\varepsilon}{2}\right]$, then $\tau_1^+ = \bar{\tau}$ and $\tau_2^+ = \tau_2 + \varepsilon$. Using these conditions, we get

$$V(x^+) - V(x) = |\tau_1^+ - \tau_2^+| - |\tau_1 - \tau_2| = \bar{\tau} - \tau_2 - \varepsilon - \bar{\tau} + \tau_2 = -\varepsilon. \tag{8.18}$$

Next, $V(x^+) - V(x)$ will be evaluated with $V(x^+) = V_{1c}(x^+)$ as in (8.15) and $V(x)$ as in (8.10):

$$\begin{aligned} V(x) &= |\tau_1 - \tau_2| \\ V(x^+) &= \tfrac{1}{\varepsilon}\left(\tau_1^+ - \tau_2^+ + 2\bar{\tau}\right)^2 + \tfrac{\varepsilon}{4}. \end{aligned}$$

Since $\tau_1 = 2\bar{\tau}$ and $\tau_2 \in \left[2\bar{\tau} - \frac{3\varepsilon}{2}, 2\bar{\tau} - \varepsilon\right)$, then $\tau_1^+ = 0$ and $\tau_2^+ \in \left[2\bar{\tau} - \frac{\varepsilon}{2}, 2\bar{\tau}\right)$. Then, using these conditions:

$$\begin{aligned} V(x^+) - V(x) &= \tfrac{1}{\varepsilon}\left(\tau_1^+ - \tau_2^+ + 2\bar{\tau}\right)^2 + \tfrac{\varepsilon}{4} - |\tau_1 + \tau_2| \\ &= \tfrac{1}{\varepsilon}\left(0 - \tau_2^+ + 2\bar{\tau}\right)^2 + \tfrac{\varepsilon}{4} - |2\bar{\tau} + \tau_2| \\ &\leq \tfrac{1}{\varepsilon}\left(-\left(2\bar{\tau} - \tfrac{\varepsilon}{2}\right) + 2\bar{\tau}\right)^2 + \tfrac{\varepsilon}{4} - |2\bar{\tau} + \left(2\bar{\tau} - \tfrac{3\varepsilon}{2}\right)| \\ &\leq \tfrac{1}{\varepsilon}\left(\tfrac{\varepsilon}{2}\right)^2 + \tfrac{\varepsilon}{4} - \tfrac{3\varepsilon}{2} \leq -\varepsilon. \end{aligned} \tag{8.19}$$

Lastly, for $x \in D_a$, we consider $V(x^+) - V(x)$ with $V(x^+)$ as in (8.16) and $V(x)$ as in (8.10), then it follows that $V(x) = |\tau_1 - \tau_2|$ and $V(x^+) = 2\bar{\tau} - |\tau_1^+ - \tau_2^+|$, respectively. Since $\tau_1 = 2\bar{\tau}$ and $\tau_2 \in \left[\bar{\tau}, 2\bar{\tau} - \frac{3\varepsilon}{2}\right]$, then $\tau_1^+ = 0$ and $\tau_2^+ \in \left[\bar{\tau} + \varepsilon, 2\bar{\tau} - \frac{\varepsilon}{2}\right]$. Then, using these conditions, we get

$$\begin{aligned} V(x^+) - V(x) &= 2\bar{\tau} - |\tau_1^+ - \tau_2^+| - |\tau_1 - \tau_2| \\ &\leq 2\bar{\tau} - (\bar{\tau} + \varepsilon) - 2\bar{\tau} - \bar{\tau} \leq -2\bar{\tau} - \varepsilon. \end{aligned} \tag{8.20}$$

■

Lemma 8.3.6 *For all* $x \in D_b := \{x \in \widetilde{D} : |\tau_1 - \tau_2| > \bar{\tau}, q_1 \neq q_2\}$,

$$\max_{g \in G(x)} V(g) - V(x) = \begin{cases} V_{2a}(g) - V_{1b}(x) & \textit{if} \quad q_1 = 1, \tau_1 = \bar{\tau}, \tau_2 \in \left[0, \frac{\varepsilon}{2}\right] \\ \\ V_{2a}(g) - V_{2b}(x) & \textit{if} \quad q_1 = 1, \tau_1 = \bar{\tau}, \tau_2 \in \left[\frac{\varepsilon}{2}, \bar{\tau}\right] \end{cases}$$

Proof First consider the point when $q_1 = 1$, then $\tau_1 = \bar{\tau}, q_2 = 2$ and $\tau_2 \in (\bar{\tau}, 2\bar{\tau})$. Such points do not belong to the set D_b due to $|\tau_1 - \tau_2| < \bar{\tau}$. Next we evaluate the point when $q_1 = 2$,

$$\tau_1 = 2\bar{\tau}, \qquad q_2 = 1, \qquad \tau_2 \in (0, \bar{\tau}).$$

It follows that

$$q_1^+ = 1, \qquad \tau_1^+ = 0, \qquad q_2^+ = 1, \qquad \tau_2^+ = \tau_2.$$

Since $\tau_1 - \tau_2 \in (\bar{\tau}, 2\bar{\tau})$ and $q_1 \neq q_2$, it follows that $V(x) = V_1(x)$. From the piecewise definition of the function V_1, for $\tau_1 - \tau_2 \geq 2\bar{\tau} - \frac{\varepsilon}{2}$ we have $V_1(x) = V_{1b}(x)$. Then, we get

$$\begin{aligned} \tau_1 - \tau_2 &\geq 2\bar{\tau} - \tfrac{\varepsilon}{2} \\ 2\bar{\tau} - \tau_2 &\geq 2\bar{\tau} - \tfrac{\varepsilon}{2} \\ \implies \tau_2 &\leq \tfrac{\varepsilon}{2}\,. \end{aligned}$$

It follows that

$$V(x) = V_1(x) = V_{1b}(x) \quad \text{if} \quad \tau_1 = 2\bar{\tau}, \tau_2 \in \left(0, \frac{\varepsilon}{2}\right] \tag{8.21}$$

When we consider $\tau_1 - \tau_2 \leq 2\bar{\tau} - \frac{\varepsilon}{2}$, the piecewise definition of V_1 results in $V_1(x) = V_2(x)$ and since

$$|\tau_1 - \tau_2| > 2\bar{\tau} - |\tau_1 - \tau_2|$$

it follows that

$$V(x) = V_1(x) = V_{2b}(x) \quad \text{if} \quad \tau_1 = 2\bar{\tau}, \tau_2 \in \left[\frac{\varepsilon}{2}, \bar{\tau}\right) \ . \tag{8.22}$$

The only option for this jump is

$$x^+ = g_3(x) = \begin{bmatrix} (2-q_1)\bar{\tau} \\ 3-q_1 \\ \tau_2 \\ q_2 \end{bmatrix} = \begin{bmatrix} 0 \\ 1 \\ \tau_2 \\ 1 \end{bmatrix} .$$

Since, $\tau_1^+ - \tau_2^+ \in (-\bar{\tau}, 0)$ and $q_1 = q_2$, we have

$$V(x^+) = V_2(x^+) = V_{2a}(x^+) \ . \tag{8.23}$$

■

Lemma 8.3.7 *For every $x \in D_b$*

$$\max_{g \in G(x)} V(g) - V(x) \leq 0.$$

Proof For each $x \in D_b$, since $q_1 \neq q_2$ we have $V(x) = V_1(x)$. Since the function V_1 is piecewise, condition (8.9) must be evaluated for each piece. Taking $V(x)$ as in (8.21) and $V(x^+)$ as in (8.23), it follows that

$$\begin{aligned} V(x) &= \tfrac{1}{\varepsilon}\left(\tau_1 - \tau_2 - 2\bar{\tau}\right)^2 + \tfrac{\varepsilon}{4} \\ V(x^+) &= |\tau_1^+ - \tau_2^+|. \end{aligned}$$

Since $\tau_1 = 2\bar{\tau}$ and $\tau_2 \in \left(0, \frac{\varepsilon}{2}\right]$, then $\tau_1^+ = 0$ and $\tau_2^+ = \tau_2 \in \left(0, \frac{\varepsilon}{2}\right]$. Then, using these conditions,

we obtain

$$\begin{aligned}
V(x^+) - V(x) &= |\tau_1^+ - \tau_2^+| - \left(\tfrac{1}{\varepsilon}\left(\tau_1 - \tau_2 - 2\bar{\tau}\right)^2 + \tfrac{\varepsilon}{4}\right) \\
&= |0 - \tau_2^+| - \tfrac{1}{\varepsilon}\left(2\bar{\tau} - \tau_2 - 2\bar{\tau}\right)^2 - \tfrac{\varepsilon}{4} \\
&= -\tfrac{1}{\varepsilon}\tau_2^2 + \tau_2 - \tfrac{\varepsilon}{4} \\
&= -\tfrac{1}{\varepsilon}\left(\tau_2 - \tfrac{\varepsilon}{2}\right)^2 \\
&\leq 0.
\end{aligned}$$

Note that $V(x^+) - V(x)$ is maximum when $\tau_2 = \frac{\varepsilon}{2}$. Next, evaluating (8.9) with $V(x)$ as in (8.22) and $V(x^+)$ as in (8.23), we obtain

$$\begin{aligned}
V(x) &= 2\bar{\tau} - |\tau_1 - \tau_2| \\
V(x^+) &= |\tau_1^+ - \tau_2^+|.
\end{aligned}$$

Since $\tau_1 = 2\bar{\tau}$ and $\tau_2 \in \left[\frac{\varepsilon}{2}, \bar{\tau}\right)$, then $\tau_1^+ = 0$ and $\tau_2^+ = \tau_2$. Using these conditions, we obtain

$$\begin{aligned}
V(x^+) - V(x) &= |\tau_1^+ - \tau_2^+| - (2\bar{\tau} - |\tau_1 - \tau_2|) \\
&= |0 - \tau_2| - (2\bar{\tau} - |2\bar{\tau} - \tau_2|) \\
&= \tau_2 - 2\bar{\tau} + 2\bar{\tau} - \tau_2 \\
&= 0.
\end{aligned}$$

■

Lemma 8.3.8 *For all* $x \in D_c := \{x \in \widetilde{D} : |\tau_1 - \tau_2| < \bar{\tau}, q_1 \neq q_2\}$

$$\max_{g \in G(x)} V(g) - V(x) = \begin{cases} V_{2a}(g) - V_{1a}(x) & \textit{if} \quad q_1 = 1, \tau_1 = \bar{\tau}, \tau_2 \in \left[\bar{\tau}, \bar{\tau} + \frac{\varepsilon}{2}\right] \\ V_{2a}(g) - V_{2b}(x) & \textit{if} \quad q_1 = 1, \tau_1 = \bar{\tau}, \tau_2 \in \left[\bar{\tau} + \frac{\varepsilon}{2}, 2\bar{\tau}\right] \end{cases}$$

Proof When $q_1 = 1$ then,

$$\tau_1 = \bar{\tau}, \qquad q_2 = 2, \qquad \tau_2 \in (\bar{\tau}, 2\bar{\tau}).$$

It follows that

$$q_1^+ = 2, \qquad \tau_1^+ = \bar{\tau}, \qquad q_2^+ = 2, \qquad \tau_2^+ = \tau_2 \in (\bar{\tau}, 2\bar{\tau}).$$

Since $|\tau_1 - \tau_2| = \tau_2 - \tau_1 \in (0, \bar{\tau})$ and $q_1 \neq q_2$, then, it follows that $V(x) = V_1(x)$. From the piecewise definition of the function V_1, for $|\tau_1 - \tau_2| \leq \frac{\varepsilon}{2}$ we have $V_1(x) = V_{1a}(x)$ leading to the following bound on τ_2:

$$\begin{aligned} |\tau_1 - \tau_2| &\leq \tfrac{\varepsilon}{2} \\ \tau_2 - \bar{\tau} &\leq \tfrac{\varepsilon}{2} \\ \implies \tau_2 &\leq \bar{\tau} + \tfrac{\varepsilon}{2}\ . \end{aligned}$$

It follows that

$$V(x) = V_1(x) = V_{1a}(x) \quad \text{if} \ \ \tau_1 = \bar{\tau}, \tau_2 \in \left(\bar{\tau}, \bar{\tau} + \frac{\varepsilon}{2}\right] \tag{8.24}$$

Looking at the case$|\tau_1 - \tau_2| \geq \frac{\varepsilon}{2}$ leads to $\tau_2 \geq \bar{\tau} + \frac{\varepsilon}{2}$. Then by the piecewise definition of V in (8.6), $V_1 = V_2$. Since,

$$|\tau_1 - \tau_2| < 2\bar{\tau} - |\tau_1 - \tau_2|,$$

it follows that

$$V(x) = V_1(x) = V_{2a}(x) \quad \text{if} \ \ \tau_1 = \bar{\tau}, \tau_2 \in \left[\bar{\tau} + \frac{\varepsilon}{2}, 2\bar{\tau}\right). \tag{8.25}$$

Since $q_1 \neq q_2$, $\tau_1 = \bar{\tau}$ and $\tau_2 \in (\bar{\tau}, 2\bar{\tau})$, the jump map used when $x \in D_c$ is g_3. Then,

$$x^+ = g_3(x) = \begin{bmatrix} (2 - q_1)\bar{\tau} \\ 3 - q_1 \\ \tau_2 \\ q_2 \end{bmatrix} = \begin{bmatrix} \bar{\tau} \\ 2 \\ \tau_2 \\ 2 \end{bmatrix}$$

Since $|\tau_1^+ - \tau_2^+| = |\tau_1 - \tau_2| \in (0, \bar{\tau})$ we have

$$V(x^+) = V_2(x^+) = V_{2a}(x^+) \ . \tag{8.26}$$

If $q_1 = 2$, then $\tau_1 = 2\bar{\tau}$. Since $q_1 \neq q_2$, then $q_2 = 1$ making $\tau_2 \in (0, \bar{\tau})$ which defines a point that is not in the set D_c. ■

Lemma 8.3.9 *For every $x \in D_c$*

$$\max_{g \in G(x)} V(g) - V(x) \leq 0$$

Proof For each $x \in D_c$, since $q_1 \neq q_2$ we have $V(x) = V_1(x)$. The function V_1 is piecewise and (8.9) must be evaluated for each piece. Taking $V(x)$ as in (8.24) and $V(x^+)$ as in (8.26), it follows that

$$\begin{aligned} V(x) &= \tfrac{1}{\varepsilon}\left(\tau_1 - \tau_2\right)^2 + \tfrac{\varepsilon}{4} \\ V(x^+) &= |\tau_1^+ - \tau_2^+| \end{aligned}$$

Since $\tau_1 = \bar{\tau}$ and $\tau_2 \in \left(\bar{\tau}, \bar{\tau} + \frac{\varepsilon}{2}\right]$, then $\tau_1^+ = \bar{\tau}$ and $\tau_2^+ = \tau_2 \in \left(\bar{\tau}, \bar{\tau} + \frac{\varepsilon}{2}\right]$. Then

$$\begin{aligned} V(x^+) - V(x) &= |\tau_1^+ - \tau_2^+| - \left(\tfrac{1}{\varepsilon}\left(\tau_1 - \tau_2\right)^2 + \tfrac{\varepsilon}{4}\right) \\ &= |\bar{\tau} - \tau_2| - \left(\tfrac{1}{\varepsilon}\left(\bar{\tau} - \tau_2\right)^2 + \tfrac{\varepsilon}{4}\right) \\ &= \tau_2 - \bar{\tau} - \left(\tfrac{1}{\varepsilon}\left(\bar{\tau} - \tau_2\right)^2 + \tfrac{\varepsilon}{4}\right) \end{aligned}$$

Defining $z = \tau_2 - \bar{\tau}$, then the solution to $z - \frac{1}{\varepsilon}z^2 + \frac{\varepsilon}{4} = (z - \frac{\varepsilon}{2})^2 = 0$ is $z_{1,2} = \frac{\varepsilon}{2}$. This implies that $V(x^+) - V(x)$ is maximum when $\tau_2 = \bar{\tau} + \frac{\varepsilon}{2}$. Then it follows that

$$V(x^+) - V(x) \leq 0$$

Lastly, evaluating (8.9) when $V(x)$ is as in (8.25) and $V(x^+)$ is as in (8.26):

$$\begin{aligned} V(x) &= |\tau_1 - \tau_2| \\ V(x^+) &= |\tau_1^+ - \tau_2^+| \ . \end{aligned}$$

Since $\tau_1 = \tau_1^+$ and $\tau_2 = \tau_2^+$, then

$$\begin{aligned} V(x) &= V(x^+) \\ \Longrightarrow V(x^+) - V(x) &= 0 \ . \end{aligned}$$

It follows that (8.9) holds. ■

Using $\bar{\tau} = 1$ and $\varepsilon = 0.3$, Figure 8.2 shows V when $q_1 = q_2$, and $q_1 \neq q_2$. Note that when $q_1 = q_2$, we have $V(x) = V_2(x)$, while when $q_1 \neq q_2$, we have $V(x) = V_1(x)$. This function was constructed in this way to eliminate points where $V(x) = 0$ outside of the compact set $\mathcal{A}$, which are points belonging to the blue lines in Figure 8.3. The function is not differentiable at these points and at points $\tau_2 = \tau_1 \pm \bar{\tau}$. The latter points, which are denoted by the green lines in Figure 8.3, will need to be removed from the basin of attraction.

The following stability result for $\mathcal{H}_{2,2}$ can be established using the Lyapunov function in (8.6) and Theorem 2.1.10.

Theorem 8.3.10 *(Timer synchronization with limited information) For every $\bar{\tau} > 0$ and $\varepsilon \in (0, 2\bar{\tau}]$, the hybrid system $\mathcal{H}_{2,2}$ is such that $\mathcal{A}$ is asymptotically stable with basin of attraction containing every sublevel set $L_V(\mu)$ with $\mu \in [0, \bar{\tau})$.*

Proof Stability of $\mathcal{A}$ for $\mathcal{H}_{2,2}$ comes from the results in Lemma 8.3.3 - lem:jumpsDc2. To show attractivity, assume that there exists a solution $\phi = (\tau_1, q_1, \tau_2, q_2)$ that always stays in the level set

$$L_V(\mu) = \{x : V(x) = \mu\}. \tag{8.27}$$

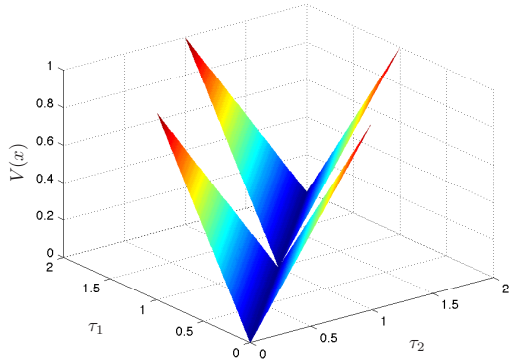

(a) $q_1 = q_2$

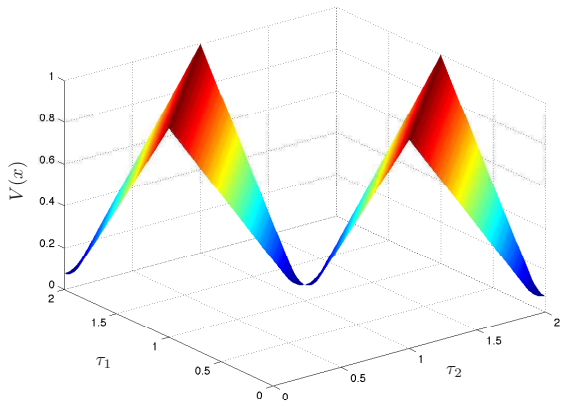

(b) $q_1 \neq q_2$

Figure 8.2: A plot of the Lyapunov function V in (8.6) for each x in $C \cup D$

When $\phi(t,j) \in D_a$, $\phi(t,j)$ jumps out of the level set immediately since, due to Lemma 8.3.5, we have $V(\phi(t,j+1)) \leq V(\phi(t,j)) - \varepsilon$. When $\phi(t,j) \in D_b \cup D_c$, we have $V(\phi(t,j+1)) - V(\phi(t,j)) \leq 0$ and the solution can evolve according to the following cases:

1. When $\phi(t_1,0) \in D_b$ and V is as in (8.21), if the solution stays in the μ level-set of V, we must have

$$\begin{aligned} V(\phi(t_1,0)) &= V_{1b}(\phi(t_1,0)) &= \tfrac{1}{\varepsilon}\left(\tau_1(t_1,0) - \tau_2(t_1,0) - 2\bar{\tau}\right)^2 + \tfrac{\varepsilon}{4} = \mu \\ V(\phi(t_1,1)) &= V_{2a}(\phi(t_1,1)) &= |\tau_1(t_1,1) - \tau_2(t_1,1)| = \mu \ . \end{aligned}$$

Then, we must have

$$\begin{aligned}
\tfrac{1}{\varepsilon}\left(\tau_1(t_1,0)-\tau_2(t_1,0)-2\bar{\tau}\right)^2+\tfrac{\varepsilon}{4} &= |\tau_1(t_1,1)-\tau_2(t_1,1)| \\
\tfrac{1}{\varepsilon}\left(2\bar{\tau}-\tau_2(t_1,0)-2\bar{\tau}\right)^2+\tfrac{\varepsilon}{4} &= |0-\tau_2(t_1,1)| \\
\tfrac{1}{\varepsilon}\tau_2^2(t_1,0)+\tfrac{\varepsilon}{4} &= \tau_2(t_1,1)
\end{aligned}$$

.

Since $\tau_2(t_1,0)=\tau_2(t_1,1)$,

$$\begin{aligned}
\tau_2^2(t_1,0)-\varepsilon\tau_2(t_1,0)+\tfrac{\varepsilon^2}{4} &= 0 \\
\Longrightarrow\ \tau_2(t_1,0) &= \tfrac{\varepsilon}{2}.
\end{aligned}$$

Along flows, the solution, $\phi(t,1)$ stays in the level set $L_V(\mu)$ for each $t\in[t_1,t_2]$. The next jump occurs when $(t_2,1)\in\operatorname{dom}\phi$ is such that

$$\tau_2(t_2,1)=\bar{\tau},\qquad q_2(t_2,1)=1,\qquad \tau_1(t_2,1)=\bar{\tau}-\frac{\varepsilon}{2},\qquad q_1(t_2,1)=1$$

and the new values after the next jump are

$$\tau_2(t_2,2)=\bar{\tau},\qquad q_2(t_2,2)=2,\qquad \tau_1(t_2,2)=\bar{\tau},\qquad q_1(t_2,2)=2\ .$$

For this jump we have $\tau_1(t_2,2)=\tau_2(t_2,2)$ and $q_1(t_2,2)=q_2(t_2,2)$. In fact, after the jump, solution $\phi(t_2,2)$ leaves $L_V(\mu)$ and reaches $L_V(0)$.

2. When $\phi(t_1,0)\in D_b$ and V is as in (8.22), if the solution stays in the μ level set of V we must have:

$$\begin{aligned}
V(\phi(t_1,0)) &= V_{2b}(\phi(t_1,0)) &&= 2\bar{\tau}-|\tau_1(t_1,0)-\tau_2(t_1,0)| &&= \mu \\
V(\phi(t_1,1)) &= V_{2a}(\phi(t_1,1)) &&= |\tau_1(t_1,1)-\tau_2(t_1,1)| &&= \mu
\end{aligned}$$

Then, we must have

$$\begin{aligned} 2\bar{\tau} - |\tau_1(t_1,0) - \tau_2(t_1,0)| &= |\tau_1(t_1,1) - \tau_2(t_1,1)| \\ 2\bar{\tau} - (2\bar{\tau} - \tau_2(t_1,0)) &= \tau_2(t_1,1) - 0 \\ \tau_2(t_1,0) &= \tau_2(t_1,1). \end{aligned}$$

For all values of $\tau_2(t_1,0) = \tau_2(t_1,1) \in (0,\bar{\tau})$, the solution satisfies $\phi(t_1,1) \in L_V(\mu)$. Then, as in the previous case, the next jump at $\phi(t_2,1)$ is analyzed. This jump has the following properties:

$$\tau_2(t_2,1) = \bar{\tau}, \qquad q_2(t_2,1) = 1, \qquad \tau_1(t_2,1) \in \left(0, \bar{\tau} - \tfrac{\varepsilon}{2}\right], \qquad q_1(t_2,1) = 1$$

$$\tau_2(t_2,2) = \bar{\tau}, \qquad q_2(t_2,2) = 2, \qquad \begin{bmatrix} \tau_1(t_2,2) \\ q_1(t_2,2) \end{bmatrix} \in \begin{bmatrix} (\varepsilon,\bar{\tau}) \\ 1 \end{bmatrix} \bigcup \begin{bmatrix} \bar{\tau} \\ 2 \end{bmatrix}$$

This jumps has several possibilities.

- For $\tau_1(t_2,1) \geq \bar{\tau} - \epsilon$, the system jumps according to g_{12} after which the solution reaches the level set $L_V(0)$, and hence, leaves $L_V(\mu)$.
- From Lemma 8.3.5, with $\tau_1(t_2,1) \in \left[\bar{\tau} - \frac{3\varepsilon}{2}, \bar{\tau} - \varepsilon\right)$, then this leads to the following:

$$V(\phi(t_2,1)) = V_{2a}(\phi(t_2,1)) = |\tau_1(t_2,1) - \tau_2(t_2,1)| = \mu$$

$$V(\phi(t_2,2)) = V_{1a}(\phi(t_2,2)) = \tfrac{1}{\varepsilon}\left(\tau_1(t_2,2) - \tau_2(t_2,2)\right)^2 + \tfrac{\varepsilon}{2} = \mu\ .$$

  Then, we must have

$$\begin{aligned} |\tau_1(t_2,1) - \tau_2(t_2,1)| &= \frac{1}{\varepsilon}\left(\tau_1(t_2,2) - \tau_2(t_2,2)\right)^2 + \frac{\varepsilon}{2} \\ |\tau_1(t_2,1) - \bar{\tau}| &= \frac{1}{\varepsilon}\left(\tau_1(t_2,2) - \bar{\tau}\right)^2 + \frac{\varepsilon}{2} \\ \bar{\tau} - \tau_1(t_2,1) &= \frac{1}{\varepsilon}\left(\tau_1(t_2,1) + \varepsilon - \bar{\tau}\right)^2 + \frac{\varepsilon}{2} \qquad \leftarrow \tau_1(t_2,2) = \tau_1(t_2,1) + \varepsilon \\ &\Longrightarrow \quad \tau_1(t_2,1) \in \left\{\bar{\tau} - \frac{5\varepsilon}{2}, \bar{\tau} - \frac{\varepsilon}{2}\right\} \end{aligned} \tag{8.28}$$

Since $\tau_1(t_2,1) \in \left[\bar{\tau} - \frac{3\varepsilon}{2}, \bar{\tau} - \varepsilon\right)$ and (8.28) cannot be simultaneously satisfied, the solution $\phi(t_2,1)$ leaves the level set $L_V(\mu)$ for any $\mu > 0$.

- For $\tau_1(t_2,1) \in \left(0, \bar{\tau} - \frac{3\varepsilon}{2}\right]$, then from Lemma 8.3.5

$$\begin{aligned} V(\phi(t_2,1)) = V_{2a}(\phi(t_2,1)) &= |\tau_1(t_2,1) - \tau_2(t_2,1)| = \mu \\ V(\phi(t_2,2)) = V_{2a}(\phi(t_2,2)) &= |\tau_1(t_2,2) - \tau_2(t_2,2)| = \mu \end{aligned}$$

Then,

$$\begin{aligned} |\tau_1(t_2,1) - \tau_2(t_2,1)| &= |\tau_1(t_2,2) - \tau_2(t_2,2)| \\ \bar{\tau} - \tau_1(t_2,1) - \varepsilon &= \bar{\tau} - \tau_1(t_2,1) \qquad \leftarrow \tau_1(t_2,2) = \tau_1(t_2,1) + \varepsilon \\ -\varepsilon &\neq 0 \end{aligned}$$

which shows that, for every $\mu > 0$, it is not possible to remain in $L_V(\mu)$ after such a jump.

3. When $\phi(t_1,0) \in D_c$ and V is as in (8.24), to determine if the solution stays in $L_V(\mu)$, consider

$$V(\phi(t_1,0)) = V_{1a}(\phi(t_1,0)) = \tfrac{1}{\varepsilon}(\tau_1(t_1,0) - \tau_2(t_1,0))^2 + \tfrac{\varepsilon}{4} = \mu$$
$$V(\phi(t_1,1)) = V_{2a}(\phi(t_1,1)) = |\tau_1(t_1,1) - \tau_2(t_1,1)| = \mu \ .$$

Then, we obtain

$$\begin{aligned} \tfrac{1}{\varepsilon}(\tau_1(t_1,0) - \tau_2(t_1,0))^2 + \tfrac{\varepsilon}{4} &= |\tau_1(t_1,1) - \tau_2(t_1,1)| \\ \tfrac{1}{\varepsilon}(\bar{\tau} - \tau_2(t_1,0))^2 + \tfrac{\varepsilon}{4} &= |\bar{\tau} - \tau_2(t_1,1)| \qquad \leftarrow \text{using } \tau_2(t_1,0) = \tau_2(t_1,1), \tau_1(t_1,0) = \tau_1(t_1,1) = \bar{\tau} \\ \tfrac{1}{\varepsilon}(\bar{\tau} - \tau_2(t_1,0))^2 + \tfrac{\varepsilon}{4} &= \tau_2(t_1,0) - \bar{\tau} \qquad \leftarrow \text{using } \tau_2(t_1,0) > \bar{\tau}. \end{aligned}$$

Solving for $\tau_2(t_1,0)$, we get

$$\tau_2(t_1,0) = \bar{\tau} + \tfrac{\varepsilon}{2}.$$

Letting the solution, $\phi(t,1)$, flow until the next jump, when $\tau_2(t_2,1) = 2\bar{\tau}$ we have

$\tau_1(t_2, 1) = 2\bar{\tau} - \frac{\varepsilon}{2}$. Then, the system jumps according to g_2 since $\tau_1 + \varepsilon > q_1\bar{\tau}$, after which the solution reaches $L_V(0)$ and hence leaves $L_V(\mu)$.

4. When $\phi(t_1, 0) \in D_c$ and V is as in (8.25), to determine if the solution $\phi(t_1, 0)$ stays in $L_V(\mu)$ note that,

$$V(\phi(t_1, 0)) = V_{2a}(\phi(t_1, 0)) = |\tau_1(t_1, 0) - \tau_2(t_1, 0)| = \mu$$
$$V(\phi(t_1, 1)) = V_{2a}(\phi(t_1, 1)) = |\tau_1(t_1, 1) - \tau_2(t_1, 1)| = \mu.$$

Then, we get

$$\begin{aligned} |\tau_1(t_1, 0) - \tau_2(t_1, 0)| &= |\tau_1(t_1, 1) - \tau_2(t_1, 1)| \\ \tau_2(t_1, 0) - \bar{\tau} &= \tau_2(t_1, 0) - \bar{\tau} \qquad \leftarrow \text{using } \tau_2(t_1, 0) = \tau_2(t_1, 1), \tau_1(t_1, 0) = \bar{\tau}. \end{aligned}$$

Since this equality is true for every $\tau_2(t_1, 0)$, we allow the system to flow until $\tau_2(t_2, 1) = 2\bar{\tau}$, then $\tau_1(t_2, 1) \in \left(\bar{\tau}, 2\bar{\tau} - \frac{\varepsilon}{2}\right]$ with $q_1(t_2, 1) = 2$. The solution, $\phi(t_2, 1)$ after the jump leads to,

$$q_2(t_2, 2) = 1, \qquad \tau_2(t_2, 2) = 0, \qquad \begin{bmatrix} \tau_1(t_2, 2) \\ q_1(t_2, 2) \end{bmatrix} \in \begin{bmatrix} (\bar{\tau} + \varepsilon, 2\bar{\tau}) \\ 2 \end{bmatrix} \bigcup \begin{bmatrix} 0 \\ 1 \end{bmatrix}.$$

This allows for the following possibilities we will investigate case by case:

- For $\tau_1(t_2, 1) \in \left[2\bar{\tau} - \varepsilon, 2\bar{\tau} - \frac{\varepsilon}{2}\right]$ we have $\tau_1(t_2, 2) = 0$ because the jump is mapped to g_2 with $\tau_1 + \varepsilon < q_1\bar{\tau}$. Then, the solution $\phi(t_2, 2)$ reaches the level set $L_V(0)$ and hence leaves $L_V(\mu)$.

- For $\tau_1(t_2, 1) \in (2\bar{\tau} - \frac{3\varepsilon}{2}, 2\bar{\tau} - \varepsilon)$, we have

$$V(\phi(t_2, 1)) = V_{2a}(\phi(t_2, 1)) = |\tau_1(t_2, 1) - \tau_2(t_2, 1)| = \mu$$
$$V(\phi(t_2, 2)) = V_{1c}(\phi(t_2, 2)) = \frac{1}{\varepsilon}\left(\tau_1(t_2, 2) - \tau_2(t_2, 2) + 2\bar{\tau}\right)^2 - \frac{\varepsilon}{4} = \mu.$$

It follows that,

$$
\begin{aligned}
|\tau_1(t_2,1)-\tau_2(t_2,1)| &= \frac{1}{\varepsilon}\left(\tau_1(t_2,2)-\tau_2(t_2,2)+2\bar{\tau}\right)^2-\frac{\varepsilon}{4} \\
2\bar{\tau}-\tau_1(t_2,1) &= \frac{1}{\varepsilon}(\tau_1(t_2,2)-2\bar{\tau})^2+\frac{\varepsilon}{4} \\
2\bar{\tau}-\tau_1(t_2,1) &= \frac{1}{\varepsilon}(\tau_1(t_2,1)+\varepsilon-2\bar{\tau})^2+\frac{\varepsilon}{4} \qquad \leftarrow \text{ using } \tau_1(t_2,2)=\tau_1(t_2,1)+\varepsilon \\
\tau_1(t_2,1) &\in \left\{2\bar{\tau}-\frac{5\varepsilon}{2}, 2\bar{\tau}-\frac{\varepsilon}{2}\right\} \qquad (8.29)
\end{aligned}
$$

Since $\tau_1(t_2,1) \in (2\bar{\tau}-\frac{3\varepsilon}{2}, 2\bar{\tau}-\varepsilon)$ and (8.29) cannot be simultaneously satisfied, the solution $\phi(t_2,1)$ leaves the μ-level set, $L_V(\mu)$ for any $\mu > 0$.

- For $\tau_1(t_2,1) \in (\bar{\tau}, 2\bar{\tau}-\frac{3\varepsilon}{2})$, we have

$$
\begin{aligned}
V(\phi(t_2,1)) = V_{2a}(\phi(t_2,1)) = |\tau_1(t_2,1)-\tau_2(t_2,1)| = \mu \\
V(\phi(t_2,2)) = V_{2a}(\phi(t_2,2)) = |\tau_1(t_2,2)-\tau_2(t_2,2)| = \mu,
\end{aligned}
$$

which leads to the following:

$$
\begin{aligned}
|\tau_1(t_2,1)-\tau_2(t_2,1)| &= |\tau_1(t_2,2)-\tau_2(t_2,2)| \\
2\bar{\tau}-\tau_1(t_2,1) &= \tau_1(t_2,2) \\
2\bar{\tau}-\tau_1(t_2,1) &= \tau_1(t_2,1)+\varepsilon \qquad \leftarrow \tau_1(t_2,2)=\tau_1(t_2,1)+\varepsilon \\
\tau_1(t_2,1) &= \bar{\tau}-\tfrac{\varepsilon}{2}
\end{aligned}
$$

Since, $\tau_1(t_2,1) = \bar{\tau}-\frac{\varepsilon}{2}$ and $\tau_1(t_2,1) \in (\bar{\tau}, 2\bar{\tau}-\frac{3\varepsilon}{2})$ cannot be simultaneously satisfied then $V_{2a}(t_2,1) = \mu$ and $V_{2a}(t_2,2) = \mu$ cannot not be true for any $\mu > 0$.

This analysis proves that the conditions for asymptotic stability presented in Theorem 2.1.10 are satisfied for the Lyapunov function (8.6). In fact, Lemma 8.3.3 establishes (8.8), Lemmas 8.3.7, 8.3.8 and 8.3.9 establishes that the condition in (8.9) is satisfied. Then, the attractivity condition was established for $v \in (0, v^*)$, where $L_V(v)$ includes every x such that $|\tau_1-\tau_2| \neq \bar{\tau}$. Then, the set $\mathcal{A}$ in (8.5) is asymptotically stable for the system $\widetilde{\mathcal{H}}_{2,2} = (\widetilde{C}, F, \widetilde{D}, G)$.

■

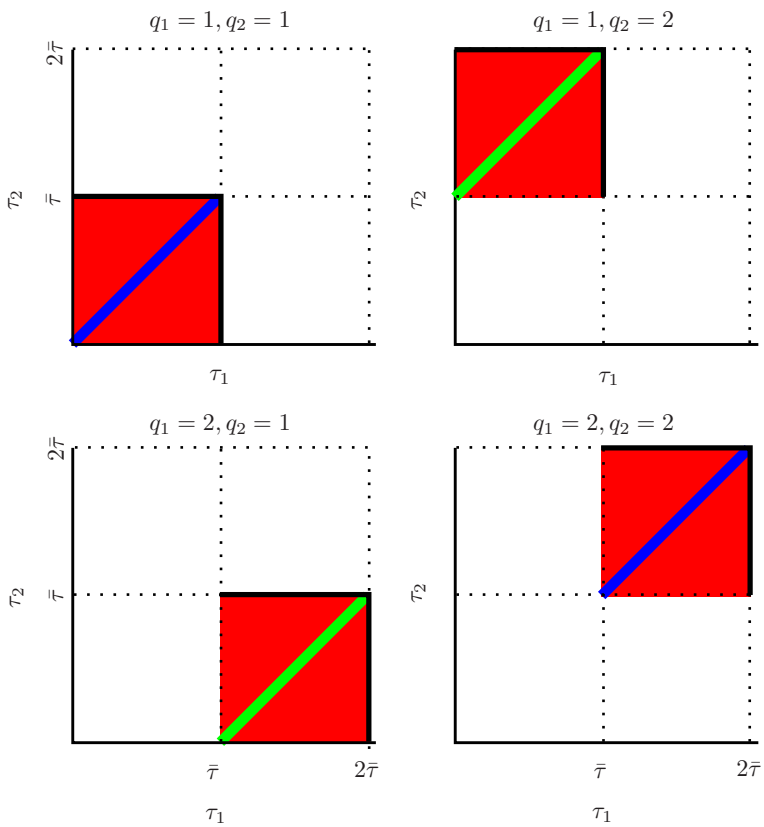

Figure 8.3: The flow set (red), the jump set (solid black), and basin of attraction with μ-level sets $L_V(\bar{\tau})$ (in blue) and $L_V(0)$ (in green) for each pair $(q_1.q_2)$

Remark 8.3.11 *For initial conditions in* $\{C \cup D \ : \ |\tau_1 - \tau_2| = \bar{\tau}, q_1 \neq q_2\}$ *solutions* $x(t,j)$ *stay in the level set* $V(\phi(t,j)) = \bar{\tau}$*. Note the green lines in Figure 8.3. For such solutions, the state does not converge to* $\mathcal{A}$ *because both agents jump simultaneously but on opposite channels, and thus missing the information transmitted. This point is corroborated by a Lyapunov local maximum at these states. Solutions from all other initial conditions in* $C \cup D$ *approach the synchronization condition defined by* $\mathcal{A}$*.*

8.4 Numerical Analysis

8.4.1 Numerical Simulation of $\mathcal{H}_{2,2}$

Solutions to $\mathcal{H}_{2,2}$ fall into three categories: always synchronized, asymptotically synchronized, and desynchronized. The simulations below show the evolution of these solution types. The parameters used are $\bar{\tau} = 1$, $\varepsilon = 0.05$.

- Always synchronized A solution that starts in the set $\mathcal{A}$ will always stay synchronized, that is, $\mathcal{A}$ is forward invariant. Figure 8.4(a) shows the evolution of such a solution. The top figure shows the timer value and the bottom figure shows the channel of the agents.

- Asymptotically synchronized A solution that starts close to $\mathcal{A}$ reaches synchronization rapidly. The initial condition for the simulation is such that $|\tau_1 - \tau_2| < \varepsilon$, so after one jump the two timers are the same. When the two timers start close to the set of points from where synchronization is not possible, the time needed to reach synchronization is much larger. The simulation in Figure 8.4(b) shows that the solution starts far from $\mathcal{A}$ but still converges. The initial conditions for these simulations are $\tau_1(0,0) = 0.3, q_1(0,0) = 1$, and $\tau_2(0,0) = 1.31$, $q_2(0,0) = 2$.

- Desynchronized When the agents start from an initial condition satisfying $|\tau_1(0,0) - \tau_2(0,0)| = \bar{\tau}$ and $q_1(0,0) \neq q_2(0,0)$, they stay desynchronized. The initial conditions $\tau_1(0,0) = 1.5$, $\tau_2(0,0) = .5$, $q_1(0,0) = 2$ and $q_2(0,0) = 1$ are used for the simulation in Figure 8.4(c). It shows that each agent has an offset leading to continually miss the other agent's transmission since they switch to opposite channels at every jump.

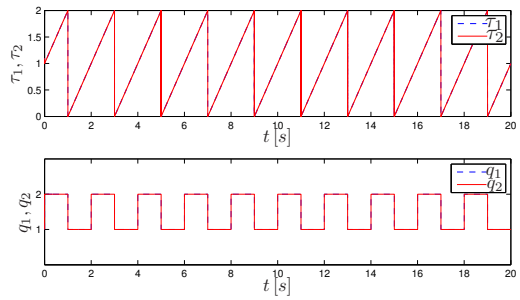

(a) A solution to $\mathcal{H}_{2,2}$ that is always synchronized.

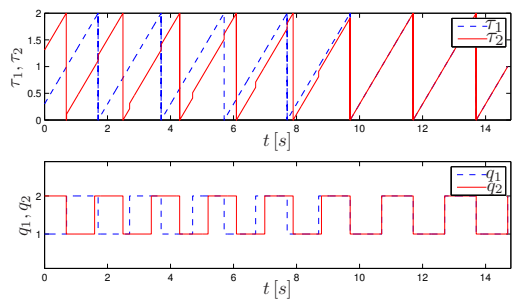

(b) A solution to $\mathcal{H}_{2,2}$ that asymptotically synchronizes after several transitions.

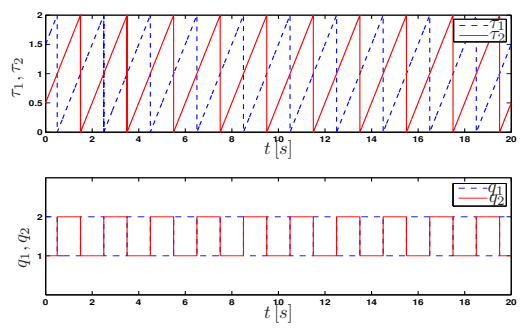

(c) A solution to $\mathcal{H}_{2,2}$ that never synchronizes.

8.4.2 Performance Analysis: Time to synchronize

The timer advance constant, ε, affects the rate at which the agents synchronize. In fact, the amount that the timers advance when a packet is received is governed by ε. If $\varepsilon \ll \bar{\tau}$, when a packet is received, the algorithm increments the timers by a small amount. If $\varepsilon \geq \bar{\tau}$ and a packet is received, the algorithm will automatically switch channels.

Figure 8.4 shows the time for convergence to synchronization with respect to the timer advance constant, ε, and as a function of the initial conditions in (8.1) and (8.3) (away from $L_V(\bar{\tau})$). A definite trend of time to convergence with respect to the value of ε: Time to convergence decreases as ε increases.

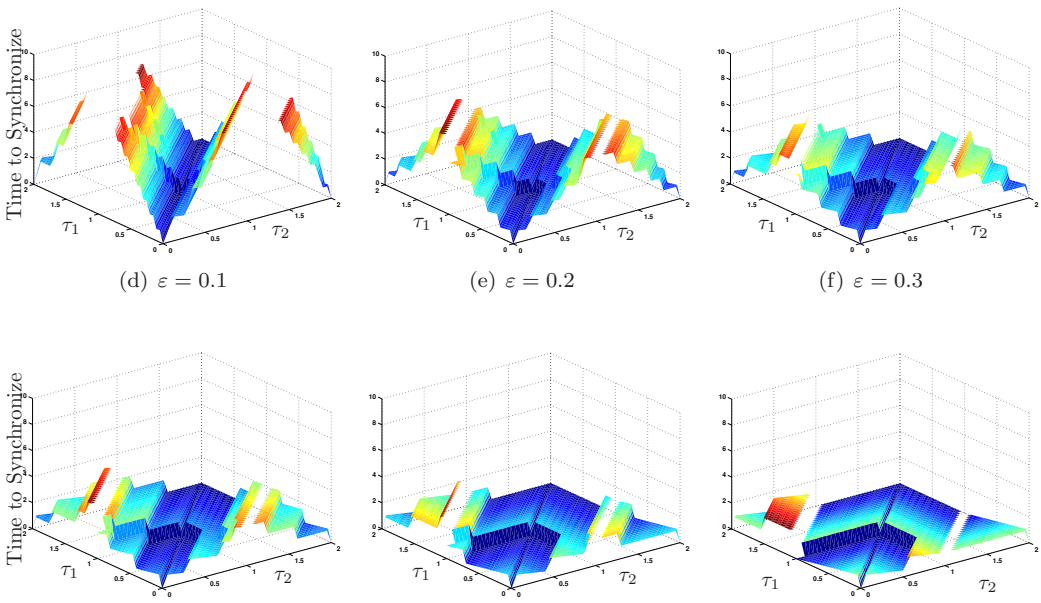

(d) $\varepsilon = 0.1$ (e) $\varepsilon = 0.2$ (f) $\varepsilon = 0.3$

(h) $\varepsilon = 0.4$ (i) $\varepsilon = 0.7$ (j) $\varepsilon = 0.1$

Figure 8.4: Time to converge to $\mathcal{A}$, i.e., time to synchronize timers and channel selections, for $\varepsilon = 0.1, 0.2, 0.3, 0.4, 0.7, 1$

A plot of the time to converge to synchronization with respect the timer advance constant, ε, can be determined by choosing a potential worse case scenario. For initial condition $x(0,0) = [1.2, 2, 0, 1]^\top$, Figure 8.5 shows time to synchronization as a function of ε. The decreasing trend present in Figure 8.5 indicates that as the timer advance constant is increased the time to convergence is decreased.

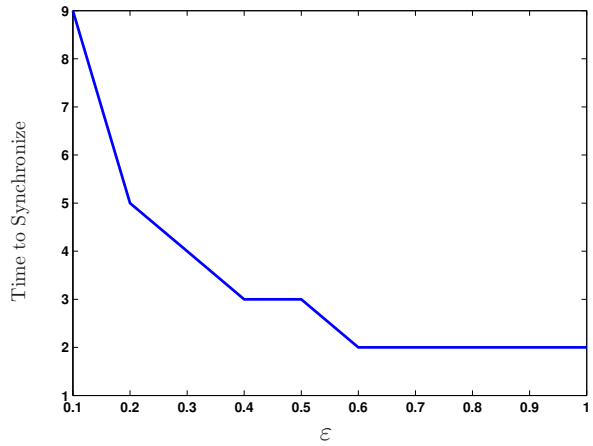

Figure 8.5: Time to synchronize as a function of the timer advance constant, ε, with x(0,0) = [1.2,2,0,1]

8.4.3 Robustness analysis to interference

The discussion in Section 8.4.2 indicates that for larger ε, the system will synchronize faster. However, ε large may compromise the robustness to adversarial attack or environmental interference. To determine the robustness of the algorithm, two sets of simulations were performed. To model environmental interference, pseudo-random times for injection of interfering packets were generated. At these time instances, a packet was injected into agent 2's correct channel, forcing it to reset and advance its timer by ε. Figure 8.6 also shows the number of injected packets versus the percentage of time on the same channel with the parameter ε equal to .3 and 1. Polynomial curve fittings were numerical generated to express the downward trend as the number of packets increase. The figure shows that the effect of the interfering packets is more significant for large ε. In fact, the agents stay on the same channel longer (for the same number of interfering packets) when ε is smaller.

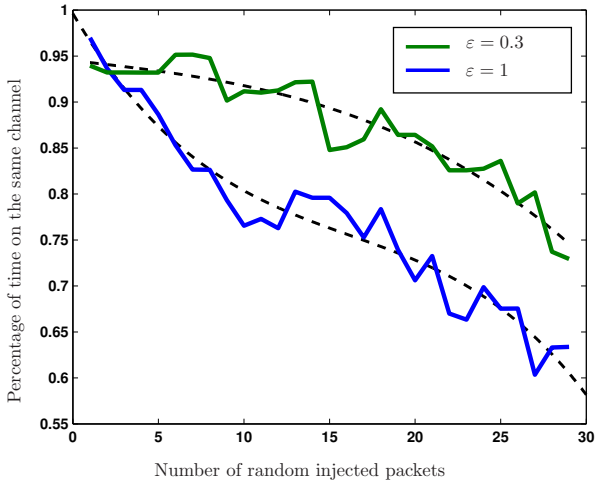

Figure 8.6: Percentage of time on the same channel versus number of interfering packets.

8.5 Experimental Results

The mechanism in the hybrid system $\mathcal{H}_{2,2}$ was implemented by using two Explorer16 demo boards with ZeroG wireless modules, both manufactured by Microchip, on a IEEE 802.11 network of two routers defining two unique SSIDs, the setup is shown in Figure 8.7. The SSIDs were configured to be uniquely named and set on different channels to simulate frequency hopping.

Figure 8.7: Test bed for experimentation with pulse-coupled oscillators Explorer16 demo boards with ZeroG wireless modules (bottom), wireless routers (top).

The boards run identical C code and are provided with SSID and IP information to identify the unique SSIDs (the channels) The states τ_1 and τ_2 are implemented via embedded clocks available within the microcontrollers. The conditions for transmissions and state resets in the jump sets are implemented as logic via if/else statements. Information is transmitted using UDP protocol. The following C code snippet summarizes the main operation modes (Run and Reset) of the implementation.

```
case Run:  // Normal run mode
    // Check if packet has been received
    if (ReceiveSignal){
        ReceiveSignal = FALSE; // clear the flag
        tau += EPS;  // increment state tau
        if (tau = taubar*qi){
             // reset state tau due to being >= threshold
             Mode = Reset;
        }
        else{
            // otherwise continue running
            Mode = Run;
        }
    }
    else if (tau = taubar*qi){
         // check if state tau expired
         SendSignal = TRUE;
         // set flags to send packet
```

```
        Mode = Reset;
    }
    else{
        // set flag to run mode
        Mode = Run;
    }
    break;


case UDP_SendSignal: // Send packet
    // Check if packet has been sent
    if (! UDPIsPutReady(UDP_SOCKET)){
        Mode = Run;
    }
    // Send packet
    UDPPut(current_channel^0xFF);
    UDPFlush();
    Mode = Run;
    break;
```

Continuous increment of the variable `tau` is performed by the internal timer in each board. Figure 8.8 shows experimental data with parameters $\varepsilon = 0.2$ and $\bar{\tau} = 30$. The first board is initialized with timer τ_1 equal zero at channel 1 (solid plots) while the second board is turned on about ten seconds later and initialized with timer τ_2 equal to zero at channel 2 (dashed plots). The oscillators reach approximate synchronization at around 300 sec. The obtained experimental results suggest that the algorithm implemented in $\mathcal{H}_{2,2}$ is robust to quantization and delays,

which are unavoidably present in the hardware implementation.

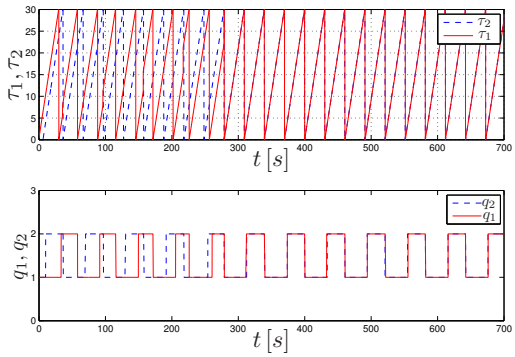

Figure 8.8: Experimental data obtained with the test bed in Figure 8.7.

8.6 Summary

A frequency hopping rendezvous algorithm was introduced for dynamic cognitive radio communication. More specifically, a hybrid synchronization algorithm proposed and modeled with two states for each agent; a channel state and a timer state, wherein, the agents used the timer state to trigger a jump between channels. Then, the synchronization problem was recast as a set stabilization problem and synchronization of a class of two impulsive oscillators was shown through Lyapunov analysis in a hybrid framework. For almost every point in the space of the timers, the oscillators synchronize. Lost packets do not effect the asymptotic stability property, but leads to slower convergence than when there is no channel constraints.

Part III

Final Remarks

Chapter 9

Conclusion and Future Directions

In this thesis, several problems of coordination of multiagent systems connected over a networks was addressed. Two main enveloping concepts were considered. The first addresses the control design of distributed controller to converge agents' states to each other when information between the agents are intermittent. The second one looks at the desynchronization of impulse-coupled oscillators.

To synchronize the state of connected agents, a typical approach is to define a controller for each agent which takes the difference between the agents state and the state of all connected agents a multiply it by a constant gain. However, when communication is intermittent, the challenge lays into how to design the gains of the controller when the time between communication events are bounded. We define a first-order controller which updates impulsively when information arrives into each agent. Then, the consensus/synchronization configuration was recast into a set stabilization problem. Depending on the specific scenario under consideration, a Lyapunov based analysis was used to certify an asymptotic stability properties. Namely, when each agent has no internal dynamics, the consensus set was determined to be pointwise asymptotically stable. When the agent has linear time-invariant dynamics, we determine the

conditions which certify exponential stability for the synchronization set.

There are numerous potential extensions to this work. With a slight modification of the synchronization set and control algorithm, a formation problem could be considered, where each agent want to maintain pre-specified distance away from its neighbors. Since actuators and communication may occur at differing times, an observer-based controller could be developed to drive the agents to synchronization. Another interesting avenue lays in the development of an event-triggered communication to drive the times at which communication occurs and uses the controllers developed to drive the agents to synchronization.

Synchronization of general hybrid systems is still an open problem. Namely, when each agent may contain both continuous and discrete dynamics, what properties do the agents need to satisfy to certify synchronization of the agents' states. Both uniform and nonuniform notions of partial state synchronization were given. It was shown that if a synchronization set was determined to be asymptotically stable then asymptotic synchronization could be certified. Through some graphical properties of the networks of the agents, it may be possible to certify synchronization for general hybrid systems. This may be done through contraction or incremental stability based analysis for hybrid systems to show that synchronization may be achieved with out the need of development of a Lyapunov function.

In a class of impulse-coupled oscillators, an asymptotically stable and robust property was shown. Moreover, a solid framework for modeling and analysis of hybrid systems was developed. Using Lyapunov stability and invariance principle, a desynchronization-like set was shown to be asymptotically stable. Moreover, we apply the techniques developed under desynchronization and apply it to both interconnection of neurons and to a frequency hopping rendezvous problem. Under the interconnection of neurons, the update of the phases of each neuron was updated by a nonlinear update law. In the frequency hopping rendezvous problem, the agents used an auxiliary channel state to indicate if communication was possible. Both cases

could be extended to consider a larger network of agents and channels. The difficulty lays in the development of a Lyapunov function to certify that the respective sets are asymptotically stable.

Bibliography

[1] Stuart Bennett. *A History of Control Engineering, 1800-1930*. Institution of Electrical Engineers, Stevenage, UK, UK, 1979.

[2] J. C. Maxwell. On governors. 16:270–283, 1868.

[3] C. Boutilier. Planning, learning and coordination in multiagent decision processes. In *Proceedings of the 6th Conference on Theoretical Aspects of Rationality and Knowledge*, TARK '96, pages 195–210, San Francisco, CA, USA, 1996. Morgan Kaufmann Publishers Inc.

[4] M. Tambe, J. Adibi, Y. Al-Onaizan, A. Erdem, G. A. Kaminka, S. C. Marsella, and I. Muslea. Building agent teams using an explicit teamwork model and learning. *Artificial Intelligence*, 110(2):215 – 239, 1999.

[5] J. A. Fax and R. M. Murray. Information flow and cooperative control of vehicle formations. *IEEE Transactions on Automatic Control*, 49(9):1465–1476, 2004.

[6] R. Olfati-Saber and R.M. Murray. Consensus problems in networks of agents with switching topology and time-delays. *IEEE Transactions on Automatic Control*, 49(9):1520–1533, Sept 2004.

[7] R. Olfati-Saber and R. M. Murray. Graph rigidity and distributed formation stabilization

of multi-vehicle systems. In *Proceedings of the IEEE Conference on Decision and Control*, volume 3, pages 2965–2971. IEEE, 2002.

[8] H. Yamaguchi, T. Arai, and G. Beni. A distributed control scheme for multiple robotic vehicles to make group formations. *Robotics and Autonomous systems*, 36(4):125–147, 2001.

[9] J. Cortés and F. Bullo. Coordination and geometric optimization via distributed dynamical systems. *SIAM Journal on Control and Optimization*, 44(5):1543–1574, 2005.

[10] R. Olfati-Saber and J. S. Shamma. Consensus filters for sensor networks and distributed sensor fusion. In *Decision and Control, 2005 and 2005 European Control Conference. CDC-ECC'05. 44th IEEE Conference on*, pages 6698–6703. IEEE, 2005.

[11] A. Sarlette, R. Sepulchre, and N. Leonard. Cooperative attitude synchronization in satellite swarms: a consensus approach. In *Proceedings of the 17th IFAC Symposium on Automatic Control in Aerospace*, pages 223–228, 2007.

[12] N. A. Lynch. *Distributed algorithms*. Morgan Kaufmann, 1996.

[13] V. N. Murthy and E. E. Fetz. Synchronization of neurons during local field potential oscillations in sensorimotor cortex of awake monkeys. *Journal of Neurophysiology*, 76(6):3968–3982, 1996.

[14] S. Phillips and R. G. Sanfelice. A framework for modeling and analysis of robust stability for spiking neurons. In *Proc. of the American Control Conf.*, pages 1414–1419, June 2014.

[15] I. Belykh, V. Belykh, and M. Hasler. Generalized connection graph method for synchronization in asymmetrical networks. *Physica D: Nonlinear Phenomena*, 224(1–2):42 – 51, 2006.

[16] Q. Hui, W. M. Haddad, and S. P. Bhat. Finite-time semistability theory with applications to consensus protocols in dynamical networks. In *Proceedings of the American Control Conference*, pages 2411–2416, July 2007.

[17] J. J. Slotine, W. Wang, and K. El-Rifai. Contraction analysis of synchronization in networks of nonlinearly coupled oscillators. In *Proceedings of the 16th International Symposium on Mathematical Theory of Networks and Systems*, 2004.

[18] D. Angeli. A Lyapunov approach to incremental stability properties. *IEEE Transactions on Automatic Control*, 47(3):410–421, 2002.

[19] S. Cai, P. Zhou, and Z. Liu. Synchronization analysis of hybrid-coupled delayed dynamical networks with impulsive effects: A unified synchronization criterion. *Journal of the Franklin Institute*, 352(5):2065 – 2089, 2015.

[20] Luca Scardovi and Rodolphe Sepulchre. Synchronization in networks of identical linear systems. *Automatica*, 45(11):2557 – 2562, 2009.

[21] L. Moreau. Stability of continuous-time distributed consensus algorithms. In *2004 43rd IEEE Conference on Decision and Control (CDC)*, volume 4, pages 3998–4003, Dec 2004.

[22] R. Olfati-Saber, J. A. Fax, and R. M. Murray. Consensus and cooperation in networked multi-agent systems. *Proceedings of the IEEE*, 95(1):215–233, Jan 2007.

[23] J. Lu, D. W. C. Ho, and J. Cao. A unified synchronization criterion for impulsive dynamical networks. *Automatica*, 46(7):1215 – 1221, 2010.

[24] T. Liu, M. Cao, C. De Persis, and J. M. Hendrickx. Distributed event-triggered control for synchronization of dynamical networks with estimators. *IFAC Proceedings Volumes*, 46(27):116 – 121, 2013.

[25] O. Demir and J. Lunze. Event-based synchronisation of multi-agent systems. *IFAC Proceedings Volumes*, 45(9):1 – 6, 2012.

[26] C. De Persis and P. Frasca. Self-triggered coordination with ternary controllers. *IFAC Proceedings Volumes*, 45(26):43 – 48, 2012.

[27] R. Goebel, R. G. Sanfelice, and A.R. Teel. Hybrid dynamical systems. *IEEE Control Systems Magazine*, 29(2):28–93, April 2009.

[28] R. Goebel, R. G. Sanfelice, and A. R. Teel. *Hybrid Dynamical Systems: Modeling, Stability, and Robustness*. Princeton University Press, New Jersey, 2012.

[29] R. Goebel. Basic results on pointwise asymptotic stability and set-valued lyapunov functions. In *Proceedings of the IEEE Conference on Decision and Control*, pages 1571–1574, 2010.

[30] S. P. Bhat and D. S. Bernstein. Nontangency-based lyapunov tests for convergence and stability in systems having a continuum of equilibria. *SIAM Journal on Control and Optimization*, 42(5):1745–1775, 2003.

[31] R. E. Mirollo and S. H. Strogatz. Synchronization of pulse-coupled biological oscillators. *SIAM Journal on Applied Mathematics*, 50:1645–1662, 1990.

[32] A. Pikovsky, M. Rosenblum, and J. Kurths. *Synchronization: A Universal Concept in Nonlinear Sciences*. Cambridge University Press, 2003.

[33] W. Gerstner and W.M. Kistler. *Spiking Neuron Models: Single Neurons, Populations, Plasticity*. Cambridge University Press, 2002.

[34] C. S. Peskin. *Mathematical Aspects of Heart Physiology*. Courant Institute of Mathematical Sciences, 1975.

[35] Y.W.P. Hong, W.J. Huang, and C.C.J. Kuo. *Cooperative Communications and Networking: Tech. and System Design*. Springer, 2010.

[36] C. Liu and K. Wu. A dynamic clustering and scheduling approach to energy saving in data collection from wireless sensor networks. In *Proc. of SECON: Data Coll. Wireless Sensor Networks*, 2005.

[37] L. F. Abbott and Carl van Vreeswijk. Asynchronous states in networks of pulse-coupled oscillators. *Physical Review E*, 48:1483–1490, 1993.

[38] A. Mauroy and R. Sepulchre. Clustering behaviors in networks of integrate-and-fire oscillators. *Chaos: An Interdisciplinary Journal of Nonlinear Science*, 18(3):037122, 2008.

[39] L. Glass and M.C. MacKey. *From Clocks to Chaos: The Rhythms of Life*. Princeton Paperbacks. Mir, 1988.

[40] R. Nagpal A. Patel, J. Desesys. Desynchronization: The theory of self-organizing algorithms for round-robin scheduling. In *Proceedings of the First Int. Conf. on Self-Adaptive and Self-Organizing Systems, '07*, pages 87–96, July 2007.

[41] J. Benda, A. Longtin, and L. Maler. A synchronization-desynchronization code for natural communication signals. *Neuron*, 52(2):347–358, Oct 2006.

[42] G. Pfurtscheller and F.H. Lopes da Silva. Event-related eeg/meg synchronization and desynchronization: basic principles. *Clinical Neurophysiology*, 110(11):1842–1857, 1999.

[43] M. Stopfer, S. Bhagavan, B. H. Smith, and G. Laurent. Impaired odour discrimination on desynchronization of odour-encoding neural assemblies. *Nature*, 390:70–74, Nov 1997.

[44] A. Nabi and J. Moehlis. Nonlinear hybrid control of phase models for coupled oscillators. In *Proceedings of the American Control Conference, 2010*, pages 922–923, July 2 2010.

[45] M. Majtanik, K. Dolan, and P.A. Tass. Desynchronization in networks of globally coupled neurons: effects of inertia. In *Proc. of 2004 IEEE Int. Joint Conference on Neural Networks*, pages 1481–86 vol.2, '04.

[46] R. Goebel and R. G. Sanfelice. Notions and sufficient conditions for pointwise asymptotic stability in hybrid systems. *Proceedings IFAC Symposium on Nonlinear Control Systems (to appear)*, 2016.

[47] C. Cai and A. R. Teel. Characterizations of input-to-state stability for hybrid systems. *Systems & Control Letters*, 58(1):47 – 53, 2009.

[48] C. Godsil and G.F. Royle. *Algebraic Graph Theory*. Graduate Texts in Mathematics. Springer New York, 2001.

[49] F. Ferrante, F. Gouaisbaut, R.G. Sanfelice, and S. Tarbouriech. A continuous-time observer with a continuous intersample injection in the presence of sporadic measurements. In *Proceedings of the IEEE Conference on Decision and Control*, pages 654–5659, 2015.

[50] F. Ferrante, F. Gouaisbaut, R. G. Sanfelice, and S. Tarbouriech. An observer with measurement-triggered jumps for linear systems with known input. In *Proceedings of the 19th IFAC World Congress*, pages 140–145, 2014.

[51] J.J.B. Biemond, N. van de Wouw, W.P.M.H. Heemels, R. G. Sanfelice, and H. Nijmeijer. Tracking control of mechanical systems with a unilateral position constraint inducing dissipative impacts. In *Proceedings of the IEEE Conference on Decision and Control*, pages 4223–4228, 2012.

[52] Adaptive sliding-mode insensitive control of a class of non-ideal complex networked systems. *Information Sciences*, 274:273 – 285, 2014.

[53] R. G. Sanfelice and L. Praly. Convergence of nonlinear observers on $\mathbb{R}^n$ with a Riemannian metric (Part I). *IEEE Trans. on Automatic Control*, 57(7):1709–1722, July 2012.

[54] Y. Li, S. Phillips, and R. G. Sanfelice. On distributed observers for linear time-invariant systems under intermittent information constraints. In *Proc. of 10th IFAC Symposium on Nonlinear Control Systems*, pages 666–671, 2016.

[55] Y. Li, S. Phillips, and R. G. Sanfelice. Robust distributed estimation for linear systems under intermittent information. *To appear in IEEE Transactions on Automatic Control*, 2018.

[56] Synchronizing linear systems via partial-state coupling. *Automatica*, 44(8):2179 – 2184, 2008.

[57] A. R. Teel, F. Forni, and L. Zaccarian. Lyapunov-based sufficient conditions for exponential stability in hybrid systems. *IEEE Transactions on Automatic Control*, 58(6):1591–1596, June 2013.

[58] T. Liu, D. J. Hill, and B. Liu. Synchronization of dynamical networks with distributed event-based communication. In *2012 IEEE 51st IEEE Conference on Decision and Control*, pages 7199–7204, Dec 2012.

[59] W. Yu, G. Chen, and M. Cao. Consensus in directed networks of agents with nonlinear dynamics. *IEEE Transactions on Automatic Control*, 56(6):1436–1441, June 2011.

[60] Ren W. and R. W. Beard. Consensus seeking in multiagent systems under dynamically changing interaction topologies. *IEEE Transactions on Automatic Control*, 50(5):655–661, May 2005.

[61] G. Como, B. Bernhardsson, and A. Rantzer. *Information and Control in Networks*. Lecture Notes in Control and Information Sciences. Springer International Publishing, 2014.

[62] D. J. Watts and S. H. Strogatz. Collective dynamics of 'small-world' networks. *Nature*, 393(6684):440–442, 1998.

[63] W. Gerstner and W. M. Kistler. *Spiking Neuron Models: Single Neurons, Populations, Plasticity*. Cambridge University Press, 1 edition, August 2002.

[64] Y. Wang and Z. Guan. Generalized synchronization of continuous chaotic system. *Chaos, Solitons & Fractals*, 27(1):97 – 101, 2006.

[65] L. Moreau. Stability of multiagent systems with time-dependent communication links. *IEEE Transactions on Automatic Control*, 50(2):169–182, Feb 2005.

[66] F. Dorfler and F. Bullo. Synchronization in complex networks of phase oscillators: A survey. *Automatica*, 50(6):1539 – 1564, 2014.

[67] L. M. Pecora and T. L. Carroll. Master stability functions for synchronized coupled systems. *Phys. Rev. Lett.*, 80:2109–2112, Mar 1998.

[68] F.H. Clarke. *Optimization and Nonsmooth Analysis*. SIAM's Classic in Applied Mathematics, 1990.

[69] S. Phillips and R. G. Sanfelice. Robust asymptotic stability of desynchronization in impulse-coupled oscillators. *IEEE Transactions on Control of Network Systems*, 3:127–136, June 2016.

[70] R. G. Sanfelice, D. A. Copp, and P. Nanez. A toolbox for simulation of hybrid systems in Matlab/Simulink: Hybrid Equations (HyEQ) Toolbox. In *Proceedings of Hybrid Systems: Computation and Control Conference*, pages 101–106, 2013.

[71] J.M. Bower and D. Beeman. *The book of GENESIS: exploring realistic neural models with the GEneral NEural SImulation System*. TELOS, 1995.

[72] B. Ermentrout. Type i membranes, phase resetting curves, and synchrony. *Neural Comput*, 8:979–1001, 1995.

[73] E. E. Brown, J. Moehlis, and P. Holmes. On the phase reduction and response dynamics of neural oscillator populations. *Neural Comput.*, 16(4):673–715, April 2004.

[74] R. Stein. Some Models of Neuronal Variability. *Biophysical Journal*, 7(1):37–68, January 1967.

[75] C. Koch and I. Segev. *Methods in Neuronal Modeling: From Ions to Networks*. A Bradford book. MIT Press, 1998.

[76] Y. Kuramoto. Phase- and center-manifold reductions for large populations of coupled oscillators with application to non-locally coupled systems. *International Journal of Bifurcation and Chaos*, 07(04):789–805, 1997.

[77] D. H. Hubel and T. N. Wiesel. Ferrier lecture. Functional architecture of macaque monkey visual cortex. *Proceedings of the Royal Society of London. Series B, Containing papers of a Biological character. Royal Society (Great Britain)*, 198(1130):1–59, July 1977.

[78] W. R. Softky and C. Koch. The highly irregular firing of cortical cells is inconsistent with temporal integration of random EPSPs. *The Journal of Neuroscience*, 13(1):334–350, January 1993.

[79] A. L. Hodgkin and A. F. Huxley. A quantitative description of membrane current and its application to conduction and excitation in nerve. *The Journal of physiology*, 117(4):500–544, August 1952.

[80] J.P. Keener and J. Sneyd. *Mathematical Physiology*. Interdisciplinary applied mathematics. U.S. Government Printing Office, 1998.

[81] A.T. Winfree. *The Geometry of Biological Time*. Interdisciplinary applied mathematics. U.S. Government Printing Office, 2001.

[82] J. Guckenheimer and P. Holmes. *Nonlinear Oscillations, Dynamical Systems, and Bifurcations of Vector Fields*. Number v. 42 in Applied Mathematical Sciences. Springer, 1983.

[83] S. Phillips and R.G. Sanfelice. Results on the asymptotic stability properties of desynchronization in impulse-coupled oscillators. In *Proc. American Control Conference, 2013*, pages 3278–3283, June 2013.

[84] R. G. Sanfelice, R. Goebel, and A. R. Teel. Invariance principles for hybrid systems with connections to detectability and asymptotic stability. *IEEE Transactions on Automatic Control*, 52(12):2282–2297, 2007.

[85] G. B. Ermentrout and N. Kopell. Frequency Plateaus in a Chain of Weakly Coupled Oscillators, I. *SIAM Journal on Mathematical Analysis*, 15(2):215–237, 1984.

[86] A. Ephremides, J.E. Wieselthier, and D. J. Baker. A design concept for reliable mobile radio networks with frequency hopping signaling. *Proceedings of the IEEE*, 75(1), 1987.

[87] L.A. DaSilva and I. Guerreiro. Sequence-based rendezvous for dynamic spectrum access. In *3rd IEEE Symposium on New Frontiers in Dynamic Spectrum Access Networks*, 2008.

[88] B. Horine and D. Turgut. Link rendezvous protocol for cognitive radio networks. In *2nd IEEE International Symposium on New Frontiers in Dynamic Spectrum Access Networks, 2007. DySPAN 2007*, pages 444–447, 2007.

[89] D. Pu, A.M. Wyglinski, and M. McLernon. A frequency rendezvous approach for decentralized dynamic spectrum access networks. In *4th International Conference on Cognitive Radio Oriented Wireless Networks and Communications*, pages 1–6, 2009.

Appendix A

List of Publications

Journal Publications

[1] S. Phillips, and R. G. Sanfelice. Robust Distributed Synchronization of Networked Linear Systems with Intermittent Information, *Automatica*, (under review).

[2] Y. Li, S. Phillips, and R. G. Sanfelice. Robust Distributed Estimation for Linear Systems under Intermittent Information, *IEEE Transactions on Automatic Control*, (accepted), April 2018.

[3] Y. Li, S. Phillips, and R. G. Sanfelice. Basic Properties and Characterization of Incremental Stability Prioritizing Flow Time for a Class of Hybrid Systems, *Systems and Control Letters*, 90:7–15, 2016.

[4] S. Phillips, and R. G. Sanfelice. Robust asymptotic stability of desynchronization in impulse-coupled oscillators., *IEEE Transactions on Control of Networked Systems*, 3(2):127–136, 2016.

Peer–Reviewed Conference Proceedings

[1] S. Phillips, A. Duz, F. Pasqualetti and R. G. Sanfelice. Recurrent Attacks in a Class of Cyber-Physical Systems: Hybrid-Control Framework for Modeling and Detection. In *Proceedings of the Conference on Decision and Control*. (accepted) Dec 2017

[2] S. Phillips, and R. G. Sanfelice. On Asymptotic Synchronization of Interconnected Hybrid Systems with Applications. In *Proceedings of the American Control Conference*. pages 2291-2296, May 2017

[3] S. Phillips, Y. Li, and R. G. Sanfelice. A hybrid consensus protocol for pointwise exponential stability with intermittent information. In *Proc. of the 10th IFAC Symp. on Nonlinear Control Sys.*. pages 146–151, Aug. 2016

[4] Y. Li, S. Phillips, and R. G. Sanfelice. On Distributed Observers for Linear Time-invariant Systems Under Intermittent Information Constraints. In *Proc. of the 10th IFAC NOLCOS*. pages 654–659, Aug. 2016

[5] S. Phillips, and R. G. Sanfelice. Robust Synchronization of Interconnected Linear Systems over Intermittent Communication Networks, In *Proceedings of the American Control Conference*, pages 5575–5580, June 2016.

[6] S. Phillips, and R. G. Sanfelice. Robust Synchronization of Two Linear Systems over Intermittent Communication Networks, In *Proceedings of the Conference on Decision and Control*, pages 5569–5574, Dec. 2015.

[7] Y. Li, S. Phillips, and R. G. Sanfelice. Results on Incremental Stability for Hybrid Systems, In *Proceedings of the Conference on Decision and Control*, pages 3089–3094, December 2014.

[8] S. Phillips, and R. G. Sanfelice. A framework for modeling and analysis of robust stability for spiking neurons, In *Proceedings of the American Control Conference*, pages 1414–1419, June 2014.

[9] S. Phillips, and R. G. Sanfelice. Results on the asymptotic stability properties of desynchronization in impulse-coupled oscillators, In *Proceedings of the American Control Conference*, pages 3278–3283, June 2013.

[10] S. Phillips, R. G. Sanfelice, R. S. Erwin. On the synchronization of two impulsive oscillators under communication constraints, In *Proceedings of the American Control Conference*,

pages 2443–2448, July 2012.